Intra-neuronal influences on development of the mammalian neuromuscular junction

Adrianna Teriakidis

Doctor of Philosophy

Institute for Adaptive and Neural Computation
School of Informatics
University of Edinburgh

2010

Abstract

During development of the nervous system an excess number of synapses are formed, most of which are subsequently pruned, resulting in functional neural networks. The precise mechanisms that determine which synapses are formed and which synapses are maintained are not thoroughly understood. The aim of this thesis is to investigate the intra-neuronal constraints and influences on synapse formation and elimination during development.

In the first part of the thesis I investigated intra-neuronal influences on synapse elimination. Synapse elimination is known to occur at polyneuronally innervated neuromuscular junctions through competition, leading to mononeuronally innervated muscle fibres. However, whether synapse elimination ever occurs in the absence of competition, leading to muscle fibres becoming denervated, has not been resolved. The data presented in this thesis suggest that only large motor units undergo a reduction in motor unit size in the absence of competition. Using the Rasmussen and Willshaw (1993) version of the Dual Constraint Model I show that these data are consistent with the prediction that synapses will be eliminated from muscle fibres when a neuron's resources become stretched, for instance as a result of the normal growth of the animal. Larger motor units, which innervate more synapses, will thus be more vulnerable to the extra demand put upon them by the growth of each synapse. The model predicts that synapse elimination in the absence of competition should occur at least over the first 6 months of life and not only during the first two postnatal weeks, when most polyneuronal innervation is normally eliminated.

In the second part of the thesis, I investigated intra-neuronal influences on synapse formation. Specifically I tested the hypothesis that each branch of a motor neuron forms synapses randomly and independently of other branches. If true there should be instances where two branches from the same neuron initially innervate the same endplate (sibling branch convergence). Sibling branch convergence was experimentally investigated in both regenerating and developing motor neurons. The evidence suggests that sibling branches can converge on the same muscle fibre and that they can competitively eliminate each other. However, it appears that convergence does not occur at the frequency that would be expected, suggesting that branches from the same

motor neuron do not form synapses independently of each other.

At present there are limitations in imaging immature networks due to the spatial resolution limit of light microscopy. The last part of this thesis explores thin serial sectioning and reconstruction as a possible technique for increasing resolution in the z-axis. This technique has potential to be developed but I show that at present it does not provide sufficient resolution to discriminate between developing motor axons in neonatal lumbrical muscles.

Acknowledgements

Many people have helped me and it was hard to decide who to acknowledge by name.

I want to thank my supervisors, Richard Ribchester and David Willshaw because they helped me most of all with the research and the thesis.

Other people whose help I appreciate and am grateful for include: Derek Thomson, David Sterratt, Hannes Saal, Oyinlola Oyebode, my parents, Danny Hamilton, Pat Ferguson and Athina Spiliopoulou.

I want to thank Jeff Lichtman and the people in his lab who helped me during my visit there, and I also want to thank Ondrej Mandula for answering my questions about microscopy.

To those who I have left off this list, I thank you also.

Declaration

I declare that this thesis was composed by myself, that the work contained herein is my own except where explicitly stated otherwise in the text, and that this work has not been submitted for any other degree or professional qualification except as specified.

(*Adrianna Teriakidis*)

Table of Contents

List of Abbreviations

α-BTX α-bungarotoxin

μ mononeuronal innervation

π polyneuronal innervation

4DL 4th deep lumbrical

ACh acetylcholine

AChR acetylcholine receptor

ANPD adults with neonatal partial denervation

AWA14 adult muscles that have been partially denervated in adult mice 14 days earlier

AWA7 adult muscles that have been partially denervated in adult mice 7 days earlier

BTX bungarotoxin

CFP cyan fluorescent protein

CNS central nervous system

EDL extensor digitorum longus

EM electron microscopy

EPP endplate potential

FWHM full width half maximum

LAL levator auris longus

LPN lateral plantar nerve

mEPP miniature endplate potential

MPS mammalian physiological solution

MU motor unit

NA numerical aperture of an objective lens

NF neurofilament

NGF nerve growth factor

NMJ neuromuscular junction

PBS 1% phosphate buffered saline

PFA 4% paraformaldehyde

PNS peripheral nervous system

PSF point spread function

SN sural nerve

SNR signal to noise ratio

TTX tetrodotoxin

YFP yellow fluorescent protein

YFP16 strain of mouse that expresses fluorescent protein in 100% of α motor neurons

YFPH strain of mouse that expresses fluorescent protein in $\sim$5% of α motor neurons

List of Figures

List of Tables

Chapter 1

Background/Introduction

1.1 Development of the mammalian nervous system

The nervous system is a connected network of specialised cells which transmit and process information in the body and the brain. In mammals it is divided into the central nervous system (CNS), which consists of everything within the brain and spinal cord, and the peripheral nervous system (PNS), which includes structures in the periphery. The important cell types in the nervous system are neurons and glia. Neurons have a spherical cell body (soma) which contains most of the cellular machinery. Long thin neurites extend from the soma, which are divided into dendrites and axons. Dendrites typically transmit information to the soma whereas axons carry information from the soma to other neurons. This idea was first proposed as the law of dynamic polarisation by Cajal. Different types of neurons have different characteristic shapes. For example, motor neurons, whose cell body is in the spinal cord, have short dendrites which receive incoming information from the brain, and a single very long axon which innervates a target muscle in the body. Although there is a single axon per motor neuron, this can branch to innervate many different muscle fibres. Neurons connect to each other through highly specialised junctions at synapses. It is presumed that neurons transmit and process most of the information, while glia serve to insulate neurons and provide trophic and structural support (Balice-Gordon, 1996). However, some work suggests that glia may also be involved in information processing (see e.g. Araque,

2008).

In mammals most of the somata of neuronal cells are found in the CNS. The PNS is composed of the autonomic ganglia, which comprise clusters of cell bodies outside of the spinal cord and participate in control of autonomic functions in the body; the neurites from motor and sensory neurons in the spinal cord, which can extend throughout every part of the body and control movement of muscles and receive sensory information; and glial cells associated with these neurites and cells. Some suggest that the nervous system is the most complicated structure in the universe. Without question it all originates in development from a single, fertilised diploid cell.

Living organisms undergo large transformations between the time they are conceived to when they reach their adult form. The fertilised ovum repeatedly divides giving rise to millions of daughter cells. These will ultimately form every part of the organism and do so by migrating to the correct positions, changing in size and shape, becoming specialised and forming connections with surrounding cells. From the earliest stages of cell division and until birth the organism is referred to as an embryo (or, from mid-gestation, a foetus). Some of the cells that are produced will become part of the nervous system.

In the early stages of development the dorsal surface of the embryo forms into two ridges, parallel to the anterior-posterior axis, which gradually grow and fuse to form the neural tube. The CNS is formed by cells which originate in the neural tube, whereas PNS cells are born in the neural crest, a region dorsolateral to the neural tube. Ventrolateral to the neural tube are the somites which give rise to skeletal muscle among other structures (Purves and Lichtman, 1985).

In order for the nervous system to function normally, both long and short range connections must be made between neurons. When axons from one part of the nervous system innervate a distant target they grow towards it as a fasciculated bundle, often following the path of a pioneer axon which grows ahead of the rest (Purves and Lichtman, 1985).

Once axons arrive at their target tissue they form synapses. In adults, there is frequently a stereotyped non-random pattern of innervation which varies little across different

individuals of a species. For example retinal ganglion cells connect topographically to cortical cells in the visual cortex; in the olfactory bulb, each glomerulus receives innervation from olfactory cells of a particular receptor type (for a review see Luo and Flanagan, 2007); and at the neuromuscular junction each muscle fibre receives innervation from exactly one axon branch (Sanes and Lichtman, 1999). These specific patterns of innervation emerge over the course of development, after much remodelling and refinement of synaptic connections.

In many areas of the developing nervous system, including all three regions mentioned above, axon branches form supernumerary synapses initially, some of which are then eliminated. Although many of these pre- and post-synaptic pairings are eliminated, the ones which are retained will grow forming larger, more intricate, or a larger number of synapses between the cells. Therefore synapses are eliminated but also added during development. This developmental remodelling is thought to allow branches to be selectively eliminated through interactions with each other, resulting in a specific pattern of innervation without the need for each synapse to be specified explicitly. This reduces the amount of genetic code needed and allows for some plasticity in the developing system.

In order to understand the developmental process and to be able to intervene if it goes wrong, it is crucial to understand the factors which affect synaptic remodelling. The neuromuscular system is particularly well suited to studying development due to the accessibility, large size and simplicity of neuromuscular synapses compared with those found in the CNS.

The aim of this thesis is to contribute to the understanding of how intrinsic properties of motor neurons affect synapse formation and synapse elimination.

1.2 The mature neuromuscular system

1.2.1 Gross anatomy of the neuromuscular system

In mature vertebrates, motor neuron cell bodies are located in the spinal cord and are thus part of the CNS. Their axons leave the spinal cord ventrally, through gaps between the vertebrae, bundled together in a spinal nerve. Spinal nerves are mainly part of the PNS, which includes nervous system structures outwith the brain and the spinal cord. Sensory axons join the spinal nerve after leaving the spinal cord dorsally. Thus, every spinal nerve is composed of motor and sensory axons. Axons in the spinal nerves are the longest in the nervous system and extend over distances of the same order of magnitude as the length of the species (metres for humans, centimetres for rats and mice, etc.) to innervate muscles, skin and joints.

Spinal nerves are branched because axons within a nerve diverge to innervate multiple different target structures. However, only a few motor axons branch within the spinal nerve. When this happens, both branches tend to innervate the same target (Lu et al., 2009b).

Once within the target muscle (intramuscularly), motor axons can branch up to hundreds of times to innervate multiple muscle fibres. A motor neuron and all the muscle fibres it innervates constitute a motor unit (MU). The number of muscle fibres in the MU is the motor unit size. Motor neurons innervate muscle fibres by forming a specialised chemical synapse, the neuromuscular junction (NMJ).

1.2.2 Anatomy of the mature neuromuscular junction

Nerves and muscles have been studied since the 18th century when Galvani noticed that frog legs would twitch in response to an electrical stimulus (Ochs, 2004), though our understanding of it has changed a lot since then. In the 1840s, before chemical synapses were understood, Doyere described how the motor nerve terminated when it reached the muscle and did not penetrate the muscle (cited in Hughes et al., 2006). As new staining and visualisation techniques were developed, including gold and silver

staining, various dyes and ultimately electron microscopy in the 1950s, NMJ morphology became better characterised (for a review see Lu and Lichtman, 2007). From these studies we now have very detailed knowledge of the distinctive form of the adult NMJ.

NMJs are primarily described in terms of three cells, the presynaptic terminal, the postsynaptic muscle fibre and the terminal Schwann cell. A fourth type of cell, the 'kranocyte', has also been associated with the NMJ (Court et al., 2008).

Motor axon branches terminate in a structure called the presynaptic terminal. The external morphology and internal constituents of the presynaptic terminal differ from that of the axon leading up to it. It consists of many short branches and is characterised by a high density of mitochondria and acetylcholine (ACh)-containing synaptic vesicles (Sanes and Lichtman, 1999). Presynaptic branches are precisely aligned with depressed regions in the postsynaptic membrane called gutters. Within these gutters the membrane forms regular folds (Marques et al., 2000). Vesicles are released from specific areas of the presynaptic membrane, the active zones, which are directly apposed to the valleys of the junctional folds in the postsynaptic membrane (Sanes and Lichtman, 1999). The postsynaptic membrane has a high density of ACh receptors (AChR) at the peaks of the folds and Na^{+} channels in the valleys of the folds. There is a 50 nm gap between the pre- and post-synaptic membranes where the basal lamina sits. The basal lamina contains acetyl cholinesterase, an enzyme which breaks down ACh released from the presynaptic terminal, and also acts as an anchor to hold the pre- and post-synaptic terminals together. Each presynaptic terminal is capped by a terminal Schwann cell, which is thought to provide trophic support to the terminal (Balice-Gordon, 1996). The NMJ is the largest synapse in the nervous system. The close apposition and complexity of pre- and post-synaptic structures, together with a high quantal content in exocytotic neurotransmitter release, ensures a high fidelity in synaptic transmission so that every presynaptic action potential causes a postsynaptic action potential (see figure 1.1).

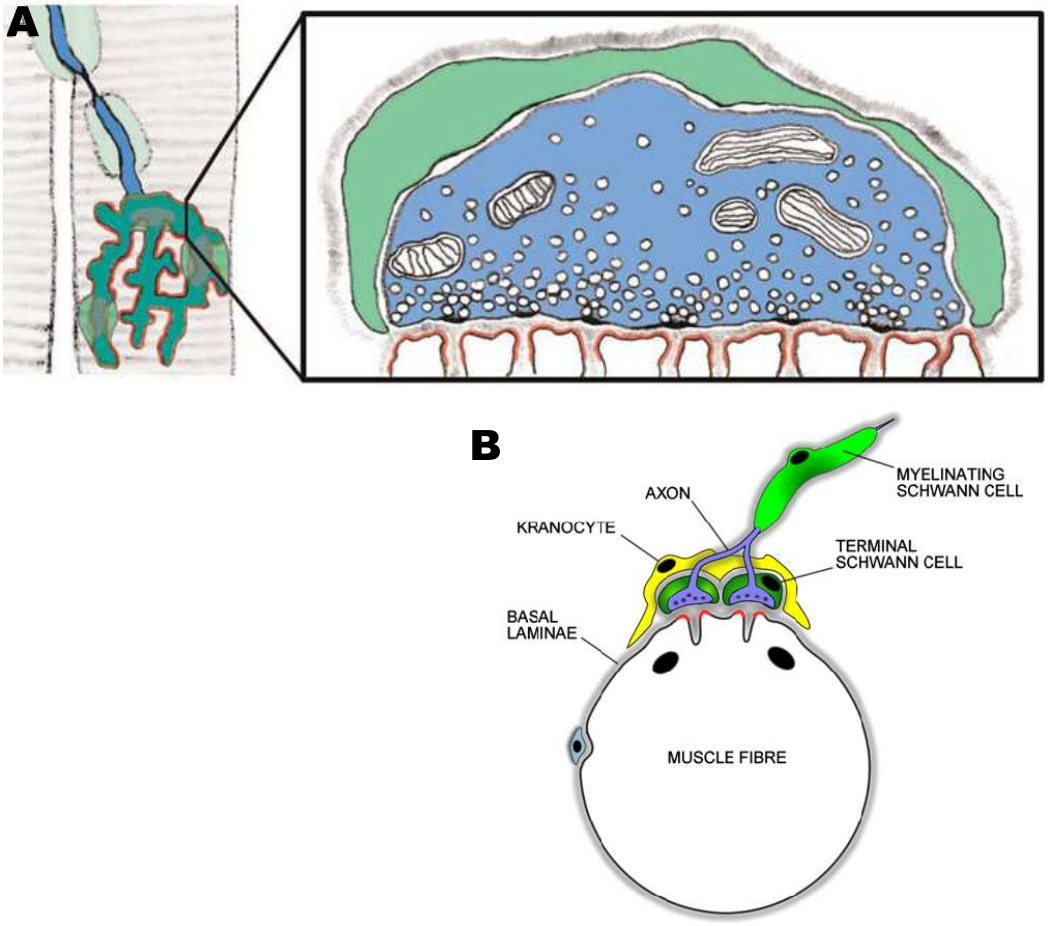

Figure 1.1: *The morphology of the NMJ. A: On the left a blue motor axon branch forms the characteristic pretzel-like synapse (NMJ - dark green) with a muscle fibre (light pink). The axon is myelinated by Schwann cells (light green) and the NMJ is covered by a terminal Schwann cell (green). The figure on the right shows a cross section through the synapse. The terminal Schwann cell (green) is covering the nerve terminal (blue) which contains mitochondria and synaptic vesicles. The junctional folds in the muscle fibre can be seen with AChRs (red) located at the peaks of the folds. In the pre-terminal axon, some of the synaptic vesicles are clustered around the active zones, the sites of release, which are directly across from the troughs of the junctional folds. The thin gray structure between the presynaptic terminal and the postsynaptic endplate is the basal lamina. This figure is from a review about glial cells by Zuo and Bishop (2008). B: NMJ morphology including the associated kranocyte (yellow). This figure is from Court et al. (2008).*

1.2.3 Motor neuron and muscle fibre types

There are two main types of motor neurons: fast and slow. As their name suggests, they differ in axon conduction velocity, but also in firing rate (Jacobson, 1978). These appear to selectively innervate fast and slow muscle fibres in the adult, so that each adult motor unit primarily consists of one type of fibre (Bennett and Pettigrew, 1976; Thompson et al., 1987).

1.3 Development of the neuromuscular system

1.3.1 Development of muscle fibres

Myogenic stem cells originate in the somites of the embryo and migrate to the limb buds, from which the muscles will form (Sanes and Lichtman, 1999). These cells divide to produce myoblasts, which are single-cell precursors to muscle fibres. Myoblasts align and fuse into polynucleated myotubes (Jacobson, 1978). The limb buds are cleaved to form individual muscles (Jansen and Fladby, 1990). Myotubes continue to elongate throughout development by the addition of myoblasts to the ends of the myotube (Bennett and Pettigrew, 1976). Myotubes mature into muscle fibres when the nuclei are displaced to the periphery (Sanes and Lichtman, 1999), though this last stage can only occur in mammals after contact with the motor nerve (Jacobson, 1978). New myotubes and muscle fibres continue to develop throughout the prenatal period and, in some muscles, for a few weeks postnatally (Bennett and Pettigrew, 1974; Betz et al., 1980).

1.3.2 Development of motor neurons

Motor neurons form in the neural tube and migrate to the ventral horn. Very soon after motor neurons arrive in the ventral horn, they extend long thin processes which will become axons and dendrites, collectively termed neurites (Purves and Lichtman, 1985). Motor neuron axons grow out of the ventral roots in a orderly fashion (Jansen and

Fladby, 1990). In the periphery they are joined by axons from sensory neurons and form a nerve bundle. Neurites grow by addition of membrane behind an organelle-dense and highly motile tip, the growth cone, which can sense and react to its environment (Purves and Lichtman, 1985). Growth cones navigate through their environment ensuring that neurites reach their target destination where they will form synapses. All axons in a nerve do not necessarily innervate the same target and therefore they may take different trajectories, causing the nerve to branch. Motor neurons in the rostral spinal cord innervate rostral muscles and similarly, motor neurons in the caudal spinal cord innervate caudal muscles (Jansen and Fladby, 1990)

Spinal nerves grow until axons reach their targets at the limb buds, around embryonic day 12 (E12) and after individual muscles have formed (Jansen and Fladby, 1990). This is followed by a period of synapse formation (see section 1.4). During the period of synapse formation about half of all motor neurons die (Harris and McCaig, 1984), which appears to be the result of insufficient access to a target derived neurotrophic factor (Purves and Lichtman, 1985).

1.3.2.1 Neurotrophin in the development of motor neurons

More than 50 years ago, Hamburger (1952) stated what much research at the time had been pointing to, that developing neurons depend on their targets for survival and growth. Coupled with the discovery of nerve growth factor (NGF) by Rita Levi-Montalcini and Stanley Cohen in 1960 (who jointly won the Nobel prize in 1986 for “their discoveries of growth factors”) (Chao, 2010), this established the hypothesis that target derived molecules contribute to cell survival and growth during development. This led to the idea that developmental cell death may be the result of limited availability of a neurotrophic factor, which neurons compete for, with the ’winners’ becoming established and the ’losers’ undergoing apoptosis. Indeed, there have been numerous studies showing that application of a neurotrophic factor during the critical period in development can rescue neurons that would otherwise have undergone apoptosis. Similarly, ablating target structures increases the prevalence of developmental cell death (reviewed in Oppenheim, 1991).

Since the discovery of NGF, many new molecules that promote the growth or survival of cells have been found, including the neurotrophin family of molecules (NGF, NT-3, NT-4, BDNF) and other trophic molecules (e.g. GDNF, LIF). Motor neurons from different pools within the spinal cord have distinct expression patterns of receptors for these molecules (for a review see Gould and Enomoto, 2009). Thus, contact with the target innervation sites appears to be necessary for the survival of motor neurons.

1.3.3 Development of Schwann cells

Schwann cells are non-neuronal cells that originate from the neural crest. They become associated with motor axons in the somites and are guided by them to their target muscle in the periphery (Mirsky and Jessen, 1996). Whether the Schwann cell will be myelinating or non-myelinating (terminal) is determined later in development (Mirsky and Jessen, 1996). In embryonic development, Schwann cells ensheath multiple different axons. Around the time of birth, the ones that will become myelinating Schwann cells begin to associate with a single axon, starting with larger radius ones (Jessen and Mirsky, 2005). During the first postnatal week, axons start to show signs of myelination extramuscularly, within the nerve. Myelination of the intramuscular portion of the axon seems to mainly occur in the second postnatal week or later (Slater, 1982).

1.4 Synapse formation

Initially, myotubes have AChRs uniformly distributed throughout their membrane, though sometimes they form small clusters. At first, they are contacted by a single pioneer axon (Bennett and Pettigrew, 1974), which induces clustering of the AChRs to the site of contact (Jansen and Fladby, 1990). Traditionally, axons are considered able to contact uninnervated myotubes at any point along the surface, although there is also evidence that some myotubes may contain preferred sites of synaptic contact (Pun et al., 2002; Kummer et al., 2006). Once contact has been made, the myotube becomes refractory to innervation elsewhere along its length, though other motor axons will form synapses within the same synaptic region (Bennett and Pettigrew, 1974).

Amphibian NMJs do not always inhibit synapse formation along the entire length of the muscle fibre, but appear to inhibit it for a certain distance around the NMJ (Bennett and Pettigrew, 1976). Hence, the number of terminals per myotube/muscle fibre increases prenatally up until the time of birth (Bennett and Pettigrew, 1974).

Consequently, at the time of birth there has already been a big reduction in the number of motor neurons, and each muscle fibre is innervated by multiple different axons (I am using the term 'muscle fibre' though I intend this to include muscle fibres and myotubes which are both present in the muscle at this time point). Since each muscle fibre will be innervated by a single axon eventually, this means that motor neurons, at the time of birth, innervate about two to five times as many muscles fibres as they will innervate in the adult.

1.5 Influences on synapse formation

1.5.1 Guidance cues

Apart from a general organisation across muscles, with rostral motor neurons innervating more rostral muscles and caudal motor neurons innervating caudal muscles, there is some evidence for a topographic organisation in the innervation of specific muscles. Moreover, it seems like this topographic specificity already exists embryonically. For example, Laskowski and High (1989) showed that the anterior serratus and diaphragm muscles are both innervated topographically from the earliest stages of synaptic development (E17-E19). Although this pattern of innervation was refined postnatally, its presence at the time when synapses are forming or have just formed suggests a systematic influence on synapse formation. This could be achieved is through the ephrin family of signalling molecules (Feng et al., 2000a). Ephrins and their ligand, Eph molecules, are more commonly known as guidance cues in the development of the retinotectal system (Luo and Flanagan, 2007). However, Feng et al. (2000a) showed that ephrins are expressed in neonatal muscles with a rostral/caudal gradient, with rostral muscles having a higher expression level. Additionally, Chadaram et al. (2007) showed that gradients of ephrin expression occur within a single muscle, in this case

the diaphragm muscle. Ephrins can inhibit neurite outgrowth, and Feng et al. (2000a) showed that rostrally and caudally derived motor neurons differ in the amount of outgrowth they achieve in the presence of ephrin. They also showed that mutant mice that were lacking the gene for a subset of the ephrin molecules, also had disrupted topographic mapping. Therefore, there is good evidence that some synapse formation may be guided by molecular cues. However, not all muscles exhibit topographic specificity. For example, in the lumbrical muscle each motor unit appears to innervate fibres randomly spread throughout the muscle (Betz et al., 1990; Gates and Betz, 1993); likewise in the soleus muscle (Fladby, 1987). It is not clear whether there is a molecular influences on synapse formation in muscles lacking topographic organisation.

1.5.2 Muscle fibre matching

There is some evidence that selective synapse formation occurs between axons and muscles of the same type. Thompson et al. (1987) found that motor units are largely homogeneous at postnatal day 8 (p8), even though synapse elimination is ongoing. However, p8 is already a week into synapse elimination and, therefore, they have not excluded the possibility that this finding is due to selective synapse elimination. In their review of development, Jansen and Fladby (1990) also reported significant homogeneity of muscle fibre types within motor units at p2 and p5 in the mouse soleus muscle, though there appeared to be some refinement between these two times. This makes a stronger case for there being selective innervation during synapse formation, although there also appears to be postnatal refinement. On the other hand, there is also evidence that motor units initially contain a mixture of fast and slow muscle fibres and become homogeneous through selective synapse elimination (Jones et al., 1987). One explanation for the matching is that muscle fibres are converted by motor neurons to be a certain type. While this may account for some of the matching, it is unlikely to account for all of it, since muscle fibre types are determined embryonically and can be determined in the absence of innervation (Thompson et al., 1990).

1.6 Development of synaptic morphology

Immediately after a synapse is formed, the presynaptic terminal is unspecialised and appears as a bulbous enlargement (Sanes and Lichtman, 1999). Pre- and post-synaptic areas are not exactly aligned, which contributes to synaptic transmission being weak (Hall and Sanes, 1993). The postsynaptic cluster of AChRs begins as a uniform plaque-like receptor dense area (Balice-Gordon and Lichtman, 1993). As development proceeds both components become specialised. Presynaptic terminals accumulate synaptic vesicles and active zones begin to appear (Hall and Sanes, 1993). At E17 to E19 in mice, the postsynaptic receptor area is slightly indented and AChRs form discrete clusters within that area. Around the time of birth, the oval postsynaptic site starts to becoming asymmetric and over the first postnatal week the junctional folds begin to form. By the end of the first week some of the endplate region will have developed junctional folds, but parts of it will still be flat. After the first postnatal week, and as junctions start to become mononeuronally innervated, the gutters in the postsynaptic membrane become more prominent (Marques et al., 2000). At the same time, small gaps in the AChR cluster within the junction begin to appear that are not overlaid by an axon (Balice-Gordon and Lichtman, 1993). This transition results in the plaque-like immature endplate transforming into the adult pretzel-like form.

1.7 Synapse elimination

Over the first two to three weeks after birth there is a period of selective synapse elimination (Redfern, 1970; Brown et al., 1976). During this time there is no further motor neuron death, but rather individual axon branches are eliminated, leading to a decrease in each axon's MU size (Brown et al., 1976). At the same time there is rapid growth of the remaining NMJs (Balice-Gordon and Lichtman, 1993). Around the end of the first three postnatal weeks each muscle fibre is innervated by a single axon. Each motor neuron still innervates many muscle fibres, but the MU size has decreased substantially (see figure 1.2; for a timeline of developmental events see figure 1.3).

Polyneuronal innervation (π) at the immature neuromuscular junction was first ob-

served by Tello in 1917, a student of Ramón y Cajal, and again by Boeke in 1932, using silver staining as the method of viewing motor axons (cited in Purves and Lichtman, 1985). However, the gradual progression from poly- to mono-neuronal (μ) innervation by synapse elimination was not appreciated until the study by Redfern (1970). He showed that the endplate potentials (EPPs) in early development were complex; in other words they resulted from the summation of responses to more than one innervating axon. He observed that EPPs became progressively simpler over time, until they were composed of the response to a single unit. He also proposed what we now know to be the case, that this is the consequence of synapse elimination.

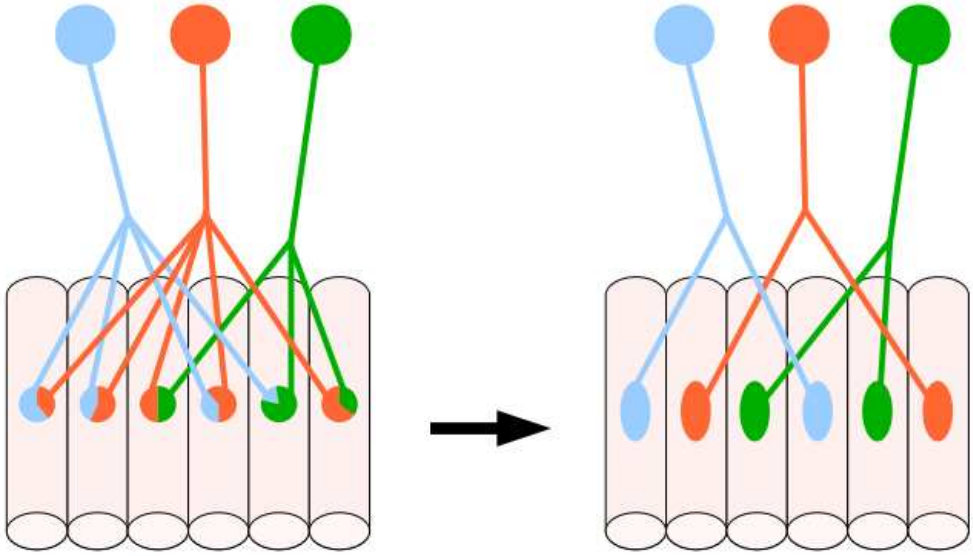

Figure 1.2: *Muscle fibres are polyneuronally innervated at the time of birth but become mononeuronally innervated through selective synapse elimination and axon branch removal over the first three weeks of development.*

1.7.1 Synapse elimination by competition

Synapse elimination is not random, because random elimination of the large number of synapses that occurs during development would lead to many muscle fibres becoming completely denervated (Willshaw, 1981). To the contrary, denervated muscle fibres are not routinely found in developing muscles (Brown et al., 1976). Therefore, axon

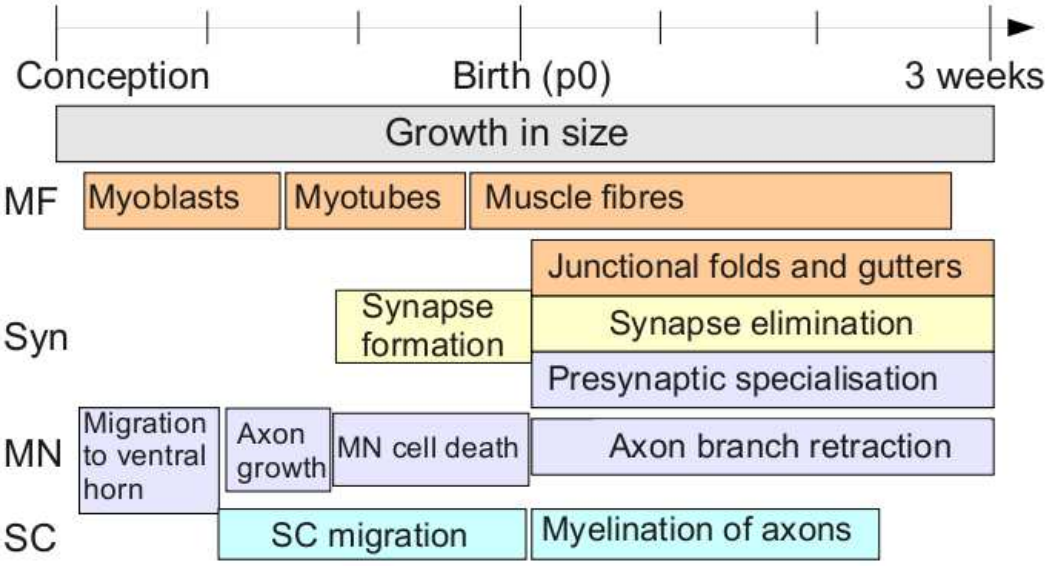

Figure 1.3: *Time line of changes that occur during rodent development. Muscle fibres (MF) develop from myoblasts which fuse to form polynucleated myotubes. After innervation myotube nuclei are displaced to the periphery at which point they are considered muscle fibres (see section 1.3.1). Synapses (Syn) are formed during the second half of the gestation period. Postnatally some synapses are eliminated while the ones which are maintained grow and become specialised pre- and post-synaptically (see sections 1.4-1.7). Motor neurons (MN) migrate to the ventral horn from which axons grow out to innervate muscles. Once contact is made about half of motor neurons die. Surviving motor neurons increase in size while some of their branches and synapses are eliminated (see section 1.3.2). Schwann cells (SC) are guided by motor axons to muscles. They begin to myelinate the nerve around the time of birth, while intramuscular myelination occurs during the first or second postnatal week (see section 1.3.3).*

branches innervating the same muscle fibre must interact in some way to ensure that exactly one remains. Indeed, multiple studies have shown that the presence or absence of other terminals at an endplate influences the fate of an axon. A number of experiments have confirmed that reducing the number of motor neurons innervating a muscle leads to a sustained motor unit size in the remaining motor units. In other words, some synapses which would have been lost during development are retained in the absence of other axons (Brown et al., 1976; Thompson and Jansen, 1977; Betz et al., 1980; Fladby and Jansen, 1987).

Some of these studies have measured the distribution of motor unit sizes in adult animals, from muscles which receive innervation through two separate nerves (AO rat soleus: Thompson & Jansen, 1977; Wistar rat lumbrical: Betz et al., 1980; mouse soleus: Fladby & Jansen 1987). By cutting the major nerve supply to the muscle around the time of birth, when muscles are polyneuronally innervated, they are able to reduce the number of branches converging on each muscle fibre, and in some cases leave a single axon innervating the muscle through the minor nerve supply. In particular, Betz et al. (1980) only examined muscles that remained innervated by a single motor unit after partial denervation. These motor units were allowed to develop in an environment with a reduced number of converging inputs and, as a result, adult motor unit sizes were found to be larger when compared to the control distribution. This phenomenon has been conceptualised as competition between axon branches innervating the same muscle fibre; therefore cutting the major nerve supply in the previously described experiments, has the effect of removing the majority of the competition and allowing more of the remaining axon branches to be retained.

Although the use of the terminology is pervasive, the nature of the competition between developing axons has not been precisely determined (for reviews see Lichtman and Balice-Gordon, 1990; Ribchester and Barry, 1994; van Ooyen, 2005). Van Essen (1982) provided a general definition for competition between axon branches originating from different motor neurons as meaning that *"the probability of survival of any given synapse depends on the presence or absence of other synapses on the same muscle fibre"*. The observation that denervated muscle fibres are not routinely found in developing muscles supports this definition, as it suggests that the probability of sur-

vival becomes close to one in the absence of other branches.

1.7.2 Morphology of synapse elimination

1.7.2.1 Synapse elimination occurs gradually

Despite early evidence that synaptic transmission abruptly stopped in synapses that were eliminated (Rosenthal and Taraskevich, 1977), subsequently, both morphological and physiological studies have provided evidence that synapse elimination proceeds gradually. Balice-Gordon et al. (1993) used spectrally distinct dyes to image two competing inputs at developing mouse sternomastoid NMJs from E17 to p14. In the early stages of development the two inputs occupied approximately equal areas of the NMJ. The absolute area occupied by both the larger and the smaller terminals increased until a few days after birth, at which point the area occupied by the smaller terminal began to decrease in size, while the area occupied by the larger one continued to increase. Despite both terminals growing in early development, the divergence in the proportion of the NMJ occupied by the largest input increases from the earliest postnatal stages, which suggests that the larger input tends to increase in size more rapidly than the smaller one.

In the second part of this study, Balice-Gordon et al. (1993) stained the terminals of competing axons with spectrally distinct markers of vesicle recycling, therefore staining only functional synapses. This part of the experiment was done on the transversus abdominis muscles in developing snakes for technical reasons, though the authors suggest that the results are generalisable to mammals as well. In agreement with the previous results, functional synaptic area was more equal in early development and the size of functional synapses diverged between the two inputs over development. It is interesting that, even when the losing branch occupied a very small portion of the NMJ, this was still functional. This observation led them to conclude that synapse elimination occurs by a gradual elimination of the losing branch's territory and, while this is occurring, the extant territory of the losing branch remains functional.

As well as gradual divergence in the size of the synaptic areas occupied by competing

axons, there is also a gradual divergence in synaptic strength. Colman et al. (1997) calculated that the difference in the quantal content, that is the difference in synaptic strength, between axon terminals at dually innervated synapses in the mouse trapezius muscle, increased as development progressed. This was due both to an absolute increase in the synaptic strength of the stronger axon and an absolute decrease in that of the weaker one. Since quantal content correlates with synaptic area, this difference could reflect a change in the synaptic areas of the two axons. However, Colman et al. (1997) also found a consistent difference in quantal sizes, that is the efficacy of a single vesicle, between the axons.

More evidence that synapse elimination proceeds gradually was provided by Gan and Lichtman (1998) who showed that there is a progressive segregation of the areas occupied by competing terminals at the developing NMJ in mouse sternomastoid muscles. At the time of birth there is a large amount of overlap in the areas occupied by each terminal, but over the first week the overlap decreased. By the second postnatal week the terminals appeared to innervate discreet regions of the endplate. Moreover, this synaptic segregation appeared to be achieved by selective elimination of branches within the terminal which were close to the other axon's territory, leading them to suggest that the signal which instigated synapse elimination acts locally, over short distances.

From these studies a consistent picture emerges: synapse elimination occurs gradually over development. Initially all inputs increase in size, though some perhaps faster than others. However, from the first postnatal week some of the terminals lose synaptic area and synaptic strength, while others continue to gain both. Despite the absolute gain in area for winning synapses, all terminals may lose parts which are near the site of innervation of other axons. This leads to synaptic segregation and, eventually, to the elimination of all but one of the inputs (see figure 1.4). As none of these studies have visualised the same junctions over time, these changes reflect the general trend over development, rather than the time-course of synapse elimination at specific junctions, which could proceed differently.

At the same time as this gradual elimination is occurring, Balice-Gordon and Lichtman (1993) showed that there is a gradual permanent loss of AChR dense areas postsynaptically, which results in the endplate shape becoming more pretzel-like, as mentioned

above. Because the deletion of postsynaptic regions only occurred at π-junctions and the deletion of a postsynaptic region was also associated with the loss of the presynaptic terminal, they concluded that this receptor depletion was related to synapse elimination. In order to determine whether the presynaptic terminals or the postsynaptic receptor dense regions were eliminated first, they repeatedly visualised both pre- and post-synaptic elements in mouse sternomastoid muscles. Postsynaptic depletion of receptors was evident before changes in the presynaptic terminal could be observed. In addition, areas of low receptor density (equivalent to faint receptor staining) always resulted in permanent loss of receptors in that area. Based on these results, they concluded that postsynaptic receptor loss induces the presynaptic terminal to withdraw.

This led to a qualitative model of synapse elimination being proposed by Colman et al. (1997) and laid out more comprehensively in a review by Nguyen and Lichtman (1996). They suggested that muscle fibres mediate the competition between axonal terminals through the distribution of AChRs. AChR density in turn is regulated by activity, so one axon's activity may have an adverse effect of AChR clusters which are not activated by it. Therefore active neurons could induce clusters of AChRs which are not activated by it to dissipate, and removing the postsynaptic support could cause the overlying terminal to withdraw (for a review see Bernstein and Lichtman, 1999). Eventually one of the axons will lose all of its points of contact with the muscle fibre, thus resulting in a single winner. The idea that inactivity of one part of the NMJ can cause the dispersal of AChRs is supported by a study by Balice-Gordon and Lichtman (1994). They showed that focally blocking a portion of the receptors at the adult NMJ led to the elimination of the blocked receptors and the withdrawal of the boutons of the presynaptic terminal opposite those receptors. However, this only occurred when the majority of receptors remained active. Blocking a larger portion, or the entire synapse, did not lead to any loss of AChRs. Therefore it is doubtful that this could be the main driving force of synapse elimination since, in the neonate, competing terminals can occupy approximately equal areas of the terminal, and the smaller terminal is capable of eliminating the larger one (discussed below).

Indeed, Walsh and Lichtman (2003) showed that synapse elimination could occur by one presynaptic terminal taking over the territory previously occupied by another ter-

minal without the loss of postsynaptic receptors. They repeatedly imaged mouse sternomastoid NMJs in p8 to p11 transgenic mice which expressed two spectrally distinct fluorescent proteins in their motor neurons. This allowed them to distinguish the synaptic territories of the different axons innervating an NMJ. They showed examples of NMJs where the postsynaptic morphology remained constant during the transition from π to μ. As the 'losing' axon withdrew its presynaptic terminals, newly vacated postsynaptic regions were innervated by the 'winning' axon. This does not falsify previous findings, that elimination can begin postsynaptically, but it does show that synaptic takeover is the most common occurrence. Walsh and Lichtman (2003) suggested that synaptic takeover could rescue postsynaptic receptors which would otherwise be lost, although they did not quantify the density of postsynaptic receptors at the points of synaptic takeover. Another interesting observation they made, is that synapse elimination did not always occur monotonically. Occasionally the axon with the smaller synaptic area in the first viewing ultimately innervated the entire junction. Similarly the larger synapse at the first viewing sometimes lost territory, and then regained it, to become the sole innervator of that particular NMJ, a phenomenon they called 'flip flop'.

Thus, although the early hypothesis that synapse elimination occurs without takeover, but rather by depletion of postsynaptic receptors, seems to provide a neat explanation for why the shape of endplates changes during development, Walsh and Lichtman (2003) unequivocally showed that synaptic takeover does occur and observed little (if any) synapse elimination associated with loss of postsynaptic receptors.

1.7.2.2 Eliminated branches retract but also shed cellular debris

Once a terminal has been completely eliminated from a synapse, the axon branch which was supporting it must also be removed. Most of the evidence suggests that eliminated branches retract back toward the parent axon, rather than undergoing Wallerian degeneration (but see Rosenthal and Taraskevich, 1977). This hypothesis was initially suggested by Korneliussen and Jansen (1976), who examined hundreds of electron microscopy (EM) images of developing NMJs, but did not find compelling evidence of additional degeneration beyond the small amount of degeneration which

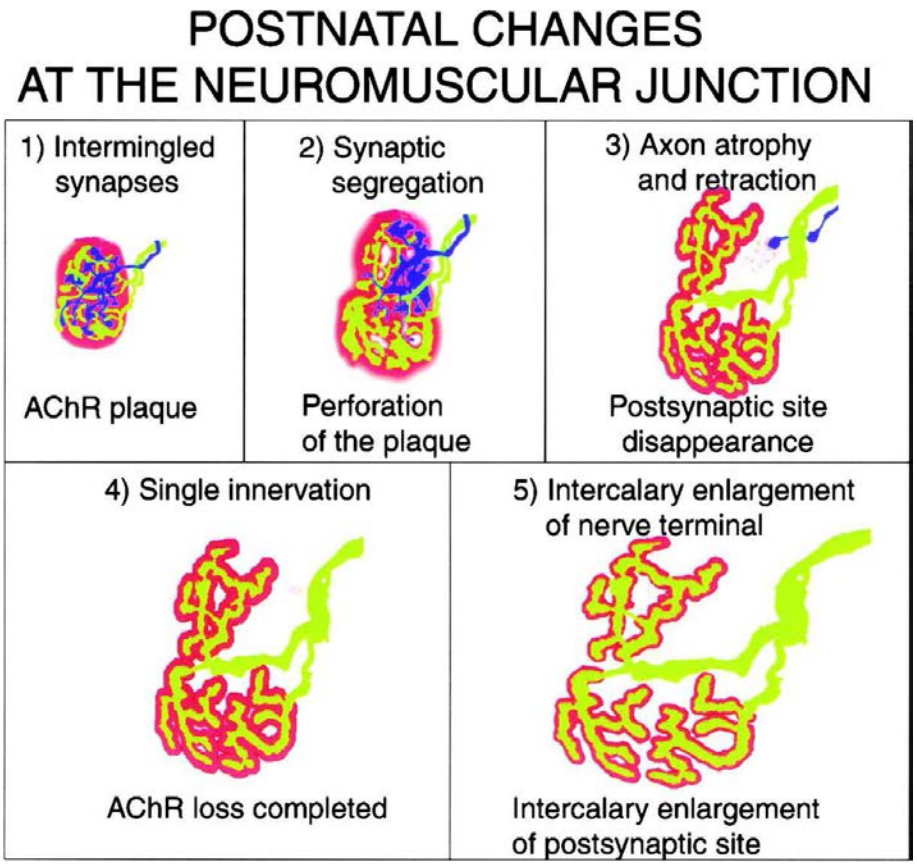

Figure 1.4: *Illustration of the postnatal change in NMJ morphology. At birth the synaptic territories of different axon branches are intermingled (1). Over the first postnatal week they become segregated, while at the same time gaps begin to appear in the postsynaptic membrane (2). By the end of the second postnatal week all but one of the synapses are eliminated. Newly eliminated synapses form retraction bulbs at their tip and appear to retract back toward the parent axon, while the last terminal which remains innervating a junction increases its territory to innervate the whole junction (3). Once single innervation is achieved the shape of the junction remains relatively stable, although there is a overall growth in size (4 and 5). This image is from a review of developmental synapse elimination by Lichtman and Colman (2000).*

is also observed in control muscles and is probably due to tissue preparation methods. Further morphological investigation of developing muscles revealed often occurrences of an intramuscular branch with a bulbous ending, termed a 'retraction bulb' (Riley, 1977; O'Brien et al., 1978). These were interpreted as being branches in the process of retraction and as they were observed both close to the endplates and close to the intramuscular branch point, Riley (1977) concluded that synapse elimination occurs asynchronously.

Subsequent studies have strengthened these conclusions by providing additional evidence. Keller-Peck et al. (2001b) have studied the innervation of entire motor units during the first two postnatal weeks and observed that axon branches of the same motor unit can occupy drastically different proportions of the synaptic area on the muscle fibre they are contacting. This suggests that at the same time as some synapses become established, others are at various stages in the competition or in the process of being eliminated. They also observed that there was no spatial bias relating to the size of the synapse, although there was a correlation between the diameter of the axon branch and the area occupied by its synapse. Specifically, thicker branches were connected to synapses which innervated a larger proportion of the endplate. Therefore they concluded that synapse elimination happens asynchronously; it is driven by local interactions at the NMJ and axon branches become thinner before they are eliminated.

Furthermore, Walsh and Lichtman (2003) imaged synapse elimination *in vivo* and have shown that branches which used to form a synapse with an endplate, but have been eliminated, do form a 'retraction bulb' which appears to be retracting back to the parent axon.

However, Bishop et al. (2004) proposed that axon branches may appear to be retracting because they are degenerating from the tip towards the branch point. Specifically, they show evidence of axonal debris being left behind and engulfed by Schwann cells. Therefore, it appears that, whilst some material may be retained within the motor neuron after synapse elimination, at least some is also shed from the motor neuron and cleared by surrounding glia. Moreover Song et al. (2008) demonstrated that retraction bulbs were associated with lysosomal activity. Lysosomes are acidic organelles which contribute to the degradation of cellular debris.

In summary, axon branches which are in the process of being eliminated become thin, end in a retraction bulb and appear to withdraw back into the parent axon, but actually leave behind cellular debris which is cleared away by surrounding glia. In addition, different branches belonging to the same neuron are eliminated asynchronously.

1.7.3 Influence of activity on synaptic competition

Activity has an important influence on both the time-course and the outcome of synapse elimination.

Increased activity seems to accelerate the process of synapse elimination, whereas blocking activity seems to decrease or suspend the withdrawal of excess synapses.

In one of the first experiments to show that activity might have an effect on the time-course, Benoit and Changeux (1975) found that cutting the tendon in four day old rats, and thus suppressing the mechanical activity in the soleus muscle, caused a delay in the elimination of poly-neuronal innervation. By three weeks, however, most of the muscle fibres were mono-neuronally innervated.

Similarly, Thompson et al. (1979) found that blocking activity in motor axons with tetrodotoxin (TTX) for two to four days slightly, but significantly, increased the number of π-junctions compared to controls, i.e. it delayed synapse elimination. Surprisingly, they also found that blocking activity for longer seemed to lead to an actual increase in the number of π-junctions. This could be explained if the activity block caused synapses that were sub-threshold, or in the process of withdrawing, to be strengthened again.

Brown et al. (1981) blocked neurotransmitter release with botulinum toxin in developing rat soleus muscle and also observed an initial decrease in the number of π-junctions, followed by an increase back to the level that existed at the time of the block.

Duxson (1982) blocked the activity in 10 day old rat soleus muscle fibres for two days by blocking AChRs with α-bungarotoxin (α-BTX) . She assessed the rate of synapse elimination by observing synaptic structures using EM (in contrast to the physiolog-

ical methods used by most other studies). She found that the number of innervating terminals (terminals were defined as vesicle-containing structures) had not decreased in the blocked muscle, in contrast to control. She also observed that the size of terminals seemed to have increased in the blocked muscle, which suggests that the terminals were still growing, despite the fact that none of them were being eliminated.

Greensmith and Vrbová (1991) also blocked activity in the muscle fibre by applying silicon rubber strips containing α-BTX to neonatal rat soleus muscle. These strips, applied at birth, caused complete block for about 24 hours, after which time synaptic function gradually returned over the next nine days. Blocking activity at birth appeared to increase the rate of synapse elimination for the first week, compared with controls. Subsequently, the amount of polyneuronal innervation remained stable up until p12 in the previously blocked muscles, which had now partially recovered, while rapidly decreasing in control muscles. From p12, synapse elimination continued in previously blocked muscles and there was an observable difference between these muscles and control muscles, even at p22. They also found that blocking at a later time point (p10), at which point their method caused a partial block, decreased the rate of synapse elimination, as evident from an increased number of π-junctions two day later. These results are hard to interpret because the activity level at each time point is unclear and the relationship between the activity level at individual synapses and the elimination which occurred at those synapses was not directly investigated.

On the flip-side, O'Brien et al. (1977) found that stimulating motor axons increased the rate of synapse elimination. Normally 90% of endplates in neonatal (p8-p10) rat soleus muscle are π-junctions. After two to three days of stimulating motor axons (at 8Hz for four hours daily), only 50% of the endplates received multiple inputs at the same developmental stage. They also hypothesised that this may occur through activity stimulating release of proteolytic enzymes. The enzymes would 'eat away' at nerve terminals until only one was left. They showed that muscles that were stimulated with ACh released proteolytic enzymes. Follow up work has shown that blocking proteases delays synapse elimination (e.g. O'Brien et al., 1984; Zoubine et al., 1996).

Thompson (1983) performed a similar experiment, but he stimulated the soleus muscle directly (which also stimulates the axons) over three to four days in seven day old rats.

He also found that stimulating the muscle increased the rate of elimination, but the pattern of muscle stimulation was important. Stimulating with high frequency bursts (100Hz every 100 seconds) caused a 50% decrease in the number of π-junctions at p10-p11 compared with controls. In contrast, stimulating continuously at 1Hz did not affect the rate of elimination, even though the total number of stimuli received were the same in both groups.

Taken together, these studies demonstrate that activity regulates the time-course of synapse elimination. There have also been studies looking at the effect of activity on the outcome of the competition between motor axons. It seems that neuromuscular synapses, like synapses in the central nervous system, follow Hebb's postulate (Stent, 1973); when the pre- and post-synaptic cells are active coincidentally, that particular synapse becomes strengthened.

Ridge and Betz (1984) used the 4th deep lumbrical (4DL) muscle, which receives innervation from both the lateral plantar (LPN) and sural (SN) nerves. They found that when they stimulated the SN, MUs in the SN were larger than expected. On the other hand, when they stimulated the LPN, MUs in the SN were smaller than expected. This indicates that neurons receiving stimulation were winning the competition at more endplates, which caused them to end up with larger motor units. This was the first suggestion that more active motor units have a competitive advantage over less active units in development.

However, Callaway et al. (1987) found unexpectedly that inactive neurons had an advantage over active neurons. They used the soleus muscle in neonatal rabbits, which also receives innervation from two spinal nerves. They blocked activity in a minority of motor units, ensuring that almost all muscle fibres still had an active input, and they found that inactive motor units were larger than in the control. This did not seem to be due to inactive synapses being eliminated more slowly, but rather to an actual advantage of inactive motor neurons when competing against active ones. This result is inconsistent with the Hebbian notion of coincident activity strengthening a synapse and non-coincident activity weakening it. The conclusions of this paper are equivocal because the method used (recording twitch tensions) has been shown to be an unreliable measure of motor unit size (Ribchester, 1988).

Another line of evidence for a Hebbian mechanism comes from studies looking at differences between natural (asynchronous) and synchronous activity.

Buffelli et al. (2002) observed that motor neuron activity naturally becomes uncorrelated during development. They looked at the activity of motor neurons innervating the tibialis anterior and soleus muscles in rats throughout early development. They found that there was a switch from synchronous to asynchronous activity, the time-course of which correlated well with the time-course of synapse elimination, lending further evidence that the asynchrony was driving the elimination process.

Personius et al. (2007) observed that connexin 40, which is a protein involved in the expression of gap junctions in motor neurons, decreases during development. They hypothesised that this led to a switch from synchronous to asynchronous activity, which could be the driving force behind synapse elimination over the same period. They found that connexin 40 knockout mice had fewer gap-junctions between motor neurons, and activity was less correlated than in controls. Synapse elimination also proceeded at a faster rate in the knockout mice, presumably because of the increased amount of asynchronous activity.

The majority of results are in agreement with a Hebbian mechanism of synapse elimination. More active axons have the competitive advantage and the more activity there is, the faster the rate of elimination. It also seems to be important to have asynchronous activity for elimination to occur.

This result creates a paradox because in adult animals smaller motor neurons are recruited first and therefore are more active than larger motor neurons (Henneman, 1985), but in development, it seems that more active motor neurons have a competitive advantage and therefore should end up innervating more fibres. It is not clear how to resolve this paradox, though one suggestion is discussed in section 1.7.7.

1.7.4 Influence of neurotrophic factors on competition

The idea that neonatal synapse elimination occurs as the result of axon branches competing for a postsynaptic neurotrophic resource is conceptually similar to that of whole

motor neurons competing for neurotrophic factors during embryonic development as described in section 1.3.2.1. However, mechanistically it may be substantially different, since these factors would be having a much more local effect in the latter case. Developmental synapse elimination occurs after developmental cell death has been completed; by this point neurons have become established and the trophic substances in question must only be affecting survival of specific branches.

There is experimental evidence that adult synapses are reliant for survival on a postsynaptic resource. McCann et al. (2007) showed that blocking protein synthesis in an adult muscle fibre leads to the terminal innervating that muscle fibre to begin retracting within 12 hours. At the same time neighbouring synapses on different muscle fibres remain intact. They argued that the morphology of the withdrawing axon branch resembles developmental synapse elimination, rather than axon degeneration, and speculated that lack of access to a postsynaptic resource may also be contributing to developmental synapse elimination. Although the first morphological changes in axons begin within 12 hours of protein synthesis inhibition, terminal Schwann cells remain in place for up to 36 hours.

Since the discovery of NGF there have been dozens of substances which evidently provide trophic support to neurons, and many of these have been tested on developing neuromuscular junctions. The overall picture which emerges from these studies seems to be that increasing the amount of trophic factors during development can delay, but not ultimately prevent, synapse elimination. Similarly, reducing the amount of trophic factor can accelerate synapse elimination, though it does not cause widespread denervation.

For example, Kwon et al. (1995) and Kwon and Gurney (1996) showed that subcutaneous administration of leukemia inhibitory factor (LIF), ciliary neurotrophic factor (CNTF), oncostatin M (OSM), brain derived neurotrophic factor (BDNF), neurotrophin-3 (NT-3) or neurotrophin-4 (NT-4) to the tensor fascia latae muscle (in the hind leg) delays synapse elimination (though only by one to two days in some cases) but does not ultimately prevent it. In contrast, fibroblast growth factor (FGF), insulin-like growth factor (IGF) and NGF did not have any effect on the rate of synapse elimination. Their studies focused mainly on LIF and BDNF, since these molecules are thought

to be expressed during normal development *in vivo*. Additionally they found that LIF knockout mice reached a state of mononeuronal innervation faster than control mice. Interestingly, they observed that the increase in π-junctions in BDNF treated muscles was largely due to non-functional synapses. Similarly, an increase in non-functional synapses was observed by Gillingwater et al. (2004) for Myo-GDNF treated re-innervated muscle fibres.

More evidence for trophic factors affecting developmental synapse elimination comes from English (1995), who examined the effect of injecting bFGF and CNTF into the lateral gastrocnemius muscle, and found both to delay synapse elimination. However, he only measured the effect up to p14, so it is not possible to tell if these factors are delaying or halting synapse elimination. Why English (1995) found bFGF to affect synapse elimination but Kwon et al. (1995) did not is unclear, but could be the result of using different muscles, different dosages or different species (Kwon et al. (1995) studied mice and English (1995) studied rats).

Jordan (1996) also examined the effect of CNTF on extensor digitorum longus (EDL) and levator auris longus (LAL) muscles. She found that CNTF treated muscles had an increased number of π-junctions compared with controls of the same age, as long as it was applied before the transition from poly- to mono-neuronal innervation was complete. She concluded that CNTF does have an effect on synapse elimination and is not acting by inducing sprouting, as it does in the adult.

Nguyen et al. (1998) found that transgenic mice in which muscle fibres over-expressed glial cell line-derived neurotrophic factor (GDNF) had an increased number of synapses on muscle fibres in the sternomastoid muscle of neonates. Also the number of synapses was correlated with the amount of GDNF over-expression, leading them to conclude that GDNF regulates the number of synapses on muscle fibres. Synapse elimination still occurred, but the time at which synapses were mononeuronally innervated was delayed in GDNF over-expressing animals.

Likewise, Keller-Peck et al. (2001a) examined the effect of GDNF injections on synapse elimination in the sternomastoid and spinotrapezious muscles of neonatal mice. They found that polyneuronal innervation persisted in mice that had been administered GDNF for up to 40 days after birth (the longest time period they tested). They also found evi-

dence of synapse elimination, but no decrease in the level of polyneuronal innervation between 30 and 40 days. This led them to suggest that synapse formation and elimination are in equilibrium at this point, and that, in contrast to CNTF, the effect is due to GDNF encouraging motor axons to branch more than they would normally, rather than affecting synapse elimination. Interestingly, if administration began after p10, GDNF did not have an effect on the motor axons, even though the appropriate receptors were still in place.

All these studies suggest that there are external substances that may regulate synapse survival, however the mechanisms by which they work and whether they exist in limiting quantities during development is far from clear.

One suggestion is that trophic factors promote activity, which in turn influences synapse elimination as mentioned in section 1.7.3. Ribchester et al. (1998) found that application of GDNF to neonatal nerve-muscle preparations increased the frequency of miniature endplate potentials (mEPPs) although not their amplitude. In contrast, none of the other factors tested (BDNF, NT-3, NT-4, LIF, IGF-1 and IGF-2) had a significant effect on mEPP frequency.

Another possible mechanism of action of trophic factors on synaptic competition was suggested by Yang et al. (2009). They showed that BDNF can have an opposing influence on nerve terminals depending on if it is in its precursor form (proBDNF) or mature form (mBDNF). Using Xenopus motor neuron cultures they showed that proBDNF is released from muscle fibres upon activation and that it acts on the p75 receptor to cause synaptic depression and axon withdrawal. However, if it is transformed into mBDNF, they suggest it could cause synaptic potentiation. This hypothesis again involves activity in the mechanism of action.

1.7.5 Other influences on synaptic competition

Kasthuri and Lichtman (2003) provide evidence that neuronal identity is important in competition. They used mice which expressed yellow fluorescent protein (YFP) and cyan fluorescent protein (CFP) in a subset of their neurons. This meant that in some muscles there were both a YFP and a CFP axon, and they could directly visualise

the motor units using fluorescence microscopy. Their evidence suggests that when two motor neurons competed at multiple muscle fibres, the outcome of the competition was the same at each site, i.e. the same neuron won at every site. Additionally, the competition seemed to follow the same time-course at every endplate that was co-innervated by the same pair of neurons. Therefore, they proposed that a hierarchy existed between neurons and that some neurons had a competitive advantage over others. Interestingly, they found some evidence that smaller motor units have the advantage. However, this experiment does not exclude the possibility that activity is the factor which determines a neuron's place in the hierarchy.

A further influence on competition might be synaptic efficacy. Buffelli et al. (2003) created genetically modified mice in which the production of choline acetyltransferase (ChAT; an enzyme which is necessary for the production of ACh at the NMJ) could be blocked. Previous studies have shown that no neurotransmission occurs in mice which lack this enzyme, although Buffelli et al. did not measure synaptic transmission in their experimental paradigm. They blocked production of ChAT in a subset of neurons at p0 and examined muscles at p11. They showed that the blocked neurons, which presumably had weaker synapses, were at a disadvantage when competing with the control neurons. This led them to conclude that synaptic efficacy is an important factor in determining the outcome of synapse elimination. In this study axons presumably were still normally active, but unable to depolarise muscle fibres.

1.7.6 Synapse elimination in the absence of competition

While synapse elimination has been documented many times to occur at π-junctions, it is not clear whether intrinsic withdrawal occurs; that is non-competitive or programmed synapse elimination. If some elimination was independent of the presence of competitors, then synapse elimination from μ-junctions could occur. Different studies have concluded both that intrinsic withdrawal does occur (Thompson and Jansen, 1977; Fladby and Jansen, 1987) and does not occur (Betz et al., 1980). This question is addressed is the first results chapter (3) and the literature relating to this issue is discussed there in more detail.

1.7.7 Models of synapse elimination

When investigating a complicated phenomenon like synapse elimination, it is hard for any one experiment or observation to provide a complete explanation. Multiple experiments and observations can help researchers to synthesise a theory which explains the data in the best possible way. Even simple theories can have unexpected or counter-intuitive logical conclusions. It is not possible to explore the logical conclusions of a theory unless the components of the theory have been precisely defined. Computational modelling of a phenomenon necessarily forces the investigator to be explicit about the components of their theory. The consequences of this theory can then be investigated by studying the model. The model could provide predictions about the system which have not already been investigated experimentally and therefore instigate new research. The model could also disagree with the observed data, in which case the component of the theory which needs to be changed can be investigated to resolve this. Therefore, computational modelling can aid the scientific understanding in a principled way. Models of synapse elimination have focused on three different types of competition: axons could compete by having a direct negative effect on their competitors ('interference' competition), they could compete for a resource ('consumptive competition') or they could compete for space.

Willshaw (1981) implemented a model of synapse elimination based on the hypothesis in O'Brien et al. (1978) that enzymes could be released at the endplate region in response to a signal (e.g. activity), which 'eat away' at the terminals innervating that endplate. O'Brien et al. (1978) hypothesised that the signal was ACh release, which is thought to increase the proteolytic activity at the NMJ. Since ACh is released by activity, this suggests a mechanism by which activity can influence synapse elimination. Willshaw proposed that each synapse has a survival strength proportional to its size and also releases a digestive enzyme proportionally to its size which acts on all synapses at the endplate, including itself. The total survival strength of a neuron is constant. Therefore, larger synapses have an advantage over smaller synapses at the endplate, but smaller motor units have an advantage over larger motor units overall. This model leads to a steady state of single innervation and can account for the decrease in variability of MU sizes over development, since smaller motor units are at

a competitive advantage. It is not clear though, how this model would account for intrinsic withdrawal and the effect of neural activity was not considered.

A similar idea was implemented by Barber and Lichtman (1999). They proposed a model where active terminals have a direct negative effect on inactive terminals. The underlying assumptions of this model are that terminals have a negative effect on competitor terminals in proportion to the amount of neurotransmitter they release, which in turn is proportional to the size of the synapse and the level of activity. However, the total amount of neurotransmitter available for release within a neuron is limited, so frequent release of neurotransmitter has an adverse effect on synapse size. This has the effect of providing a short term advantage to large active synapses, but a long term disadvantage to the motor neuron as a whole, which could provide an explanation for the seemingly conflicting results that more active neurons seems to have a competitive advantage, yet eventually in the adult, less active neurons tend to have larger motor units (Henneman, 1985). One drawback of this model is that competitive elimination only occurs when axons are active asynchronously, although experimental evidence shows that inactive axons are also capable of competing (Costanzo et al., 2000, and see section 1.11). Moreover, although there is a limited presynaptic resource in this model, elimination is the result of a negative effect of other axons. Therefore, it is not clear that it can account for 'intrinsic withdrawal'. Although it cannot account for all the experimental findings, this model does make some interesting predictions. Because activity influences, not only the outcome, but also the rate of competition, one prediction is that more active axons will win or lose their competitions earlier than less active axons. In addition, this is the only model which demonstrates the possibility for the 'flip flop' phenomenon described by Walsh and Lichtman (2003), whereby the larger of two competing synapses may lose area to become smaller and then regain it to become the eventual winner.

Others have supposed that axons compete for a limited resource. Gouzé et al. (1983) created a model of synaptic stabilisation during development. They assumed there is a postsynaptic resource μ which diffuses from the muscle fibre to the presynaptic terminals to form some stabilising factor s. The postsynaptic resource μ is suggested to be a substance from the NGF family. Once a terminal captures enough μ to form

a critical amount of $s > S$, that terminal becomes stabilised. In this model, the other terminals do not withdraw explicitly, but once the amount of s that they have becomes very small it is assumed that they are not stabilised. This model also incorporates the effect of activity by assuming that the rate of conversion of μ to s is proportional to the activity rate of the neuron. However, there is no limit in the number of synapses belonging to one motor neuron that can be stabilised, so, in the absence of competition, no elimination would occur. In other words, this model could not account for 'intrinsic withdrawal'. Furthermore, the threshold has to be set differently depending on the number of axons and muscle fibres, so the end-state of mononeuronal innervation is not very robust.

The idea of competing for a resource was extended by Bennett and Robinson (1989), who formulated a model of synapse elimination based on both a pre- and a post-synaptic resource. They assumed that each presynaptic neuron has a certain quantity of receptors, which become distributed to all the terminal axon branches of the neuron. Postsynaptic muscle fibres release a neurotrophic factor, which can bind to the presynaptic receptors. The more receptors there are on each axon, the more of this factor it captures and thus the larger the terminal grows. This means that motor neurons with fewer terminals, and therefore smaller MU sizes, would have more receptors per axon terminal and so they would have a competitive advantage, assuming each motor neuron started with the same amount of presynaptic resource. For synapse elimination to occur in this model the initial conditions must be such that each motor neuron innervates a different number of muscle fibres. Although not a large problem, assuming initial innervation is random, it can be overcome by introducing a shallow affinity gradient. If the receptors in some neurons have a greater affinity to bind the trophic factor than others, then a 'symmetry breaking' initial configuration is not necessary. This idea is interesting in light of the neuronal hierarchies that Kasthuri and Lichtman (2003) claim exist. The rate of synapse formation is proportional to the amounts of free postsynaptic resource, the number of unbound receptors and the size of the existing synaptic area raised to a power an. If synaptic area has no influence, an can be set to zero. In order for competition to occur, synapse size has to positively reinforce synapse formation. Bennett and Robinson (1989) suggest that synapses could exert an electrotonic force on molecules, attracting them to the synapse, so that the bigger synapses will grow

disproportionately more. Increasing *an* will increase the rate of elimination. They claim that manipulating *an* captures the effect of activity on synapse elimination, since blocking activity slows or halts elimination whereas increasing activity increases the rate of elimination. Synapses degenerate only proportionally to their existing size.

Rasmussen and Willshaw (1993) modified Bennett and Robinson (1989)'s model by giving a dynamical explanation which explicitly describes how the distribution of the presynaptic resource between the soma and the terminals of the motor neuron arises. They showed that the so called Dual Constraint Model could replicate many of the experimental results; for example that intrinsic withdrawal was found to occur in the soleus but not in the rat lumbrical muscle. They also showed that mononeuronal innervation is a stable state of the model. In subsequent years, other papers have re-analysed this model to account for further phenomena. For example van Ooyen and Willshaw (1999) showed by stability analysis that polyneuronal innervation could also be a stable state of this model, which could account for the finding of stable π-junctions after activity block in regenerating muscles (Barry and Ribchester, 1995, see section 1.11).

Jeanprêtre et al. (1996) conceptualised a model of competition for neurotrophic factor which is assumed to be released postsynaptically. They assume there is a uniform concentration of neurotrophic factor, which is taken up into terminals in proportion to the number of neurotrophic receptors they have. This factor is continually produced and degraded and receptors are bound and unbound stochastically with certain association and dissociation constants. They analysed their model mathematically, rather than computationally, and they showed that only one axon branch will survive, and that the surviving branch will be the one with lowest threshold for the concentration of trophic factor which yields no growth. Two other states supported by the model are: denervation as a consequence of removal of neurotrophic factor, and stable polyneuronal innervation in the case where more than one axon have the same threshold value. Another interesting feature of the model is that increasing the amount of trophic factor does not increase the number of surviving branches, despite the fact that branches are competing for a limited resource. A weakness of this model is that it does not take into account how growth of one branch affects other sibling branches from the same neuron.

van Ooyen and Willshaw (1999) created one of the most biologically detailed models of synapse maturation and elimination. In their scheme, a neurotrophic factor is released from a postsynaptic target at a certain rate and is degraded. Presynaptic boutons have receptors for this factor and the receptors are inserted as a function of the neurotrophic factor uptake rate (they tested three different functions). The kinetic constants were set to match what is known about NGF and its receptor. This model can support both mono- and poly-neuronal innervation as stable states, but was only tested in the case where there was a single postsynaptic target. When there are multiple postsynaptic targets, polyneuronal innervation can often be the steady-state, depending on the ratio of the motor unit sizes of competing neurons (Groen, 2008).

Deppmann et al. (2008) created a model of the developmental elimination of sympathetic neurons. This system is slightly different from the neuromuscular junction because, in this case, each neuron has a single arbour with no presynaptic resource limitations. It has similarities as well, especially from a biological point of view where the pathways might be the same. Their model incorporates both competition for neurotrophic factor and direct negative influences between neurons. In order for competition to occur between neurons, the levels of TrkA in the neuron have to be NGF dependent, as does the duration of the trophic effect. This was confirmed experimentally and had also been predicted by the van Ooyen and Willshaw (1999) model. Competition is sped up by introducing direct negative effects of neurons on other neurons.

Van Essen et al. (1990) implemented a model of developmental synapse elimination where synapses compete for space. Each terminal has a bias function, which dictates how likely it is to sprout or retract. Terminals both sprout and retract in a probabilistic manner, although if a terminal tried to sprout into an occupied space it is blocked. This competition continues until there is a single terminal left. Although, during development, terminal growth does seem to be dynamic, it is not clear whether this is the case at adult mononeuronally innervated junctions, which do not change much morphologically over time (see section 1.9.1) .

Nowik (2009) analysed competition from a game theoretic point of view in order to try and reconcile the seemingly conflicting results that more active neurons have a competitive advantage at the synapse, though less active neurons seems to win more

endplates overall. The model is rather abstract and assumes that each neuron has an equal probability of winning. However, when a competition has been won the neuron has to divert resources to that endplate, which lessens its competitive advantage. It also assumes that more active neurons complete their competition first and less active ones complete their competition later on. This is one of the consequences of the Barber and Lichtman (1999) model but has not been shown experimentally. A consequence of these assumption is that more active neurons win earlier, but win less overall. This idea is interesting, though not grounded very soundly in biology. Although it could be the case, it is not clear why 'winning' a synapse would require more resources than innervating a polyneuronally innervated synapse.

Modelling studies have provided some interesting insights into the question of intrinsic withdrawal (discussed more in chapter 3). Specifically the dual-constraint (Bennett and Robinson, 1989; Rasmussen and Willshaw, 1993) models have demonstrated that intrinsic withdrawal, if it does occur, is not necessarily due to genetically programmed synapse elimintion but rather could occur because of a limit on the intrinsic capacity of the motor neuron. In addition, they have demonstrated that intrinsic withdrawal does not necessarily occur as a separate mechanism to between-unit competition, but rather the limited intrinsic resource can work to influence the outcome of the competition. Therefore, it may only be observed in situations where between-unit competition has been removed. At present it is not clear if intrinsic withdrawal does occur. Supposing it does, it is also unclear if its occurence is due to limited neuronal resources, therefore, modelling studies could potentially provide useful predictions for testing this hypothesis.

1.8 Summary of developmental events

In summary, there is a complicated series of developmental events which result in the mature functioning NMJ. They start with the birth and migration of motor neurons and myoblasts, continue with the maturation and first interactions between these cells, including synapse formation and conclude after a few weeks of synaptic remodelling, during which time the majority of synapses are eliminated (figure 1.3). Synaptic mod-

ification during development has been studied extensively, yet many questions still remain about what determines the fate of individual synapses.

1.9 Changes in NMJ morphology in adulthood

1.9.1 Changes during unperturbed maturation

Once the developmental period of synaptic remodelling is complete, NMJ morphology remains relatively stable through adulthood. However, there is some evidence (discussed below) for a small amount of plasticity after mononeuronal innervation has been established. There are some additions or deletions of receptor dense areas, small modifications of the presynaptic terminal by the addition of pre-terminal branches and an overall increase in size. This does not preclude the possibility that there is a small amount of synapse formation and elimination ongoing during adulthood. A number of studies have quantified aspects of NMJ morphology at different ages, including some which have repeatedly visualised the same NMJ at different points in time.

1.9.1.1 Change in size

The biggest observable change that occurs in NMJ morphology, after mononeuronal innervation is established, is a three to four fold increase in size (Balice-Gordon and Lichtman, 1990; Wærhaug, 1992). The increase in terminal size is highly correlated with the increase in nose to rump length, muscle length and muscle fibre perimeter (Balice-Gordon and Lichtman, 1990; Ip, 1974). In addition, Balice-Gordon and Lichtman (1990) showed that NMJs grow predominantly by intercalary addition of AChRs, in other words new AChRs are added in between existing ones. They found that physically stretching the muscle caused elongation of both pre- and post-synaptic elements and accordingly they suggested that the postsynaptic endplate region grows as a consequence of the muscle fibre growth, while the presynaptic terminal grows as a consequence of its adherence to the postsynaptic membrane.

The rate of increase is approximately linear and fairly rapid, from very shortly after

NMJs have been formed embryonically until about four to six months of age (Balice-Gordon and Lichtman, 1990; Balice-Gordon et al., 1993; Courtney and Steinbach, 1981). From about six months, and for the remainder of the lifetime of the animal (maximum about 36 months), the growth rate tails off, though it is not clear if NMJ size remains constant from beyond six months (Andonian and Fahim, 1989), or if it continues to grow at a slower rate (Balice-Gordon and Lichtman, 1990). Andonian and Fahim (1989) found that the nerve terminal area of mouse EDL and soleus muscle remained flat from four to thirty-two months of age. In contrast, Balice-Gordon and Lichtman (1990) showed a continuous increase in NMJ size in mouse sternomastoid muscles over the first 16 months, with the added advantage that they were repeatedly visualising the same NMJs over time. Wærhaug (1992) measured NMJ size over the first 30 months in rat EDL, soleus and diaphragm muscles and found an increase over the whole period in EDL and soleus but only up to six months in the diaphragm.

These data suggest that NMJs rapidly increase in size over the first four to six months of life of the animal. There may be differences between muscles in the rate of growth, but there appear to be instances where NMJs continue to increase in size throughout the lifetime of the animal and this increase in size is correlated with the growth of the muscle fibres, muscles and animal in general.

1.9.1.2 Presynaptic changes

There is evidence for minor remodelling of the presynaptic terminal as the animal grows older. Specifically the number of pre-terminal branches increases with age. An early study showing plasticity in normal adult motor axons was undertaken by Barker and Ip (1966). The imaged cat, rabbit and rat motor axons and found evidence of sprouting and pre-terminal branching in adults. These finding were extended by Tuffery (1971). He observed that in young adult cats the ratio of terminals with a single branch to terminals with two branches in the soleus muscle was 99:1, whereas in six year old cats this ratio was 60:36 (the rest of the terminals having more than two branches). He also found that the increase in complexity did not arise from new endplates being formed on the muscle fibre, but rather what he called rejuvenation, where a sprout from the last node of the terminal axon branch innervated the same endplate

as the main branch. Courtney and Steinbach (1981) also observed the same pattern in rat sternomastoid muscle: the number of NMJs innervated by more than one terminal branch increased up until 13 months of age after which there was no further increase up to 30 months of age. The same result was recorded by Tweedle and Stephens (1981) who observed rat soleus, adductor longus, rectus femoris and plantaris muscles up to two and a half months of age and found an increase in NMJs with multiple pre-terminal branches from six weeks onwards. Evidence of this remodelling in action comes from Cardasis and Padykula (1981) who examined three to five month-old rat soleus muscle, and observed frequent instances of postsynaptic junctional folds which were not associated with a pre-terminal axon. Wernig et al. (1984) also observed the presence of empty postsynaptic gutters in the synaptic region of adult mouse soleus muscles. These observations are consistent with the interpretation that there was ongoing synaptic remodelling and the presynaptic terminal had withdrawn from that portion of the muscle fibre, though it could likely be replaced. In the same study, Wernig et al. (1984) found evidence for an increase in complexity of the presynaptic terminal up to 11 months, by the addition of terminal branches (these are branches within the terminal region as opposed to branches originating from the final node of the innervating axon). This result suggests that there is some postsynaptic remodelling to match the presynaptic remodelling, though they did not image the distribution of postsynaptic receptors, nor did they find evidence of new postsynaptic regions (i.e. regions with a presynaptic terminal which had not developed mature gutters and junctional folds). Postsynaptic changes will be discussed more in the next section. Fahim et al. (1983) found no increase in the number of pre-terminal branches between seven and twenty-nine month old mouse EDL muscles, though they did find an increase in the number of terminal branches, as well as a corresponding increase in the number of primary postsynaptic cleft branches. They interpret the lack of additional pre-terminal branches between seven and twenty-nine months as consistent with earlier studies, which demonstrate that the number of pre-terminal branches only increases for roughly the first year of life. In contrast to these studies, Lichtman et al. (1987) report no significant changes to the structure of individual terminals which were followed over periods of up to six months.

Therefore there appears to be some addition of presynaptic terminal branches as the

animal grows, though this process seems to be restricted to the early adult life of the animal.

1.9.1.3 Postsynaptic changes

In addition to some presynaptic plasticity, there is also evidence of minor postsynaptic plasticity at the NMJ. As described in the previous section, Fahim et al. (1983) found an increase in the number of primary cleft branches in older compared to younger adult mouse EDL NMJs. This means that the main postsynaptic gutter had more side-branches in older animals. Similarly Wigston (1989) made repeated visualisation of adult mouse soleus muscles separated by up to six months. He found that, although NMJ structure remained largely stable, 44% of the endplates he viewed had small additions or deletions of postsynaptic receptor areas on the second viewing. He also stained the nerve terminals after the second viewing and confirmed that newly added regions were associated with presynaptic innervation. In addition the nerve terminal was removed from deleted regions, thus suggesting that both pre- and post-synaptic remodelling were occurring.

In contrast Balice-Gordon and Lichtman (1990) repeatedly visualised mouse sternomastoid NMJs up to a year old and found only 4% of them had any additions or deletions of postsynaptic area. Moreover, they found that pre-and postsynaptic structures were always closely apposed, although they did find that one third of presynaptic terminals underwent an addition or a deletion over a time period of 18 months.

The cause of the discrepancy between these studies is not clear, but they all agree that the postsynaptic structure remains largely stable with possible minor alterations. How common these alterations are is unclear. Fahim et al. (1983) suggest the reason for terminal re-organisation with ageing is to compensate for reduced synaptic strength per area.

1.9.2 Plasticity after paralysis or injury

Although NMJ morphology remains relatively stable with only minor changes under normal conditions, a large amount of plasticity can occur in response to injury or paralysis. Motor axons sprout in response to paralysis or injury of neighbouring NMJs, but they can also regenerate in response to injury of their own axon.

1.9.2.1 Paralysis

In this context, sprouts are axon branches which have been newly formed and grow from the nodes of Ranvier of existing branches (nodal sprouts) or from the presynaptic terminal (terminal branches). New branches are normally very thin, but they may be short or long and they may terminate in a synapse or not. As discussed previously, the increase in pre-terminal branches with age is due to newly formed sprouts, which originate at the last node of Ranvier near a junction and innervate a portion of that same junction. However, sprouting has been shown to be up-regulated in response to paralysis (Duchen and Strich, 1968; Meunier, 2002) and partial denervation.

Paralysing the muscle with botulinum toxin (colloquially known as Botox) induces synaptic terminals to sprout (Duchen and Strich, 1968) and chronic stimulation after paralysis can suppress sprouting (Ironton et al., 1978). Botulinum toxin causes paralysis by acting presynaptically to inhibit transmitter release (Meunier, 2002). Other paralysing agents (e.g. tetrodotoxin) also have the same effect, though interestingly, paralysis only seems to induce terminal sprouts (Ironton et al., 1978). Paralysis as an assay for inducing terminal sprouting is robust and has been used routinely in order to investigate various aspects of sprouting (for example Wright and Son, 2007, used botulinum toxin to show that transgenic neurons lacking ciliary neurotrophic factor could indeed sprout, contrary to what was previously concluded).

1.9.2.2 Injury

Sprouting is also a response to denervation. In the adult, when some of the endplates in the muscle become vacant, the remaining intact motor axons can produce nodal and

terminal sprouts, which re-innervate the denervated junctions. One of the ways this can be achieved is by partially denervating the muscle, in other words injuring some of the axons which innervate a specific muscle while leaving other ones intact. When muscles are partially denervated, intact motor neurons produce sprouts to innervate the denervated endplates and can increase their motor unit size by up to five-fold (Brown and Ironton, 1978). Thompson and Jansen (1977) suggest there is a cap on the number of muscle fibres that an adult motor neuron can innervate based on their data showing a linear increase between the total number of innervated muscle fibres and the number of intact motor axons. Each additional intact motor axon appeared to contribute an extra 550 innervated muscle fibres in the rat soleus muscle. A motor unit size of 550 is approximately four times larger than the average motor unit size in unoperated muscles. Terminal Schwann cells are very important for re-establishing innervation and have been shown to extend processes in response to denervation of the NMJ they are associated with. These processes can form bridges to innervated endplates and guide sprouts to the denervated muscle fibres (Son and Thompson, 1995a). Kranocytes may also be involved in regeneration as they show morphological changes very soon after denervation and before any noticeable difference in the morphology of terminal Schwann cells (Court et al., 2008). However, the exact contribution of kranocytes is unclear. There is also some evidence that there is a difference in the sprouting response of fast and slow muscles. Fast muscles (composed predominantly of fast muscle fibre types) have relatively more nodal sprouts compared with slow muscles which have more terminal sprouts (Brown et al., 1980).

Interestingly, neonatal motor units do not appear to have the same capacity for sprouting in response to partial denervation (Thompson and Jansen, 1977; Betz et al., 1980; Lubischer and Thompson, 1999). This could be related to the fact that terminal Schwann cells undergo apoptosis at denervated neonatal endplates (Trachtenberg and Thompson, 1996; Lubischer and Thompson, 1999) as opposed to the facilitatory role they take on in the adult.

1.9.3 Plasticity during regeneration

The second major remodelling event that can occur in adult muscles is degeneration of motor axons after damage and regeneration of damaged motor axons. When motor axons are damaged, the part of the axon distal to the injury undergoes Wallerian degeneration within 24 hours (Beirowski et al., 2004). This leads to denervation of the muscle fibres innervated by that axon. The proximal tip of the axon then regrows and can re-innervate muscle fibres at the pre-existing endplate sites (Nguyen et al., 2002). During regeneration, axons grow along pre-existing paths (Nguyen et al., 2002) and are also guided to the old endplate region by terminal Schwann cells (Son and Thompson, 1995b).

Regeneration resembles development in that there is a period of transitory polyneuronal innervation when axons first form synapses, followed by competitive elimination, which results in most synapses becoming mononeuronally innervated. Polyneuronal innervation during regeneration was observed by Boeke in 1916 (cited in Ribchester and Barry, 1994) and first shown physiologically by McArdle (1975). McArdle recorded from EDL muscle fibres at regular intervals after nerve crush and showed that the incidence of polyneuronal innervation, as indicated by recording complex EPPs, peaked at 18 days post-crush with 31% of endplates having complex EPPs and then decreased again, so by 60 days only 3% of endplates showed this evidence of polyneuronal innervation. A similar time-course was shown in rat soleus muscle by Benoit and Changeux (1978), also through intracellular recordings of EPPs. The peak incidence of polyneuronal innervation in soleus muscle occurred around three weeks after the nerve was crushed, although at this time only about 20% of muscle fibres had π-junctions.

Presumably the mechanism of synapse elimination in development and regeneration are the same (for more discussion of this see sections 1.10 and 1.7.1).

1.10 Comparison of synapse formation between development and regeneration

Despite the similarity in synapse elimination, there are important differences in synapse formation between development and regeneration.

First, following nerve injury, motor axons degenerate but the pathways they followed remain intact for some time. Therefore, regenerating axons can follow the same pathways as axons did previously. Nguyen et al. (2002) found that in some cases the mechanical guidance from non-neuronal tubes can be so influential that regenerating axons reoccupied the same precise pathways that occurred before the injury. During development, axons do not have supportive infrastructure in place to guide them to their targets and, in fact, Schwann cells tend to be guided by axons, rather than the other way around (Sanes and Lichtman, 1999).

Second, the synaptic machinery at the endplate is preserved after the axon undergoes Wallerian degeneration and regenerating axons preferentially form synapses at the pre-existing endplates. In development motor axons induce endplate formation (Jansen and Fladby, 1990), or at least synaptic specialisations develop concurrently pre- and post-synaptically.

Third, neonatal motor units have been shown to have gap junctions connecting them so their activity pattern is synchronous during synapse formation (Personius et al., 2007). Although gap junctions are also present on injured axons, it is not clear if the extent of coupling is functionally equivalent between development and regeneration (Chang and Balice-Gordon, 2000).

Fourth, the number of π-junctions at any one time during regeneration appears to be less than in development ($<$50% of junctions during regeneration compared to 100% each innervated by two to five axon branches in development). This could be the result of synapse formation and elimination happening concurrently, rather than consecutively, during regeneration. Therefore, the overall amount of synapse formation may not differ, but the incidence at any one time does.

Fifth, in regeneration, guidance cues may be lost, reduced or expressed differently.

Feng et al. (2000a), for example, showed that ephrin was undetectable on intact adult muscle fibres and, while levels were up-regulated after denervation, they were not as high as the levels found in the neonate. Indeed Laskowski and Sanes (1988) showed that re-innervated adult muscle fibres are not as topographically innervated as control muscle fibres, though it is not clear if this is due to a difference in the pattern of synapse formation or less selective synapse elimination. There could also be other molecular differences in neonate versus adult muscles which are important for synapse formation.

There may be other differences due to the larger size of the muscle, the larger distance between the motor neuron cell body and its terminals, or some change in the properties of motor neurons.

1.11 Comparison of synapse elimination between development and regeneration

Synapse elimination of regenerating motor axons is thought to occur by the same mechanisms that influence developmental synapse elimination. The effect of activity has been studied in regenerating axons and it appears that synapse elimination in the adults is also driven by Hebbian rules.

Ribchester and Taxt (1983) were the first to test the effect of differential activity on synapse elimination. They used the 4th deep lumbrical muscle for their experiments, which receives dual innervation from the lateral plantar and the sural nerves, as mentioned previously. They took advantage of this dual innervation to block activity only in the LPN. This resulted in active SN axons competing with inactive LPN axons. They found that after blocking the LPN, MU size in the SN was larger than in the control and MU size in the LPN was smaller. However, because a substantial amount of the muscle was blocked, some blocked muscle fibres may have become hypotrophic, while some active ones became hypertrophic, which could have skewed the results. But other techniques used in this study corroborated the result that active neurons have a competitive advantage over inactive neurons.

Similarly, Ribchester and Taxt (1984) showed that more active neurons have an ad-

vantage over less active neurons. They used the 4DL preparation in adults again and they crushed the SN. This resulted in the LPN axons sprouting to completely innervate the muscle. After about 20 days SN axons had grown into the muscle and started to compete with the established LPN synapses. On average SN axons took over 2.5% of the synapses. However, when activity in LPN was blocked they took over 6.5%. When the LPN was actually cut, then SN motor axons innervated about 30% of the muscle. These differences show that inactive synapses are still more competitive than degenerating synapses, but less competitive than active synapses.

Busetto et al. (2000) found that when natural (asynchronous) activity was replaced by synchronous activity, fewer synapses were eliminated over the same amount of time. This was done by transplanting the fibular nerve so that it grew into the soleus muscle. When the fibular axons reached the muscle, soleus axons were cut and the fibular nerve innervated the muscle. Natural activity was blocked with TTX and the nerve was stimulated below the block with frequencies that ranged between 15-80Hz. They found that synchronous activity imposed on nerve block had the same effect as just the block on its own. However, synchronous activity imposed on natural (asynchronous) activity had the same effect as natural activity on its own. Therefore the presence of activity was not sufficient for synapse elimination to proceed at a normal rate, rather it was important that some activity was asynchronous. This seems to conflict with previous results (O'Brien et al., 1977; Thompson, 1983) which found that increasing activity by stimulation increased the rate of synapse elimination. Busetto et al. suggest that this discrepancy may be due to using adult muscles during re-innervation rather than neonatal muscles. However, another difference is that they were investigating synapse elimination of a transplanted nerve. Based on these results Busetto et al. (2000) concluded that asynchronous activity is what drives elimination.

More recently Favero et al. (2006) confirmed these results in experiments investigating synapse elimination following regeneration of a crushed nerve into the soleus muscle of adult rats. There was a delay in synapse elimination in muscles where synchronous activity was imposed on nerve block. Thus, it appears that it is asynchronous activity specifically which is driving synapse elimination.

However, activity is not a necessary prerequisite for competition. Inactive synapses can

still compete and displace other inactive synapses. Ribchester (1993) and Costanzo et al. (2000) showed that regenerating inactive axons displaced more established inactive axons than in controls, where both regenerating and established synapses had normal levels of activity. Costanzo et al. (2000) suggest that regenerating axons may gain an advantage when activity is blocked because this may stimulate the muscle to produce growth factors, and regenerating axons may respond better to growth factors than established ones.

Moreover, activity is not sufficient for competition to proceed. Barry and Ribchester (1995) showed that in the 4th deep lumbrical muscle, polyneuronal innervation was preserved for some time by activity block, and remained stable after activity resumed for at least eight weeks. Therefore, while activity still seems to influence synapse elimination in regenerating axons, as it does in development, it is not necessary or sufficient.

Synapse elimination in regeneration may have some differences compared to development but the sequence of events appears similar. Since regenerating motor axons are larger and easier to work with regeneration has proved to be a useful model for studying synapse elimination.

1.12 Outline of the thesis

The aim of my studies was to examine influences on synaptic modification that are intrinsic to the neuron. In this introduction I have outlined many studies which have investigated the external influences on the fate of synapses during synapse formation and elimination in development, for example the activity of other neurons, molecular cues, trophic substances and fibre-type mis-matches. However, there could be properties of the motor neuron itself which influence which synapses are formed and which are maintained. I investigate how sibling branches, that is branches belonging to the same parent motor neuron, interact with each other during development to influence the pattern of innervation that emerges.

In chapter 3, I present an experiment which re-investigates synapse elimination in

the absence of competition. The most important finding is direct evidence for both competition and intrinsic withdrawal influencing motor unit development in mouse 4th deep lumbrical muscle. Moreover, it appears that only large motor units lose synapses in the absence of competition and I show that these results are consistent with the hypothesis that synapse elimination can occur as a result of the strain put on the neuron because of the natural growth of the animal.

In chapter 4, I investigate whether synapses from the same neuron are made randomly and independently of each other. Assuming that is the case, there should be frequent instances of within unit convergence on the same endplate. I show that this does not happen as frequently as would be expected in development and therefore axon branches belonging to the same neuron may influence where each makes a synapse. I do show some instances where within-unit convergence has occurred, more commonly so in regenerating motor axons. I further show that although this is found at early stages of regeneration and development it is not found in unoperated adults and appears to decrease at later stages of regeneration, suggesting axon branches from the same neuron can eliminate each other.

Although the experiments described in chapters 3 and 4 have provided strong support for the interaction of sibling branches in the formation and elimination of connections, the results are not 100% conclusive. For that, a better technique for visualising motor units would be needed. In Chapter 5, I therefore investigate a method for imaging neonatal motor units at higher resolution than confocal microscopy is able, in order to tackle the connectomic challenge of determining the innervation pattern and motor unit sizes in neonates. While I show that this method does improve on the resolution offered by a confocal microscope, it still is not enough to resolve fine neonatal axons in all instances.

Chapter 2

Methods

2.1 Animals

All animal procedures were carried out in accordance with UK Home Office regulations. Thy1-YFP16/BL6 and thy1-YFPH/BL6 mice were originally obtained from Jackson Labs (Bar Harbour, Maine) and used to establish in house breeding colonies.

These mice are genetically modified to express yellow fluorescent protein (YFP) driven by the modified thy1.2 gene promoter (Caroni, 1997; Feng et al., 2000b). YFP is expressed in the cytoplasm of neuronal cells and freely diffuses throughout the entire cell structure. It is a variant of green fluorescent protein (GFP), which was first purified from the jellyfish Aequorea victoria (GFP has been such an important development in biological chemistry that the 2008 Nobel prize in chemistry was awarded to Osamu Shimomura, Martin Chalfie and Roger Y. Tsien ”for the discovery and development of green fluorescent protein”).

In the thy1.2-YFP16 strain, expression begins embryonically (Feng et al., 2000b) and 100% of motor neurons express YFP. In contrast in the thy1.2-YFPH strain an apparent random subset (5%) of motor neurons express fluorescent protein, and the age at which fluorescent protein is visible in motor neurons varies, but is mainly post-natal (Keller-Peck et al., 2001b).

2.2 Surgery

2.2.1 Adult Surgery

All surgical instruments (Fine Science Tools) were sterilised using a bead steriliser (Fine Science Tools). Adult animals were placed in an induction chamber (sealed plexi-glass box) and exposed to either Halothane (2-5% in 1:1 O_2/N_2O; Merial Animal Health Ltd) or Isofluorane (2-5% in O_2) until deeply anaesthetised. This was confirmed by noting slowness in breathing and absence of the pinch reflex.

Hair on the inside of the ankle was then trimmed with small scissors to expose the skin. Animals were placed under a dissecting microscope (Zeiss) and anaesthetic administration was continued using a Fluovac system (International Market Supply) at 2-4% anaesthetic. A small incision was made on the medial side above the ankle, and the tibial and sural nerves were exposed by blunt dissection.

For nerve cuts, a 1mm section of the nerve was removed using watchmaker's No 5 forceps and surgical scissors. Nerve crush was achieved by a single application of constant pressure to the nerve with a pair of No 3 forceps for 5-10 seconds.

After the cut or crush, the wound was sutured using 7/0 mersilk thread (Ethicon). In most cases only a single suture was required. The procedure was performed bilaterally in all instances.

After the procedure, animals were removed from the anaesthetic mouthpiece and returned to their cages to recover. Animals were monitored until the effect of the anaesthetic had worn off, as indicated by their level of activity.

2.2.2 Neonate Surgery

Mouse pups (up to p5) were anaesthetised by chilling in ice for 5-10 minutes, until they did not exhibit vital signs (i.e. breathing and heartbeat). The moribund pups were placed under a dissecting microscope and a small incision was made above the ankle, as in adults. The tibial nerve was exposed by blunt dissection and approximately 1mm

was removed. The wound was sutured using 8/0 silk thread (Ethicon). This procedure was performed bilaterally. Afterwards, the pups were warmed to physiological temperature and vital signs quickly returned. The animals were then returned to their cage.

2.3 Sacrifice

All animals were sacrificed by a Schedule 1 method, either by stunning and cervical dislocation or by overdose of anaesthetic and cervical dislocation. Pups were sacrificed by cervical dislocation or by overdose of anaesthetic.

2.4 Tissue Preparation

2.4.1 Dissection

2.4.1.1 Lumbrical Muscle Dissection

Immediately after sacrificing the animal, both legs were cut at the thigh and the skin was removed. Legs were placed in oxygenated mammalian physiological solution (MPS) containing 120 mM NaCl; 5 mM KCl; 2 mM $CaCl_2$; 1 mM $MgCl_2$;0.4 mM NaH_2PO_4 23.8 mM $NaHCO_3$ and 5.6 mM D-glucose (chemicals purchased from VWR International Ltd). For dissection, legs were placed in a Sylgard 184 (Dow Corning) coated petri dish with the plantar surface facing upward and secured in place using 0.1-0.2mm minutien pins (Fine Science Tools).

In adults, lumbrical muscles were removed still attached to the tendon and pinned into a separate petri dish for fixing and staining, before further dissection of the muscles from the tendon and mounting the muscles on glass slides.

In neonates the tendons were not always fully formed and, specifically, the tendon supplying the 5th toe was often poorly formed. Therefore in neonates the lumbrical muscles were exposed by removing the flexor digitorum brevis muscle and overlying

tissue. Muscles were then fixed and stained before the 4th deep lumbrical muscle was dissected from the foot and mounted on a slide.

2.4.1.2 LAL Dissection

For LAL dissections both neonate and adult animals were sacrificed by an overdose of anaesthetic and decapitated. This was done in order to ensure the LAL muscle, which is behind the ear, was not damaged before the dissection. A small incision was made between the eyes from which the skin was carefully cut down the midline of the head and around the ears. Then, while holding up the ear, the connective tissue underneath was cut away on both sides until the LAL attached to the ears could be removed and pinned into a Sylgard coated dish containing MPS solution, for fixing and staining. After fixing, the LAL was further dissected and mounted on a slide.

2.4.2 Fixation

Tissue was fixed in 4% paraformaldehyde (PFA; Fisher Scientific) in 1% phosphate buffered saline (PBS; containing 137 mM NaCl, 2.76 mM KCl, 8.1 mM Na_2HPO_4 and 1.47 mM KH_2PO_4; chemicals from VWR) for 15-30 minutes on a rocking platform. After fixing, tissue was washed in at least 3 changes of PBS for 10 minutes each time.

2.4.3 Staining

All staining was done on a rocking platform.

2.4.3.1 TRITC-α-BTX

ACh receptors at the synapse were stained using 5μg/ml tetramethyl rhodamine isothiocyanate conjugated α-bungarotoxin (TRITC-α-BTX,Molecular Probes or Biotium, Inc.) in MPS or in PFA for 10-20 minutes, followed by at least 3 washes in MPS or PBS.

2.4.3.2 Anti-Neurofilament staining

A standard immunostaining protocol was followed. Samples were fixed and stained with TRITC-α-BTX before incubation with permeabilising solution consisting of 4% bovine serum albumin (Sigma) and 0.5% Triton-X (Sigma) in PBS for 30 minutes at room temperature. Then, samples were incubated with 1:300-1:1000 by volume of the primary antibody (mouse anti-neurofilament; $2H_3$; Hybridoma Bank) in blocking solution overnight at room temperature, given 2x10 minute washes in PBS and then incubated in 1:1000 by volume secondary antibody (polyclonal rabbit anti-mouse-FITC, Dako) in PBS for 2-4 hours at room temperature. Finally, samples were washed in PBS at least 3 times for at least 10 minutes.

2.4.3.3 Anti-GFP staining

Anti-GFP staining follows the same protocol as above except the primary antibody was used at 1:1000 and was rabbit anti-GFP (Millipore) and the secondary was swine anti-rabbit-FITC (Dako) or anti-rabbit-488 (Jackson Labs).

2.4.4 Mounting Tissue on Slides

Whole muscles were placed on glass slides (VWR) and sealed under a glass coverslip (VWR) with either 2.5% 1,4-diazabicyclo [2,2,2] octane (DABCO) in glycerol or Vectashield (Vector Labs). Some tissue was flattened between two magnets to reduce the imaging depth necessary.

2.5 Data Collection

The methodology used throughout this thesis is imaging of experimental specimens and quantification or observation of the images. In a typical light microscope light from a source is defocused with the condenser (which is a lens) in order to uniformly illuminate the sample which sits on a stage. The light passes through the sample and

is collected by the objective lens. The light then passes through the tube to reach the eyepiece or camera. Both the objective lens and the eyepiece lens (which are more commonly a collection of multiple lenses) magnify the image.

2.5.1 Fluorescence Microscopy

Fluorescence has been a big step forward for imaging, be it fluorescence expressed endogenously by genetically modified mice or fluorescent probes attached to structures through immunolabelling. Fluorescent molecules have a special property that they absorb and emit energy from a defined range of wavelengths of light. The maximum emission is normally at a longer wavelength (lower energy) than the excitation optimum wavelength. This means that they can be illuminated with a certain wavelength, the return path of which is blocked by a dichroic mirror so no reflected light is seen, but the shifted (emission) wavelength is allowed to pass. When these molecules are attached to the structure of interest, this can greatly increase the contrast between it and the background. The shift in the wavelength is called the Stokes shift and is caused by electrons being excited by the illuminating wavelength to a higher energy state. As they relax back to their ground state they only release part of the energy they absorbed in the form of light, which means the emitted wavelength of light is of lower energy than the absorbed wavelength. This means that only emitted light is visible, therefore only the structures labelled with the fluorescent protein are visible on a dark background. This improves the contrast of the image.

The principle of fluorescent microscopy is exactly the same as a normal light microscope with the exception of a carefully placed filter which will block out the reflected light and let the fluorescent light pass. Also illumination is by a narrow range of wavelengths rather than white light.

An Olympus BX50WI microscope with Olympus 10x 0.3 NA, 20x 0.5 NA and 40x 0.85 NA air objectives and illuminated by a mercury lamp was used in order to examine fluorescent samples in the first instance. It was also used to select muscles with single fluorescent axons where that was necessary and to count the number of endplates in muscles. YFP and FITC were visualised using Olympus filter blocks with 460-490

nm excitation filter, 505nm dichroic mirror and 515nm barrier filter and TRITC was visualised with a 520-550 nm Excitation filter, 565nm dichroic mirror and 580 nm barrier filter.

2.5.2 Confocal Microscopy

There are two major differences between confocal microscopy and light microscopy. Firstly the illumination light is focused to a point rather than defocused to uniformly illuminate the plane. Each diffraction limited spot is illuminated in turn and the returning light is gathered through a confocal pinhole so that only the light from the in-focus plane is gathered. The presence of a pinhole for light collection is the second difference. Since each spot is illuminated serially the image is not collected all at once, but rather it is built up by scanning along the specimen. For this reason, confocal microscopy is also called laser scanning microscopy. Again, in the case of fluorescence filters are used to separate only the wavelengths of interest.

Three confocal microscopes were used to acquire images in this thesis. A Biorad Radiance 2000 attached to a Nikon microscope with 10x 0.3 NA air and 40x 1.3 NA oil objectives was used with Lasersharp 2000 software. A Zeiss axiovert 510 LSM and Zeiss Pascal LSM with 10x 0.3 NA air and 20x 0.8 NA and 63x 1.4 NA oil objectives were used with Zeiss software. YFP and FITC were excited with an Argon laser at 488 nm emission and emitted light was collected around the 510 nm wavelength. TRITC was excited using a Helium Neon (HeNe) laser exciting at 543 nm and emitted light was collected around 590 nm.

2.5.3 Counting

In order to find the number of endplates present in a muscles they were viewed under the fluorescence microscope and the number of endplates was counted three times. The average of the three counts was taken to be the number of endplates in that muscle. In some instances endplates were counted from confocal images. The number of axons was determined either by viewing the muscle through the fluorescence microscope or,

in ambiguous cases, by using images taken on the confocal microscope. Quantifying the samples blind was not possible because there were such large differences between different types of muscle (e.g. neonatal, adult, adult with neonatal partial denervation) that it would have been obvious by looking at the muscles which group they belonged too. However, I did not anticipate that this would affect the results because the quantifications were relatively unambiguous (e.g. counting the innervated endplates, total endplates, etc.).

2.5.4 Measuring lengths/widths

Measurements of axon branch lengths were done on 3D confocal stacks in ImageJ (Rasband, 2009, available from:http://rsbweb.nih.gov/ij/) or Fiji ('Fiji Is Just ImageJ' pre-packaged with image processing software, http://pacific.mpi-cbg.de) using the Simple Neurite Tracer plugin developed by Mark Longair. Diameter measurements were done by using the line tool in ImageJ to measure the width of the axon at two locations near the endplate in a 2D slice and using the average of those measurements.

2.6 Data Analysis

Image processing, including creating montages from multiple image tiles and altering the colour levels to enhance signal brightness in images was done in Fiji, Adobe Photoshop and Gimp (GNU Image Manipulation Program, http://www.gimp.org/). Alignments were done using Reconstruct (Fiala, 2005). All statistical analysis was performed using R (R, 2005, available from:http://www.r-project.org/) and SPSS. Graphs were made in R and in Matlab (R2008b, Mathworks). All modelling was done in Matlab.

Chapter 3

Results: Intrinsic Withdrawal and Competition

3.1 Introduction

It is well established that the presence of multiple axons converging on the same endplate, which are thought to interact through competition, is a very significant factor driving synapse elimination during development of the NMJ (Brown et al., 1976; Betz et al., 1980). However, it is not clear whether competitive interactions are a sufficient explanation for all synapse elimination that occurs in the first few postnatal weeks. It has been suggested that motor neurons may withdraw synapses in the absence of other converging axon branches, which would result in some muscle fibres becoming denervated (Thompson and Jansen, 1977; Fladby and Jansen, 1987). Synapse elimination which occurs independently of other branches has been termed intrinsic withdrawal.

Intrinsic withdrawal has mainly been revealed by partially denervating a muscle and investigating whether the remaining motor units still lose synapses despite the absence/reduction of the majority of competitors. Key to this type of investigation is the use of muscles which are innervated via two separate nerves, facilitating partial denervation. There are several such muscles which have been used, for example the soleus muscle in the AO strain of rats (in which the innervating nerve bifurcates allow-

ing for the muscle to be partially denervated without cutting one of the spinal nerves, Thompson and Jansen, 1977) and the 4th deep lumbrical in rats (Betz et al., 1980).

Brown et al. (1976) were the earliest to describe a reduction in MU size in spite of a reduction in competition. They cut the main spinal nerve (L5 root) to the soleus muscle of rats, which resulted in approximately 30% of muscles becoming completely denervated. The remaining 70% continued to be innervated by a subset of motor neurons through a different spinal nerve that supplies the soleus, albeit with a reduced amount of competition. They assessed MU size by measuring twitch tensions and they found that the time course of elimination appeared slower in partially denervated muscles than in the contralateral control muscle and that the remaining units were more easily fatiguable, meaning that the tension generated by the muscle contraction decreased faster after repeated stimulation on the operated side. This decrease in the tension could be caused by several mechanisms, for example it could be due to weakening of synaptic transmission due to depletion of synaptic vesicles of ACh in the pre-synaptic terminal. The fact that muscles were more fatiguable after partial denervation could be an indication that the remaining motor units were more stretched than control motor units typically are. In five out of the ten units they examined (the remaining five all being from the same muscle), MU size was closer to the average adult size and smaller than average MU size at the time of denervation. This was the first suggestion that some synapse elimination had occurred despite the reduced amount of competition.

This observation was examined more systematically in a subsequent paper by Thompson and Jansen (1977). Using the same muscle, but in AO strain rats, they found that the mean MU size of motor units was larger at the time of partial denervation (just after birth) than the size of the remaining motor units was at maturity (2-20 weeks after partial denervation). Based on these results, they concluded that synapses can be eliminated in the absence of competition. Although the difference in the distributions of motor unit sizes is quite striking, there are certain criticisms of this study which weaken its conclusions. Although they used the standard method of measuring motor unit size at the time, their measurements are indirect. In both neonatal and adult muscles that had been partially denervated neonatally they measured the tension generated by motor units relative to the whole muscle tension and converted that proportion to

number of muscle fibres. They determined the number of muscle fibres in each preparation by counting the number of profiles in a cross section through the muscle. They mention themselves that it was difficult to determine the number of muscle fibres in neonates due to some very small cross sections. Moreover, in adults that had been partially denervated there will have been many denervated atrophic fibres which they had to decide whether to include or exclude from the total number of muscle fibres. In addition this method assumes that each muscle fibre contributes equal tension and that tensions sum linearly which may not be the case, especially in neonatal muscles. Also the neonatal muscles they were comparing were not age-matched and, although Brown et al. (1976) found no reduction in the number of fibres that are polyneuronally innervated up to p5, that does not imply that there is no synapse elimination. In fact it is probable that motor unit sizes are already decreasing during this period. Finally, none of the muscles examined in either of the two studies had a single remaining motor axon. This means that in all cases some reduction due to competition was expected, and so it is hard to show convincingly that the reduction observed was occurring in the absence of competition.

In order to address some of these concerns, Betz et al. (1980) re-examined the question by using the rat 4th deep lumbrical muscle. This muscle also receives innervation from two nerves (the lateral plantar and the sural) and has the advantage that often there is a single axon innervating through the smaller (sural) nerve. This allowed them to examine MU size only in muscles with a single remaining axon and thus no competition. They investigated 23 adult muscles which had been partially denervated zero to two days after birth and in which a single axon remained intact innervating the muscle. They found that the mean motor unit size in these muscles was not significantly different from neonatal motor unit size and was significantly greater than unoperated adult MU size. From this they concluded that all synapse elimination can be accounted for by competition between converging axon branches. There are also a few factors which complicate the interpretation of these results. The rat lumbrical muscle undergoes addition of muscle fibres during post-natal development, unlike the soleus, and thus some new synapses are formed postnatally. Also they used the same indirect method of measuring MU size in neonates as the previous study (estimating from the percentage tension and the number of neonatal muscle fibres). In adults with neonatal partial

denervation, the number of innervated muscles fibres was estimated by counting the innervated fibres in the cross section of the muscle, as there was a single motor unit innervating all fibres. They used a more sophisticated method for determining which fibres were innervated based on measuring the size of all muscle fibres and labelling as denervated those that fit the distribution of sizes found in completely denervated muscles. This assumes that denervated muscle fibres in completely denervated and partially denervated muscles atrophy at the same rate. Moreover, as both methods are indirect they could have separate biases in the measurement.

Fladby and Jansen (1987) re-addressed this question using mouse soleus muscle. This muscle does not have an increase in muscle fibres after birth (Slater, 1982) and it has fewer motor units and muscle fibres than rat muscles. They found that adult muscles with up to about five remaining units after partial denervation had average motor unit sizes of less than expected if just competition was causing elimination. This led them to conclude that intrinsic withdrawal was occurring. Their criticism of the earlier papers is that twitch tensions seem to underestimate motor unit size in neonatal muscle but not in adult. Therefore neonatal motor unit size may have been underestimated in Betz et al. (1980) and thus masked the effects of intrinsic withdrawal.

Although they have tried to be more accurate with their MU size estimates, they are still comparing estimates of motor unit size from tension measurements to estimates of motor unit size from fibre diameter measurements. Their estimate of neonatal motor unit size is probably correct because they verified using several different methods (Fladby, 1987) but they have not directly measured motor unit size in adults with neonatal partial denervation.

Other studies have also addressed this question using even less precise methods for comparing motor unit sizes and concluded both that intrinsic withdrawal does and does not occur. For example Gates and Ridge (1992) investigated this question using the rat 4th deep lumbrical muscle again. They found that mean estimated motor unit size in adults with neonatal partial denervation was not different from neonatal motor unit size as reported by Betz et al. (1979). Also Fisher et al. (1989) partially denervated rat soleus muscles and suggested that the neonatal field of innervation was maintained into adulthood. On the other hand, Connold et al. (1992) using similar methodology

concluded that intrinsic withdrawal does occur in the EDL muscle of rats, even though the EDL is primarily composed of fast muscle fibres like the lumbrical and in contrast to the slow soleus.

Thus, given these conflicting results, it is unclear whether any synapse elimination does in fact occur in the absence of other competing neurons.

In the first part of this chapter I have described the mouse 4th deep lumbrical muscle which is used as the preparation for subsequent experiments.

In the second part of this chapter I have re-examined the question of whether some synapses withdraw from muscle fibres in the absence of competing axon branches, leaving them uninnervated. The mouse 4th deep lumbrical preparation allowed the study of single unit muscles after partial denervation and I have quantified motor unit size by using transgenic YFP mice to directly visualise motor units. This direct visualisation is the primary improvement over the physiological methods used to measure motor unit size in all previous studies which have examined the question of intrinsic withdrawal.

I found evidence for both intrinsic withdrawal and competition. In the absence of competition only the largest motor units seem to decrease in size, which suggests that larger motor units are more susceptible to intrinsic withdrawal.

If there is a limit, an interesting question is why neurons have to withdraw some of their collateral branches instead of just failing to expand. One suggestion is that intrinsic withdrawal could be the result of an intrinsic genetic program to decrease the number of synapses at a certain time point during development. An alternative explanation is that it is not necessarily the number of terminals which is limited, it could be total synaptic area, total amount of neurotransmitter or total intracellular volume to name just three. This is not a new idea, for instance Fladby and Jansen (1987) suggested: *"if the limiting 'capacity' of the motoneurons were the total amount of transmitter which could be delivered to all its terminals, the number of terminals would have to be restricted as more transmitter was required for each"*. Therefore if neurons produce a limited amount of substances necessary for growth, sibling branches may compete with each other for it, resulting in some branches growing at the expense of others.

Neurite growth requires protein synthesis and trafficking of intracellular structural proteins, like tubulin and neurofilaments, proteins which can affect stabilisation and branching like microtubule associated proteins (MAPs), and cell membrane structures, as growth requires the addition of new membrane (Futerman and Banker, 1996; Kiddie et al., 2005; Kobayashi and Mundel, 1998). Substances required for neurite outgrowth are produced in finite amounts and may be a limiting resource for the growth of the neuron. In fact there is evidence that neurons have a limited capacity for growth because preventing it in one area will lead to increased growth in another and vice versa.

For example Vital-Durand and Jeannerod (1975) claim that some types of neurons have a tendency to conserve the total outgrowth of their arbours. They describe a series of experiments looking at the branching pattern of retinal ganglion cells and neurons in the lateral olfactory tract (LOT). They showed that when they ablated part of the branching structure, there was increased branching in the intact area. Moreover in the LOT when they removed some of the competing inputs, thus causing the LOT axons to cover a larger area than usual, there was a decrease in the distal outgrowth. These data led them to suggest that a conservation of outgrowth takes place which has the effect of 'compensatory sprouting' and 'compensatory stunting'. Since then other studies have also induced compensatory sprouting or stunting (e.g. Gan and Macagno, 1997).

This has also been observed at the level of individual neurons, for example Hutchins and Kalil (2008) found that cortical axon branches with higher calcium concentrations grew rapidly while sibling branches from the same parent neuron retracted. Also Murphey and Lemere (1984) found that in individual cricket sensory neurons the excess growth of one region was associated with reduced growth in another. In addition, Samsonovich and Ascoli (2006) showed that there was a negative correlation between the sizes of the apical and basal dendritic trees of individual hippocampal pyramidal neurons. This is consistent with the idea that there is a constraint on the total outgrowth of the cell.

The idea that sibling axon branches may compete with each other for some resource permissive to elongation was nicely described by Smalheiser and Crain (1984) and a computational model of competition between neurites of the same cell for tubulin

has been proposed by van Ooyen (2001). The idea that there is a neuronal resource, like tubulin or some substance neccessary for synaptic function, which limits the total amount of outgrowth or the total synaptic size that a motor neuron can support, is interesting in light of the experimental findings in this chapter. If each motor neuron had a similar capacity for growth then the intrinsic resources of the large motor units would be more stretched than those of smaller motor units. This could result in the observation that only the largest motor units in this study appeared to lose synapses. Perhaps elimination was caused by competition within the neuron for presynaptic resources.

One hypothesis is that the natural growth of the animal is what puts stress on motor units. Interestingly, none of the models of synapse elimination take into account the fact that the animal is growing, not only during the period of synapse elimination, but also after that period is finished.

In the third part of this chapter I have altered the model of synapse elimination by Rasmussen and Willshaw (1993) to include a variable postsynaptic resource, which increases in proportion to the growth of the animal. I have used this model to investigate the effect of synaptic growth on motor unit size during the first few weeks postnatally and into adulthood.

3.2 Methods

There are three parts to this chapter: (1) characterisation of the mouse 4DL, (2) investigation of synapse elimination in the absence of competition and (3) modelling the effect of growth on motor units in control and partially denervated muscles.

3.2.1 Anatomy of the 4th deep lumbrical muscle

First I characterised the morphology of the mouse 4DL. For this, 4DL muscles were dissected from YFP16 and YFPH adult mice and YFP16 pups between the ages of p5-p9 (see 2.3-2.4.1). Endplates were labelled with Rhodamine-α-BTX (see 2.4.3.1), fixed (2.4.2) and mounted on slides (2.4.4). These samples provided information about

the number of endplates, number of motor and sensory axons, mean motor unit size and motor unit size distribution in the mouse 4th deep lumbrical muscle (see 2.5.3). Data specifically about the number of motor and sensory axons innervating through the smaller sural nerve were obtained from partially denervated samples (see next section).

3.2.2 Synapse elimination in the absence of competition

I used a similar experimental design to previous studies (e.g. Betz et al., 1980). The 4th deep lumbrical muscle of neonatal (p5) YFP16/Bl6 mouse pups was partially denervated by cutting the tibial nerve (see section 2.2.2). Pups were allowed to recover either two days (to p7) or more than four weeks (to adult) before the 4DL muscle was dissected, fixed, stained with rhodamine-α-BTX and mounted on a slide (see sections 2.3-2.4.3.1). The number of sensory and motor axons which remained (i.e. those which innervated the muscle through the sural nerve) were counted and muscles with a single motor axon were selected for further study. Motor unit size was calculated in these muscles by counting the number of innervated endplates. MU size of single remaining units at two days after partial denervation (neonatal) was compared to MU size of single remaining units more than four weeks after partial denervation (ANPD).

The difference between this study and previous studies is that MU size is assessed morphologically rather than physiologically and is therefore a direct measure of the number of muscle fibres innervated by a single unit. Additionally, as in Betz et al. (1980) but in contrast to Thompson and Jansen (1977) and Fladby and Jansen (1987), only muscles where a single motor unit remained after partial denervation were used in the analysis. Therefore these units developed in the complete absence of competition. Moreover, mouse 4DL was used which has not been used in any of the previous studies and neonatal MU size was estimated two days after partial denervation rather than at the time of partial denervation. Therefore both groups have undergone exactly the same treatment but for different lengths of time.

The number of innervated endplates was also assessed in adult muscles which had been partially denervated in neonates and had two or three remaining axons. This

was compared with an estimate of how many endplates should be innervated if no intrinsic withdrawal occurred. The estimate was made by randomly choosing two or three motor units from a density plot constructed from the neonatal MU size data gathered from neonatal muscles with a single remaining axon. The expected overlap was calculated between these units and used to find the number of unique endplates that would be expected to be innervated once a state of mononeuronal innervation was reached (see appendix A).

3.2.3 Modelling the effect of growth on motor units

The model of synapse elimination described in Rasmussen and Willshaw (1993) was implemented in Matlab with the difference that the value for B_0, the postsynaptic resource, was replaced by a function which describes how synapses grow over time. The form of the function was determined by gathering data from the literature and choosing the best fit function as determined by the summed squared error (SSE).

3.3 Results

3.3.1 Anatomy of the mouse 4th deep lumbrical (4DL) muscle

The mouse 4DL inserts into the 5th digit in the mouse hindlimb and is innervated by axons travelling both in the lateral plantar (tibial) and in the sural nerves as can be seen in figure 3.1A. Figure 3.1B shows an image of an unoperated adult mouse 4DL. All averages quoted are given as mean $\pm$ standard deviation unless otherwise stated.

On average there were 5.45 ± 1.34 axons innervating the 4DL muscle (n = 11 muscles). More than half of the muscles examined (7/11) had at least one sensory ending (as determined by the presence of an annulospiral Ia afferent ending innervating a muscle spindle, figure 3.1C). Therefore the average number of motor neurons supplying the 4DL is 4.81 ± 1.43.

In the adult mice I studied there were 223 ± 38 endplates per muscle (n = 40 muscles).

A

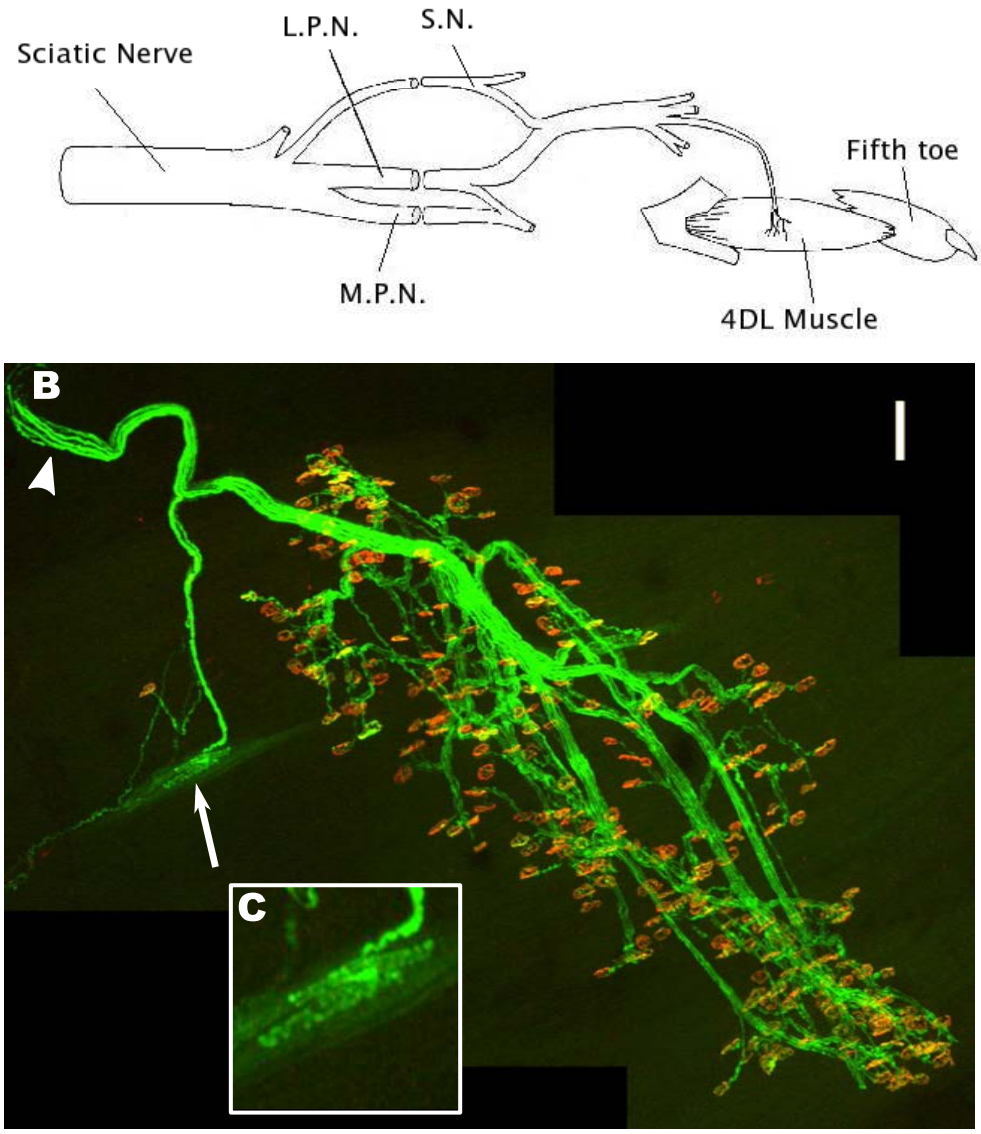

Figure 3.1: *The mouse 4DL. A: Drawing of the mouse 4DL and its innervation. LPN=Lateral Plantar Nerve, MPN=Medial Plantar Nerve, SN=Sural Nerve. Image from Richard Ribchester based on the rat lumbrical muscle in Ribchester and Taxt (1983). B: A maximum intensity projection of a confocal z-stack of an unoperated adult YFP16 mouse 4DL. All axons express YFP in the cytoplasm (shown here in green) and the postsynaptic AChRs have been labelled with rhodamine-α-BTX (red). The overlap between presynaptic and postsynaptic areas appears yellow. The axons enter the muscle at the top left (arrowhead) and a sensory ending can be seen innervating a spindle (arrow). C: Magnified image of the muscle spindle seen in B. Scale bar: 100 µm*

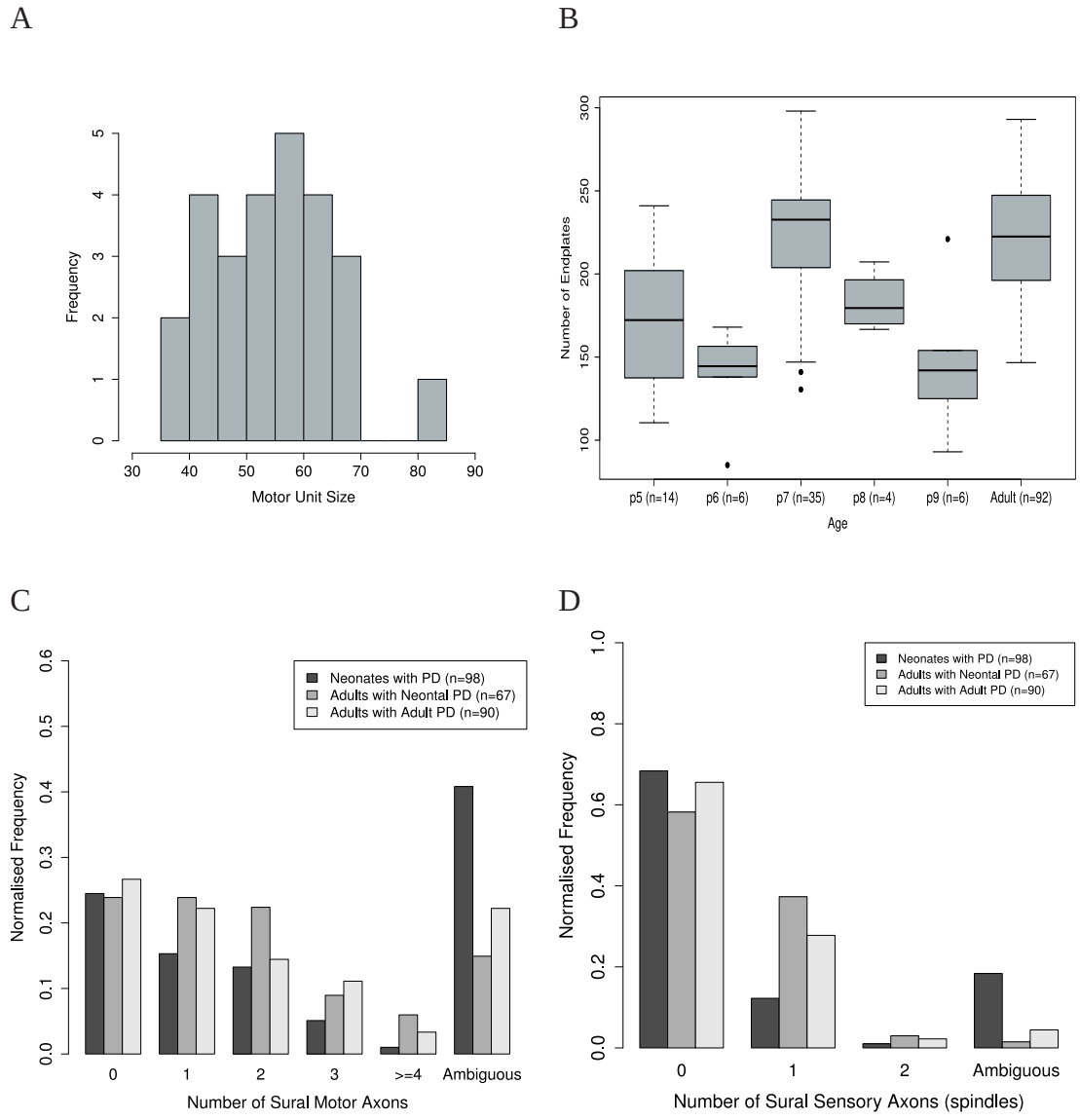

Figure 3.2: *Characteristics of the mouse 4DL. A: Distribution of motor unit sizes from unoperated adult YFPH 4DL muscles with a single fluorescent motor unit. B: Number of endplates in 4DL muscles over development and in the adult. C:Histogram showing the relative frequency of different numbers of motor axons innervating the 4DL through the sural nerve. D: Same as in C but for sensory axons (ending in a muscle spindle).*

There was no significant difference in the number of endplates between 4DLs from male and female or YFP16/YFPH mice (2-way ANOVA, ns). The average motor unit size was 54 ± 15 and there was no significant difference in sizes calculated from YFPH (54 ± 11) and YFP16 (52 ± 23) muscles (t-test, 2-sided, ns). The distribution of motor unit sizes was not significantly different to a normal distribution (Kolmogorov-Smirnov, ns; figure 3.2A). Given that YFPH and YFP16 mice have a similar number of endplates and MU sizes, it is assumed that units from the two strains can be compared.

Number of endplates over development The number of endplates in the muscle appeared to increase by about 60 post-natally (ANOVA, $p<0.001$, figure 3.2B). This is an indication that the number of muscle fibres increases, as each muscle fibre has been found to have exactly one endplate. Post-hoc t-tests (with bonferroni correction) reveal that there are the same number of endplates at p5 and p6 and they are significantly fewer than at p7 or in adulthood (see table 3.1). In addition there is no difference in the number of endplates between p7 and adult muscles. Surprisingly, the number of endplates in p9 muscles is significantly lower than in adult or p7 muscles and not significantly different from p5/p6. It seems unlikely that some endplates at p7 are removed by p9 and then new ones are added by adulthood. A more parsimonious explanation is that the p9 muscles are not a representative sample, as there are only six muscles and they are all from the same litter. In addition, the neonatal muscles used in subsequent experiments are from p7 pups which have contributed to this data. Therefore it is concluded that there appears to be addition of about 60 fibres between p5 and p7 at which point the full adult complement of muscle fibres is reached and there is very little, if any, further addition.

Sural nerve axons Betz et al. (1980) showed that after cutting the LPN, the number of intact units in the SN did not change in the rat 4DL. Similarly, here, I have shown no change in the number of motor units innervating the mouse 4DL through the sural nerve after partial denervation. Figure 3.2C shows the distribution of motor axons innervating the 4DL through the sural nerve in neonates, in adults with partial denervation as neonates and in adults with partial denervation as adults. Despite the seemingly smaller proportion of muscles with one or more axons in neonates, these distributions do not significantly differ from each other (χ^2, ns). Considering that there are a very

	p5	p6	p7	p8	p9	adult
p5		ns	<0.001	ns	ns	<0.001
p6			<0.001	ns	ns	<0.001
p7				ns	<0.001	ns
p8					ns	ns
p9				ns		<0.001
adult						

Table 3.1: *Table showing the p-values for the post-hoc comparisons between number of endplates at different ages. Graph showing the number of endplates by age can be seen in figure 3.2B.*

similar number of muscles which receive no innervation from the sural nerve, the difference probably reflects the fact that neonatal axons are harder to resolve when they are present, as can be seen by the increase in the number of muscles in which the number of innervating axons was ambiguous. Therefore the most reliable data are the adult data which show that in approximately a quarter of muscles there are no motor axons from the sural nerve, in approximately a quarter there is a single axon, in 20% there are two, in 10% there are three and in about 5% there are four or more axons innervating through the sural nerve. The remaining 15% make up the ambiguous group and therefore have at least one axon.

Similarly, figure 3.2D shows the distribution of sensory axons through the SN. There are significantly fewer muscles with one sensory axon in the neonatal group (χ^2, $p<0.0001$) but again, this is probably due to there being more ambiguous cases in the neonatal group. Approximately 60% of muscles had no sensory innervation though the sural nerve, about 30% had one sensory and about 2% had two sensory axons in the SN.

Since about one third of muscles receive sensory innervation through the SN and about two thirds overall have a sensory ending, approximately the same number of muscles (one third) must receive sensory innervation from the LPN. Conversely, it seems like most of the motor innervation comes through the LPN since the average number of motor axons in the SN is one.

The mouse lumbrical muscle is therefore smaller than the other muscles used to study synapse elimination in the absence of competition, although the mean MU size is larger than that measured in adult mouse soleus, which is about 30 (Fladby and Jansen, 1987). Like the rat lumbrical there appears to be some addition of muscle fibres post-natally, though this seems to occur before p7 which is the time point at which neonatal motor unit size was measured.

3.3.2 Synapse elimination can occur in the absence of competition

The next part shows three separate results which are all consistent with the hypothesis that some synapse elimination can occur in the absence of competition.

3.3.2.1 Only large motor units decrease in size after neonatal partial denervation

MU sizes from muscles which had been partially denervated at p5 to leave a single remaining motor unit were compared at two different time-points: neonatal (p7, two days after the partial denervation) and adult (4+ weeks after the partial denervation) and also to unoperated control motor units. MU sizes were normally distributed in all three groups ($p>0.8$ for all three comparisons, Kolmogorov-Smirnov test). MUs from both neonates and ANPD were significantly larger than control YFPH adult motor unit sizes (mean $\pm$ S.E. for neonates:137 ± 18, ANPD:103 ± 9, control:54 ± 2, $p<0.001$ for both comparisons, post-hoc Dunnett's C after ANOVA, figures 3.3 and 3.4 and 3.5). The difference in mean MU size between neonatal and ANPD muscles is not significant (ns, Dunnett's C after ANOVA, figure 3.3), although the variances of the two distributions are different (Levene's test, p=0.006). While the smallest MUs in each distribution are around the same size as each other (43/44) and in the range of control MU sizes, half (6/11) of the neonatal motor units innervate more endplates than the largest ANPD motor unit. This suggests that specifically the large motor units have decreased in size in the absence of competition.

I also did some experiments looking at the sprouting response of adult motor units (figure 3.3). Motor unit sizes appeared to increase in adults either 7 (AWA7) or 14

(AWA14) days after partial denervation, as expected. Despite the increase in mean motor unit size, there was still a wide range is motor unit sizes, many of which fell within the normal range of sizes. Adult sprouting was not investigated any further.

3.3.2.2 The number of innervated endplates in ANPD with two remaining axons is less than expected though with three remaining axons is at the expected level

Additional evidence for intrinsic withdrawal is provided by looking at the number of endplates innervated in adult muscles which have been partially denervated at p5 and have two, or three axons remaining. When there are two or three axons remaining, there will still be π-junctions after the cut, and therefore some competition will persist. However, if no intrinsic withdrawal occurs, the number of endplates which are innervated should remain the same. I estimated the number of endplates that should be innervated when two or three axons are left based on the neonatal motor unit sizes from the muscles with a single axon (see appendix A for details). This was done by creating a density distribution from the 11 data points, selecting two or three motor unit sizes randomly from this distribution and calculating how many distinct endplates would be innervated given that each motor neuron forms synapses randomly. As can be seen in figure 3.6, when there are two remaining axons the number of innervated endplates is less than that predicted (one-sample t-test compared with mean of 95 $p=0.045$, and compared with a mean of 94 $p=0.058$; data shown in the graph is divided by the number of axons to give an average MU size per motor neuron). However, when there are three motor neurons left innervating the muscle, the predicted number of innervated endplates is practically identical to the observed number (one sample t-test comparing to mean of 70, ns). This suggests that when there are only one or two axons left some synapses are eliminated from μ-junctions leaving the muscle fibre uninnervated, however when there are three (and presumably more) axons left all elimination occurs at π-junctions.

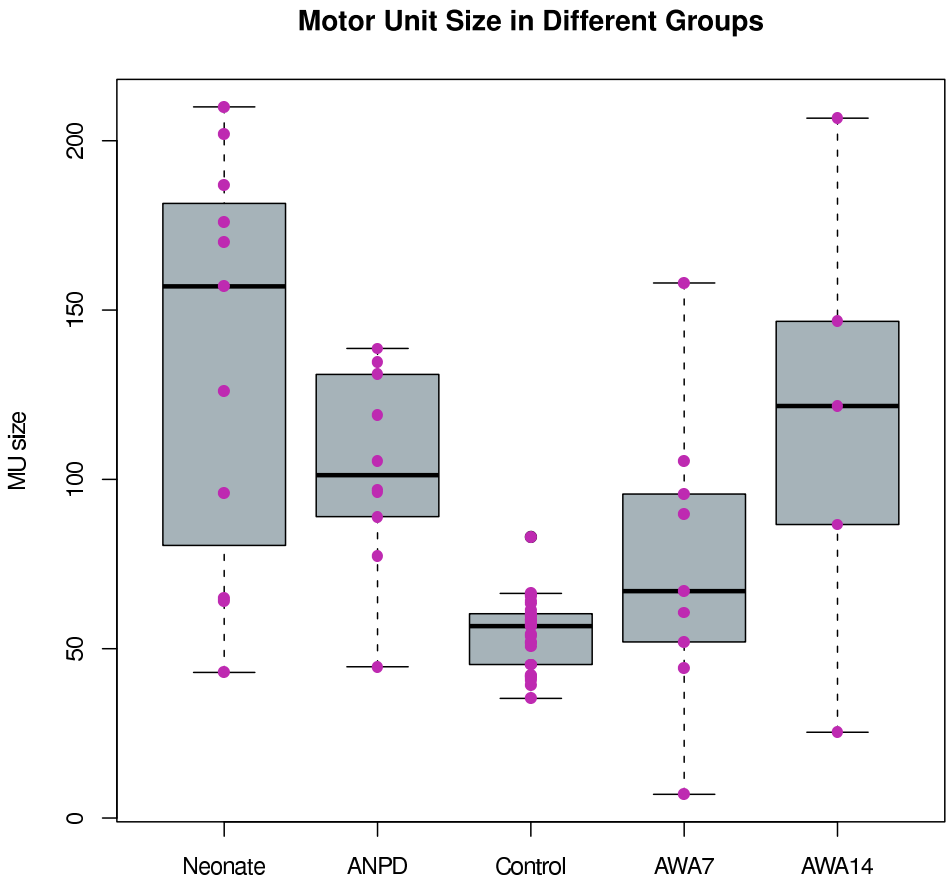

Figure 3.3: *Boxplots showing the distribution of MU sizes in control YFPH animals (control) and at different time points after neonatal or adult partial denervation. Control = unoperated YFPH adult MUs; Neonate=2 days after neonatal partial denervation; ANPD= more than four weeks after neonatal partial denervation; AWA7= 7 days after adult partial denervation; AWA14=14 days after adult partial denervation. Superimposed on the boxplots are the actual data points. Each pink dot corresponds to the MU size of the single remaining motor unit after partial denervation in the operated muscles or of the single fluorescent motor unit in the control muscles.*

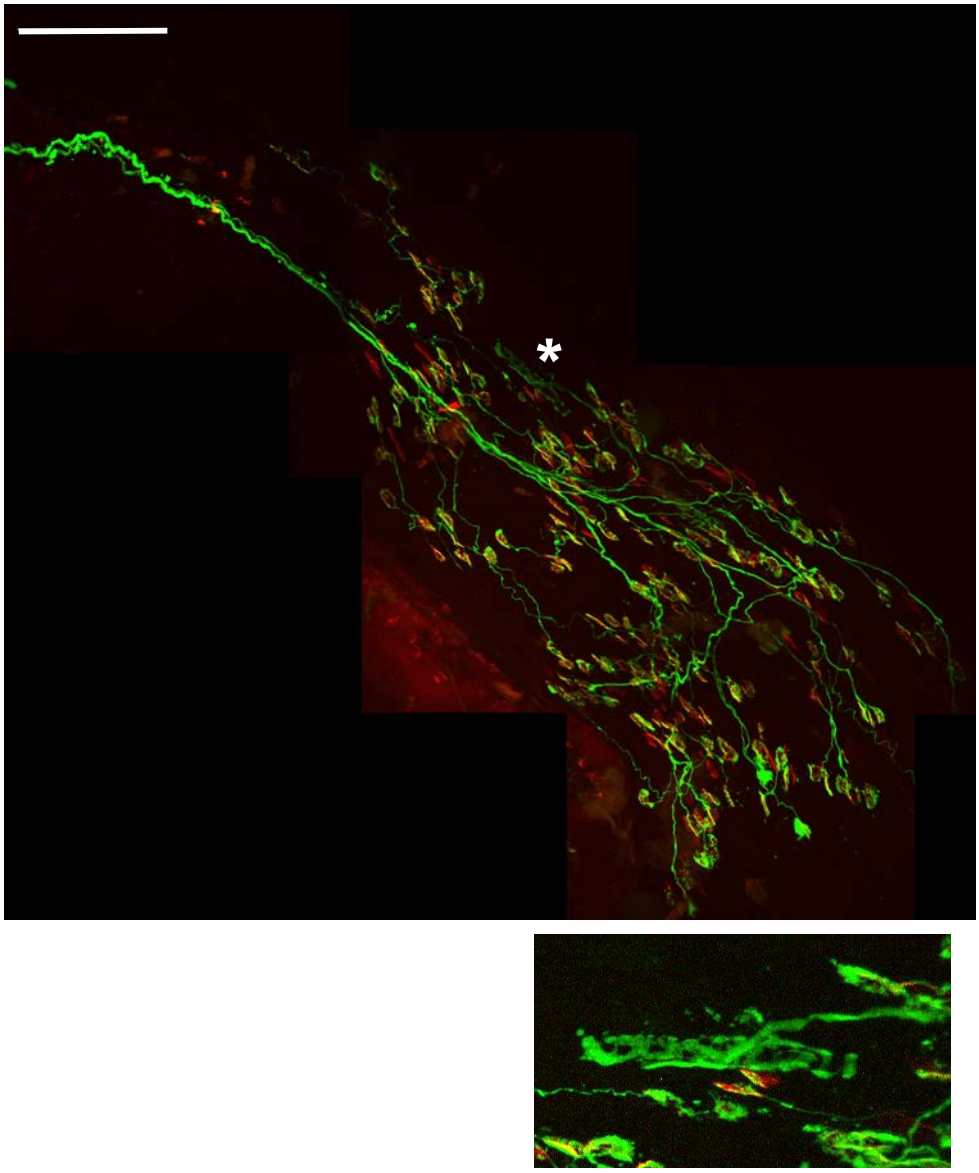

Figure 3.4: *Single fluorescent motor unit in a neonatal muscle (p7) two days after partial denervation. The muscle also has a sensory axon innervating it (∗, and magnified in lower box). Axons express cytoplasmic YFP (green) and endplates are tagged with rhodamine-α-BTX (red). The visible motor axon is the only motor axon present. Scale bar: 100 µm*

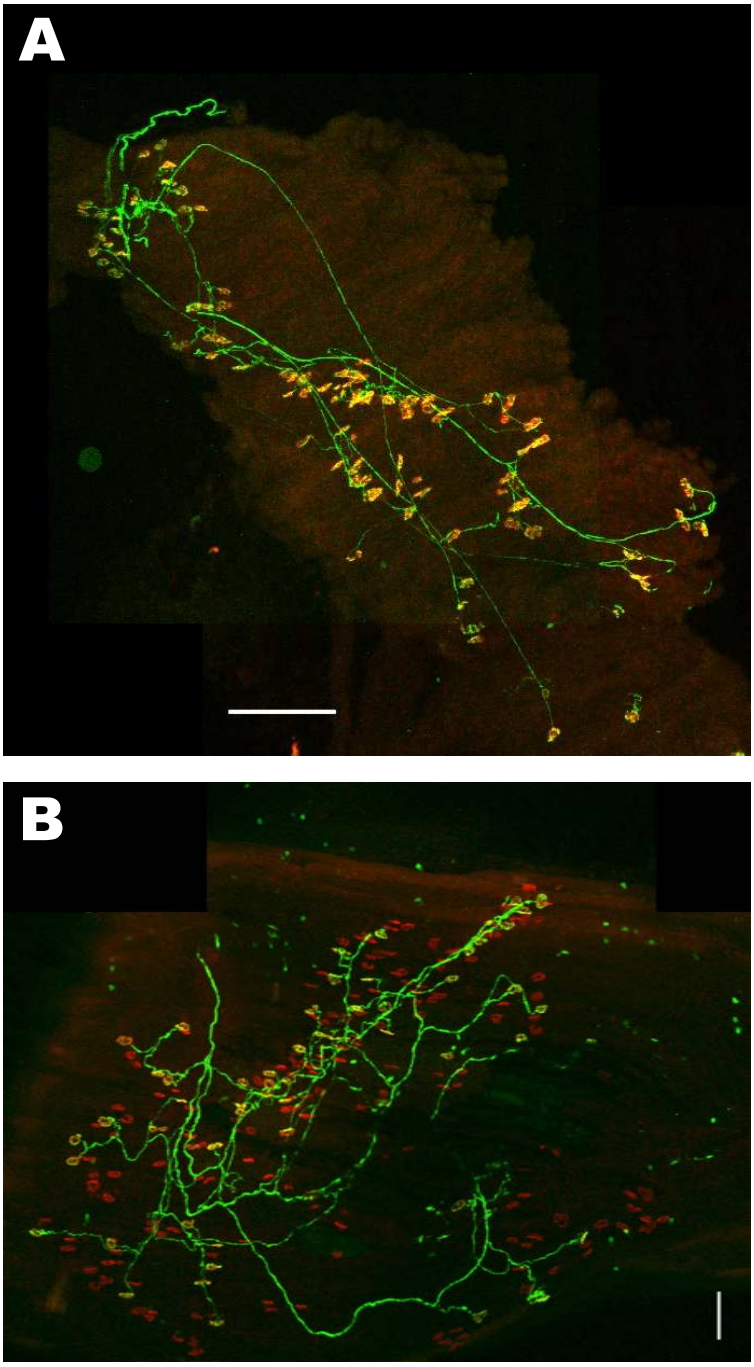

Figure 3.5: *Single fluorescent motor units in: an adult muscle with neonatal partial denervation (A) and an adult YFPH (B). Axons express cytoplasmic YFP (green) and endplates are tagged with rhodamine-α-BTX (red). In A the muscle was partially denervated at p5 and the visible axon is the only remaining motor axon. Notice that there are no uninnervated endplates even though the axon is only innervating around 100 endplates. This is typical for adult muscles which have been partially denervated as neonates but have some remaining axons. In B there are non-fluorescent units which innervate all the endplates not innervated by the fluorescent axon. Scale bars: 100 µm*

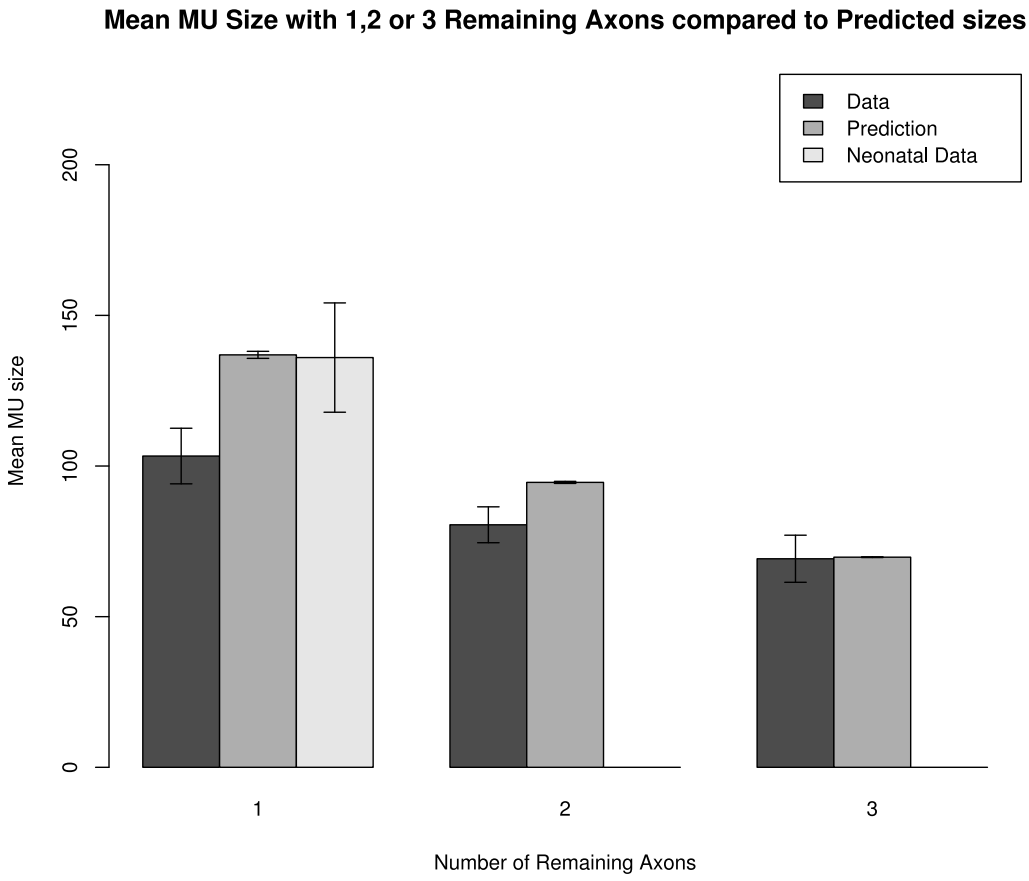

Figure 3.6: *Average MU size with one, two or three remaining axons. Dark gray bars show the actual data from ANPD, medium gray show predicted MU sizes and the lightest gray shows the actual neonatal MU sizes. Error bars show the standard error of the mean.*

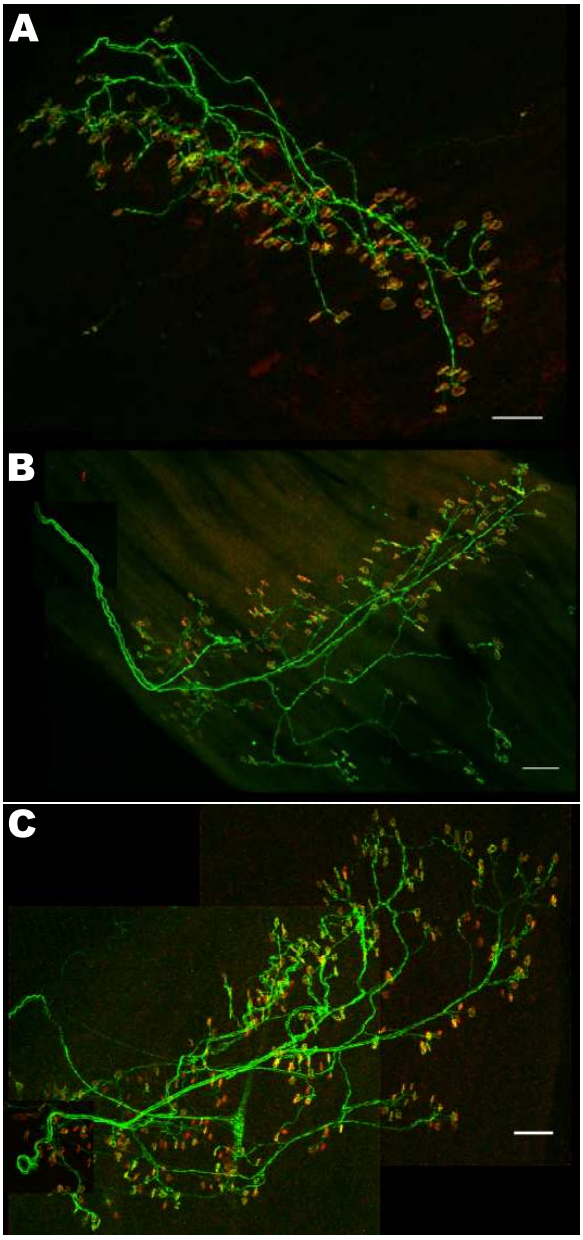

Figure 3.7: *Examples of adult muscles which were partially denervated at p5 and have one (A), two (B) or three (C) remaining axons. Note that there are no denervated endplates in any of these examples. Scale bars: 100 µm*

3.3.2.3 Morphological Evidence

Another line of evidence for intrinsic withdrawal comes from morphological features of adult muscles after neonatal partial denervation. In most cases, when there is at least one motor neuron present, every surviving endplate is innervated. This is not because all muscle fibres become innervated, since the number of endplates is significantly lower than in unoperated adults; rather it is most likely because denervated muscle fibres have degenerated or at least the AChRs on denervated fibres have dispersed. This contrasts with the case where the muscle is completely denervated where there are still AChR clusters and some of the endplates even appear as 'pretzels', see figure 3.9. In some ANPD muscles with a remaining axon however, there were a few (less than five usually) uninnervated endplates (see figure 3.8). These are indistinguishable from the innervated endplates. These could be endplates which have been recently vacated by intrinsic withdrawal.

In one of the adult muscles that had been partially denervated at p5 there were many uninnervated adult endplates and signs of retraction bulbs (figure 3.10). This was the only example where the denervation was so extensive. It is not clear if the denervation in this case represents intrinsic withdrawal or is due to some other factor. For example there may happen to be a non-fluorescent unit in this muscle and elimination is occurring through competition, or the muscle or nerve may have been inadvertently damaged at some point before the dissection.

In summary I have provided three pieces of evidence which suggest that motor neurons can withdraw axon branches from μ-junctions leaving the muscle fibres uninnervated. None of the three lines of evidence is conclusive. In the first case the variance in motor unit sizes is significantly different in single unit muscles from neonates two days after partial denervation and adults more than four weeks after partial denervation, and half of the neonatal motor units are larger than the largest ANPD unit. However, the difference in the mean motor unit size is not significant. In the second case the average ANPD motor unit size in muscles with two remaining axons is less than what it is predicted to be in the absence of intrinsic withdrawal and this difference is marginally significant. In the third case there is some morphological evidence consistent with what we would expect to see if intrinsic withdrawal did occur, namely some uninnervated

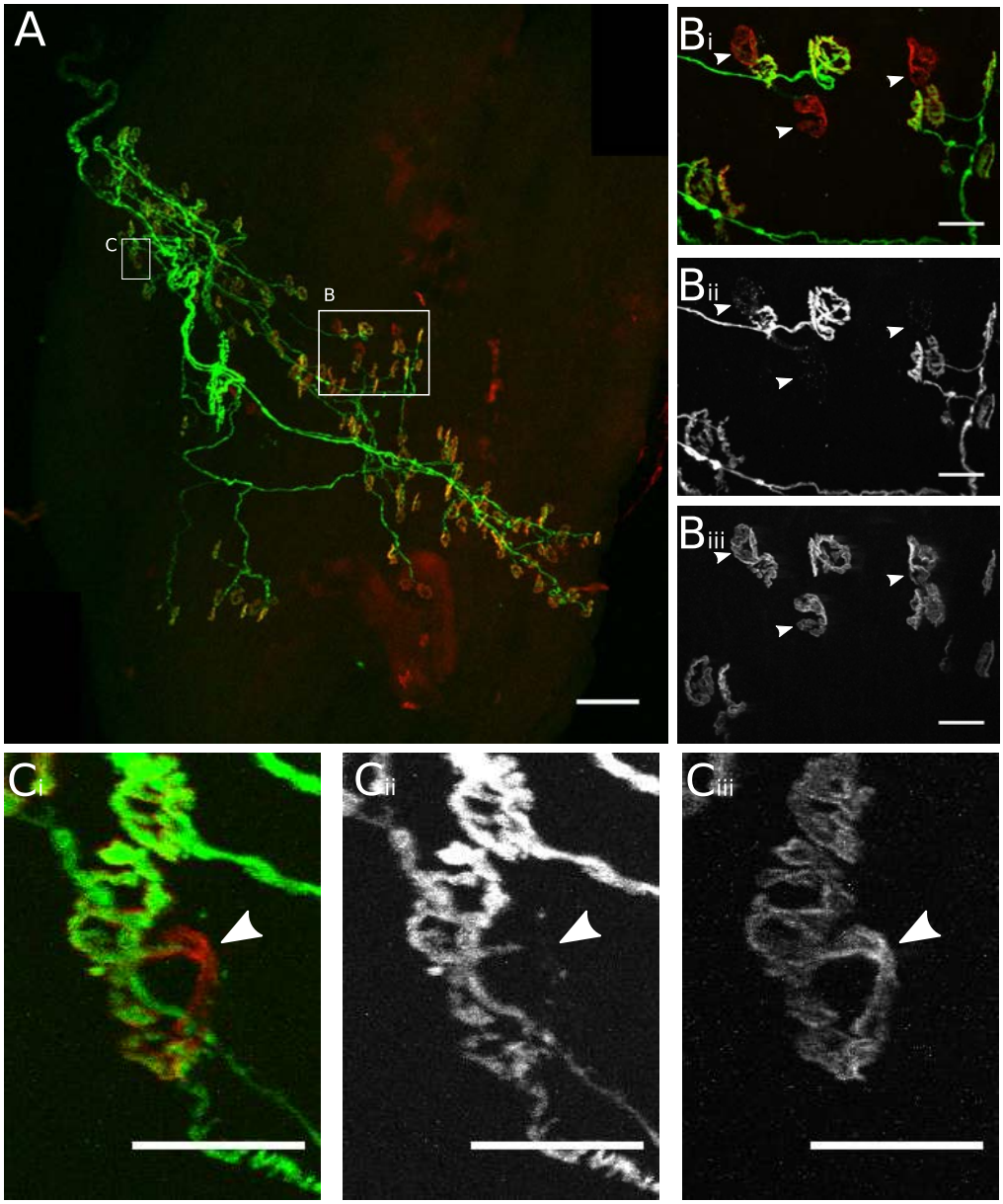

Figure 3.8: *ANPD muscle with 3-4 uninnervated endplates. A: Montage of entire adult muscle which was partially denervated at p5 and has a single remaining motor axon. B: Region with three uninnervated adult looking endplates (arrowheads). Bi: merged image, Bii: axons only, Biii: endplates only. C: Region of the muscle with a partially occupied endplate (arrowhead). Ci: merged image, Cii: axons only, Ciii: endplate only.*

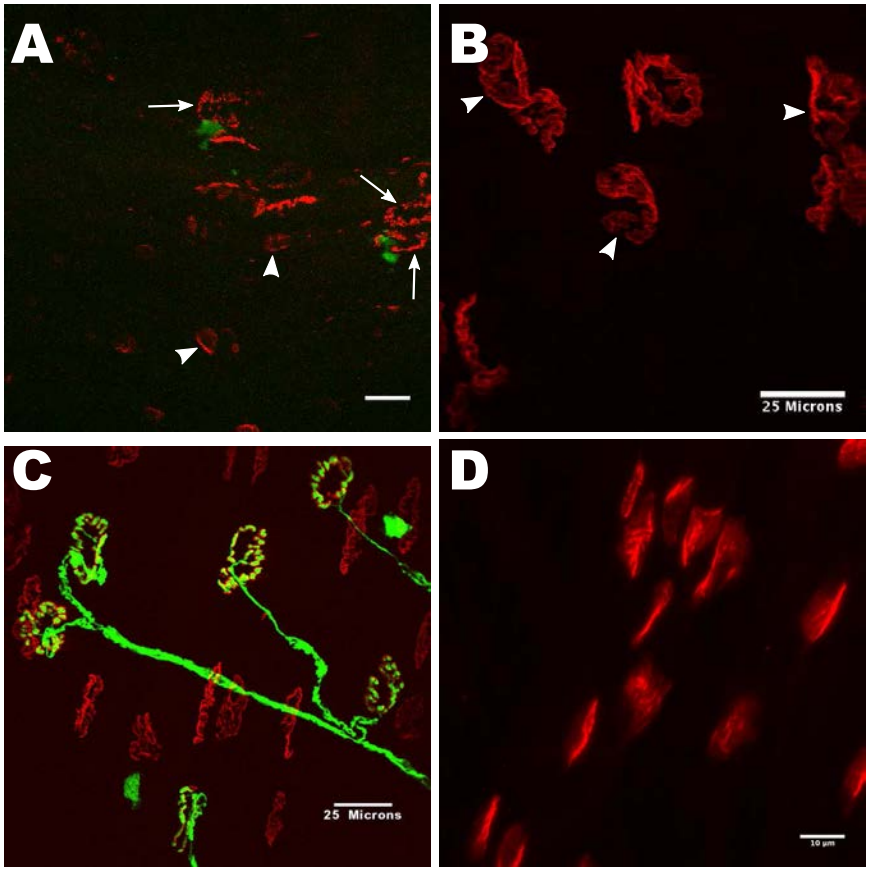

Figure 3.9: *Endplates in adult muscles that were A: completely denervated at p5 (with green channel overlaid but no axons present), B: partially denervated at p5 (without axons overlaid), C: unperturbed development of YFPH (with fluorescent axon overlaid) and D: p5 endplates (without axon overlaid) . Notice that in the muscle that was completely denervated at p5 there is still evidence of endplates. Some look like neonatal endplates (arrowheads, compare to D) and others have grown and resemble adult endplates though they are not as full (arrows). B is part of the image shown in figure 3.8 Biii. It is from an adult muscle which was partially denervated at p5 and has a single remaining axon. The arrowheads distinguish the uninnervated endplates. The other endplates in the image are innervated by an axon which is not shown here. There is no morphological difference between the innervated and uninnervated endplates or the appearance of endplates in unoperated muscles (C). Scale bar in A: 10 µm*

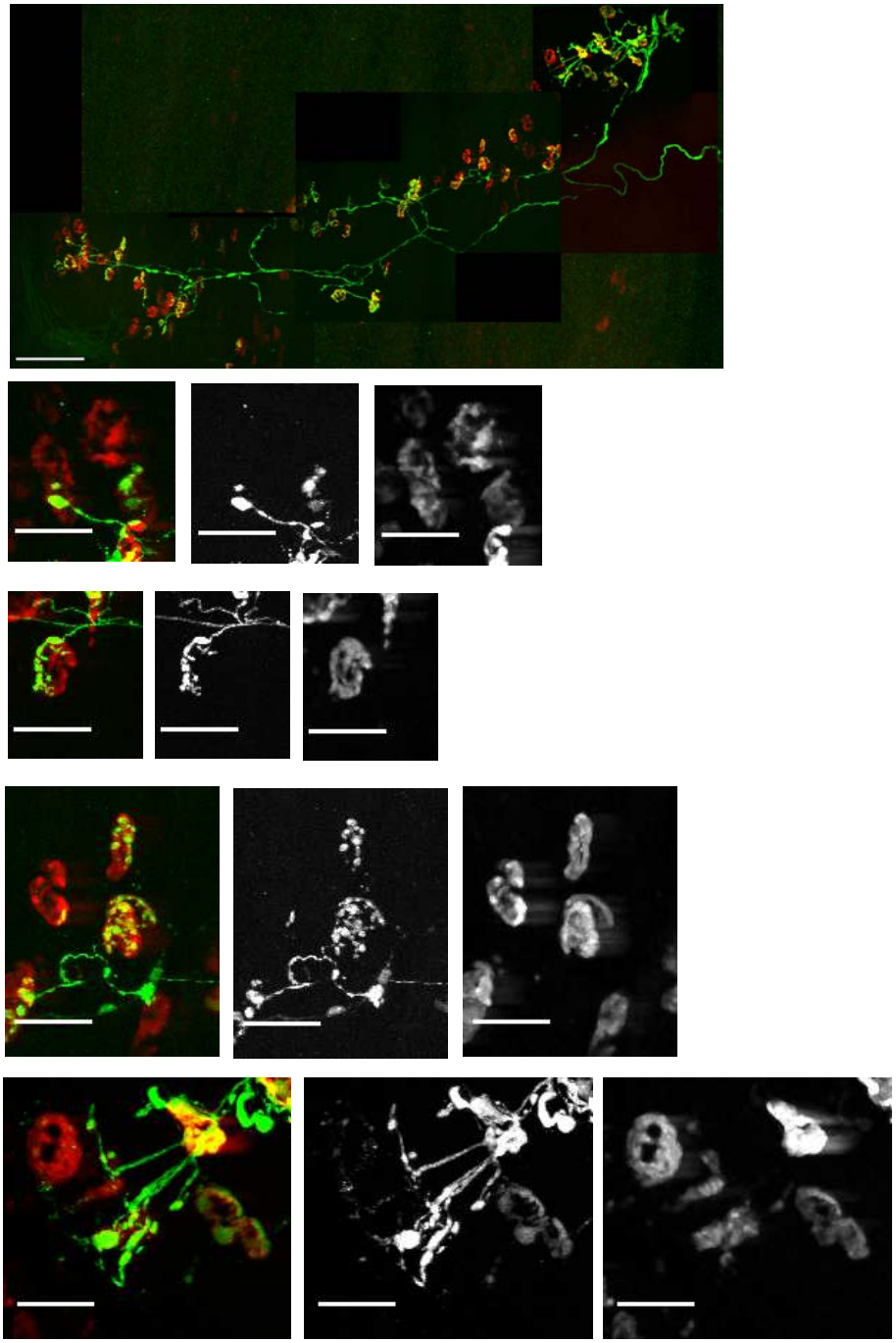

Figure 3.10: *Muscle with many uninnervated muscle fibres. This muscle looked different from the other ANPD muscles because of the extensive denervation. There are multiple examples of partially denervated endplates and axon branches ending in what appear to be retraction bulbs. Axons express YFP (green) and endplates are labelled with rhodamine α-BTX (red). Top image shows a montage of the whole motor unit. Next four rows show magnified images of individual endplates. Left images are merged axons and endplates, middle images are the axons only and right images are the endplates only.*

fully formed endplates. However, there could be alternative explanations for these empty endplates as well (see Discussion). Therefore while none of the three provides conclusive evidence on its own, put together they make a strong case for the occurrence of intrinsic withdrawal.

3.3.3 Modelling

Based on the previous results, intrinsic withdrawal is hypothesised to occur because the neuron has limited resources and therefore there are a limited number of synapses it can support. The Rasmussen and Willshaw (1993) model of synapse elimination already supports the idea of intrinsic withdrawal in cases where the presynaptic resource a neuron has is less than the postsynaptic resource available to it. However, in this model, neither the presynaptic nor postsynaptic resources vary over time. Therefore, once developmental reorganisation is concluded the system is stable and no other changes occur. Rodents are still growing well into their adult life. I have implemented Rasmussen and Willshaw's model with a growing postsynaptic resource, which reflects the growth of the animal, and investigated the effect of this on synapse elimination over its lifetime.

3.3.3.1 Implementation of Rasmussen and Willshaw model

First I implemented the model described in Rasmussen and Willshaw (1993). Each muscle is characterised by certain attributes: the number of muscle fibres (M), the number of motor neurons (N), the spread of neonatal motor unit sizes and the amount of polyneuronal innervation at birth (see below for the specific values). There is a presynaptic resource A associated with each motor neuron and a postsynaptic resource B associated with each muscle fibre which combine in a reversible chemical reaction to form C, a binding complex which is proportional to the area of the NMJ. A and B are suggested molecular substances which interact in the synaptic cleft. Each motor neuron, n, has a fixed amount of A (A_0) which either exists in the soma (A_n) or is distributed to each axon branch in proportion to the size of the synapse at the end of each branch. Initially, each muscle fibre, m, has a fixed amount B_0 of B, which axons

innervating the same muscle fibre compete for. The equations which govern how the amount of A at each terminal (A_{nm}) and the amount of C at each junction (C_{nm}) change over time are given by equations 3.1 and 3.2 respectively.

$$\frac{dA_{nm}}{dt} = \gamma\frac{A_n}{\nu_n} - \delta\frac{A_{nm}}{C_{nm}} \tag{3.1}$$

$$\frac{dC_{nm}}{dt} = \alpha A_{nm}B_mC_{nm} - \beta C_{nm} \tag{3.2}$$

At each iteration the amount of pre-synaptic resource in the soma and the amount of unbound postsynaptic resource in the muscle fibres can be calculated by equations 3.3 and 3.4 respectively.

$$A_n = A_0 - \sum_{i=1}^{M} A_{ni} - \sum_{i=1}^{M} C_{ni} \tag{3.3}$$

$$B_m = B_0 - \sum_{j=1}^{N} C_{jm} \tag{3.4}$$

$\gamma, \delta, \alpha, \beta$ are rate constants and are given the same values as in the original model, namely γ = 3, δ = 2, α = 45 and β = 0.4. ν_n is the number of synapses that motor neuron n makes, and is calculated from the data at each iteration. In all subsequent simulations ten thousand iterations are equivalent to one week.

Rasmussen and Willshaw showed that the ratio $\frac{A_0}{B_0}$ is proportional to the maximum number of terminals a motor neuron can support. They set the postsynaptic resource, B_0, to 1 and the pre-synaptic resource, A_0, of each neuron to the maximum motor unit size for each muscle based on physiological measurements. In all the subsequent simulations A_0 was set to 80 which was roughly the maximum motor unit size observed in the adult lumbrical muscle. B_0 was set to 1 for replication of the results and was then varied as discussed below.

I show that my implementation of the model gives results comparable to those in Rasmussen and Willshaw (1993) (see figure 3.11). I have used parameters from mouse soleus muscle for comparison with the paper and mouse lumbrical for comparison with my experimental results.

3.3.3.1.1 Mouse soleus parameters For mouse soleus I used identical parameters to those in Rasmussen and Willshaw (1993). There are 600 muscle fibres and 20 motor neurons. Initially there are 6 ± 1 terminals converging on an endplate and the initial spread of motor unit sizes is two-fold.

3.3.3.1.2 Mouse lumbrical parameters For the mouse lumbrical muscle I used the parameters derived for the 4DL previously. I used 222 muscle fibres and 5 motor units. The initial amounts of convergent innervation and spread of MU sizes are unknown so I arbitrarily set the numbers to be 4 ± 1 and two-fold respectively, effectively reusing the parameters from the soleus, though with a slightly reduced convergence rate since there are many fewer motor neurons.

3.3.4 Determining the NMJ growth function from literature

Next I searched the literature to find data on how NMJs grow over time (Courtney and Steinbach, 1981; Robbins and Fahim, 1985; Andonian and Fahim, 1987, 1989; Balice-Gordon and Lichtman, 1990; Wærhaug, 1992; Balice-Gordon et al., 1993). I found that the growth pattern is remarkably consistent across muscles in both mice and rats (figure 3.12A&B) and seems to increase about four-fold over the lifespan of the animal. The length, width and area all increase by a similar amount, in contrast to what would be expected if an oval was increasing, namely that the area would increase by the $width \times height$. NMJ's are not solid structures though and it is interesting that the area appears to increase linearly with the length. Growth of the NMJ is also correlated with the growth of the animal and the growth of the muscle (Balice-Gordon and Lichtman, 1990).

The growth function, as determined by the literature, was used to model the change

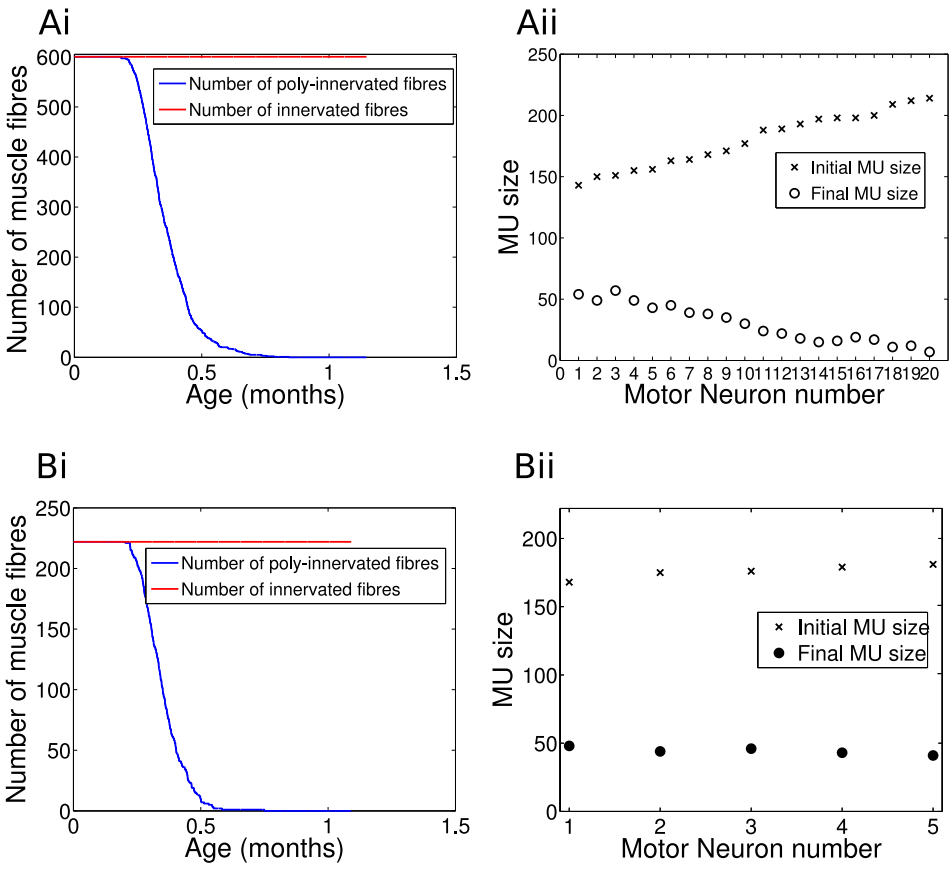

Figure 3.11: *Replication of results from Rasmussen and Willshaw (1993). A: results for mouse soleus muscle and B: for mouse lumbrical. In both muscles the process of elimination is complete at around three weeks (Ai and Bi blue lines) during which time no muscle fibres become denervated (red lines). Once competition is complete the model is in a stable state and no more elimination occurs. All MUs reduce in size, though the larger ones reduce slightly more than the smaller one (Aii and Bii). Thus smaller MUs have a competitive advantage over larger MUs.*

in post-synaptic resource (B_0), even though the data describe the size of the synapse, which is represented by C in the model. This was done because B_0 is a parameter which can be set in the model whereas C is determined by the dynamics during the simulation. Nevertheless, as can be seen in figure 3.14 the change in size of C has the same shape as the change in size of B_0.

In order to fit the NMJ area data I considered age 0 to be the time of conception and 21 days to be the time of birth (ie p0). Using the `fminseach` function in Matlab, I minimised the sum squared error (SSE) for four different equations and chose the best fit (see table 3.2).

The equation used to model the change in NMJ area with time t is of the form

$$B_0 = a + b \times log(t) \tag{3.5}$$

with the parameters shown in table 3.2. Each muscle fibre in the model has a postsynaptic resource given by this equation $\pm 10\%$. This symmetry breaking is necessary for the increase in postsynaptic resource to have an effect in the model. Here I report the results from running the model with this equation only but I have also tried using $B_0 = a + \frac{b}{t}$ and $B_0 = \frac{a}{b+e^{c+dt}}$ and both give comparable results. (See discussion (section 3.4.4) and appendix (C) for differences)

3.3.5 Running the model with variable postsynaptic resource

Next I re-ran the simulations with the new increasing function for B_0. In order to keep the original values of the other parameters I normalised B_0 so that it is equal to one at three weeks (which is the end of the developmental period). All simulations were run for the equivalent of three years. Since the amount of B_0 is continually increasing the simulation never reaches a steady state. The elimination of polyneuronal innervation follows a similar time-course as before and during this time all muscle fibres remain innervated (figure 3.13 Ai, Bi). Figure 3.15 shows the competition at 24 representative endplates during the first three weeks of development. However, as the postsynaptic resource grows, axon branches of the same neuron start to compete with each other for

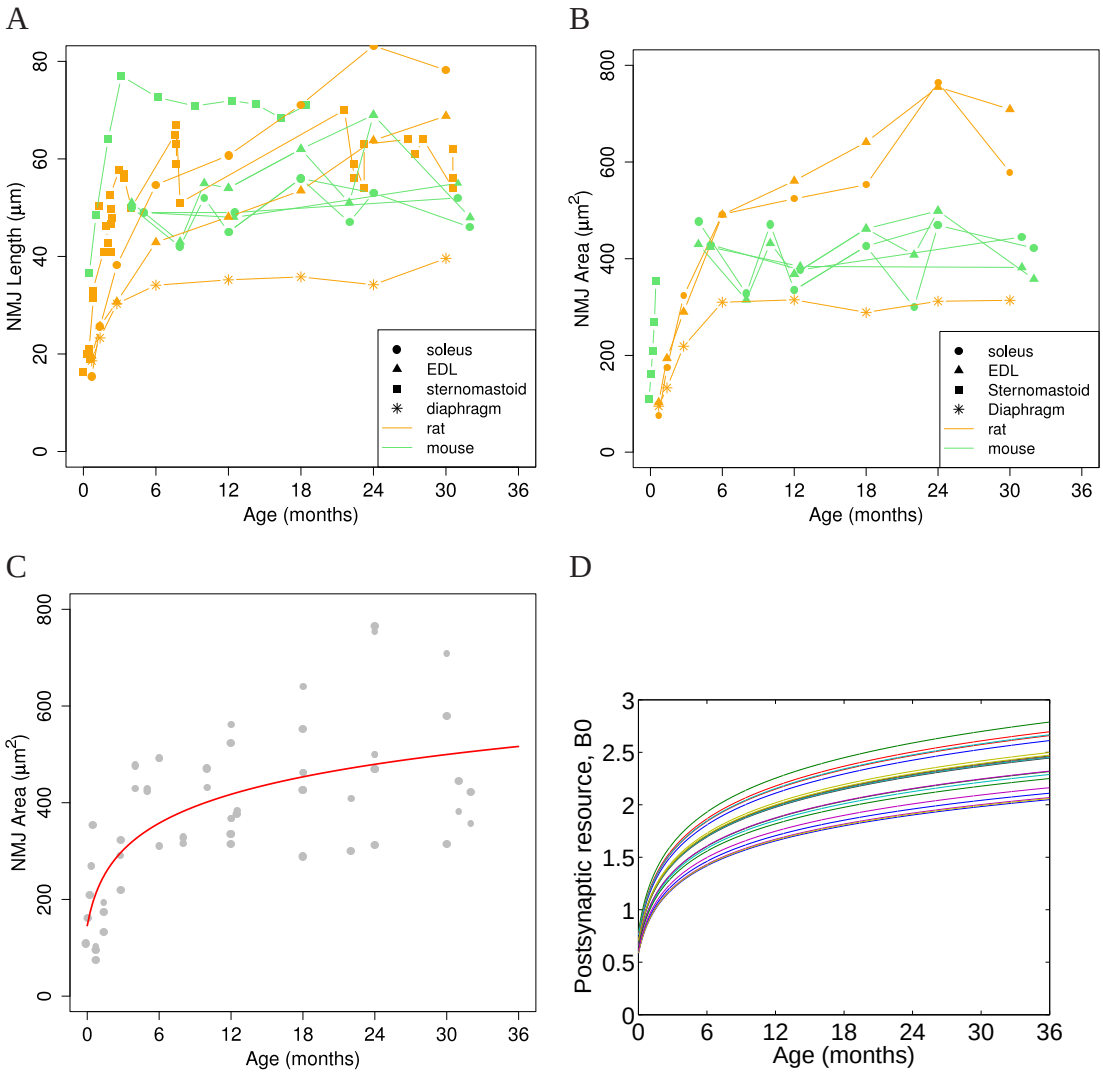

Figure 3.12: *NMJ growth with age. Growth in length (A) and area (B) seem remarkably similar in both mice (green) and rats (orange) across different muscles (see symbols in legend). I found the best fit to all the area data from both mice and rats (C, red line) and used this as the growth function for* B_0. *D. The amount of* B_0 *over time in a random selection of 20 muscle fibres. In the model I randomly alter the size by* $\pm 10\%$ *in order to create a distribution of sizes.*

	Equation	Fit	SSE	$\frac{\sqrt{SSE}}{n}$	parameters
1	$B_0 = a + b * log(t)$	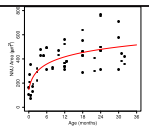	6.96×10^5	14.64	a=180.35, b=93.31
2	$B_0 = \frac{a}{b+e^{-t}}$	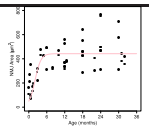	7.14×10^5	14.83	a=55.67, b=0.13
3	$B_0 = ab^t$	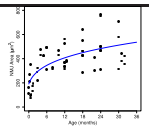	7.27×10^5	14.96	a=210.4, b =0.26
4	$B_0 = a + \frac{b}{t}$	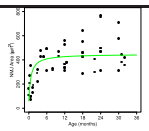	8.11×10^5	15.8	a=448.09, b=-267.75
2(b)	$B_0 = \frac{a}{b+e^{c+dt}}$	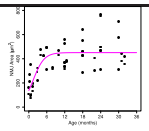	6.81×10^5	14.48	a=7.94, b=0.02, c=-2.84, d=-0.55

Table 3.2: *Table showing the fits of four possible equations. Equations 1 and 3 have very similar shapes and are continually increasing. Equation 4 is also continually increasing but has a faster rate of increase in the beginning and then the growth tails off. Equation 2 reaches a limit after about six months with no further increases. Although equation 2(b) has a slightly lower SSE than equation 1, it needs four parameters instead of two for this. The model was run with both and they give comparable results with slightly different time-courses (see appendix C. Here the results from equation 2 are reported.*

presynaptic resource, which is necessary for further growth of the synapses. Around nine months of age some motor units begin withdrawing a few of their synapses because they cannot maintain the number of synapses that they have ended up with (see figure 3.14). This makes sense considering that the maximum number of terminals a motor neuron can support is proportional to $\frac{A_0}{B_0}$. As B_0 grows this fraction will continually decrease. There is no sprouting built into this model, however if this elimination occurred in reality one might expect that the empty endplates would be innervated by sprouts from other motor neurons. Also it is interesting to note that during synapse elimination the largest motor units lose disproportionately more synapses to become the smallest motor units. With further maturation the originally smallest MUs which are the largest after synapse elimination, are the first to lose synapses (figure 3.13Aii, Bii), indicating that the competitive advantage of smaller motor units is everything to do with them spreading their resources to fewer synapses. The relationship would not be so strict if motor neurons had a variable presynaptic resource as well.

Each of the sub-figures in figure 3.14 represents the synaptic areas of one motor neuron. Each line in the sub-figure shows the area of a synapse made by that motor neuron. When the area drops to zero, that synapse has been eliminated. There is one sub-figure for each of the 20 motor neurons in the soleus simulation. Some motor units did not lose any synapses after the developmental period is over, while others have lost a few synapses from about nine months onwards. These neurons do not lose all their synapses at once, but as time progresses and B_0 continues growing they lose more and more synapses.

Another observation is that there are instances where the axon which occupies the largest area of a synapse at one point in the competition ends up being overtaken and eliminated by an originally smaller axon. Similarly, as the synapse grows the axon occupying the most area may be overtaken by a faster growing axon but can then grow again, eliminating other axons. Viewed in terms of relative occupancy of the synapse, this resembles the flip-flop phenomenon described in Walsh and Lichtman (2003), although none of the synapses actually shrink in absolute size to then grow again at this stage. In figure 3.16 there is an example of a synapse where the axon which originally has the largest area is overtaken by a smaller axon but then manages

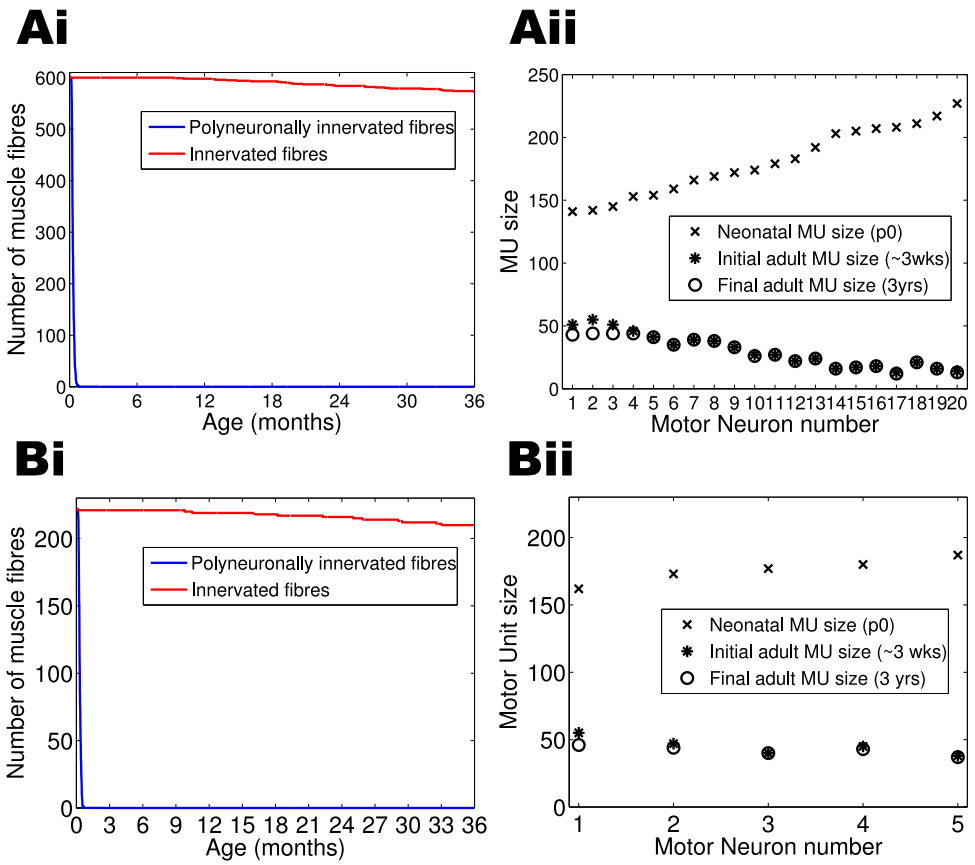

Figure 3.13: *Simulation of synapse elimination with a variable postsynaptic resource. A: Results for the mouse soleus muscle; Ai shows that the time-course of developmental synapse elimination is the same as before. However, the number of innervated fibres begins to decrease at about nine months of age and continues to decrease up to three years of age. Aii shows motor unit sizes at birth (x), at the time when synapse elimination is complete (*) and at the end of three years (o). Some MUs lose synapses after the developmental period is complete. B:Same but for the mouse lumbrical muscle.*

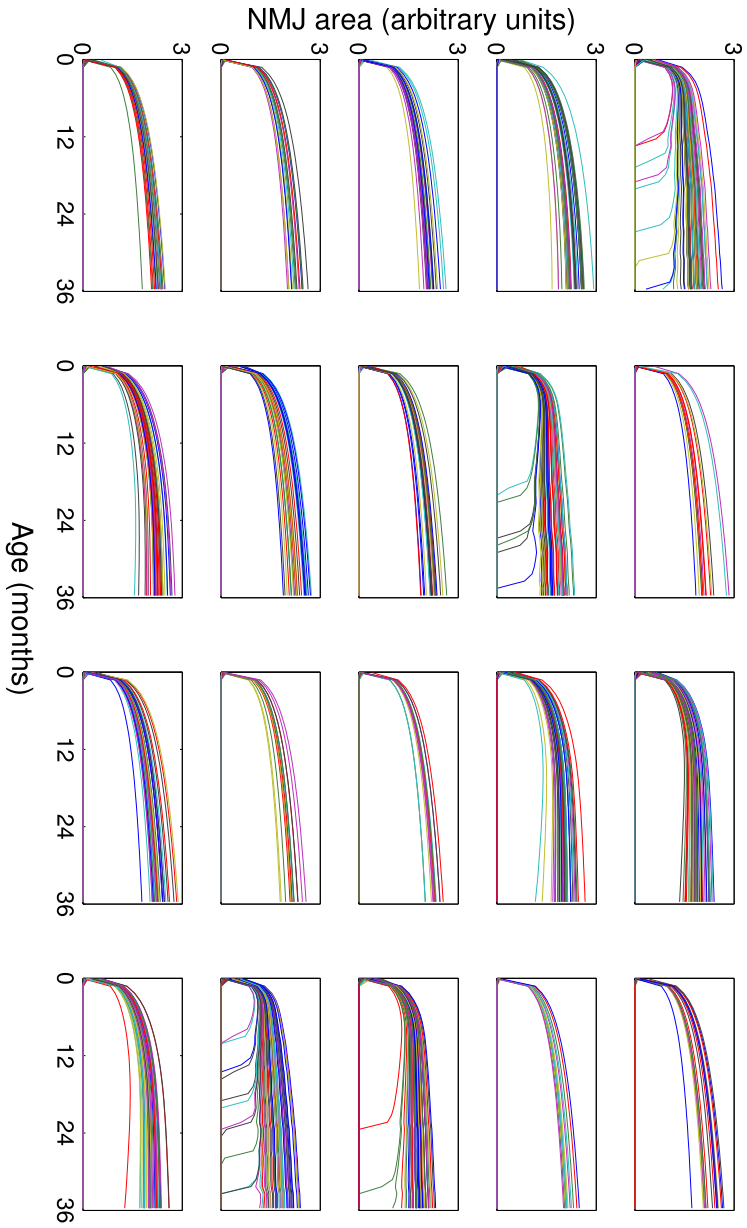

Figure 3.14: *MUs from the mouse soleus muscle over time. All 20 MUs from the simulation are shown in a separate sub-figure. Each line shows how the area of one of the synapses that neuron has formed varies over time. Some of the motor units lost synapses throughout the lifetime of the animal (three years).*

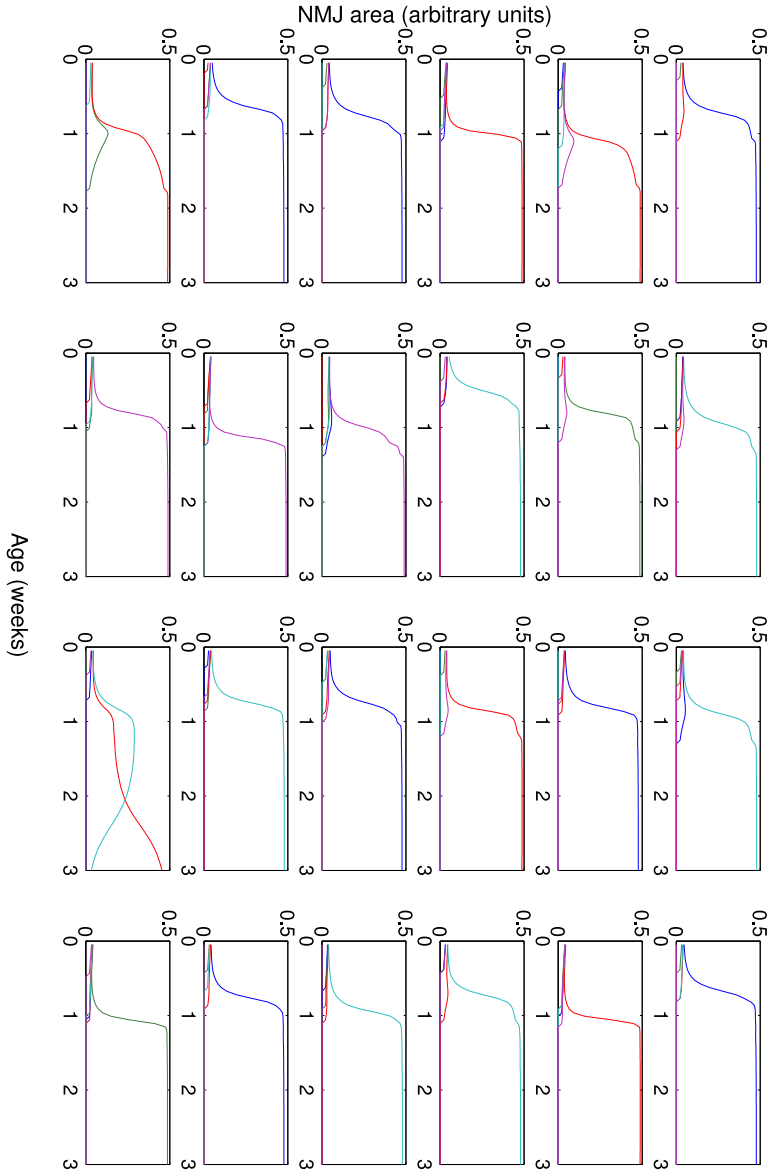

Figure 3.15: *Competition at 24 representative synapses in the soleus muscle. Each graph represents one endplate and each line represents the area occupied by the synapse of one motor neuron at that endplate. When more than one axon has positive area the synapse is polyneuronally innervated. Most synapses become mononeuronally innervated by two weeks of age.*

to win the competition. This is also a feature of the original model.

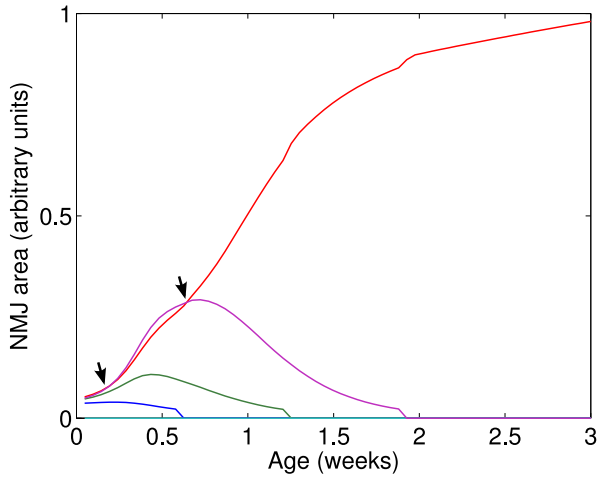

Figure 3.16: *The red synapse is originally larger but the magenta one grows faster and is larger for 2 days after which the red one becomes larger again.*

3.3.6 Replication of the experiment; Partially denervating the revised model at p5

I used the model with the growing postsynaptic resource to replicate the experiment described in section 3.3.2. The model was run as before for the first five days of development, with the only difference being that in the initialisation I manipulated the size of one of the motor units in order to get a wider range of sizes. At p5 I removed all but one of the motor neurons and allowed the remaining one to develop as before but in the absence of competition. The model ran for the equivalent of three years (the full lifespan of the animal), as before. After about one month only the largest motor neurons had decreased in size, whereas medium and smaller ones remained roughly the same size (Fig 3.18). Some examples of synaptic areas and intrinsic withdrawal up to three weeks of age can be seen in figure 3.17. Interestingly, the largest motor units reduced more in size than other units that also lost some synapses. Rather surprisingly, almost all motor units at three years after partial denervation had reduced to about 50 muscle fibres. This can also be seen by looking at figure 3.18A which shows the time

course of elimination for individual units. Here it is clear that motor unit size decreases gradually over the whole lifespan of the animal. If the neuron has more presynaptic resource (A) than it is using in its synapses at the time of partial denervation, then the MU size is maintained until the growth of the animal uses up all the A and causes branches of the same neuron to compete with each other. As the postsynaptic resource continues to grow, neurons gradually lose more and more synapses. Therefore the model suggests that in one month old animals only neurons with motor unit sizes above a certain value will have decreased compared to their size at p5. However, at later time points the MU size in ANPD should be smaller than that observed at one month.

Replicating the experiment with a fixed post-synaptic resource gives similar results at one month after partial denervation, although the value of A_0 would have to be changed for it to match the experimental results quantitatively (see appendix D). However, it does not predict any further decrease in motor unit size after the first 3 weeks of development.

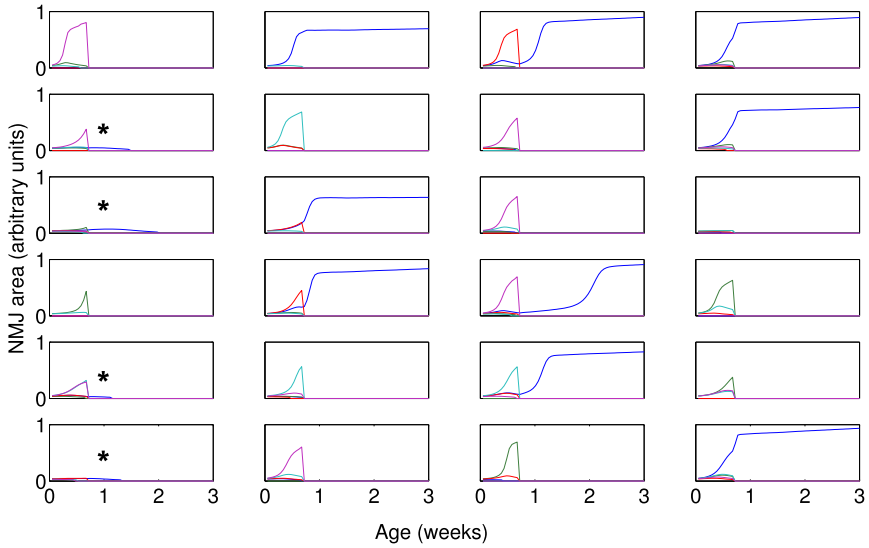

Figure 3.17: *Example of synapses after partial denervation. An $*$ denotes synapses which remained innervated at the time of partial denervation but subsequently became denervated.*

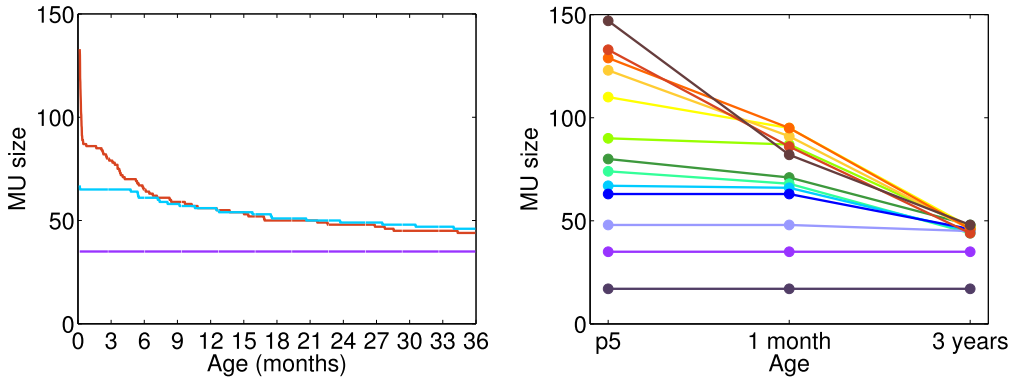

Figure 3.18: *Results from simulating the experiment of partially denervating at p5. A: Motor unit size from p5 onwards for three of the motor units. Units are coloured the same in B. B: Motor unit sizes at the time of partial denervation (p5), at one month (which corresponds to the the age of ANPD in the experiment in section 3.3.2) and at three years (maximum lifespan of mice).*

3.4 Discussion/Conclusions

In this chapter I have (1) characterised the mouse 4th deep lumbrical muscle, (2) presented three separate pieces of evidence which suggest that intrinsic withdrawal does occur and specifically in larger motor units and (3) used a modified version of the Rasmussen and Willshaw model to show that the experimental data is consistent with the hypothesis that intrinsic withdrawal occurs as a consequence of the normal growth of the animal. Based on the results of the model, I have predicted that intrinsic withdrawal may occur over the whole lifespan of the animal. I will discuss each of these in separate sections below.

3.4.1 Characteristics of the 4DL muscle

The mouse fourth deep lumbrical muscle is very small with, on average, 5 ± 1 motor axons innervating 223 ± 38 muscle fibres, and the mean motor unit size in mouse 4DL is 54 ± 11. Approximately 60% of muscles are also innervated by a sensory axon.

3.4.1.1 Distribution of MU sizes

Mean YFP16 and YFPH motor unit sizes are not significantly different. YFP16 motor unit sizes represent an average size per lumbrical muscle, so they should be less variable than YFPH MU sizes, each of which is from a single MU. However, there does not appear to be a difference in the spread of MU sizes. Mean MU sizes in YFP16 range from 24-89 whereas the range of YFPH MU sizes is 35-83. This could be due to several reasons.

If the variance in MU size within a muscle is quite low, but between muscles is higher (possibly due to variance in the number of axons innervating a relatively constant number of muscle fibres) then the mean range calculated from YFP16 muscles could match the range of YFPH. In other muscles the range of motor unit sizes can be between three-fold (Brown et al., 1976) to many-fold (e.g. in the interscutularis muscle where the largest MU was 38 and the smallest 1, (Lu et al., 2009b))

Another possibility is that the large range in the MU size calculated from YFP16 is artifactual. Since the means were calculated by dividing the number of endplates by the number of axons (excluding axons innervating muscle spindles), the very low values could be due to fluorescent gamma motor neurons which do not innervate many muscle fibres or non-spindle sensory neurons. Some of the muscles observed in the lab did have a fluorescent tree-like structure which was not an α-motor neuron. The very large MU sizes could also be over-represented as 3/11 YFP16 4DL's quantified were from the same litter and had only three motor axons innervating. This could have artificially increased the average MU size. Excluding those data points, the average number of motor units is 5.5 per muscle and the average MU size is 39 which is smaller than the YFPH estimate.

A third possibility is that fluorescence expression in motor neurons from YFPH mice is not entirely random, but restricted to motor units of a narrower range of sizes than is found in the general population of MU sizes. The distribution of motor unit sizes in the mouse interscutularis muscle was found to be skewed with many smaller ones and fewer larger ones (Lu et al., 2009b) which is in agreement with previous evidence from rat soleus (Betz et al., 1979) and rat lumbrical (Betz et al., 1979) muscles. The

distribution of motor unit sizes from YFPH units in the mouse lumbrical muscle did not significantly differ from the normal distribution. There are not enough YFP16 estimates to be able to determine if the underlying distribution is normal or skewed. This could be an indication that YFPH motor units are not representative of all motor units even though their average size does not differ from YFP16.

One or more of these reasons could account for the fact that the range of mean motor unit sizes from YFP16 mice is approximately the same as the range of YFPH MU sizes. Despite these issues, mean motor unit sizes are not different between YFPH and YFP16, so YFPH MU sizes provide the best current estimate of lumbrical MU sizes and are used as the control adult MU size.

Neonatal motor units ranged in size by at least four times from about 50-200. This is smaller than the range found in rat soleus (Thompson and Jansen, 1977, 200-1200) or lumbrical (Betz et al., 1979, 20-300). Fladby (1987) reports a three-fold range in tension measurements at p1 which subsequently decreases. In this study, sizes were estimated by partially denervating the muscle at p5 and, in muscles with a single remaining axon, counting the number of innervated endplates at p7. Two days after the nerve cut all cut axons had completely degenerated and there was no trace of YFP from these axons even after amplifying the YFP signal by immunolabelling.

3.4.1.2 Postnatal addition of muscle fibres

In the mouse soleus there is no significant addition of muscle fibre postnatally (Slater, 1982) though Betz et al. (1979) concluded that there is an approximately two-fold addition of muscle fibres postnatally in the rat 4th deep lumbrical muscle. The data in this chapter suggest that the number of muscle fibres in the 4DL increases up to p7, at which point the number is equal to that found in adults. Neonatal motor unit size was assessed at p7 and the average number of muscle fibres in these muscles was 242 ± 8 (mean $\pm$ SE). It seems likely that there was no addition of muscle fibres between the two time-points at which MU size was assessed after partial denervation, though there may have been some addition (about 60 fibres) between the time of partial denervation (p5) and p7.

3.4.1.3 Number of motor and sensory axons in the sural nerve

Finally there is the issue of how many MUs innervate through the sural nerve and whether this changes after partial denervation. Although the number of muscles with one or more axons through the sural nerve was greater in adults with neonatal partial denervation than in neonates, most likely this can be accounted for by the fact that neonatal muscles are smaller and axons are harder to resolve leading to a higher number of ambiguous cases. Further support that the distributions are the same in both cases comes from the fact that the number of muscles with no motor axons innervating through the sural nerve was the same in adults and neonates. Based on these data, approximately 25% of muscles are innervated by a single axon through the sural nerve, thus providing a good model system where all competition can be removed by cutting the tibial nerve.

In conclusion, the 4DL muscle provides a good model system, as it is a small muscle with a single motor unit innervating through the sural nerve approximately 25% of the time. Based on the evidence discussed above I am assuming that YFPH MU sizes are representative of 4DL motor unit sizes and that no addition of muscle fibres occurs after p7.

3.4.2 Synapse elimination during development in the presence and absence of competition

3.4.2.1 Influence of competition

Adult motor units which developed in the absence of competition from p5 onwards were significantly larger than adult motor units measured from unoperated YFPH muscles in which a single axon was fluorescent. This result confirms that competition is an important factor in the reduction of MU size during development.

3.4.2.2 Synapse elimination in the absence of competition

The evidence for synapse elimination in the absence of competition comes from three different lines of evidence.

First, there appears to be a reduction between p7 and adulthood in the MU size of large motor units which have developed in the absence of competition. The difference in the means is not significant but the variance is significantly different between the two groups. In addition, 6/11 neonatal units are larger than the largest ANPD unit although the smallest units are about the same size.

Second, the predicted mean motor unit size in muscles with two remaining motor axons was larger than that observed. This prediction is based on the observed neonatal MU sizes under the assumption that each axon innervates a muscle fibre randomly and there is no intrinsic withdrawal (i.e. every muscle fibre which is innervated will remain innervated). When there are three axons remaining after partial denervation the predicted and observed sizes are nearly identical.

A criticism of the prediction method may be that axons tend to fasciculate intramuscularly, and if two axons travel along the same path their field of innervation may overlap more often than if they were innervating independently. If this was the case then the prediction would overestimate the number of muscle fibres that should be innervated in all instances. However, when there are three remaining axons the predicted mean MU size is almost identical to the measured mean MU size. One reason why it may not overestimate when there are three axons is because the maximum number of muscle fibres that can be innervated is capped at 223. Thus any overestimate would be capped as well. However, the prediction and the data give the mean number of innervated muscle fibres in this case as 210 and not 223 so a higher estimate was possible.

Therefore the prediction does not seem to be biased in any systematic way. This suggests that in the case of two remaining axons there is still some synapse elimination occurring which cannot be explained purely by competition. With three remaining axons competition is a sufficient explanation for all synapse elimination.

This result is comparable to what Fladby and Jansen (1987) found, namely that MU

sizes in muscles with up to five motor units were smaller than would be expected if no intrinsic withdrawal occurred, however muscles with seven remaining motor units (or more, presumably, though data for more than seven MUs was not shown) had the expected MU size.

This result is consistent with the idea that there is a maximum MU size, possibly determined by the intrinsic resources of the neuron, above which neurons retract some of their synapses (Rasmussen and Willshaw, 1993). The more neurons left after partial denervation the more π-junctions that will remain with ongoing competitive interactions. This competition acts to decrease the number of synapses of each neuron. If the MU size is decreased sufficiently by competition no intrinsic withdrawal will occur, however if there is too little competition the neuron may not be able to maintain each synapse.

Taken together these data support the conclusions of Thompson and Jansen (1977) and Fladby and Jansen (1987) that synapse elimination can still occur in the absence of competition. Moreover it appears as though the largest motor units are sensitive to non-competitive elimination and when competition sufficiently reduces MU sizes no intrinsic withdrawal occurs.

The third line of evidence is morphological. Most adult muscles with neonatal partial denervation did not have any uninnervated endplates. This is consistent with previous results that uninnervated muscle fibres atrophy over development. Fladby and Jansen (1987) comment that partially denervated mouse soleus muscles contained fewer uninnervated muscle fibres than completely denervated muscle. It is plausible that the active motor neurons hasten the degeneration of uninnervated fibres. There were some muscles fibres with more pretzel-like endplates in completely denervated muscles though these were distinguishable from innervated adult endplates. Pun et al. (2002) found that endplates could form in the absence of innervation in some muscle fibres whereas in others they did not. While most adult muscles with neonatal partial denervation had no uninnervated endplates, there were a few muscles in which a handful of endplates were uninnervated. One interpretation of these images is that the axon has recently withdrawn its synapses from these endplates. As these are static images it is not possible to be certain about this interpretation. Other possibilities are that the

endplates were damaged during the dissection causing the YFP to leak out or that the endplates are innervated by an axon that happens to not be fluorescent. Both these explanations are unlikely. In figure 3.8B there are three uninnervated endplates in different areas next to fluorescent endplates. If the axon had been damaged there should be a pool of fluorescence around the endplate (see appendix B) and the uninnervated endplates should all be in the same area (unless the muscle was damaged once in each area and only the YFP from the endplate region escaped). The second alternative explanation is also not likely because this is a YFP16 muscle and in control muscles I have never seen a group of uninnervated endplates (indicating a non-fluorescent axon). Furthermore the smallest MU size seen in the unoperated adult 4DL is 35 which is ten times larger than a motor unit with only three endplates. Despite this, it is not clear if the empty endplates really are the morphological manifestation of intrinsic withdrawal or whether they are due to unintentional damage to the muscle by the mouse some time before the dissection or some neurological abnormality. They are however consistent with the idea of intrinsic withdrawal and taken together with the other two lines of evidence strengthen the conclusion that it does occur.

3.4.3 Criticisms of the experimental design

I have shown that synapse elimination occurs, but I have not shown that it is caused by intrinsic properties of the motor neuron rather than external environmental changes due to the procedure. Lubischer and Thompson (1999) have argued that partial denervation experiments are not a good model for testing intrinsic withdrawal because the motor units remaining after partial denervation are not normal and the changes that happen after partial denervation could lead to synapse elimination as a secondary consequence. Because this is important for the interpretation of this experiment I will address the criticisms one by one.

Synapse elimination could occur after partial denervation because some small synapses may be at the point of no return at the time of denervation and, even though the competition is removed, they still withdraw. While the idea that synapses can reach a 'point of no return' seems plausible and is predicted by the models of synapse elimination

(Rasmussen and Willshaw, 1993) this is unlikely to have influenced my results. In order to measure neonatal MU sizes I partially denervated at p5 and waited 48 hours until measuring MU sizes. Synapses can gain and lose area in less than 24 hours during development (Walsh and Lichtman, 2003) so two days should be enough time for any synapses at the point of no return to have been eliminated.

Another criticism is that synapse elimination might occur in response to other changes brought about by partial denervation. Trachtenberg and Thompson (1996) showed that terminal Schwann cells degenerate in neonates after denervation. However, this should not affect the terminal Schwann cells at the endplates that are still innervated and accordingly Lubischer and Thompson (1999) mention that there is loss at denervated but not at innervated junctions although they do not quantify this. Therefore the Schwann cells are assumed to be intact in innervated endplates after partial denervation.

Moreover Lubischer and Thompson (1999) found that synaptic strength of preserved motor units decreases after partial denervation. This may lead to the criticisms that very small terminals do not provide enough signal to activate the muscle fibre which may then degenerate as if it has been denervated. However, as stated before synapses can grow and retract quickly during development and therefore should be able to grow sufficiently to activate the synapse or be eliminated by two days later. Specifically Colman et al. (1997) say that their analysis shows that *"1 day or less is necessary for fibres to become singly innervated once their inputs differ in quantal content by at least a factor of 4"* and when the quantal contents differ by a factor of four the weaker input can still elicit a postsynaptic response.

The fact that synapses become weaker is consistent with the idea that as the animal is growing, extra strain is put on the motor neuron. Lubischer and Thompson (1999) even mention this at the end of the discussion: *"Our results are consistent with the hypothesis that increased nerve growth at some sites along the axon can cause loss of terminal branches at other sites.*" With relation to the modelling, this describes the competition for and redistribution of the pre-synaptic resource, A_0, amongst branches belonging to the same parent motor neuron.

In conclusion the experimental design of assessing neonatal motor unit size two days after partial denervation, although done as a necessity, since the resolution would not

otherwise permit the assessment of neonatal MU size, is also an advantage because it results in both the neonatal and adult MUs having undergone exactly the same procedure so any systematic error introduced by partial denervation should affect both samples.

3.4.4 Discussion about the modeling

The experimental evidence suggests that intrinsic withdrawal does occur and, specifically it occurs to a higher degree in larger motor units. The cause of intrinsic withdrawal is not known, but one strong hypothesis is that intrinsic withdrawal occurs due to the motor neuron having a limited size capacity. There is certainly abundant evidence in the literature that neurons may have a limited capacity for growth as discussed in the introduction to this chapter. Moreover the idea that the phenomenon of intrinsic withdrawal in motor neurons may be specifically due to the limited resources of the neuron has been previously proposed many times (e.g. Lubischer and Thompson, 1999). Studies on the limited capacity of neurons have looked at growing branches before they reach their targets and assessed the amount of extension or retraction. Postnatally at the NMJ, axons have already reached their targets and formed synapses, but at the same time animals are still growing during development and throughout at least the first six months of life. This means that the distance from the motor neuron cell body to the synapse is getting larger, each synapse is getting larger and the diameter of the axons is getting larger. For example a mouse's length can increase by three times from the end of the developmental period until six months of age (Balice-Gordon and Lichtman, 1990)

The hypothesis I examined in the third part of this chapter, using a modified version of the Rasmussen and Willshaw (1993) model, is that intrinsic withdrawal could be the result of the motor neuron not having the resources to keep up with the normal growth of the animal, leading sibling branches to compete with each other for the motor neuron's internal resources and some of the branches to be withdrawn.

The Dual Constraint Model, as implemented by Rasmussen and Willshaw (1993) assumes there is a presynaptic resource and a postsynaptic resource which combine to

form a product which is proportional to synaptic area. Although the postsynaptic resource has been thought to be some kind of neurotrophin in these types of models, increasing the postsynaptic resource does not lead to sustained polyneuronal innervation. In contrast it leads to more intrinsic withdrawal. Therefore, perhaps it is more accurate to think of the postsynaptic resource as some structural element necessary and perhaps encouraging to the growth of the synapse. The more of this postsynaptic resource there is the more presynaptic resource will be required to match it and the more strain will be placed on the neuron, leading to stronger competition between the axon branches which it is supporting.

I have implemented the Dual Constraint Model as described in Rasmussen and Willshaw (1993) and shown that my implementation works just as described in the paper. This original model already can account for the experimental results (see appendix D), as each motor neuron in the simulation has the same capacity, which is proportional to $\frac{A_0}{B_0}$, and therefore any motor neuron that starts off with more synapses than is specified by its capacity must lose some synapses. However, both the pre- and post- synaptic resources are fixed at birth. Therefore, there is no additional plasticity after synapse elimination is complete and each synapse has reached its maximum value. In mice synapses continue to grow at least throughout the first six months of life. I wanted to investigate the effect this growth would have on motor units during and after the developmental period and therefore I modified the model by making the postsynaptic resource increase in line with how NMJs increase in size over time. Four different types of equations were used to model the growth of synapses over time. The main difference between these is whether they are bounded (ie reach a maximum value) or keep growing forever. It is not clear from the data whether synapses reach a maximum before the end of the lifetime of the rodent or not. In the equation I have used for these simulations, synapses grow continually, but I have also tried a bounded equation and the effect is predictable, namely: synapses can be lost up until the point at which synapses stop growing and motor units remain stable from then onwards. This model assumes that neurons do not have a fixed capacity on the number of synapses they can maintain but rather this number changes as the size of each synapse changes. Therefore, each neuron can maintain more smaller synapses and fewer larger ones. In my simulation I have kept the presynaptic resource constant although the same effect

might occur if the presynaptic resource increased at a slower rate than the postsynaptic resource.

This version of the model is also capable of replicating the experimental results. Additionally, it provides the prediction that after six months further decreases in motor unit sizes will have occurred. In other words it predicts that intrinsic withdrawal should not only occur over the first three weeks of development but rather, if it is driven by increases in size, then it should occur over the first six months at least. Without this assumption is it hard to understand why the animal might have a specific restricted capacity at three weeks but then continue to grow two to four times in size without any additional elimination necessary.

Finally I used this model, with an increasing postsynaptic resource, to investigate normal development. In this case no muscle fibres were denervated during the developmental period, suggesting that, while the limited presynaptic resource may weaken a neuron's synapses, the weakest are always chosen for elimination and these always correspond to polyneuronally innervated muscle fibres. Thus, as proposed by Rasmussen and Willshaw, the intrinsic capacity of the neuron seems to influence synapse elimination in conjunction with competition and not as an additional separate mechanism. Interestingly, once each muscle fibre is mono-neuronally innervated, this model predicts that some intrinsic withdrawal may occur as the animal increases in size if one of the neurons has 'won' too many synapses. The model does not incorporate sprouting, but in a real muscle the empty endplate would be expected to be re-innervated by a sprout from a different motor neuron. There is evidence for a limited amount of synaptic re-organisation in adult muscles and some instances have been observed in our lab of terminal sprouts innervating a synapse in unoperated adult muscle. This could be an indication that the specific endplate was vacated at some point after the developmental elimination period.

One property of motor neurons which is not accounted for in this model is the sprouting response after partial denervation in the adult. Although there is evidence that the sprouting response weakens with age (Kerezoudi and Thomas, 1999; Jacob and Robbins, 1990), adult motor units can sprout up to four to five times their original size in response to partial denervation. If they have this capacity since birth, i.e. if the ratio

$\frac{A_0}{B_0}$ is such that the maximum number of synapses a motor neuron can support is four to five times as many as seen normally, then intrinsic withdrawal must not be the result of a limited capacity but rather it must occur for some other reason. Alternatively, after partial denervation the capacity of the neuron (A_0) may increase for some reason, either due to genetic changes within the neuron which could result from the release of neurotrophic factors from muscle fibres or glia cells or for some other reason.

These data suggest that intrinsic withdrawal does not normally occur during the developmental period. Rather the intrinsic capacity of the neuron serves to influence the outcome of competition.

3.4.5 Conclusion

In conclusion I have provided good evidence that intrinsic withdrawal can occur and that when it does it is the neurons with large MUs that are more affected. I have attributed this to the neurons having a limited presynaptic resource and as the animal grows, the neuron is able to maintain fewer synapses. I have tested the consequences of this hypothesis by modifying the Rasmussen and Willshaw (1993) model to include an increasing postsynaptic resource which increases in line with the normal growth of the animal. This model provided two specific predictions which can be tested experimentally.

First, the range of motor unit sizes should decrease as the animal grows older. This could be tested by measuring the range of motor unit sizes at various ages in YFP animals.

Second the mean motor unit size after partial denervation should decrease as the animal ages. This could be shown by replication of this experiment but with multiple endpoints covering a wider range of the lifespan of the animal. The prediction is that motor units should be closer to the normal adult size (i.e. undergone more intrinsic withdrawal) the older the animal is. The only study which has looked at sizes at multiple time-points is that by Thompson and Jansen (1977) and there is no obvious trend for longer time points to be associated with smaller motor unit sizes. However, the authors lumped together all the observations above four weeks.

Chapter 4

Results: Sibling Convergent Innervation

4.1 Introduction

During the initial development of the peripheral nervous system it is thought that axons are guided by molecular cues and geometric constraints to innervate the correct region (Jacob et al., 2001; Jansen and Fladby, 1990; Jacobson, 1978), but within these target regions models of synapse formation and elimination assume that synapses are initially formed non-selectively (Willshaw, 1981; Jacobson, 1978).

At the neuromuscular junction, synapse elimination is at least partly driven by competition between axon branches converging on the same endplate (Betz et al., 1980; Thompson and Jansen, 1977; Fladby and Jansen, 1987, and see chapter 3). The outcome of this competition is evidently influenced by differences in neuronal activity (Ribchester and Taxt, 1983; Ridge and Betz, 1984; Barry and Ribchester, 1995), hierarchical identity (Kasthuri and Lichtman, 2003) and synaptic strength (Buffelli et al., 2003).

This chapter investigates the assumption that synapses formed by motor axons onto muscle fibres are initially random, a key principle in most published models of neuromuscular synaptic competition (Willshaw, 1981). This is an important issue because

given this tenet, there should be frequent instances where two or more branches from a single motor axon converge to innervate the same motor endplate. However, apart from occasional pre-terminal branching, this is not observed in adult muscles. If sibling convergence does indeed occur during development, this would not only be consistent with the idea that initial innervation patterns are formed randomly, it would also suggest that all but one branch must be selectively eliminated through competition with the others. This is important because competition at the NMJ is always discussed under the assumption that the competing arbours belong to different neurons. None of the published models of competition discusses whether it could accommodate competitive within-unit synapse elimination. In fact, the factors which have been shown experimentally to influence the outcome of synaptic competition rely on inter-neuronal differences. Specifically, distinct neurons have asynchronous activity patterns and differ in their intracellular constituents (which could suggest differences in a presynaptic resource). It is not clear how axon branches from the same neuron could be differentiated.

In this chapter I used both regenerating and developing motor axons to address the question of whether within-unit convergence on a single muscle fibre occurs. In order to study the patterns of connections made by single fluorescent motor units from the earliest stage of re-innervation, transgenic thy1.2:YFPH mice were used, in which only a small, random subset ($\sim$5%) of motor neurons are fluorescently labelled (Feng et al., 2000b; Keller-Peck et al., 2001b).

Two muscles were used for investigating developing motor axons: motor units in the levator auris longus (LAL) muscle were imaged at high resolution from p5-p6 transgenic thy1.2:YFPH mice and single motor units in the 4th deep lumbrical muscle of thy1.2:YFP16 mice were imaged at p8 after partial denervation at p5.

The data show unequivocally that (1) regenerating sibling axon branches can and do innervate the same muscle fibre, and developing motor axon branches appear able to do so as well, but (2) the frequency with which intra-neuronal convergence occurs appears lower than expected in a random and independent model, both for regenerating and developing motor units, and (3) converging branches are absent from control adult muscles and their frequency declines in later stages of regeneration, raising the issue

of how such convergent sibling connections can ultimately be eliminated or pruned.

4.2 Methods

In order to investigate sibling convergence three different systems were used.

4.2.1 Regenerating lumbrical motor axons

Adult (8-46 weeks, mean age:21 weeks) YFPH/BL6 mice were anaesthetised and the tibial and sural nerves were crushed bilaterally (for details see section 2.2). Mice were allowed to recover either 12-14 days, 34-35 days or $>$70 days and compared with control YFPH/BL6 mice (6-17 weeks, mean age: 12 weeks). Mice were sacrificed by a schedule 1 procedure and the lumbrical muscles 1-4 were removed, stained, fixed and mounted on glass slides (see sections 2.3 to 2.4.4). Lumbricals were viewed under a fluorescence microscope (see section 2.5.1) and muscles with a single fluorescent motor unit (non-fluorescent units were also present in these preparations) were selected for further analysis. These muscles were imaged using a Biorad Radiance 2000 confocal microscope and almost every innervated endplate was captured using a 40x 1.3NA oil lens (see section 2.5.2).

4.2.2 Neonatal LAL motor units

Neonatal (p5-p6) YFPH/BL6 pups were sacrificed by overdose of anaesthetic and decapitated. The LAL muscle was dissected (see section 2.4.1), AChR were stained with TRITC-α-BTX and fixed in PFA. YFP was amplified using anti-GFP immunolabelling (section 2.4.3.3) and muscles were mounted on glass slides (see sections 2.4.2 to 2.4.4).

Muscles with a single fluorescent unit (non-fluorescent units were also present in these preparations) were imaged on a Zeiss inverted confocal microscope using a 63x 1.4NA oil objective (see section 2.5.2).

4.2.3 Neonatal lumbrical motor units

Neonate (p5) YFP16/BL6 pups were anaesthetised by chilling and the tibial nerve was cut bilaterally, causing partial denervation of the 4th deep lumbrical muscle (see section 2.2 and figure 3.1 for a schematic of the dual innervation of the 4th deep lumbrical).

Three days later (p8) pups were sacrificed by cervical dislocation and the 4DLs were dissected, stained with TRITC-α-BTX, fixed in PFA. YFP signal was amplified with anti-GFP immunolabelling and muscles were mounted on glass slides (see sections 2.3 to 2.4.4).

Muscles with a single remaining motor unit (no non-fluorescent units were present in these preparations) were selected for further imaging with a Zeiss inverted confocal microscope using a 63x 1.4NA oil objective.

4.2.4 Image Analysis

All images were analysed in ImageJ, Fiji, Adobe Photoshop and Gimp. Axons were traced and axon length measured using the 'Simple Neurite Tracer' plugin for Fiji. Diameter was estimated by measuring the width of the axon, using the ImageJ line tool. Montages were made using the 'Stitching' plugin in Fiji and by hand in Gimp and Adobe Photoshop (see sections 2.5.3 and 2.5.4).

4.2.5 Statistical Analysis

Statistical tests were performed in R or SPSS. Quoted values are mean ± SD unless otherwise stated.

4.3 Results

4.3.1 Sibling branches are expected to converge during development

During development, motor axons form more synapses than they ultimately retain. Similarly, supernumerary innervation occurs during the re-innervation of muscle fibres by regenerating motor axons. If each axon branch forms synapses randomly and independently from other branches, there would be no mechanism to prevent two branches of the same neuron (sibling branches) innervating the same motor endplate. Here I show the calculation for finding the expected amount of sibling convergence, given a specified number of muscle fibres and axon branches.

Note that if sibling convergence does occur, then the number of branches the axon of a neuron has and the number of endplates it innervates, both of which are thought of as being the motor unit size, are no longer equal. In this chapter motor unit size will refer to the number of endplates innervated by a motor axon and may be smaller than the number of branches a motor unit has.

The frequency with which sibling convergence is expected to occur can be calculated exactly if the number of branches the axon of a motor neuron has and the number of potential innervation sites (i.e. muscle fibres) are known. The more branches a motor axon has and the fewer muscle fibres, the higher the incidence of sibling neurite convergence is expected to be. Section 4.3.2 shows the calculation in full. Based on this calculation, the probability of sibling branch (i.e. within motor unit) convergence for lumbrical and soleus muscles in mice and rats is shown in figure 4.1. According to the analysis all four of these muscles, given their respective estimated neonatal MU sizes, would be expected to contain on the order of 10-60 convergently innervated endplates by each motor unit at birth.

However, in control adult muscles, sibling convergent branches are not present. Examination of 165 NMJs from three different un-operated adult lumbrical muscles revealed only instances of short pre-terminal branches converging on an endplate. Specifically, there were 24 examples (15%) of pre-terminal branches with a mean length of 8.6 $\pm$

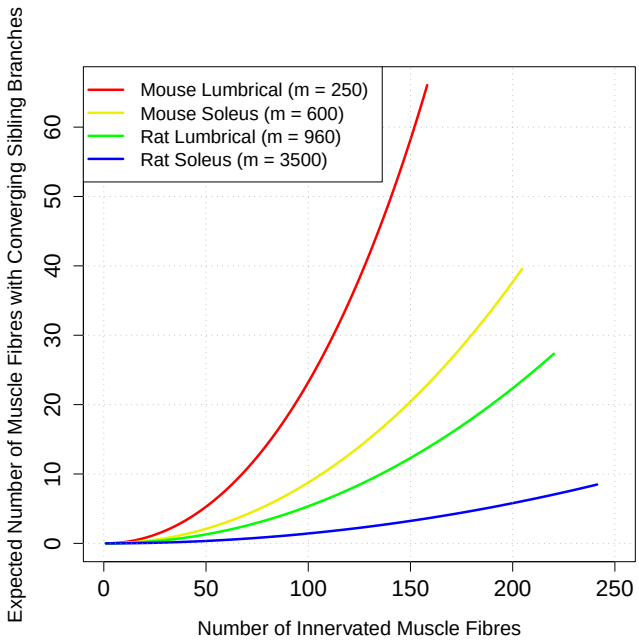

Figure 4.1: *Expected number of endplates convergently innervated by sibling axon branches of a single neuron plotted against the total number of endplates innervated by that neuron. The more branches an axon has and the fewer muscle fibres available to be innervated, the greater the number of expected convergently innervated endplates. For example in the mouse lumbrical muscle which has approximately 250 muscle fibres and neonatal motor unit size can be around 150, more than one third of endplates are expected to be innervated by more than one branch, if each branch innervates independently of other branches.*

6.3 μm (Range:2-17 μm, figure 4.3) and 141 (85%) NMJs which had a single branch innervating the endplate. There were an additional 39 endplates examined, in which the site of innervation was not resolvable, so these were excluded from all analysis. Figure 4.5A shows the three longest examples of pre-terminal branches (white arrows) found in the un-operated adult NMJs examined.

A consequence of these two results is that either sibling branches do converge on the same endplate, and are capable of competitive elimination; or branches from the same axon do not form synapses randomly and independently, ensuring that convergence does not occur.

4.3.2 Calculating the expected amount of convergence

Suppose a motor axon has b branches, each of which randomly and independently innervates one of m muscle fibres. The number of muscle fibres with two or more converging inputs from this same motor neuron will equal the total number of muscle fibres minus the number of muscle fibres that are innervated by either none or exactly one of the b branches.

$$M(2+) = m - M(0) - M(1) \tag{4.1}$$

Since each muscle fibre has an equal probability of being innervated, the probability that any given branch b_i will innervate a given muscle fibre m_j is $\frac{1}{m}$. Therefore the probability that m_j is not innervated by branch b_i is $1-\frac{1}{m}$. Since there are b branches, the probability of a muscle fibre not being innervated by any branch is $(1-\frac{1}{m})^b$. Thus, the number of muscle fibres which will be innervated by no branches is given by

$$M(0) = m(1-\frac{1}{m})^b \tag{4.2}$$

The probability of a given muscle fibre m_j being innervated by the first branch (b_1) and none of the others is equal to $\frac{1}{m}(1-\frac{1}{m})^{(b-1)}$. This is one way in which an endplate could be contacted by exactly one branch. Another way would be if it was only innervated by the second branch $(1-\frac{1}{m})\frac{1}{m}(1-\frac{1}{m})^{(b-2)}$ and so on. There are therefore b

different ways in which an endplate can become innervated by a single branch (one for every branch), so the total probability of an endplate being contacted by exactly one branch is $b\frac{1}{m}(1-\frac{1}{m})^{(b-1)}$. The number of endplates which will be innervated exactly once will be

$$M(1) = mb\frac{1}{m}(1-\frac{1}{m})^{(b-1)} = b(1-\frac{1}{m})^{(b-1)} \tag{4.3}$$

Therefore, by substitution in equation 4.1, the expected number of muscle fibres innervated by converging sibling branches is

$$M(2+) = m - m(1-\frac{1}{m})^{b} - b(1-\frac{1}{m})^{(b-1)} \tag{4.4}$$

Equation 4.4 calculates the numbers of endplates with converging sibling branches given a certain number of branches. From this it is also easy to calculate the number of endplates expected to have converging branches given the number of endplates which are innervated (i.e. the motor unit size). This is done by using equation 4.2 to solve for b, the total number of branches required to get the observed motor unit size, given the number of endplates.

$$\frac{M(0)}{m} = (1-\frac{1}{m})^{b} \Rightarrow \frac{\log(\frac{M(0)}{m})}{\log(1-\frac{1}{m})} = b \tag{4.5}$$

In order to calculate the number of converging branches expected in various observed muscles, equation 4.5 was used to calculate how many branches are needed to result in the observed motor unit size and b was then substituted in equation 4.4. This gives a very similar but slightly smaller result to just finding the difference between b and the motor unit size, because the latter way does not take into account that some endplates might be innervated by more than two converging branches.

Both regenerating and developing motor axons were examined to determine if, and how often, sibling branches converge on the same muscle fibre.

4.3.3 Regenerating motor axons

During re-innervation after nerve crush motor axons form excess synapses leading to polyneuronal innervation which are then eliminated again resulting in mononeuronal innervation. The period of polyneuronal innervation after regeneration was used as a model for development because it is easier to visualise and resolve labelled axons in re-innervated adult muscles than it is in neonates. The tibial and sural nerves of adult mice were crushed once near the ankle, causing Wallerian degeneration of the distal axons, and allowed to regenerate between 12-131 days, before sacrificing the mice and observing the muscle. The operated mice were split into three groups, which were allowed to recover for different lengths of time. These groups reflect different stages during the regeneration process. Recovery times were 12-14 days, 34-35 days and $>$70 days.

The number of partially occupied endplates (defined as having less than 90% occupancy) differed between the groups, with approximately 20% (11/58) of endplates partially occupied at 12-14 and 34-35 days, compared with no partially occupied endplates in the control group and 1/32 (3%) in the $>$70 day group (these numbers are based only on endplates with converging sibling branches). This was taken as an indication that polyneuronal innervation is present up to 35 days after crush, but excess synapses have largely been eliminated by 70 days post-crush. Two examples of partially innervated endplates can be seen in figure 4.2.

Motor unit sizes were not significantly different between these groups, nor compared with control motor unit sizes (ANOVA, p=0.23). This is contrary to the expectation that, during the period of polyneuronal innervation, motor units may have an expanded motor unit size. However, since these are regenerating units, and the extent of polyneuronal innervation at any one time is lower than in development, it could be anticipated that there will not be a big difference in motor unit size at any one time.

Based on the occupancy data, it is assumed that muscles from the first two time points after nerve crush (12-14 days and 34-35 days; early regeneration) are still in a dynamic state of re-organisation with ongoing synapse elimination, whereas muscles from later time points ($>$70 days) have a more stable morphology largely devoid of polyneuronal

innervation.

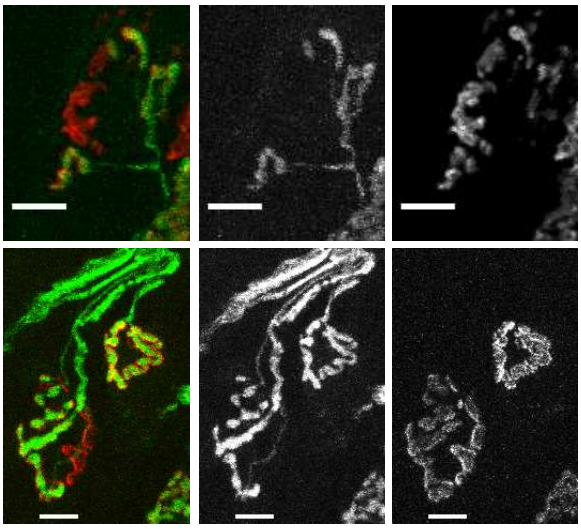

Figure 4.2: *Two examples of partially innervated endplates from 34 days after crush. On the left are the merged confocal image projections, centre shows the axon only (YFP) and right shows the endplate only (α-BTX). Scale bars 10 µm.*

4.3.3.1 Regenerating sibling branches can converge on the same endplate.

All of the muscles used in this analysis had a single fluorescent axon which only branched intramuscularly. Therefore any converging branches found would be from the same axon. Other, non-fluorescent axons were also present in the preparation. I imaged 700 NMJs from nine different muscles in the early stages of re-innervation (12-14d and 34-35d). Of these 176 (25%) were not adequately resolved and excluded from further analysis. Of the remaining 524, 67 endplates (13%) were innervated by more than one branch (figure 4.5B & C) and 457 endplates (87%) were innervated by a single un-branched terminal. The convergently innervated endplates included instances of normal pre-terminal branching, similar to that seen in control animals, as well as instances of converging branches which were quantitatively and qualitatively different.

4.3.3.2 Quantitative difference between the groups

Branch lengths were not normally distributed in any group (as determined by the Kolmogorov-Smirnov test), and therefore the data were transformed by taking the logarithm before performing statistical tests. After the transformation the distributions of lengths were normally distributed, but their variances were still significantly different. The post-hoc Dunnett's T3 test was used which does not assume equal variances.

The average length of branches (including terminal and converging branches) from the common branch point to the endplate was 28.4 ± 33.8 μm at 12-14 days after crush and 26.9 ± 36.8 μm at 34-35 days after crush (figure 4.3) both of which are significantly longer than control values (both comparisons $p<0.01$, Dunnett's T3 after ANOVA) but not significantly different from each other($p=0.99$, Dunnett's T3 after ANOVA).

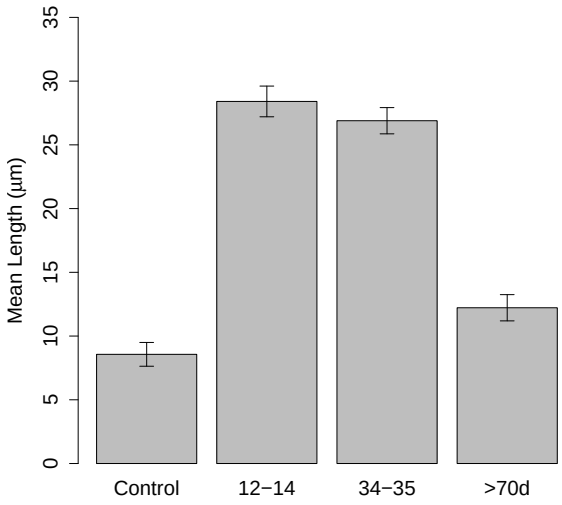

Figure 4.3: *Average lengths from the common branch point to the endplate for muscle fibres which are innervated by two branches. These means include both pre-terminal branches and converging sibling branches. Error bars show SEM. Converging sibling branches are longer up to 35 days after crush which presumably reflects the fact that the population is made up of a mixture of pre-terminal and converging sibling branches.*

4.3.3.3 Qualitative difference in branches between groups

Additionally, there were 18 instances where one of the converging branches was a sub-branch of the axonal arbour at the common branch point, i.e. the axon branched one or more times between the common branch point and the convergently innervated endplate (see figure 4.7). In most of these cases (13; 19.4% of all convergently innervated endplates) the other sub-branch innervated a different endplate. In a minority of cases (5; 7.5%) the additional sub-branch innervated the same endplate (triple convergent innervation). The first case was never observed in the control group. In the >70d group there were only two instances of this (5.4%). Triple innervation was also seen in three cases in the control group (12.5%) and in three cases in the >70d group (8.1%).

There were also three instances in the non-ambiguous endplates where one of the converging branches appeared to be a terminal sprout from a different endplate. Overall, there were more examples of this, but these were often ambiguous as it was not possible to tell which endplate the sprout had originated from and which it was innervating. Again, this was never observed in the control group and only once in the >70d group (figure 4.5D third from left; there was also an example where both branches were terminal branches from the same endplate, see figure 4.5D left image).

Figures 4.9 and 4.10 show an entire regenerating motor unit which has been traced and represented in a diagram. Many of the unusual morphological features described above can be seen in this example. For instance, endplate 28 is innervated by one collateral which has branched three times since the common branch point and a second one which is a terminal branch from endplate 23. A magnified image of this endplate is shown in figure 4.5B, middle image.

4.3.3.4 The frequency of convergence is less than expected by chance

As mentioned above, the motivation for looking for converging sibling branches was based on calculating the expected number of converging sibling branches for a given number of muscle fibres (m) and a given motor unit size, under the assumption that each branch innervates muscle fibres independently and randomly.

In muscles up to one month after nerve crush there are significantly fewer endplates with converging sibling branches than predicted based on the assumptions above. For each muscle, I calculated the ratio of the observed number of endplates with converging branches divided by the predicted number of endplates with converging branches. The ratio will be one if the prediction matches the observation. Numbers below one mean there was more convergence predicted than observed and numbers above one mean there was less convergence predicted than observed.

The mean ratio for the early regeneration groups was 0.62 ± 0.4 and was significantly different to one (one-sample t-test, p=0.023). This is despite the fact that the number of endplates counted as being innervated by converging branches presumably represents a mixed population, containing endplates with pre-terminal branches and endplates with sibling converging branches.

A complication when interpreting this result arises because some synapse elimination has already occurred and therefore it is not clear whether to attribute the reduced number of converging branches to selective synapse formation or selective elimination. In other words it is not possible to use these images, in order to differentiate whether fewer than expected converging synapses were formed or whether some have already been eliminated.

4.3.3.5 Converging sibling branches may be competitively eliminated

The fate of these long converging branches was investigated in the group of animals which were left to recover for $>$70 days (range: 74-131 days, mean: 100.8 days). By this point it is assumed that synapse elimination is complete and the morphology is largely stable. Images of 427 endplates from eight different muscles were analysed. Of these, 100 (23%) were excluded due to inadequate resolution. Of the remaining 327, 37 (11%) were convergently innervated by more than one branch and 290 (89%) were singly innervated. Overall the average length of the branches which were convergently innervating endplates in this group was significantly shorter than those measured at 12-14 days after crush (p=0.032 compared to 12-14d, Dunnett's T3 after ANOVA), though they were not significantly different from those measured 34-35 days after

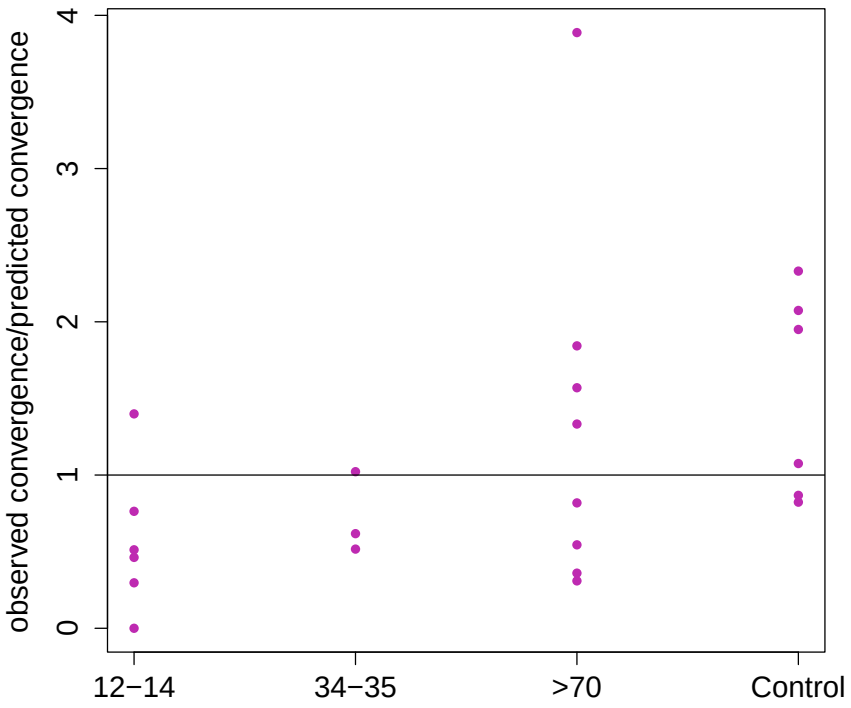

Figure 4.4: *Ratio of actual double innervated endplates over predicted convergence. If all double innervated endplates were due to converging branches then this ratio should equal 1 (see line). However, some of the double innervated endplates are due to pre-terminal branches. Despite possibly overestimating the number of convergently innervated endplates, there are still fewer than would be expected in early regeneration, given the motor unit sizes. Another interesting observation is that in the control group, where there are only pre-terminal branches, these seem to outnumber the expected convergence. Therefore it seems likely the control group has more pre-terminal branches than the experimental groups. Indeed, here the groups are ordered according to the age of the synapses and there is a tendency for an increase in the number of observed double endplates (compared to that predicted) while at the same time the average branch length of converging branches is decreasing.*

crush or control lengths (range: 2.6-46.6 μm, mean: 12.2 $\pm$ 9.3 μm, ns, Dunnett's after ANOVA, figure 4.3). Figure 4.5D shows the four longest examples of converging sibling branches from this group.

The lack of long branches $>$70 days after crush can be seen more clearly in figure 4.6. Histograms of branch lengths show that at 12-35 days after crush there are some long branches which do not exist in control animals nor $>$70 days after crush. These data support the hypothesis that converging sibling branches can competitively eliminate each other.

Additionally, there is some morphological evidence consistent with the idea that converging branches can eliminate each other. Figure 4.8 shows two examples of what appear to be retraction bulbs (arrowhead) close to an endplate with a vacated area of synapse (arrow).

4.3.3.6 There does not appear to be a consistent relationship between the length of converging branches and the ratio of their diameters

Taking the fact that there are longer branches in early regeneration, together with the fact that a higher proportion of branches have an unusual morphology, suggest that converging sibling branches can be competitively eliminated. Given that axon thinning has been shown to precede synapse elimination and some of the long converging branches in early regeneration seemed to be innervated by a thin and a thick branch, I tested whether there was a difference in the ratio of the diameters (largest/smallest) of converging sibling branches, a possible indication that one branch was in the process of being eliminated. Diameter ratios and branch lengths were not normally distributed (p¡0.05, Kolmogorov-Smirnov) and therefore non-parametric tests were used. First I tested whether there was a correlation between branch length and diameter ratios, since pre-terminal branches were short and might have more equal diameters than long converging branches, where one branch was destined to be eliminated. However, there was no significant correlation between the average branch length and the ratio of the diameters of each branch, as determined by Spearman's rho test (see figure 4.11). Next I tested whether there was a difference in ratios between the different groups, as elim-

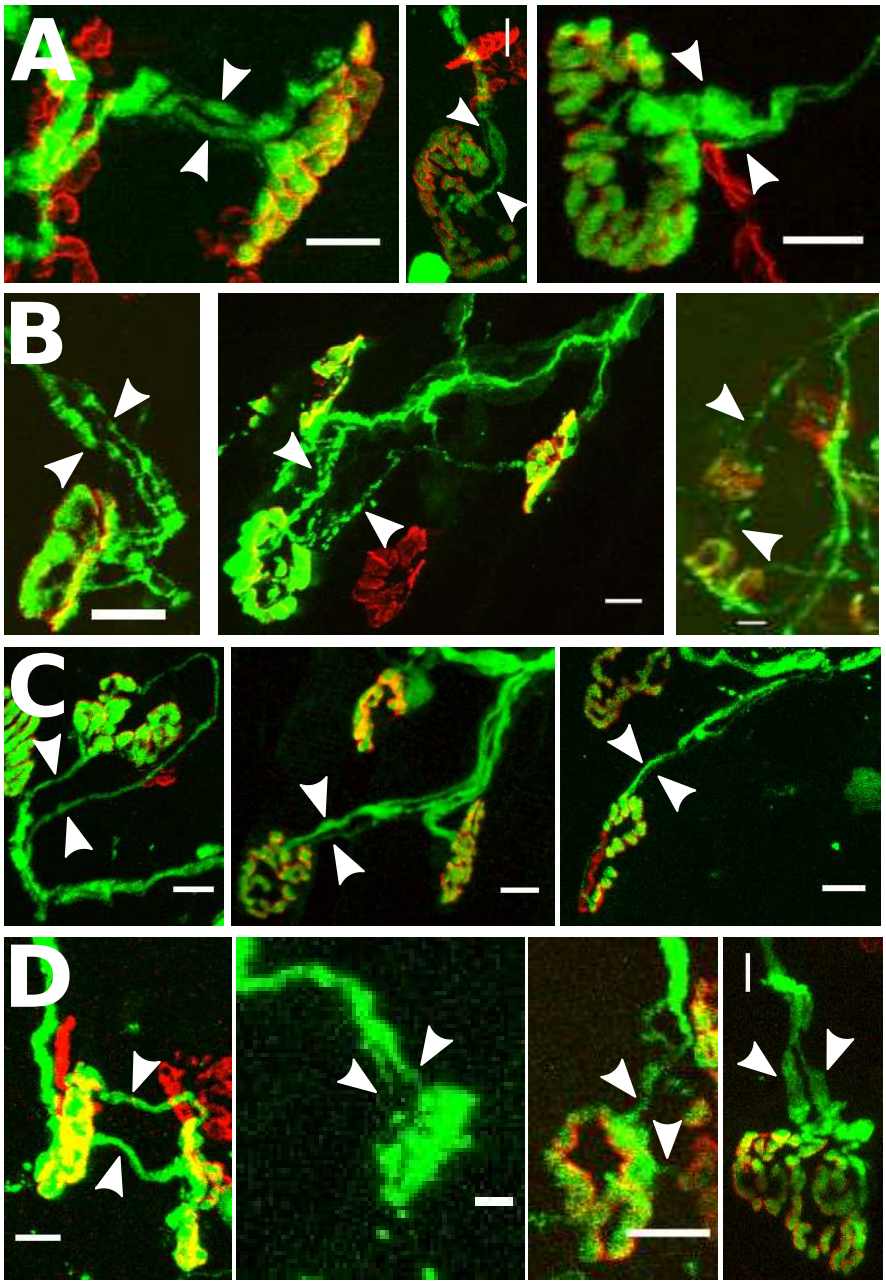

Figure 4.5: *Examples of endplates which were counted as being innervated by two branches in (A) control, (B)12-14d, (C)34-35d and (D) >70d groups. The converging branches shown from the control and the >70d groups show the* longest *examples in these groups. White arrowheads indicate the two innervating branches in each image. Scale bars: 10 µm*

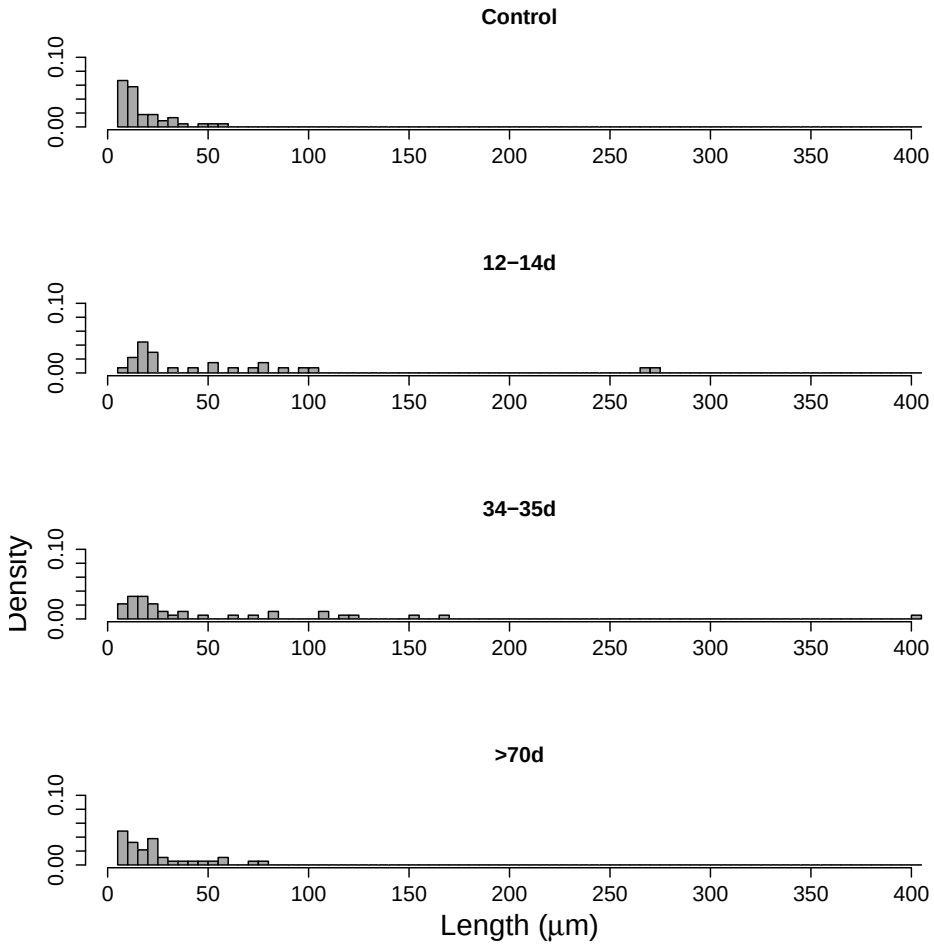

Figure 4.6: *Histograms of the distribution of branch length in the four groups. Early in regeneration (12-35 days) there are a few very long converging branches. Such long branches do not appear in either the control or $>$70d groups. Their absence from the $>$70d group suggests that one of the converging branches has been competitively eliminated.*

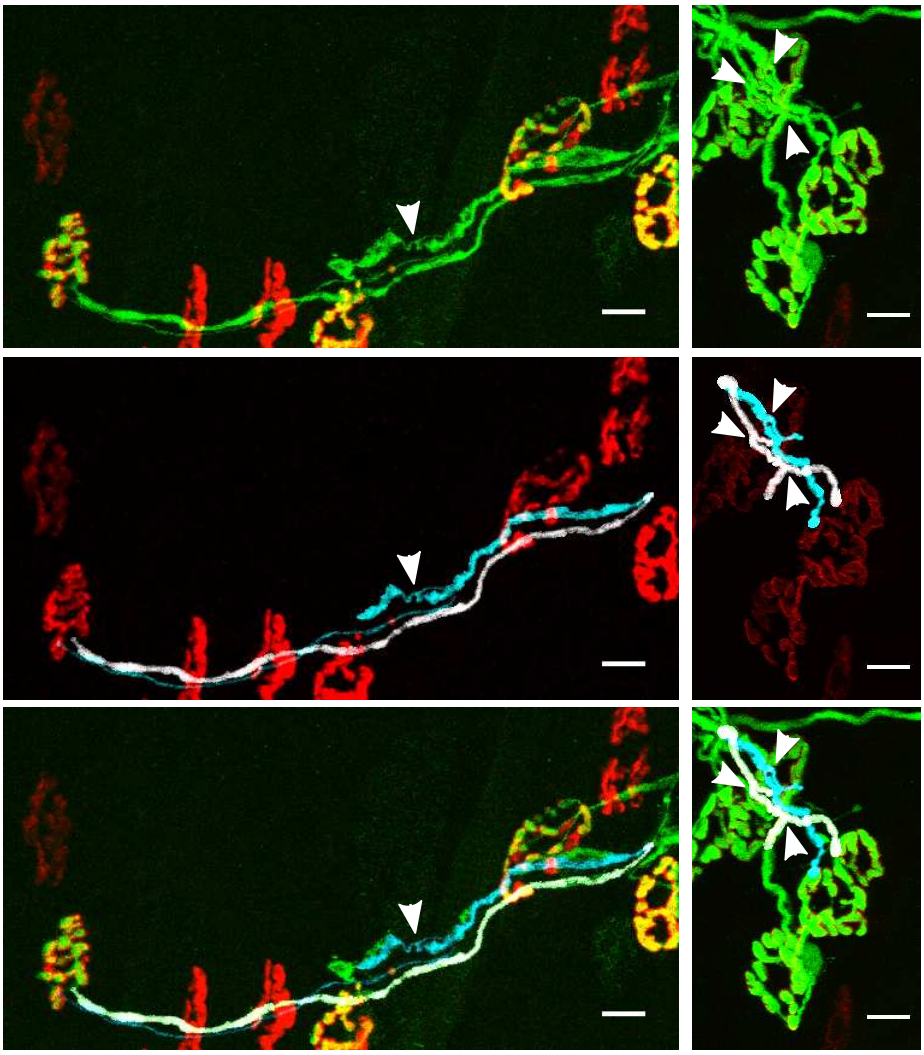

Figure 4.7: *Two examples of endplates which are innervated by long converging sibling branches that branch after the common branch point before innervating the endplate. This morphology is never seen in control motor units and only one example was found in the >70 day group. Top images show the axon (green) and endplates (red), middle show the traces and the endplates and bottom show the traces superimposed on the axons and the endplates. Scale bars: 10 µm*

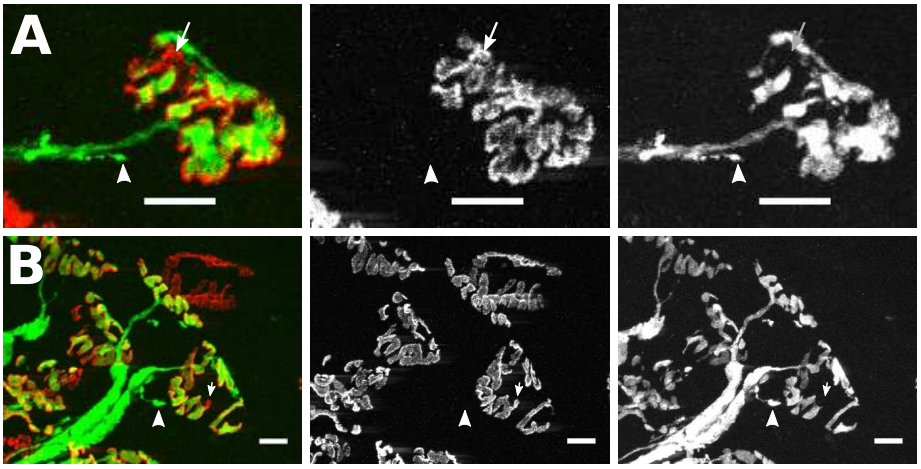

Figure 4.8: *Two examples of of what appear to be retraction bulbs (arrowheads) near endplates with a vacant postsynaptic area. Right panels show YFP only, middle panels show TRITC-α-BTX and left panels show the merge. Both examples are from the same muscle, which was dissected 12 days after nerve crush. Scale bars: 10 µm*

ination was only expected to be occurring in the early regeneration groups, so these might have higher ratios than the control and late regeneration group. Again there was no difference in the median ratios between the four groups (ns, Kruskall-Wallis). Therefore, these data do not support the hypothesis that there is a difference in the diameters of sibling converging branches.

4.3.3.6.1 Conclusion from regeneration experiment I have shown that sibling branches can converge on the same endplate during the first month of regeneration and they appear able to eliminate each other, since long converging branches are not seen at late time-points after crush. The frequency of convergence in early regeneration is less than expected by chance, though it is not clear if this is due to selective synapse formation or selective elimination.

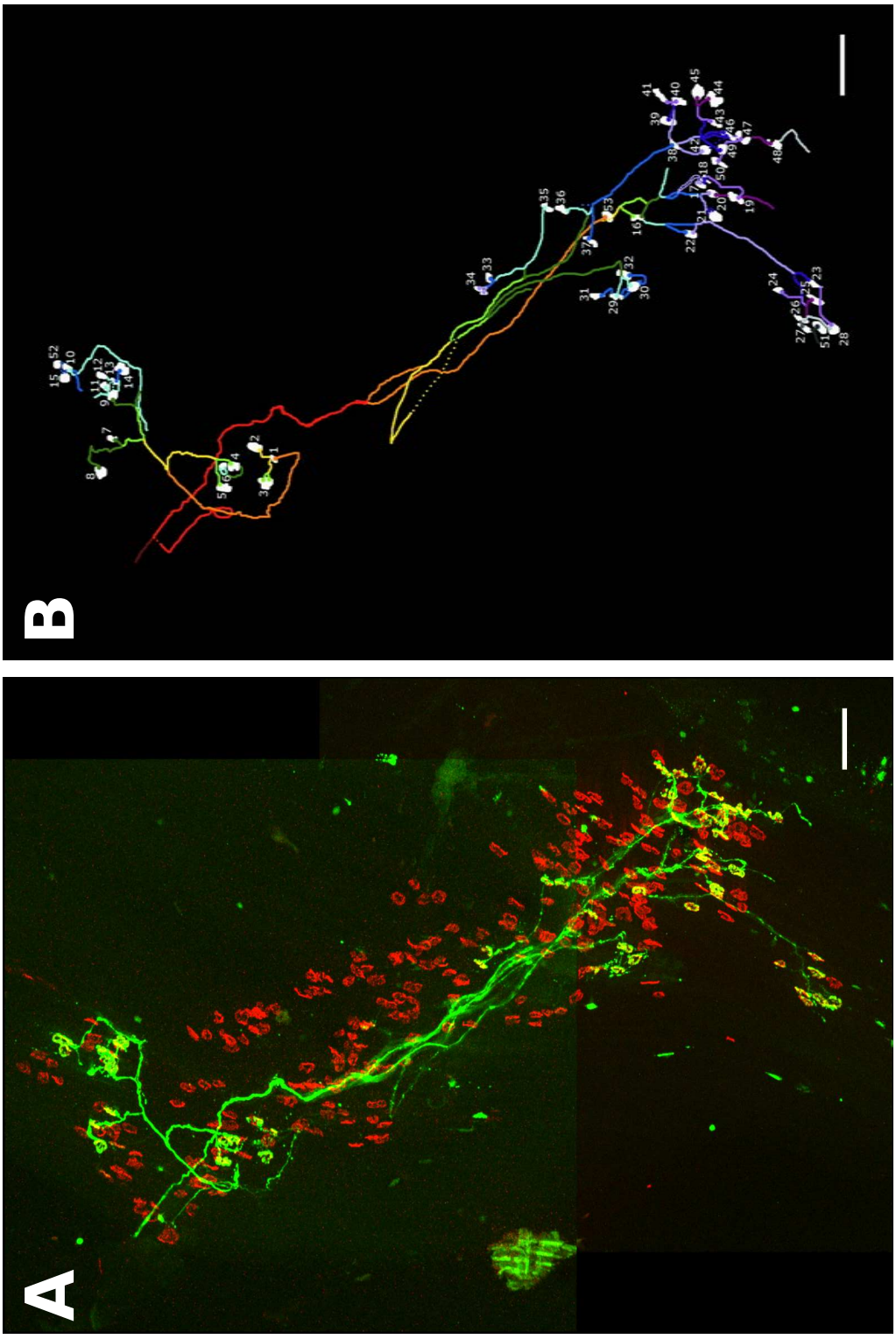

Figure 4.9: *A: An entire motor unit from 14 days post-crush. B: Traced motor unit in A. Each time the axon branches the colour changes, starting from dark red. Therefore, colour represents branch order. Each endplate is numbered and the numbering corresponds to that in figure 4.10. Dotted regions are regions of uncertainty. Scale bars: 100 µm*

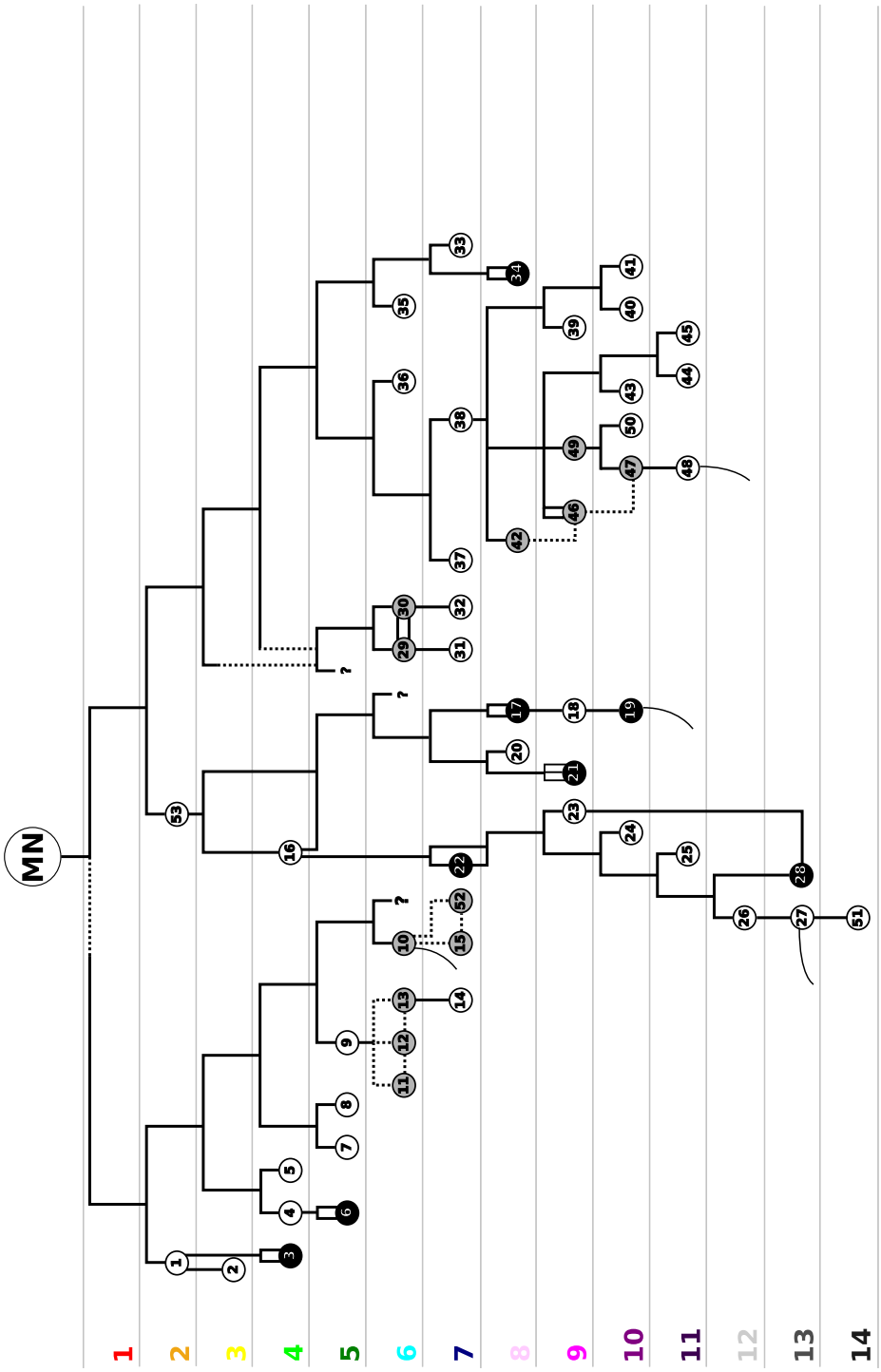

Figure 4.10: *Branching diagram of an entire motor unit from 14 days post-crush. Every endplate is numbered (numbers correspond to figure 4.9B). White indicates single innervation, black double innervation and gray endplates that are ambiguous. The level of each endplate is colour-coded to indicate branching order. For example, an endplate on line 5 shows that the axon has branched 5 times from entering the muscle to innervating the endplate. The colours are also used in figure 4.9B for showing the axons.*

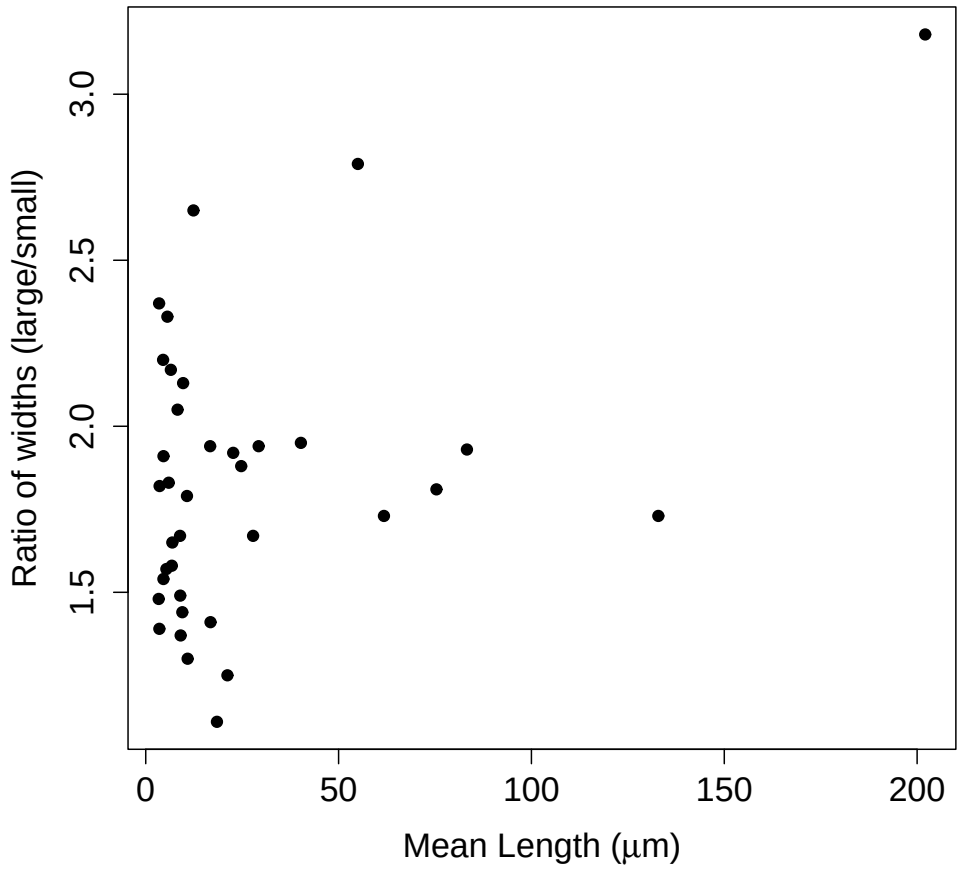

Figure 4.11: *Mean length of branches innervating an endplate plotted against the ratio of their widths (largest/smallest). There is no significant correlation between these variables.*

4.3.4 Developing Motor Units 1: Neonate YFPH LAL

In order to address whether sibling branches converge on the same endplate during development I imaged five single fluorescent motor units from three different p5- p6 mouse LAL muscles. This is a segmental muscle behind the ear (for details see methods section 2.4.1). Because of incomplete dissections it is unclear whether the axon trees imaged represent the entire motor unit or one branch of the motor unit. The number of innervated endplates varied between 15 and 61, (15,15,16,22,61, see figure 4.12).

Inspection of each of the 129 innervated endplates revealed 4 endplates which seem to be convergently innervated by two branches, 3 of which are part of the same motor unit (figure 4.13). A multi-layer tiff showing the 3D projection of each of the endplates shown in figure 4.13 can be found on the DVD submitted with this thesis in `Chapter_4.../neonate_LAL/`. In the 3D projection, endplates are shown in red and axons are shown with a 'fire' look up table. These files can be opened using Fiji or ImageJ. The 4th endplate is unusual as two endplates seem to be connected by a terminal branch (figure 4.12C although it is not clear which endplate the branch originated from. This pattern of innervation was seen during regeneration, but has not been observed in unoperated adult motor units. The rest of the endplates appeared to be innervated by a single branch.

The expected number of convergently innervated endplates can only be estimated after making certain assumptions (see section 4.4.1). Firstly, because this is a segmental muscle with motor units restricting their tree to one portion of the muscle (Murray et al., 2008) it is unclear how many possible innervation sites exist for each of the motor axons. I have made a rough estimate of the total number of endplates by only counting endplates close to the axon branches. These were between 31 and 224.

A second assumption involves specifying how many of the converging synapses will have already been eliminated by p6. Assuming none is eliminated, the number of convergently innervated endplates expected in these samples varied between 0.6-9. In total, across all muscles, 19 convergently innervated endplates would be expected although this number would be lower if more potential innervation sites had been in-

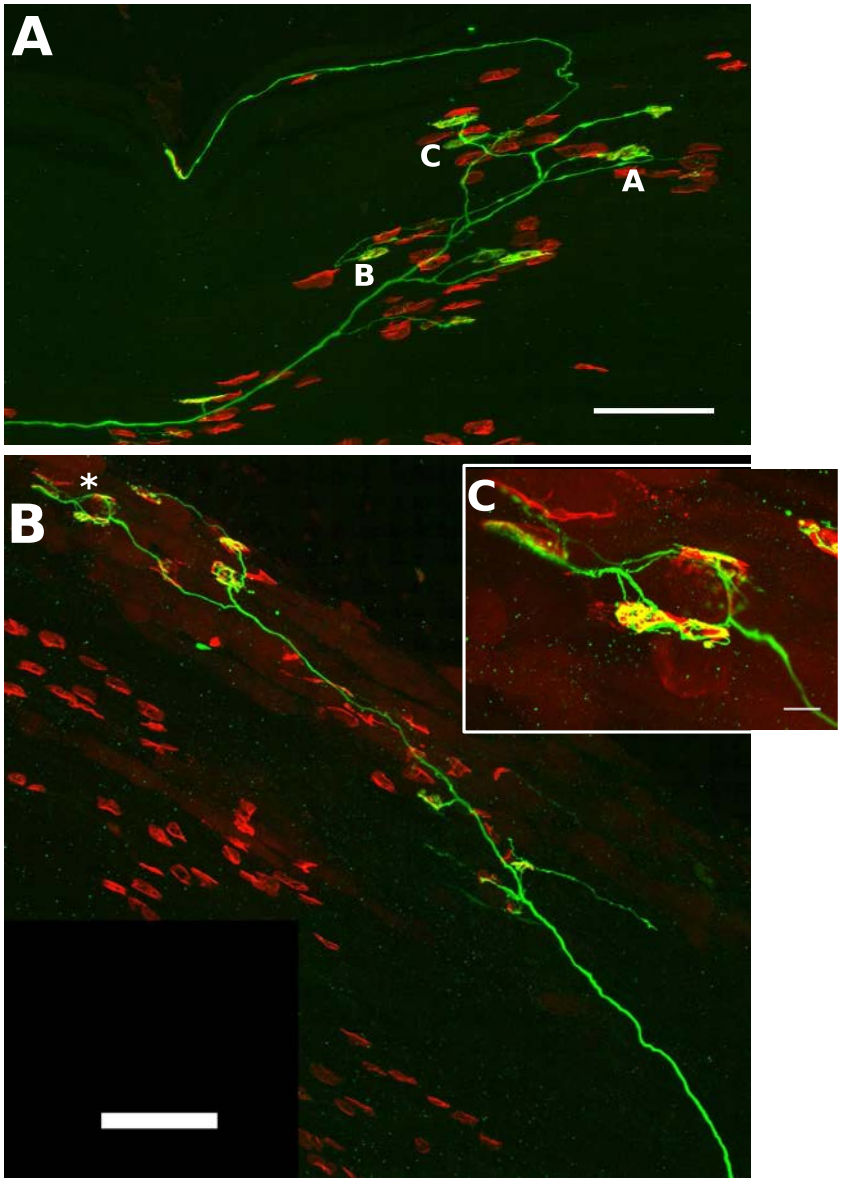

Figure 4.12: *Two YFPH LAL motor units. A: Motor unit with 15 synapses. The three best examples of convergence were found in this motor unit and are marked with letters which correspond to the images in figure 4.13. B: Motor Unit with 16 synapses. This motor unit had what appeared to be a loop between two synapses marked in the image by a star and shown in C. Scale bars A&B: 100 µm, C: 10 µm*

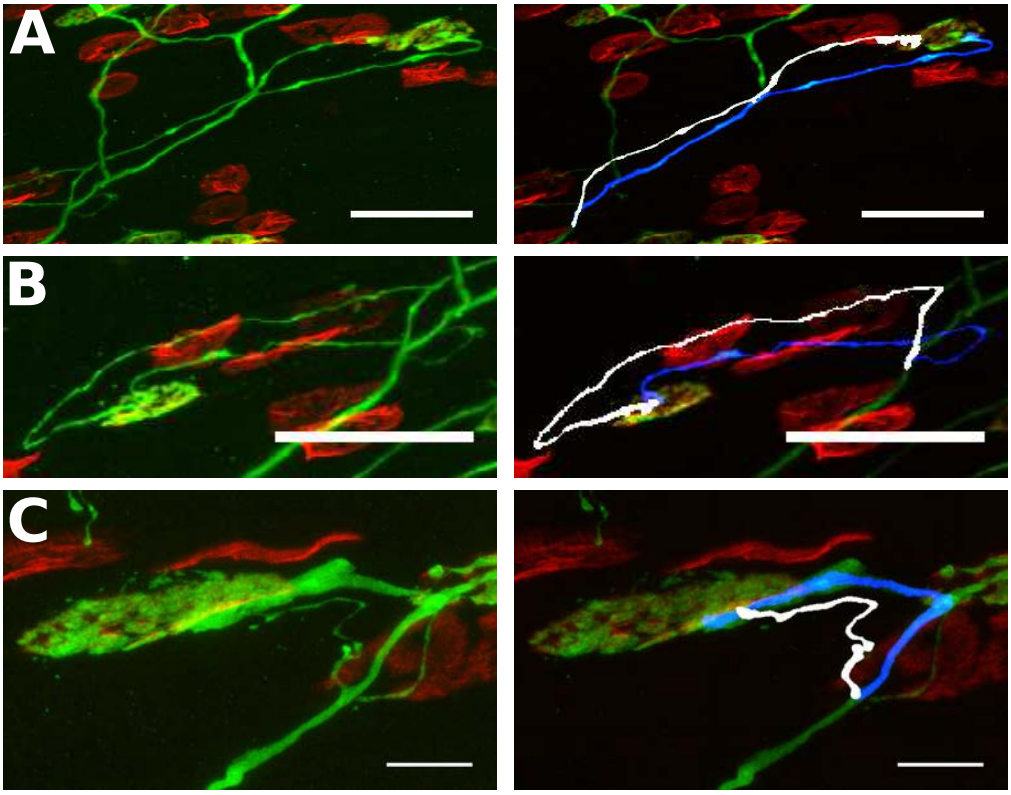

Figure 4.13: *Examples of three convergently innervated endplates from the motor unit shown in figure 4.12A. Scale bars in A&B: 50 µm, C: 10 µm.*

cluded.

From these data, it appears that sibling neurite convergence can occur during development. The fact that 4 examples were found is strong evidence that sibling branches can eliminate each other, since adult muscles do not seem to exhibit convergence. There are no examples in adult lumbrical muscles and there have been no reports of sibling convergence in adult LAL muscles. Murray et al. (2010) published a representative trace of an adult LAL motor unit which did not contain any sibling convergence. There were no examples of sibling convergence in the interscutularis connectome published by Lu et al. (2009b). However, it is not clear from these data whether sibling convergence occurs with the expected frequency.

One striking feature of these images is that, while more than one axon tend to fasciculate, when there is a single axon, branches do not travel along the same paths. This provide a clue to a possible mechanism where sibling branches repel or otherwise prevent each other from getting too close (see figure 4.14). A consequence of this mechanism could be the observation that sub-trees of a single motor unit innervate non-overlapping territories in contrast to sub-trees belonging to different neurons (Lu et al., 2009b). This was not observed to be the case for regenerating motor axons, where branches of a single axon was frequently found to fasciculate.

4.3.5 Developing Motor Units 2: Neonate YFP16 4DL

In addition to LAL motor units, I explored whether converging sibling branches exist in developing lumbrical muscles. Because YFPH is not expressed early enough in the lumbrical muscles, 4DLs from YFP16 mice were partially denervated at p5 and imaged three days later at p8. The degeneration of axons supplied by the LPN allowed observation of the full arboreal extent of intact sural nerve units. Two 4DL muscles with a single unit were imaged at high resolution. Both motor units were large and innervated more than 70% of the muscle (motor units sizes of 161 and 214). Since the lumbrical is not a segmental muscle and there does not seem to be a spatial bias in the innervation pattern, counting the total number of endplates is sufficient to determine the number of possible innervation sites. From the previous chapter, the adult average

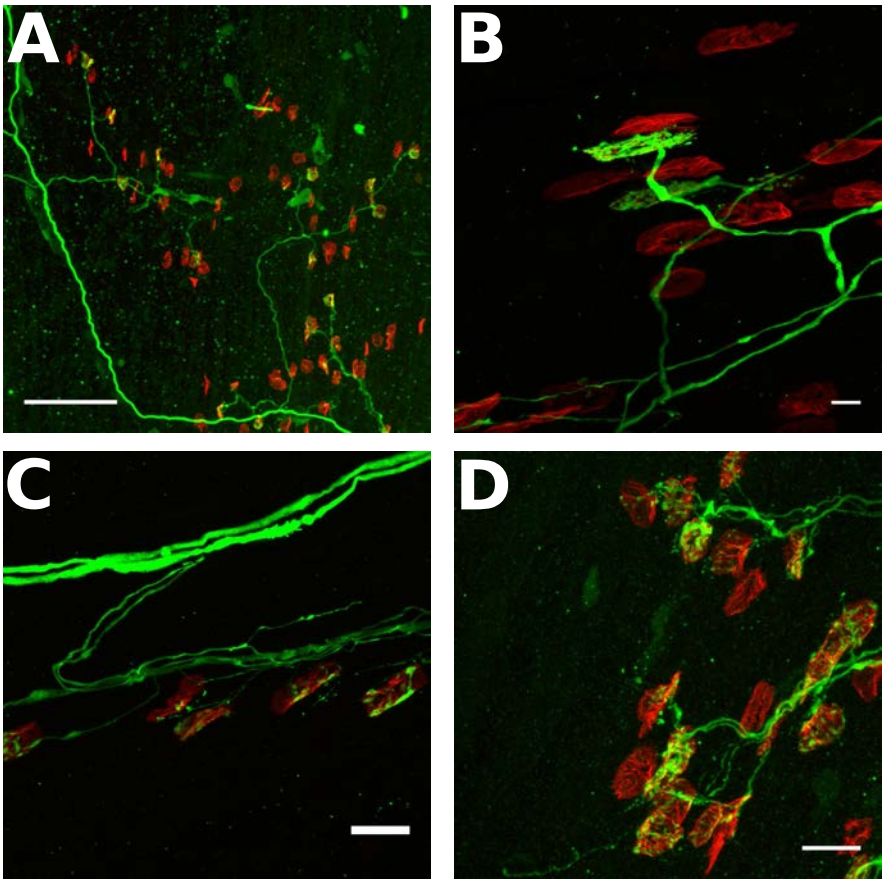

Figure 4.14: *Branches from multiple neurons fasciculate but branches from a single neuron do not. Examples of intramuscular nerves where there is a single fluorescent neuron (A&B) or more than one different fluorescent neuron (presumably, as there is more than one axon entering the muscle) (C&D). Axons from multiple neurons tend to fasciculate but branches from a single axon do not. Scale bar: 100 µm in A and 10 µm in B,C and D.*

motor unit size is found to be ∼50 which is three to four times smaller than these motor units. The average size of adult motor units that have been partially denervated at p5 is about 100. Therefore it seems likely these motor units were destined to decrease in size still by at least one third and up to four-fold.

Figure 4.15 shows low resolution images of the entire units. Given the motor unit sizes and the total number of endplates for these two units, approximately 100 endplates in each muscle are expected to be convergently innervated, assuming random and independent innervation.

Each endplate was scrutinised and most endplates appeared to be singly innervated. It is more difficult to assess the innervation pattern in the lumbrical because it is smaller than the LAL and the motor units are large. Despite the difficulty is assessing each endplate, in one muscle (figure 4.15A) there were no endplates which appeared to be convergently innervated. In the second muscle (figure 4.15B) there were approximately 10-15 endplates which were unresolvable from each other and a further 4 which could potentially be convergently innervated (figure 4.16). The 3D projection of each endplate in figure 4.16 can be found on the DVD submitted with this thesis in `Chapter_4.../neonate_4DL/`. However, there are no unambiguous or compelling examples of convergently innervated endplates, despite the fact that the expected number of convergently innervated endplates could be up to 100 in each of the muscles. This suggests that in the lumbrical muscle, convergence during development does not occur as often as would be expected by chance; in other words that there is some interdependence for synapse formation between different branches belonging to the same parent neuron.

For comparison, images of adult muscles with neonatal PD used in the previous chapter were scrutinised. Unfortunately most were not high enough resolution to determine how endplates were innervated. Of those that were, 77 innervated endplates were found of which 2 were innervated by a double branch. Both of these were most likely terminal branches, as their lengths were quite short (maximum length 6.8 μm) and within the normal terminal branch range. There were also 10 endplates innervated by terminal branches, which shows that these branches have the ability to become stabilised, and one endplate which appeared to be innervated by two terminal branches

(figure 4.19)

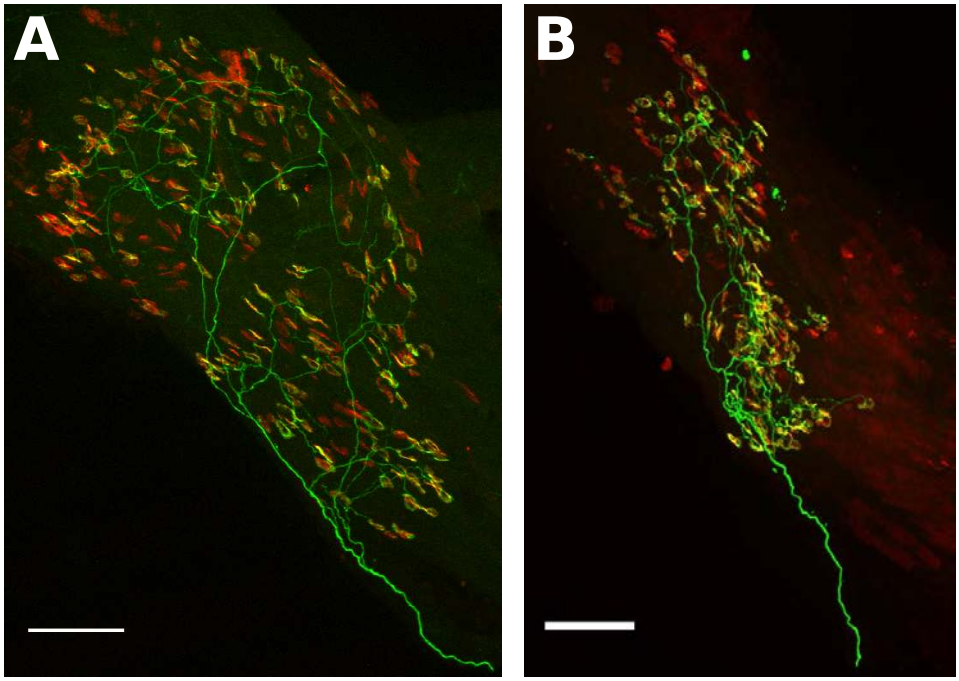

Figure 4.15: *Two 4th deep lumbrical motor units from muscles partially denervated at p5 and imaged at p8. A:motor unit size = 214, B: MU size = 161. Scale bars: 100 µm*

One interesting observation which came out of scrutinising every endplate is that many endplates in the lumbrical muscle appeared to be innervated by branches extending from synapses on other muscle fibres. These sprouts resemble the terminal sprouts that are typical in both partially denervated or chronically paralysed muscle (figure 4.17). Neonatal motor units have been reported not to sprout in response to denervation (Lubischer and Thompson, 1999). However, it appears that terminal sprouts may be relatively common in the lumbrical muscle. This is in contrast to LAL where there was perhaps one terminal sprout out of all the endplates examined.

Data from the neonatal lumbrical muscle therefore argue quite strongly that convergence does not occur as often as expected, if at all, in the 4DL.

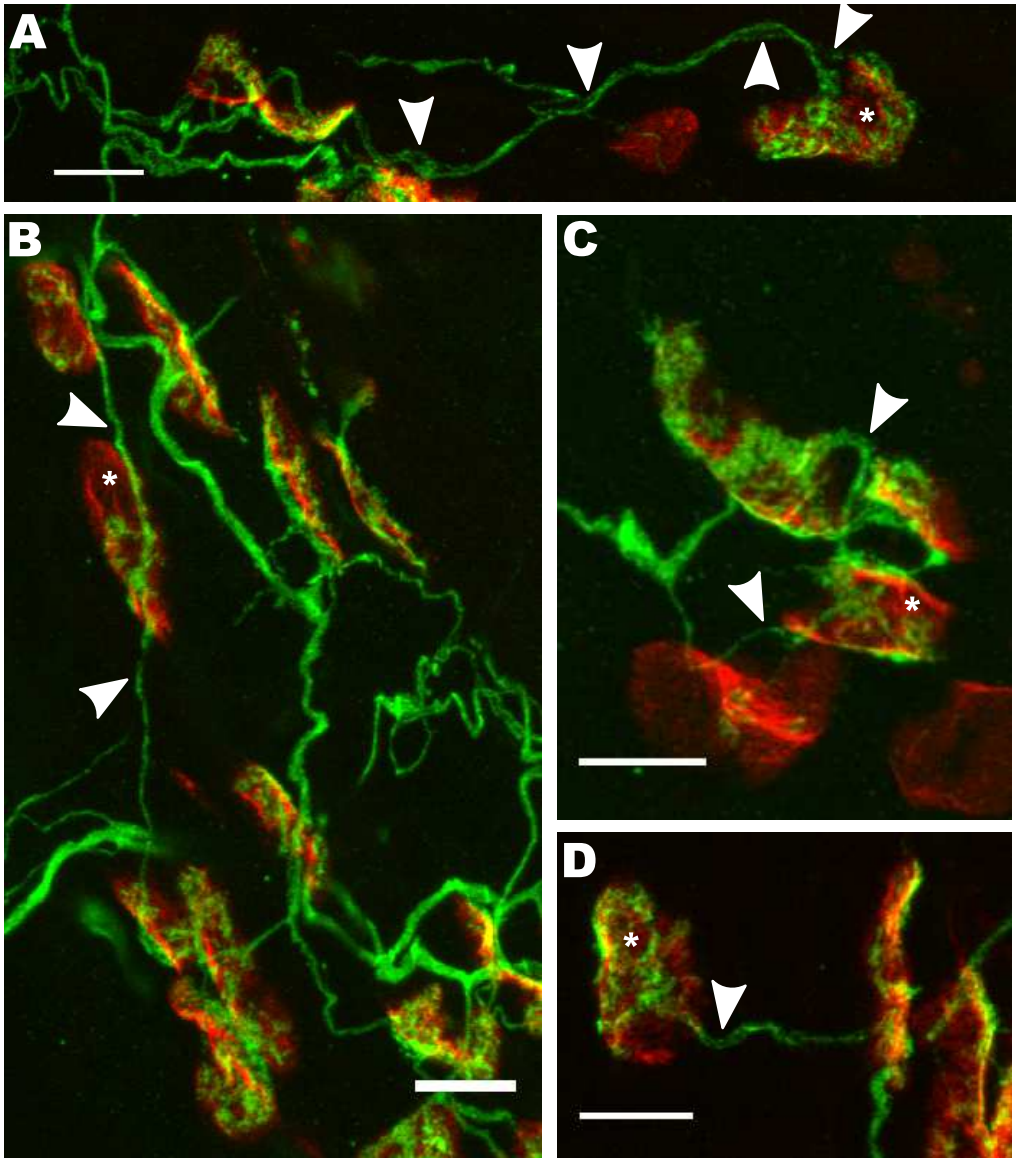

Figure 4.16: *Four examples of endplates which are possibly convergently innervated. The endplate which is possibly convergently is marked with a* $*$ *in each case. A and D appear to have two branches travelling along the same path very close together. Arrowheads indicate locations where there is reasonable doubt that the nerve contains a single branch. B is the most convincing. The marked endplate has a branch coming from the top and another from the bottom (see arrowheads). Both appear to connect to the endplate with a synapse and neither is an obvious terminal branch. C is not a high enough resolution image to be able to be certain of the innervation pattern. Two branches pass very close to the endplate (arrowheads) though the bottom branch could travel passed to innervate a different endplate. Scale bars: 10* μm

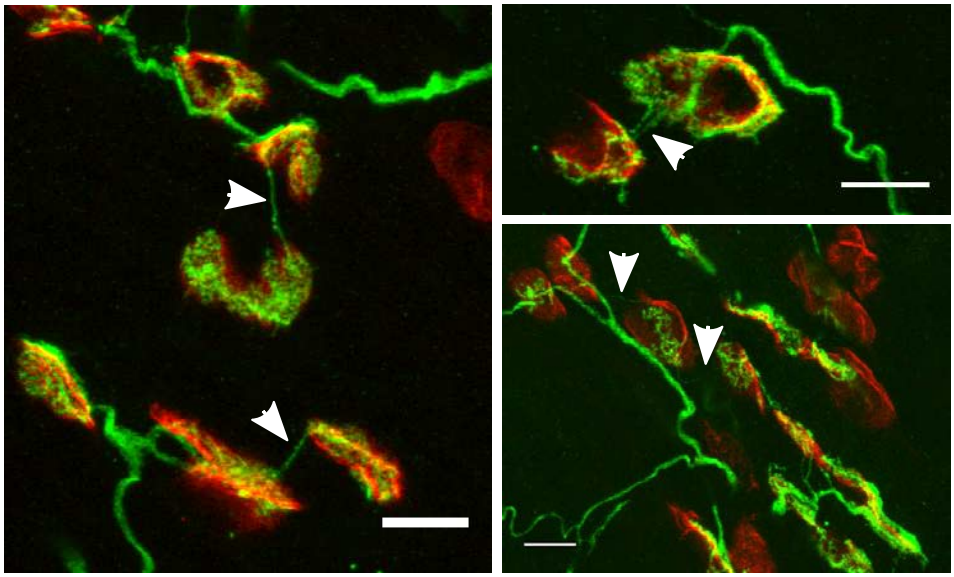

Figure 4.17: *Some examples of what appear to be terminal branches from p8 neonatal 4DL muscle which was partially denervated at p5. Scale bars: 10 µm*

4.3.6 Conclusion from neonatal data

It appears that sibling branch convergence rarely occurs, suggesting that axon branches from the same neuron do not form synapses independently of each other. Nevertheless there were examples of convergently innervated endplates in LAL and possibly in lumbrical muscles which are not present in adult muscle. Taken together these data suggest that sibling branches can eliminate each other if they converge on the same endplate, though this does not happen as often as predicted assuming each branch innervates randomly and independently from its siblings. Therefore axon branches probably do not innervate in this way.

4.4 Discussion

The motivation for these experiments is provided by the observation that two axon branches originating from the same motor neuron are never seen converging on the same endplate in adult 4DL muscles. This is also supported by published traces of

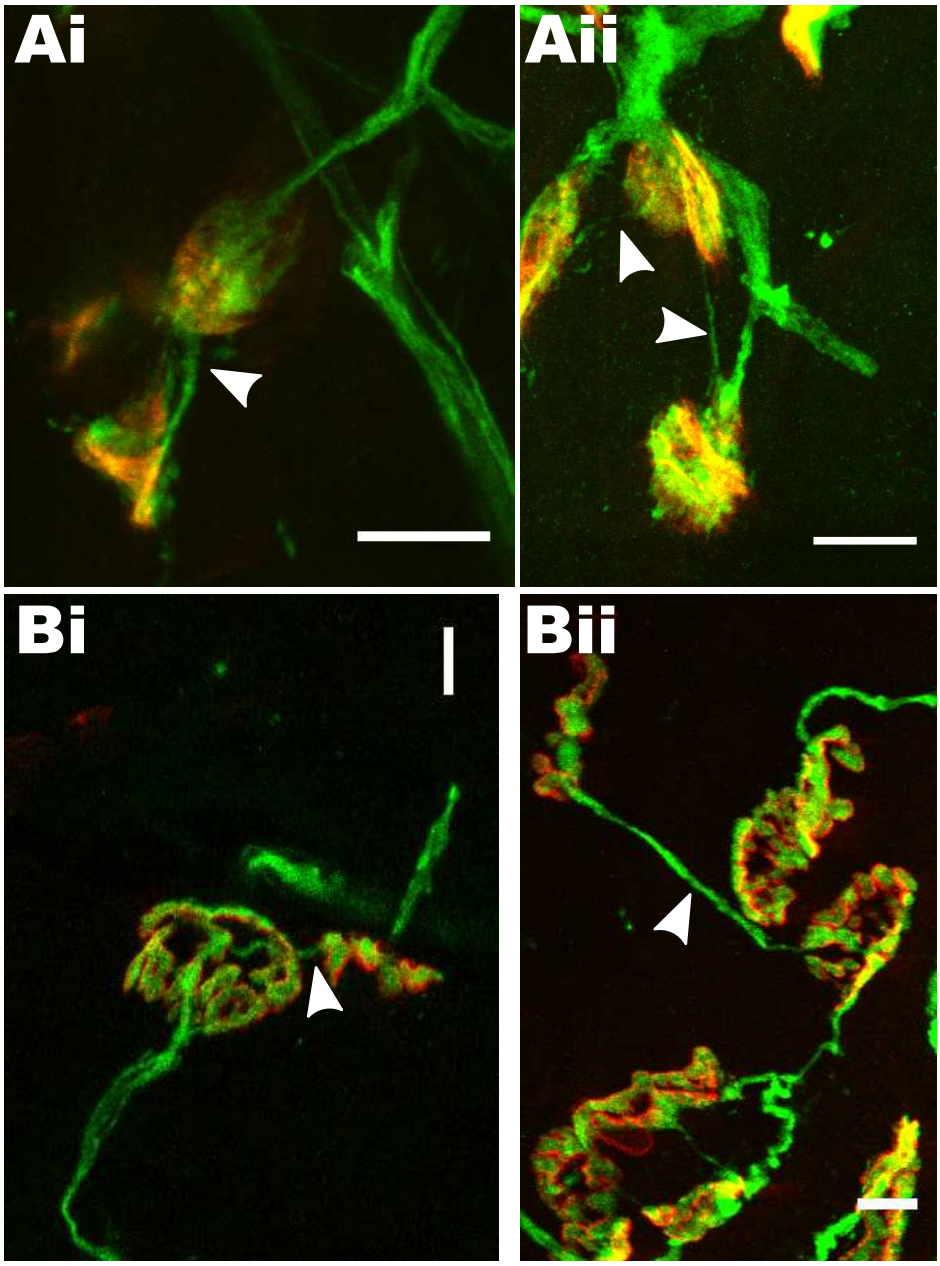

Figure 4.18: *Some examples of what appear to be terminal branches in A:unoperated p5 YFP16/BL6 mouse lumbrical and B: Adult lumbrical muscle with partial denervation at p5. Scale bar: 10 µm*

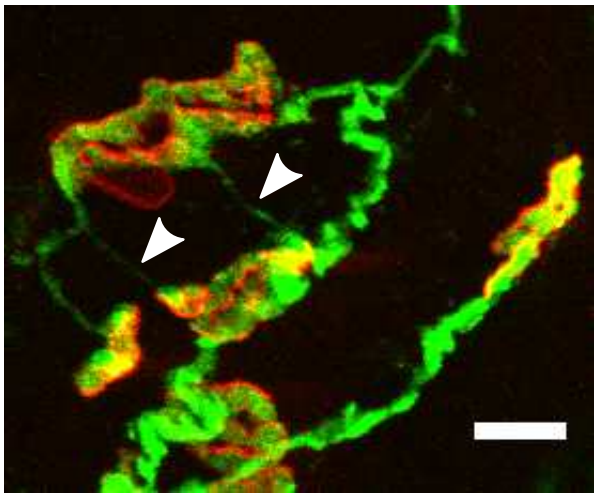

Figure 4.19: *One examples of what appears to be two terminal branches converging on the same endplate in an adult 4DL muscle which had been partially denervated at p5. An endplate innervated by two terminal branches was also seen in the late stage of regeneration (figure 4.5D first on the left). Scale bar: 10 µm*

motor units in other adult muscles (e.g. Lu et al., 2009b). However, assuming motor axon branches innervate endplates randomly and independently of other branches, a few tens of muscle fibres in each 4DL would be expected to be innervated more than once by the same neuron. This necessarily entails that either motor axon branches do not innervate endplates randomly and independently of each other or sibling branches are capable of eliminating each other.

This chapter addresses three questions:

1. Do sibling branches (that is, axon branches originating from the same parent motor neuron) ever converge to innervate the same endplate?

2. Does this occur as frequently as would be expected under the assumption that sibling branches form synapses randomly and independently of each other?

3. Can converging sibling branches competitively eliminate one another?

These questions were addressed using data from three different systems: regenerating lumbrical motor axons, developing LAL motor axons and developing lumbrical

motor axons. All three of the data sets are consistent with the conclusion that sibling branches do occasionally converge on the same endplate, though much less often than is expected under the assumptions above and that sibling branches are capable of competitively eliminating each other.

Each system provides varying amounts of support for these conclusions and has its limitations, though the fact that the results from all three are consistent strengthens this conclusion.

Below I will discuss the method used to estimate how often sibling branches were expected to converge on an endplate and then I will discuss each system separately.

4.4.1 Calculating the expected frequency of convergence

In order to calculate the expected frequency of sibling branch convergence, assuming that sibling branches innervate muscle fibres randomly and independently of each other, three further assumptions must be made.

First, an accurate estimate of the number of potential innervation sites is needed. In the lumbrical muscle, given its size and innervation pattern, it seems fair to assert that every endplate is *de facto* a possible innervation site and every endplate can be counted. In the LAL it is less clear since the muscle is a flat sheet and axonal trees are restricted to one band of the muscle (Murray et al., 2008). Even within that band they might not innervate each region. I have considered only endplates in close proximity to the axonal tree as potential innervation sites, though this may underestimate the number of possible innervation sites, which would lead to overestimation of the amount of sibling convergence expected.

Second, an estimate of the total number of axon branches originating from a neuron is needed. This has been estimated by counting the number of innervated endplates at the time of dissection. However, assuming some branches have already been eliminated prior to the time of dissection, the number of innervated endplates will have decreased already. Therefore this may lead to an underestimation of the expected frequency of sibling convergence. Note that if neonatal lumbrical motor neurons have sprouted

leading to larger motor units, this will not bias the frequency calculation as long as the sprouts also innervate endplates randomly and independently.

Third, the calculation does not take into account that some converging sibling branches may have been eliminated by the time of dissection. I have provided evidence that sibling branches are able to eliminate each other, but also some instances of convergence could be eliminated by a third axon branch from a different neuron innervating the same muscle fibre. Therefore the expected frequency might overestimate the number of converging sibling branches expected to be in the sample at the time of dissection.

The second and the third assumption will partly cancel out. They would completely cancel if elimination were random, but, because it is selective, it is not clear exactly what effect these approximations will have on the final result.

Despite these limitations it is useful to be able to derive an approximate 'best guess' estimate of the number of converging sibling branches expected in order to see how it compares with the observed frequency.

4.4.2 Regenerating Deep Lumbrical Motor Axons

Regenerating motor axons are often used as a model of development because they are larger and thus more easily resolvable and technically easier to work with. When axons regenerate they do so in a similar manner to development, by forming excess synapses, leading to polyneuronally innervated endplates, with subsequent elimination of excess branches. However, as discussed in section 1.10, there are differences. Since the muscle has already grown into its adult form before the motor axon is damaged, the other major structures, e.g. AChRs, Schwann cells and terminal Schwann cells, are already in place when motor axons are regenerating. During regeneration axons can grow along existing glia tracks (Nguyen et al., 2002) and they innervate the pre-existing endplate sites. Therefore synapse formation is not entirely random during regeneration, but somewhat constrained by the existing architecture of the adult muscle. However, the pre-existing architecture does not entirely dictate the innervation pattern, since polyneuronal innervation and its subsequent elimination still occur in the adult after injury. The results from regeneration are interesting in their own right,

as well as alluding to what may occur during development.

I imaged single fluorescent motor units from YFPH lumbrical muscles at three different time points after nerve crush, 12-14 days, 34-35 days and >70 days. The first two groups are considered to represent 'early regeneration' when synapse formation and elimination are ongoing. The latter group is considered to represent late regeneration when most of the changes have occurred, the morphology is largely stable and there are few if any polyneuronally innervated endplates left.

This distinction is supported by the observation that in the first two groups (12-35 days) approximately 19% (11/58) of the endplates analysed (ie those with more than one innervating fluorescent branch) were partially occupied by the fluorescent unit, in contrast to none in control muscles and only 3% (1/32) in the group that had recovered from crush for >70 days. This provides evidence that the endplate could also be innervated by a non-fluorescent neuron. Keller-Peck et al. (2001b) showed that endplates partially occupied by fluorescent motor axons in neonates were always additionally innervated by a non-fluorescent neuron (ie there were no uninnervated postsynaptic areas). During regeneration this may not always be the case since the endplates remain morphologically intact during the denervation and re-innervation period, however the fact that there were only 3% (1/32) in the group that had recovered from crush for >70 days confirms at least that there is ongoing plasticity up to 35 days.

Regenerating motor axons were expected to have an expanded motor unit size. However, this was not supported by the data. There are three possible reasons why motor unit size was not significantly larger up to 35 days after nerve crush when there is presumed polyneuronal innervation. Firstly, for this experiment, any lumbrical muscle with a single fluorescent unit was used, not just the 4DL. The mean motor unit size for the other three lumbricals is not known, though, if it is different from that of the 4DL, comparing MU sizes between groups which contain units from a unique mix of muscles may not be informative. Secondly the variance in motor unit sizes may be too large for the difference to reach statistical significance with only a few samples (3-8) and thirdly it is possible that motor unit size does not vary as much during regeneration because there is a smaller incidence of polyneuronal innervation. For example, McArdle (1975) found that only 31% of EDL muscles were multiply innervated at

early times in regeneration. Since the phases of synapse formation and elimination overlap more, regenerating MUs may not change in size so drastically. In neonates, in contrast, almost every muscle fibre has more than one input.

No long converging sibling branches were observed in 165 NMJs from three unoperated adult lumbrical muscles. However, there were 24 endplates with short pre-terminal branches. Pre-terminal branches are known to occur at the NMJ and are thought to be the result of remodelling after the mature synapse has been formed. Courtney and Steinbach (1981) showed that the number of endplates with pre-terminal branches increases with age in rat sternomastoid muscle. From observing a static image of the morphology it is not possible to conclude whether two innervating branches are the result of local remodelling at the mature synapse (referred to as pre-terminal branches) or the convergence of two axonal arbours, each of which could have innervated any endplate, on the same endplate (referred to as sibling branch convergence). Only the latter of the two is of interest in this study.

This presents a problem of how to classify endplates with two innervating branches as having either pre-terminal branches or converging sibling branches. In order to circumvent this problem, I measured the lengths of all instances of two or more innervating branches, from the common branch point to the endplate. The reasoning is that local remodelling should result in short branches, whereas sibling convergence could occur for any length of branch. Accordingly, a population with only pre-terminal branches would be expected to have a shorter mean branch length than a population containing both pre-terminal branches and converging sibling branches.

Indeed, the mean length from the common branch point to the endplate in the control group was significantly shorter than mean branch length in the early regeneration groups. This comparison demonstrates the existence of long converging branches during regeneration, which are far outside the distribution of normal pre-terminal branch lengths.

These long converging branches were also absent at longer time points after crush. The mean length in the $>$70 day group was significantly shorter than those at the earliest time of regeneration studied (12-14 days), but not significantly different from 34-35 day branches or control. This could indicate a progressive elimination of long

converging branches.

In addition, the morphology of some of the converging branches was qualitatively different from that seen normally in pre-terminal branches, namely some converging branches bifurcated between the common branch point and the endplate, with these sub-branches innervating different endplates. This was never seen in control muscles and only once at later time points during regeneration.

These data strongly suggest that the long branches in early regeneration are converging sibling branches and that one of the long converging branches is eventually eliminated. This sequence would explain the reduction in mean branch length and absence of unusual morphology during late regeneration.

It is unlikely that the reduction in mean branch length of converging branches is due to remodelling which makes branches appear shorter.

Other studies have found that axon branches become thin before they are eliminated. I tested the relationship between branch diameter and length of the branch, with the hypothesis that longer branches, which may be transient, would have a bigger difference between their branch diameters than shorter branches. However, no correlation was found between the average length of converging branches and difference in their diameters. Moreover, there was no difference in the ratio of the diameters between the four groups. The possible reason for failure to find a relationship are threefold. First, thinning could be a very brief stage before withdrawal and therefore thin branches may be a rare occurrence. Second, it may not be a feature of elimination during regeneration, even though it is during development and third, the variance in diameter ratios might be too large to show a difference in such a small sample.

The frequency with which convergence occurred in early regeneration was less than expected assuming each branch innervates a random endplate independently of other branches. This is despite the fact that the observed number of convergently innervated endplates in the early regeneration group is presumed to contain pre-terminal branches, which would inflate the measured number of occurrences. Since there are spatial constraints in adult muscles, it is not surprising that re-innervation is not entirely random.

There appear to be proportionally more pre-terminal branches in control muscles and

during late regeneration than there are during early regeneration. Pre-terminal branches have been shown to increase with age (see section 1.9.1.2). However, it is not clear whether it is the age of the animal or the age of the synapse which is the critical factor. These data are consistent with the notion that it is the age of the synapse which is important, as synapses would be more recently formed in early regeneration than in the other two groups. This question of when pre-terminal branches arise is open to further investigation.

An experiment to resolve this would be to crush the sciatic nerve unilaterally in adult mice and allow the axons to regenerate. The number of terminal branches in the lumbrical muscles in both operated and unoperated legs could be quantified at different time points. If the number of pre-terminal branches were the same on each side this would suggest that the age of the animal affects pre-terminal branching, whereas if the regenerated synapses contained less pre-terminal branching this would suggest that the age of the synapse is the important variable.

Despite the fact that regenerating adult axons are larger than neonatal axons, the exact innervation patterns are not always resolvable. This led to a number of endplates being disregarded in the analysis, due to them not being sufficiently resolved.

The calculation of the frequency of convergence between sibling branches assumes that the endplates which have been disregarded are representative of the whole sample, i.e. they are not biased towards a particular type of endplate. This is not necessarily the case since more than one innervating branch might be harder to resolve than a single one. Therefore there is a possibility that a higher proportion of the endplates in the ambiguous group are innervated by more than one branch than in the classified population. If this is the case I have underestimated the number endplates with converging branches.

Given the environmental constraints on innervation sites and the possibility of having underestimated the number of endplates with converging branches, it is not possible to be certain whether sibling branches have a higher probability of avoidance than branches from two different neurons or whether the incidence of convergence was low due to other factors.

In conclusion, regenerating lumbrical motor axons provide a number of examples of sibling branches converging on the same endplate and provide very strong evidence that one of the branches becomes eliminated. The frequency of sibling branch convergence appears to be less than expected, although it is hard to estimate this number and therefore it is unclear whether this is representative of a tendency for sibling branches to avoid innervating the same endplate more than branches from different neurons do, or whether the low incidence is the result of ongoing elimination.

4.4.3 Developing LAL Motor Units

The YFPH line is a good biological resource for imaging single fluorescent motor units in the adult because only a subset of neurons express fluorescent protein and are visible. However, fluorescent protein expression in this line does not begin as early as YFP16, which is expressed embryonically (Feng et al., 2000b). Motor neurons in YFPH animals express visible levels of YFP at different stages of development. No fluorescent motor neurons were found in lumbrical muscles up until at least p10, making this an unsuitable system to study early development. The triangularis sterni was also investigated, but no fluorescent units were found there either. However, other muscles express it earlier in this line, and particularly the LAL muscle had a high incidence of fluorescent motor units from p5 and later (three out of four muscles examined contained at least one fluorescent unit at p5).

The LAL is larger than the lumbrical muscle and therefore easier to resolve. It is a segmental muscle with a rostral and a caudal band, which are innervated by distinct populations of motor neurons. There are two caudal regions and five rostral regions of endplates. Motor neurons have been found to innervate more than one endplate region (Murray et al., 2008). Lanuza et al. (2001) showed that approximately 50% of terminals are polyneuronally innervated at p5 in the rat. Whether this is also the case in the mouse in unknown, although there were some endplates which were only partially occupied by the fluorescent axon, which suggests that the elimination period was not complete.

Out of 129 endplates that were innervated by five different units in three different

muscles only 4 endplates (3%) were found that appeared convergently innervated, 3 of which were all part of the same unit. This conclusively demonstrates that sibling convergence can occur in neonate muscles.

In order to determine if sibling branches can competitively eliminate each other, the incidence in neonates needs to be compared with the incidence in the corresponding adult muscle. To the best of my knowledge no studies have reported sibling converging branches in adult LAL or any other muscle. Specifically, Murray et al. (2010) provided a trace of a typical LAL adult motor unit which does not contain any convergence. Likewise Lu et al. (2009b) provided traces of all the motor neurons in the interscutularis muscle and none contained examples of sibling convergence. Coupled with the data in this thesis showing a lack of sibling converging branches in adult lumbricals, this supports the idea that sibling convergence is not present in adult muscles. Therefore the fact that some examples of sibling convergence have been found in neonatal muscles provide strong evidence that these branches are capable of eliminating each other.

The final question is whether convergence occurs as often as expected under the assumption of random and independent innervation. This question is again harder to answer.

One problem may be that the imaging resolution is not high enough to distinguish two innervating branches at this age, leading to underestimating the number of convergently innervated endplates. However, when there is more than one fluorescent axon innervating a certain region, two separate axons can be resolved for most of the length of the nerve they are travelling along. Therefore, it seems unlikely that there are a significant number of instances where there are two long branches which innervate the same endplate and they are continuously so close together that they are unresolvable.

A bigger problem is that the LAL is a different and segmental muscle, so there is a different expectation for how many converging endplates would be expected to be present. I calculated that the expectation of convergent innervation is about five times larger than the number I measured it to be (19 expected and 4 observed). Additionally, there were three muscles that did not appear to contain any converging sibling branches. The expected number for these muscles was 9, 2 and 0.5, which is small

enough that it is unclear whether lack of converging sibling branches implies that they occur less often than would be expected.

In conclusion, the LAL, despite its shortcoming, has provided the best example of a neonatal endplate innervated by two sibling converging branches, thus showing that this can occur during development. Since it has not been reported in adult muscles it seems likely that one of these branches was destined to be eliminated. It is not clear whether the frequency of occurrence matches the expected frequency.

4.4.4 Developing Lumbrical Motor Units

The third system I used to investigate this question is the neonatal lumbrical muscle. Since fluorescence is not visible in the lumbrical muscles of p5 YFPH strain pups, in order to be able to resolve single units, I partially denervated the lumbrical muscle at p5 and analysed only muscles with a single remaining unit at p8. The 4th deep lumbrical muscle is smaller than the LAL and is uniformly innervated. I imaged two such muscles at high resolution, amounting to a total of 375 innervated endplates. Both motor units were very large, innervating more than 70% of the muscle.

Because of the large size of the motor units and because the lumbrical muscle is smaller than the LAL, it was harder to resolve the axon branches innervating the endplates. Out of the 375 endplates imaged there were only 4, all from the same muscle, which were potentially convergently innervated. Two of these seemed to be convergently innervated by terminal branches.

None of these 4 examples provides an indisputable example of convergent innervation. If they are examples of convergent innervation, this strongly implies that convergent branches are able to eliminate each other, since no examples were found in adult lumbrical muscles nor in adult muscles which had been partially denervated at p5.

Interestingly there were quite a few of what appeared to be terminal branches; that is, branches which extended out from an innervated endplate. Terminal branches are not seen often in adult muscles (though some examples have been found in our lab in adult lumbrical muscles). They are found in adult muscles after neonatal partial denervation

as well as in unoperated neonatal muscles. There are three ways to account for these sprouts. First, they could be illusory, due to an axon branch innervating a terminal 'en passant' with a small branch which is closer to the endplate than the smallest resolvable distance in the image, causing it to look like a terminal branch. Second, these branches could be present and selectively eliminated during normal development but retained for some reason after partial denervation. Third, they they could arise in response to partial denervation. The first reason probably accounts for some of the examples seen. However, since adults with neonatal partial denervation retain some terminal sprouts, it seems likely that at least some endplates really are innervated by terminal sprouts in the neonate after partial denervation. Whether this is due to a failure of selective elimination or to terminal sprouting is not clear, though previously it has been reported that neonatal units do not produce terminal sprouts in response to partial denervation (Lubischer and Thompson, 1999).

In this preparation it is easier to calculate the expected frequency of convergence, since the assumption that every endplate is a possible innervation target is more likely to be true. Moreover, the whole muscle has been dissected and it contains fewer endplates, so every endplate can be counted. In both muscles examined the expected number of endplates with converging sibling branches was around 100 (101 and 105). This is very different from the numbers observed (4 and 0).

Part of this discrepancy could be accounted for by the fact that by p8 some of the converging branches will have been eliminated (assuming the previous conclusion that they can eliminate each other is correct). Additionally, there may be some instances of sibling convergence which are not resolvable. However, neither of these two factors, even combined, seem able to account for the whole difference.

It is interesting that there were more examples of sibling neurite convergence in the adult reinnervated lumbrical than in the neonate even though motor unit sizes of regenerating motor units were smaller. If there is a mechanism which prevents sibling branches from converging, it could be the case that it is less potent or absent in adult muscles. For example, there is a decrease in the concentration of putative guidance cues like ephrin in adult muscles (Feng et al., 2000a). In addition, regenerating axons could grow in a different manner to neonatal axons which could result in a different

shape of the axonal tree. This could relate to the observation that neonatal branches do not seem to fasciculate with sibling branches whereas in the adult this occurs more commonly. Finally there is the possibility that some sibling convergence in the neonate was not identified due to the constraint of the image resolution.

In conclusion, it is not clear whether sibling convergence does occur in the neonatal lumbrical muscle but these data provide strong evidence that sibling convergence does not happen as often as is expected if innervation was random and independent within a motor unit.

4.4.5 Conclusion

Taken together, all these data suggest that sibling branch convergence can happen, although it does not happen as often as would be expected. This suggests that either motor axon branches do not grow independently of each other or that growth is not random or both. A possible scheme where axons grew non-randomly would be where different sub-trees were guided to innervate different regions of the muscle. If this was the case, branches would still innervate independently of other branches (ie the choice of endplate of one branch would not affect the choice of a different branch) but convergence may still be prevented by the separation in space, due to each branch not innervating a target randomly. On the other, hand non-independent innervation would describe a situation where axons could still innervate endplates randomly but the fact that one axon has innervated an endplate somehow influences the probability that others will converge there. There are several plausible mechanisms which could result in non-random or non-independent growth.

First, it has been shown that some neurons are able to recognise themselves. For example leech comb cells grow into intricate comb-like patterns without any overlap between processes from the same neuron (Baker and Macagno, 2007). This is achieved through contact-mediated retraction.

Second, non-randomness could be related to the method of growth. If axon branches tend to grow out in opposite directions the resulting tree might contain fewer overlaps than if branches grew out in a random direction. Also if axons could form synapses

along the length of the axon instead of just at the tip of the axon, this could give rise to many short branches from just a few primary collateral branches and not much overlap. These synapses might have the appearance of 'en passant' synapses. Fully understanding the consequences of how growth could affects the innervation pattern probably requires simulations.

Despite the fact that there may be a preventative mechanism, sibling convergence in neonates can occur at early time points in development and regeneration, as shown in the LAL muscle and in regenerating 4th deep lumbrical muscle, but is not present at later time points. Therefore it appears that sibling branches can eliminate each other and models of synapse elimination need to be able to explain this type of elimination.

Chapter 5

Results: Imaging Neonatal Motor Units

5.1 Introduction

One of the ways neuroscientists try to understand the intricacies of the nervous system is through observations of the form and connectivity of neurons and brain regions. The scale at which the nervous system is organised spans many orders of magnitude, from angstroms (10^{-10}m) to metres, though the naked eye can typically only resolve structures on the order of millimetres or larger. Light microscopes, invented around the turn of the 17th century, can assist in the resolution of small structures up to a theoretical limit (about 200 nm).

Neuroscientists commonly study the morphology of individual neurons, despite the difficulty in obtaining complete neural reconstructions. Recently there has been interest in reconstructing more complete maps of the connections between many neurons. A map of all the connections within the nervous system of an organism has been termed a 'connectome' (Lichtman and Sanes, 2008). The only complete connectome to date is that of C. elegans reconstructed by White et al. (1986) using serial sectioning and electron microscopy. This connectome contains approximately 300 neurons and, although very difficult and complicated to reconstruct, is orders of magnitude simpler than any mammalian connectome.

Recently, there has been a substantial drive towards creating the right tools to be able to

reconstruct connectomes with several leading scientists advocating for more research to be done to this end (Sporns et al., 2005; Lichtman and Sanes, 2008; Smith, 2007; Briggman and Denk, 2006). In order to make this task feasible, new visualisation and analysis techniques are being developed (Livet et al., 2007; Lu et al., 2009a; Micheva and Smith, 2007). This is a mammoth task, which is not only very laborious, but at the moment it is not clear what the best approach to it is. There are many imaging techniques and they have their advantages and disadvantages. For example EM has the highest resolution, making it possible to resolve structures on the order of nanometres. However, this form of imaging must be done in a vacuum (precluding live imaging) and typically more structures are visible in the image than with fluorescence microscopy, where, for example, only the neurons of interest could be visible. The downside of everything being visible is that image analysis and reconstruction times are increased, since there is much more information to deal with. On the other hand, light and confocal microscopes have very good signal to noise and contrast, allowing images with only the structures of interest to be visible. They suffer however from the fundamental resolution limit, which is a limitation of all light microscopes (see section 5.1.1).

The first mammalian connectome was published by Lu et al. (2009b), and is of the interscutularis muscle in the adult mouse. This is a relatively small muscle and motor neurons are large compared to neurons in the central nervous system, so confocal microscopy, combined with manual tracing, were sufficiently good techniques to complete this project. In order to create connectomes of large circuits, many techniques will have to be combined to enable both high resolution and dealing with a feasible amount of data.

With the bigger goal of creating connectomes, and leading on from the results of the previous chapters, it would be interesting to map out the connections in a neonatal 4th deep lumbrical muscle. This would provide answers to questions like: What is the distribution of motor unit sizes in a typical unoperated neonatal 4DL? What is the extent of polyneuronal innervation at p5 and what is the time-course of elimination? What, if any, is the incidence of terminal branching? How often do sibling branches converge on the same endplate? Tracing each neuron in a neonatal 4DL muscle is challenging because the muscle is much smaller than in adults, the axons are thinner,

more abundant and the distance between different axons is smaller, since they are not all necessarily myelinated yet.

5.1.1 Optical resolution in light microscopes

Microscopes have an intrinsic limitation to their resolving power by virtue of the nature of light: that it is a wave which can interfere with itself and that it travels in all directions. There is a hard limit to the spatial frequencies which can be imaged by a specific objective lens, and this is called the Abbe limit, named after Enrst Abbe (Heintzmann and Ficz, 2006). The Abbe limit is equal to $\frac{\lambda}{2NA}$, where λ is the wavelength of light and *NA* is the numerical aperture of the objective. This means that the minimum spatial frequency that can be imaged by a 1.4 NA objective using visible (530 nm) light is about 5 lines per μm. In other words, the finest resolvable grating will contain lines separated by about 200 nm.

The image of an infinitesimally small point of light, after it has passed through the microscope lenses, will have a definite size and shape. The way the imaging apparatus spreads the light from a point source is called the point spread function (PSF) of the microscope (see figure 5.1). The actual dimensions of the PSF depend on the characteristics of the specific lenses and the wavelength of light used. In the lateral direction (parallel to the plane of imaging) the PSF appears as a bright central disk (the Airy disk) surrounded by dimmer concentric circles (figure 5.1A). The bright center of the PSF is elongated in the z-axis and the dim concentric circles form an hourglass shape (figure 5.1B). Since every point of light is blurred by the PSF, the image which is captured by a microscope is the convolution of the true image with the PSF. The size of the PSF is related to the Abbe limit and the image resolution is limited by the size of the PSF.

In confocal microscopy, because the image is generated by focusing light to a diffraction limited point in the specimen and the returned light is collected through a pinhole, the PSF is roughly equal to the squared PSF of a widefield microscope. In other words, the difference in intensity between the peak of the Airy disk and the diffraction rings is magnified, which overall results in a smaller PSF and a higher contrast image.

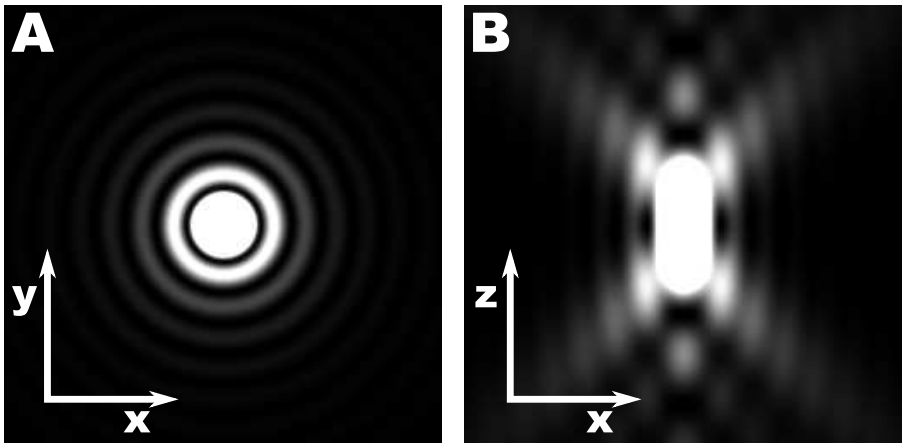

Figure 5.1: *Theoretical PSF of a widefield microscope generated using the PSF generator plugin in Fiji. A: Theoretical PSF in the lateral (XY) direction. The bright central circle is the Airy disk. B: Theoretical PSF in the axial (XZ) direction. Pixel intensity has been brightened to make the interference patterns more visible.*

Image resolution is a very important concept in microscopy. In everyday language we say we can resolve two objects if we can visually distinguish them. In a microscopy image, the ability to distinguish two objects is affected by the image resolution, which is specifically related to the point spread function, but also by the image contrast and the signal to noise ratio.

In a grayscale image, contrast refers to the difference between the brightest pixel and the dimmest pixel. If there is no difference in intensity between the structure of interest and the background, then it is not possible to resolve the structure of interest, whatever the resolution of the image may be. A common problem in microscopy used to be that there is not much difference in the brightness of different biological structures, leading to low contrast images. Many techniques were developed to counter this problem, e.g. phase contrast, darkfield and fluorescence. By using fluorescent markers to tag the structure of interest, it is now possible to acquire very high contrast images in which the structure of interest appears bright on a dark background.

Noise is a measure of the variation in intensity of single pixels that is due to stochastic fluctuations rather than variation in the specimen. There are a few points in the imag-

ing process at which noise could be introduced. For instance, during image acquisition of fluorescent images noise can arise in the emission stage as there is stochastic fluctuation in the amount of fluorophore that will be excite; it can arise during the detection stage, as there is variation when the number of photons are amplified in order to be detected and it can arise in the detection system. The signal-to-noise ratio (SNR) is a measure of how much bigger the signal is than these random fluctuations in signal. A low SNR may also decrease our ability to distinguish two objects even if the objective resolution is enough.

Confocal microscopy produces a vast improvement in contrast, by eliminating out of focus light from the image, and a modest increase in resolution due to the slight decrease in the width if the PSF (about 1.4x). With a combination of confocal and fluorescence it is possible to achieve high contrast and high signal to noise images, though noise can be a problem when imaging at low light levels, with a small pinhole or at short dwell times, for instance when attempting to minimise bleaching. Both SNR and contrast contribute to our ability to distinguish objects in a microscopy image, but ultimately the image resolution is determined by the PSF.

Although there is a hard limit on the frequencies which can be imaged by a microscope, given assumptions about the shape and intensities of the objects which are being imaged, these may still be distinguishable close to that limit. There are several criteria for calculating the minimum resolvable distance in an image based on the point spread function. For example, the Sparrow criterion states that two points are resolvable if there is a dip in the peak of their combined diffraction pattern. (In this case the minimum resolvable distance is also dependant on the intensities of the spots and the signal to noise ratio. For example, if one point is dimmer than the other they would need to be further apart for there to be a dip in their summed point spread functions.)

Another measure of resolution sometimes quoted is the full width half maximum (FWHM) of the PSF. Generally this term refers to the width of a curve at the point where its height is half of the maximum height. The curve in this case is the intensity profile of the PSF. The theoretical FWHM of the PSF of a confocal microscope with a 1.4 NA objective and 543nm light is 149nm laterally and 420 nm axially (Schrader et al., 1996).

A more commonly used rule is the Rayleigh criterion. The Rayleigh criterion posits that two points are resolvable if the peak of the central disk of one PSF is no closer than the first dark ring of the other PSF. This means that the minimum resolvable lateral (XY) distance, according to the Rayleigh criterion, is the distance from the centre of the Airy disk to the first dark ring (in other words the radius of Airy disk) and for a confocal microscope is equal to $\frac{0.4\lambda}{NA}$ where λ is the wavelength of light and *NA* is the numerical aperture of the lens. In the axial (XZ) direction this distance is equal to $\frac{1.4n\lambda}{NA^2}$ where *n* is the refractive index of the imaging medium, which is usually oil for high NA objectives (Formulae from the Olympus website, see (Spring et al., nd)). Therefore, according to the Rayleigh criterion, using a 1.4 NA objective lens (which is typically the highest NA lens available in microscopy labs) and 530 nm light (which is the peak emission wavelength of YFP), theoretically, the minimum resolvable lateral distance is 155 nm and the minimum resolvable axial distance is 571nm. For a conventional microscope these values are calculated using $\frac{0.61\lambda}{NA}$ for lateral and $\frac{2n\lambda}{NA^2}$ for the axial resolution and are equal to 231nm and 817nm respectively.

However, these are theoretical minima. In practice the minimum distance at which we can be certain there are two objects instead of one also depends on contrast, SNR as well as our assumptions about the shape of what is in the image. For example if we know we are imaging round beads, we can be fairly certain that an elongated structure in the image is due to the presence of more than one bead. Axons, although generally long and thin can vary a lot in shape and orientation and even in intensity, so it is harder to determine the number of objects in an image if they are not well separated.

Moreover, imaging apparatus is never perfect and imperfections lead to aberrations, noise and, ultimately, to lower resolution.

The resolution of the acquired image can also be affected during the digitisation of the image. The image volume which corresponds to a single pixel is determined by the magnification applied to the specimen. Each pixel is associated with a particular intensity value between 0-255 for 8-bit images, and between 0-4095 for 12-bit images. Therefore, the information in the image volume corresponding to a pixel is captured by a single number. According to the Nyquist sampling theorem, in order to preserve features of a certain frequency in a signal, it must be sampled at least at twice that

frequency. In relation to imaging this means that in order to capture spatial details of a certain size, e.g. 200 nm which is close to the theoretical lateral resolution limit, the size of the area corresponding to one pixel must be half that size or smaller. Therefore, images with pixel sizes of 100 nm or smaller will preserve all the information that it is possible to capture from a lens with minimum resolution 200 nm. Imaging at lower magnification (and therefore larger pixel sizes) will not utilise the full resolving power of the microscope.

In this chapter I concentrate my efforts on imaging neonatal (p5) 4DL motor units. I show that confocal microscopy does not provide enough resolution to visually separate developing motor neurons, even after deconvolution. Furthermore, I show that serially sectioning a muscle, imaging, and aligning the sections increases the z-resolution compared to confocal microscopy but still does not reveal enough fine detail to resolve developing axons in all instances.

Most of the work in this chapter was carried out on a visit to the lab of Professor Jeff W. Lichtman. Other members of his group who are involved with this technique and who assisted me with this project are Ken Hayworth who designed and built the automatic tape collecting machine and Juan Carlos Tapia, Richard Schalek, Hirohide Iwasaki, and Narayanan Kasthuri who are all involved in serial reconstruction projects.

5.2 Methods

5.2.1 Tissue preparation

5.2.1.1 Dissection

Neonatal (p5) 4DL muscles were dissected from YFP16/Bl6 and YFPH/Bl6 mouse pups as described previously in section 2.4.1.

5.2.1.2 Fixation and fluorescent labelling

All muscles were fixed in PFA (see section 2.4.2) and stained with alexa-555-BTX or Rhodamine-α-BTX to mark AChRs at the endplate. Fluorescent muscles (i.e. from YFP16 mice) were stained with rabbit anti-GFP antibody and 488-anti-rabbit secondary(Jackson) to amplify native fluorescence in nerves. Muscles without fluorescence were immunolabelled with mouse anti-NF primary and rabbit anti-mouse FITC secondary antibody in order to fluorescently tag neurofilaments (see section 2.4.3 for details).

5.2.1.3 Embedding muscles in LR WHITE for serial sectioning

Immunostained 4DL muscles were embedded in LR White plastic in preparation for slicing according to the following protocol. Muscles were first dehydrated by incubating in increasing concentrations of ethanol at 4^oC (2x10 minute incubations in 50% ethanol followed by 2x10%incubations in 70% ethanol). Muscles were not incubated in higher than 70% ethanol in order to preserve the fluorescence. Muscles were then immersed in a 1:1 mixture of 70% ethanol and LR White for 30 mins followed by 2x 10 minute incubations in 100% LR White. Finally, muscles were incubated for at least four hours in 100% LR White at 4^oC, before polymerisation of the LR White at 60^oC overnight. It was not possible to control the orientation of embedding of the muscle since it is so small. If a different orientation is desirable, one possibility is to embed the muscle in agarose initially and then embed the agarose block in LR White.

5.2.2 Section preparation

5.2.2.1 Tissue sectioning

A Leica microtome with a diamond knife controlled by custom made software were used to section the muscle into 100-200 nm slices.

5.2.2.2 Tape collection

A custom made automatic tape-collecting device (ATUM - Automatic Tape-collecting UltraMicrotome, designed and manufactured by the Lichtman Lab) was used to collect every slices on a reel of tape made from mylar, kapton or polycarbonate. Cover tape was affixed over the slices which were stored in this fashion for imaging.

5.2.2.3 Slide preparation

Segments of tape with up to 12 sections were cut and placed on a slide. The cover tape was removed and the sections were sealed under a coverslip with Vectashield and nail polish.

5.2.3 Imaging slices

Slices were imaged using a Zeiss Pascal confocal microscope with a 63x 1.4 NA objective lens. Each slice was captured in a montage of 2-8 images. (1024x1024, 0.1 step).

5.2.4 Aligning images

Images were post-processed using Fiji (see 2.6). Montages were created using the Stitching plugin and saved as 8-bit tiff files for importing into Reconstruct and manual alignment.

5.3 Results

This chapter investigates ways to achieve sufficient resolution to image neonatal (p5) 4DL muscles. Figure 5.2 shows a montage of the maximum projections of about 40 image tiles, which cover an entire p5 4DL muscle.

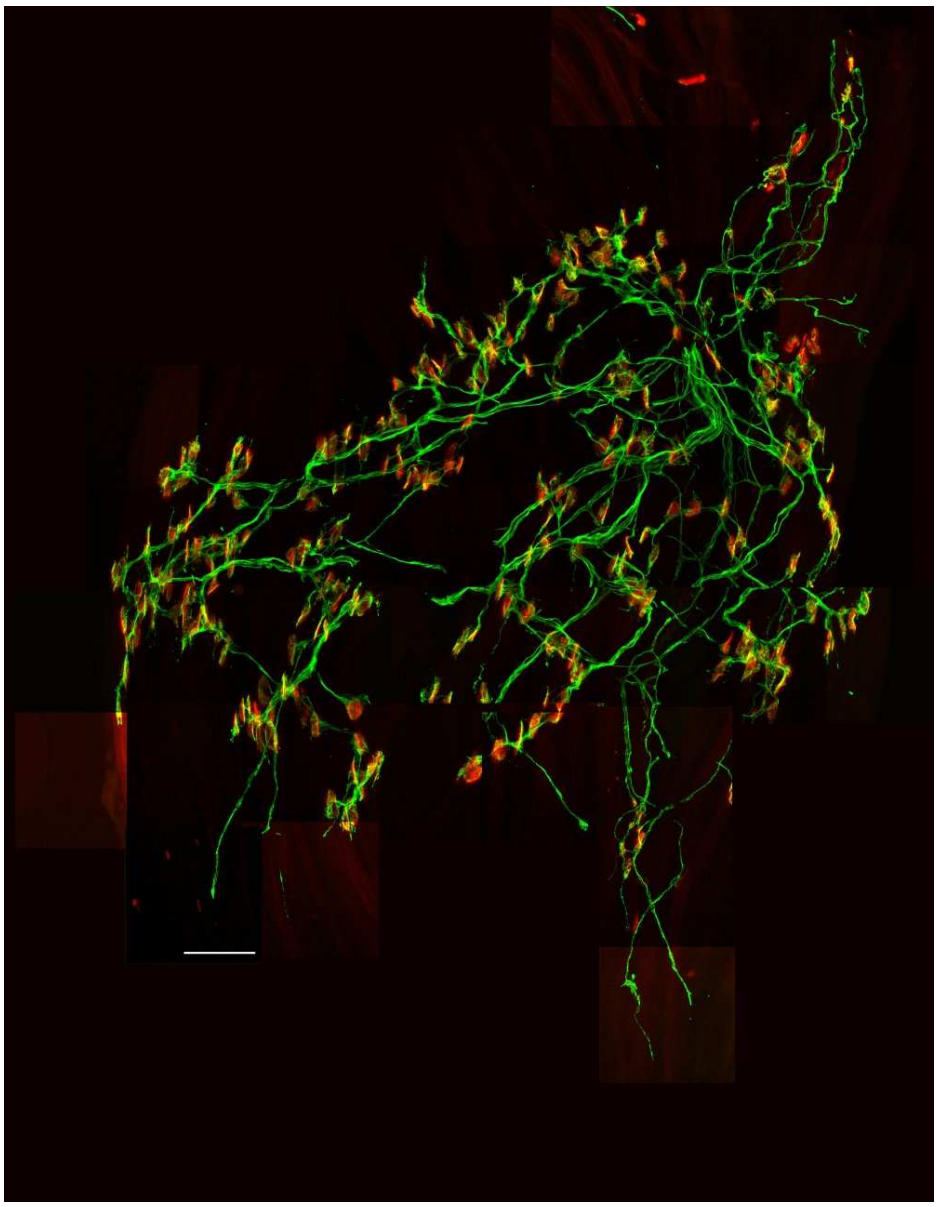

Figure 5.2: *Image showing a YFP16 p5 4th deep lumbrical muscle. This image is a montage of maximum intensity projections of about 40 image tiles. Axons (green) express YFP endogenously, which is amplified by immunolabelling. AChRs (red) are labelled with alexa-555-BTX. Scale bar: 50 µm.*

5.3.1 Confocal imaging of neonatal 4DL marked by YFP/Neurofilament

First of all, I tried imaging a neonatal 4DL muscle at the highest possible resolution with a confocal microscope. A 4DL muscle from a YFP16 mouse (which expresses YFP in every motor neuron) was imaged with a 63x 1.4 NA objective lens. The pixel size of the collected images corresponds to 93, 93 and 300 nm in x, y and z respectively. These images do not provide sufficient resolution to distinguish between axons (see figure 5.3). Furthermore, axons appear thicker and more easily resolved at the point of entry than they are in the intramuscular nerve bundles or as they approach the endplates. This makes it difficult to determine how many axon branches are innervating an endplate in most circumstances. Moreover, as endplates can appear to have terminal branches (whether they do or not in neonates is unclear) observing two branches converging on an endplate does not distinguish whether there are two different branches innervating the endplate or the same branch either innervating the endplate at one location and travelling away as a terminal branch or simply travelling past the endplate at a distance less than the resolution limit.

In addition, I tried imaging muscles without endogenous fluorescence in which the neurofilament (NF) in motor neurons had been fluorescently labelled. There are two potential benefits to NF labelling. Most synaptic boutons contain little or no NF and therefore are not labelled, which may help in determining how many branches innervate an endplate. Moreover, axons with fluorescence bound to the NFs may appear slightly narrower than axons with YFP freely diffusing in the cytoplasm, although any difference would certainly be small. The x, y and z dimensions of each pixel in these images corresponds to 57, 57 and 200 nm respectively. However, axons with fluorescently labelled NF are also not always resolvable in neonates (see figure 5.4). Although muscle fibres were clearly polyneuronally innervated, in most cases the number of different branches innervating an endplate was ambiguous.

Finally, Huygens deconvolution was performed on the images of NF-labelled axons. The PSF of the microscope was not measured during this imaging session but estimated from the parameters of the objective lens used and the excitation and emission wavelengths. The deconvolved image appeared less noisy, but it did not contain sufficient detail to allow individual axons to be distinguished (figure 5.5).

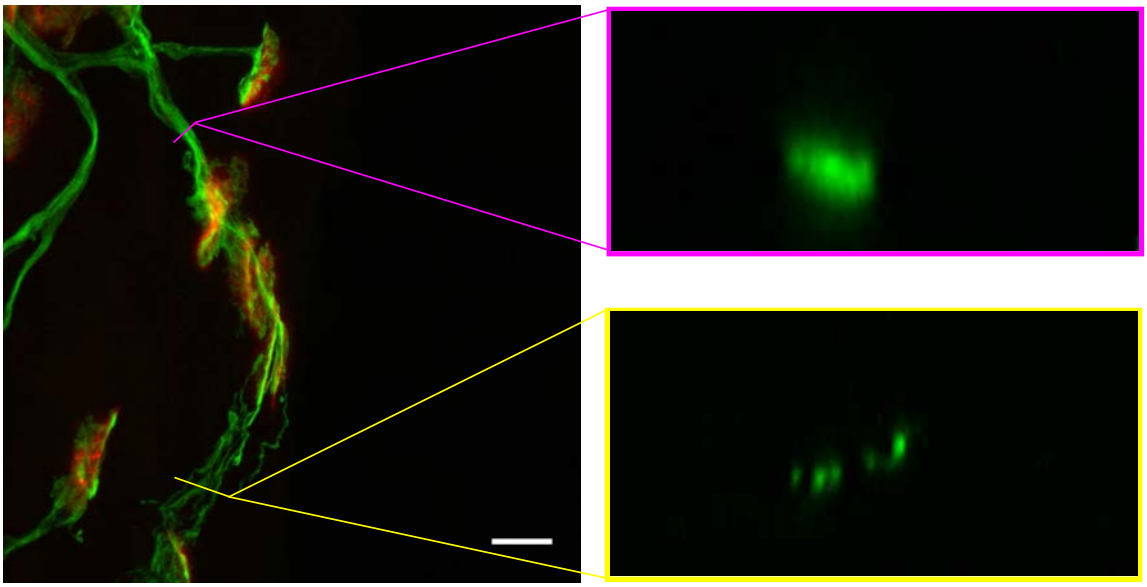

Figure 5.3: *One tile from the montage shown in figure 5.2 (left box). Axons endogenously express YFP (green) and endplates are stained with alexa-555-BTX (red). The yellow and pink boxes show cross-sections throught the image at the location shown. Non-orthogonal cross-sections in this and figure 5.4 were created using the 'Volume Viewer' plugin in Fiji. There are parts of the intramuscular nerves where single branches are resolvable (yellow box). However, there are also many areas where it is not possible to resolve individual axons(e.g. pink box). Scale bar: 10 µm*

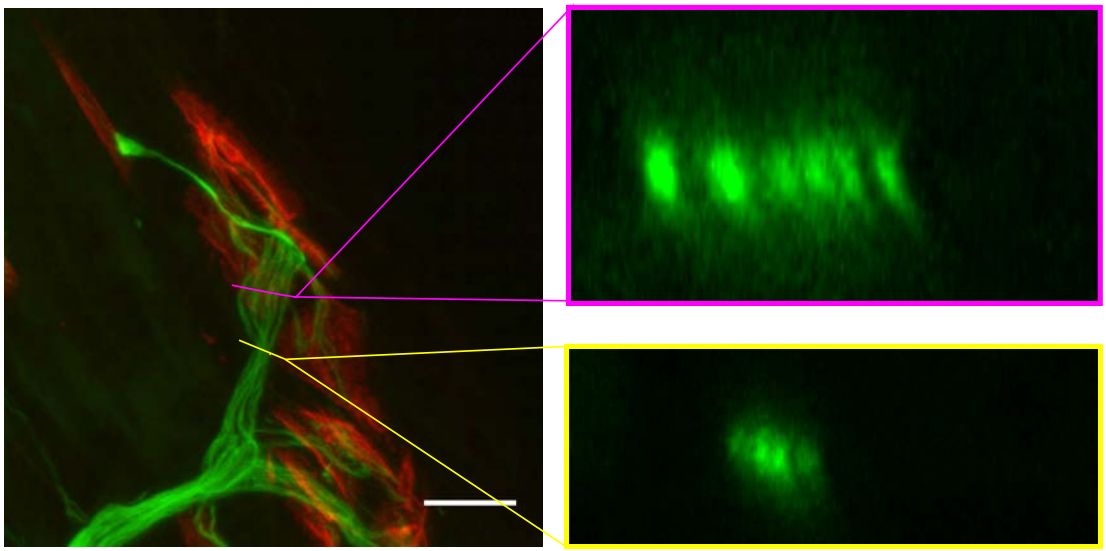

Figure 5.4: *Motor axons with fluorescently labelled NF (green) and end-plates labelled with Rhodamine-α-BTX (red). The yellow and pink boxes show cross-sections throught the image at the location indicated by the lines. Single axons cannot be resolved at some points in the image (yellow box) while they can be resolved at other points (pink box). Scale bar: 10 µm*

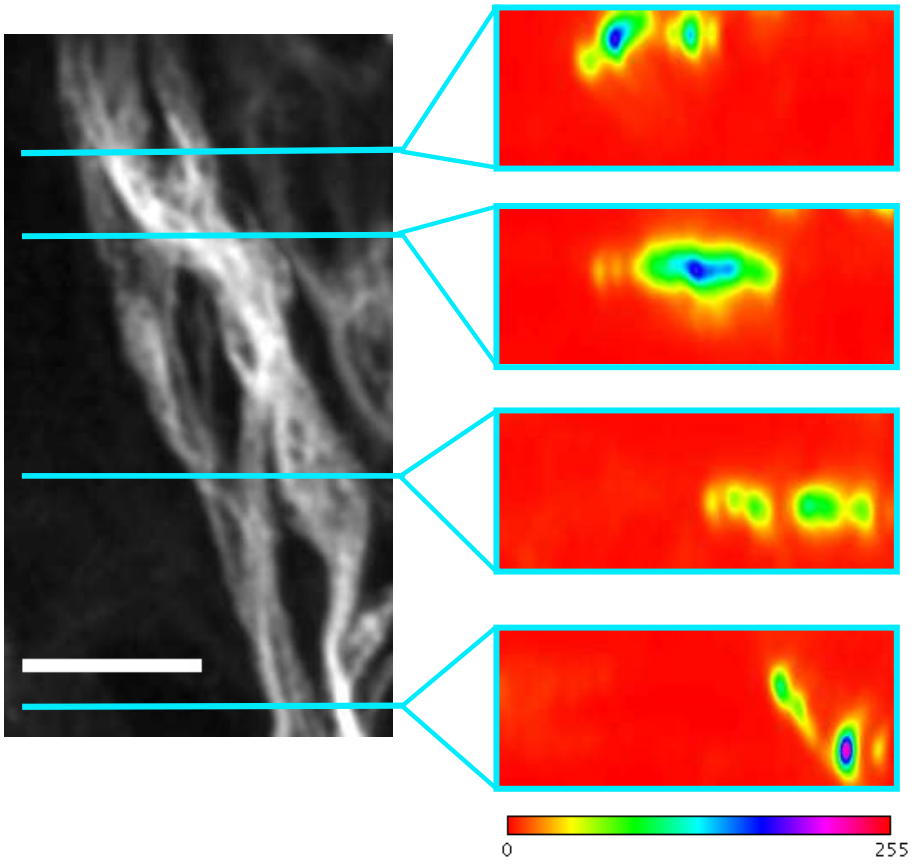

Figure 5.5: *On the left is the maximum intensity projection of the deconvolved image of NF stained axons in the 4DL. Individual axons were still unresolvable. Boxes on the right show the XZ cross-section of the image at the y-coordinate indicated by the blue lines. Grayscale images are displayed with a spectrum look-up table for ease of visualisation. The mapping of pixel intensity to colour is shown on bottom right. Scale bar (left image): 5µm*

Additionally it was not possible to visualise single units using YFPH mice, in which only 5% of motor neurons express fluorescent protein, because no fluorescence was visible in the lumbricals up to p10, even after YFP amplification with anti-GFP staining.

Therefore confocal microscopy does not provide sufficient resolution to distinguish between neonatal axons in the 4DL muscle. In order to achieve this other methods which can circumvent the classical resolution limit must be used. There are a number of methods being developed (see discussion). One method in particular which I tried on the neonatal 4DL muscle is reconstructing ultra-thin serial sections.

5.3.2 Serial sectioning 1: optimising the technique

One of the limitations of conventional and confocal microscopy is that the axial resolution is 3-4 times worse than the lateral resolution. The axial resolution can be increased by sectioning the specimen, thus ensuring that the signal from fluorescent axons in each section does not contribute any photons to the signal in neighbouring sections (because they are physically separated). This will result in the axial resolution being limited by (and equal to) the thickness of each section. Figure 5.6 shows a small (500 nm) fluorescent spot on a 100 nm section. It is not clear what the true image of the spot in x/y is (i.e. what its dimension are) but the length along the z-axis should be 100 nm, which is the thickness of this particular section. In contrast, the axial length appears to be about 1 μm due to the PSF of the microscope. Similarly, the FWHM of the intensity profile along the centre of the spot is approximately 1 μm (see figure 5.6 bottom graph). Hence, physically sectioning at 100 nm increases the axial resolution about ten times compared to optical sectioning.

In order to trace the axonal trees within the muscle, every section must be imaged and the image must be aligned so the signal in each section can be related to signal in other sections. Good alignment between section is only possible if the sections do not contain distortions like wrinkles, folds, stretches or skew. Therefore it is important that each section is as flat as possible for imaging.

A combination of parameters were tried in order to achieve this. These were: slice

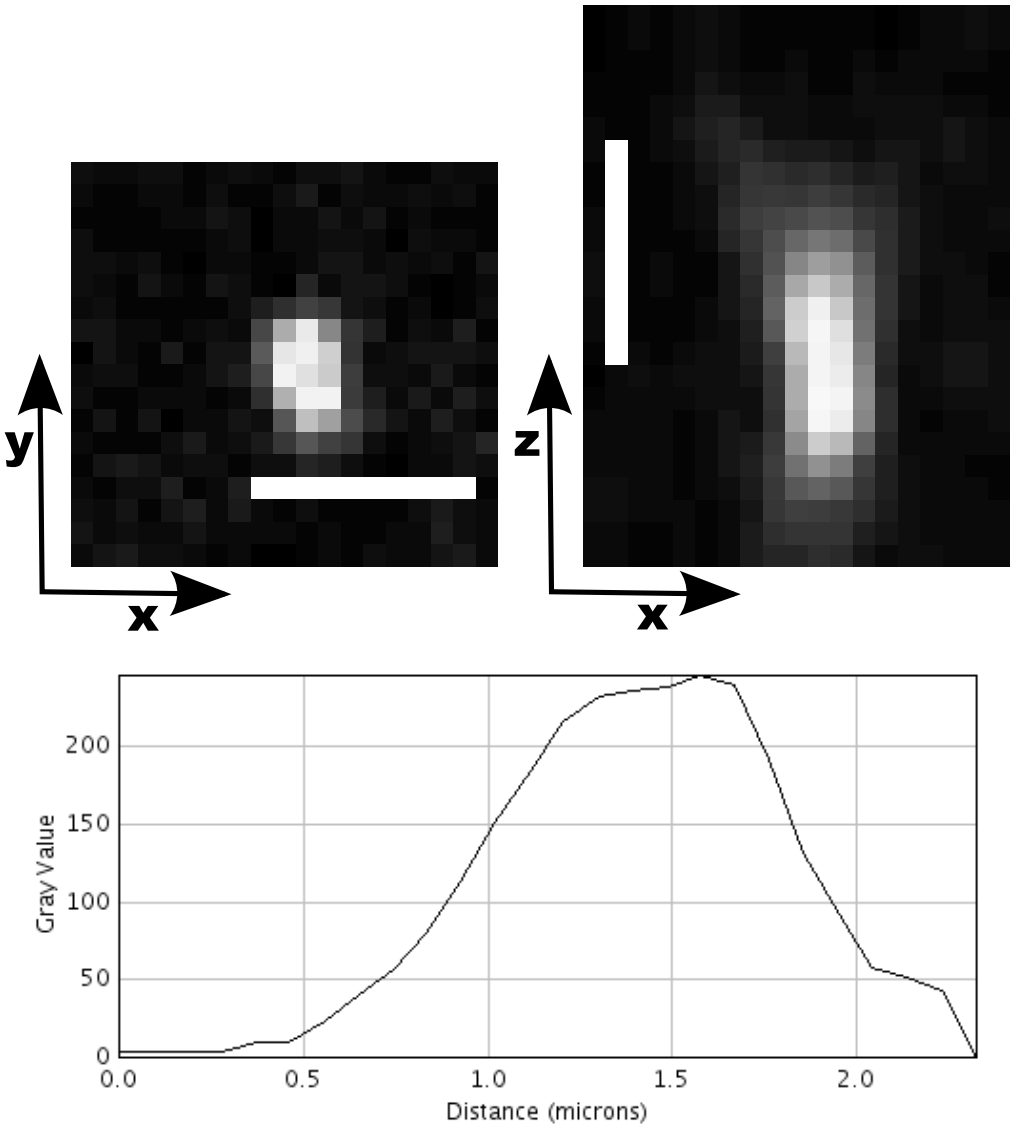

Figure 5.6: *The x/y profile of a small (500 nm) fluorescent spot is shown on the left. This is not a uniform bead, but rather a small spot of fluorescence on a 100 nm slice through the muscle. On the right is the x/z image of the spot. Although the z-thickness is known to be 100 nm, this image shows that it appears to be 1 µm or larger. Scale bars: 1 µm. The bottom graph shows the intensity profile along the z-axis through the centre of the spot. The FWHM is the width at 127.5 intensity value and is equal to just over 1 µm*

thickness, tape substrate, and mounting method. Firstly, slices were cut at two different thicknesses. At 200 nm thick they appeared to have wrinkles (see figure 5.7C arrowheads) whereas no wrinkles were apparent in 100 nm slices (see figure 5.8 for example). It is not clear why 200 nm slices become wrinkled and 100 nm slices do not, although it could be related with the way the slice interacts with the substrate. An alignment of 13 tiles of 200 nm thick sections can be seen as a movie on the DVD submitted with this thesis. It can be found at `Chapter_5.../200nm_on_mylar_wrinkles.avi`. The wrinkles cause the alignment to be jerky.

There was also a choice of different tape materials for collecting the slices on: mylar, capton and polycarbonate. Polycarbonate tape had the lowest autofluorescence of the three, but slices appeared very wrinkled on it. There was no noticeable difference between mylar and kapton in terms of how flat the slices appeared.

Kapton had the highest level of autofluorescence, which was apparent in both the green and the red channel (see figure 5.8B). Because the signal in the red channel (from the BTX) was dim anyway, kapton autofluorescence completely masked it (figure 5.8Biii). Mylar is also autofluorescent, but the signal in both the red and green channels remained visible (figure 5.8A). I briefly experimented with trying to transfer the slices directly onto the coverslip without success.

Apart from wrinkles which are local, the flatness of the slice is also compromised if the slice is tilted with respect to the imaging plane. Tilt is largely the result of how the slices are mounted on slides.

I tried various methods for mounting the sections. Using no medium (just air) between the slide and the cover slip did not produce good images and led to the slices bleaching easily. Optical glue that is optically invisible and solidifies under UV light preserved the fluorescence but did not cure very well. In addition, the thickness of the glue was not uniform, which could lead to distortions in the imaging. Finally, I tried various methods of applying Vectashield, varying the amount and whether the preparation was flattened between magnets. A small amount of Vectashield with hardly any pressure on the coverslip worked the best and preserved the fluorescence adequately.

Each section did not fit into a single field of view (95x95 μm^2) so multiple image-tiles

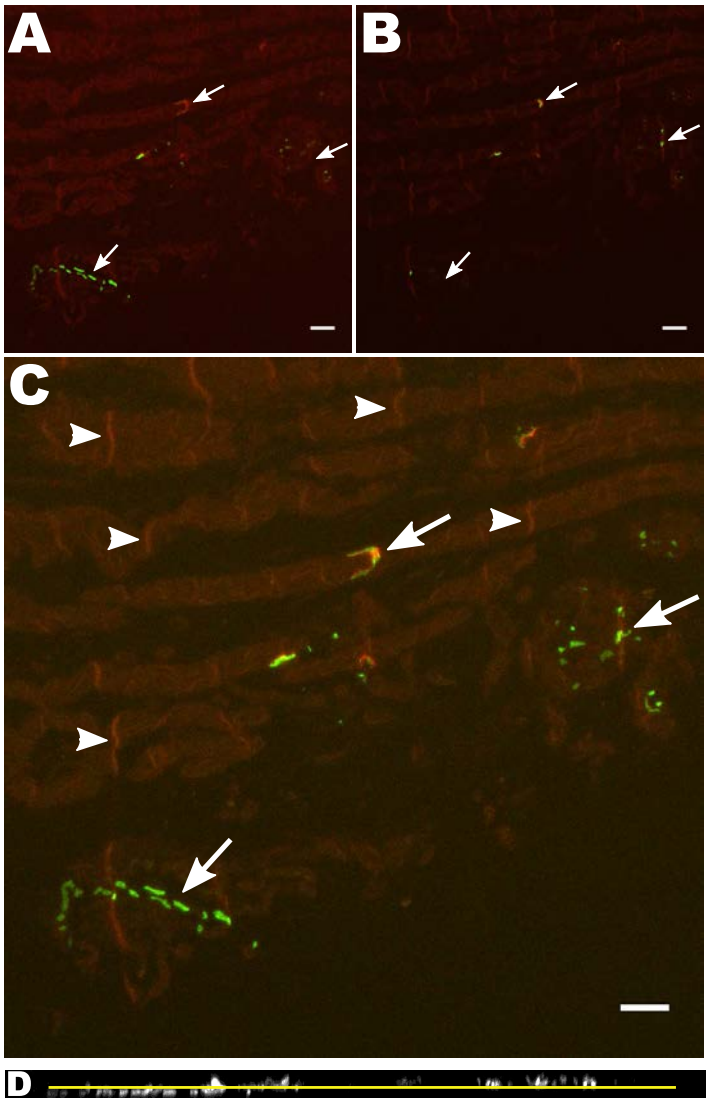

Figure 5.7: *Image showing one tile from a 200 nm slice. Note the presence of wrinkles (arrowheads in C) which could distort the image, making alignment of the sections harder. Apart from wrinkles, the slice is not flat on the slide. This can be seen because different parts are in focus in different z-planes. A and B show optical slices which are separated by 2100 nm. Different parts of the slice are in focus in each (see arrows). C is the maximum projection. D shows the maximum projection of the x/z cross-section. Note the fluorescence on the right is higher (along the z-axis) than the fluorescence on the left, indicating that this slice is tilted with respect to the image plane. These distortions will have to be compensated for during alignment for an informative image to be produced. Scale bars: 10 µm*

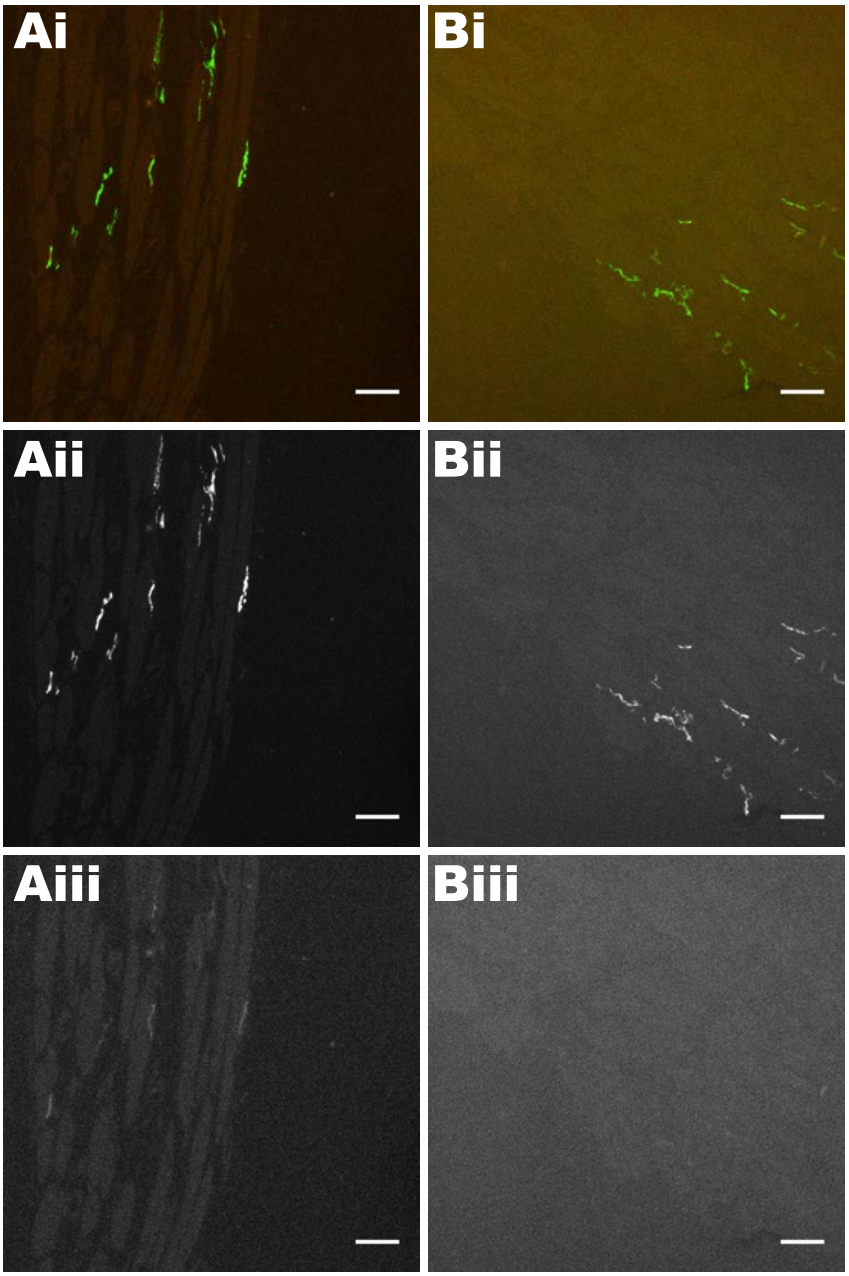

Figure 5.8: *Autofluorescence levels of A: mylar and B: kapton tape. Top row shows merged image, middle row shows green channel only (axons) and bottom row shows red channel only (endplates). Notice that YFP is bright enough to be visible on both tapes, though the contrast is higher on mylar (A) which has a lower autofluorescence. Both tapes have high autofluorescence in the red channel, although receptors on the mylar slice are still faintly visible. In contrast, nothing is visible on the kapton. Both slices shown here are 100 nm thick. Notice there are no visible wrinkles like in the 200 nm slices in figure 5.7, although in 200 nm thick slices the SNR is better. Scale bars: 10 µm.*

were captured of each slice and stitched together. Because the signal can be sparse, it was difficult to stitch the slices together in the x/y plane. In order to facilitate this, a third channel was used to collect the reflected light produced by the 543 HeNe laser. In order to minimise the imaging time per slice I oriented the slices on the slide so as to minimise the number of tiles needed to cover the entire section. Furthermore, I tried to reduce the number of z-slices through which I imaged. However, if there was some tilt in the slice I necessarily had to increase the number of z-steps.

Using the reflected light for alignment worked well most of the time (see figure 5.9). However, occasionally the image was dimmer and blurry around the edges and in these cases it was not as easy to find the exact x/y alignment. This may have been caused by distortions due to misalignment of the microscope.

In view of these findings an attempt was made at a reconstruction using 100 nm slices collected on mylar tape. The tape was then cut into short (roughly 5cm) segments containing up to 12 slices on each segment. These were mounted on the slides using a small amount of Vectashield and by gently laying a cover slip over them without much pressure.

I cut through most of a 4DL muscle producing around 1700 slices of 100 nm thickness. Given that each slice can be covered by a 1x4 grid of tiles which are 95x95 μm^2, the 4DL appears to be contained within a volume of 100x200x400 μm^3.

Of these about 300 sections were imaged at high resolution.

5.3.3 Serial sectioning 2: reconstruction

After imaging, the most in-focus image plane was chosen from each stack and saved as a tiff file. Occasionally the slice was tilted resulting in different features being in focus in different image planes. When this occurred, maximum projections were saved instead of just a single plane (though this only was the case for a handful of images used in the final reconstruction). Generally, using the maximum projection is slightly worse than the in focus plane because the optical sections are not always perfectly aligned with each other. Therefore, the maximum projection may cause some

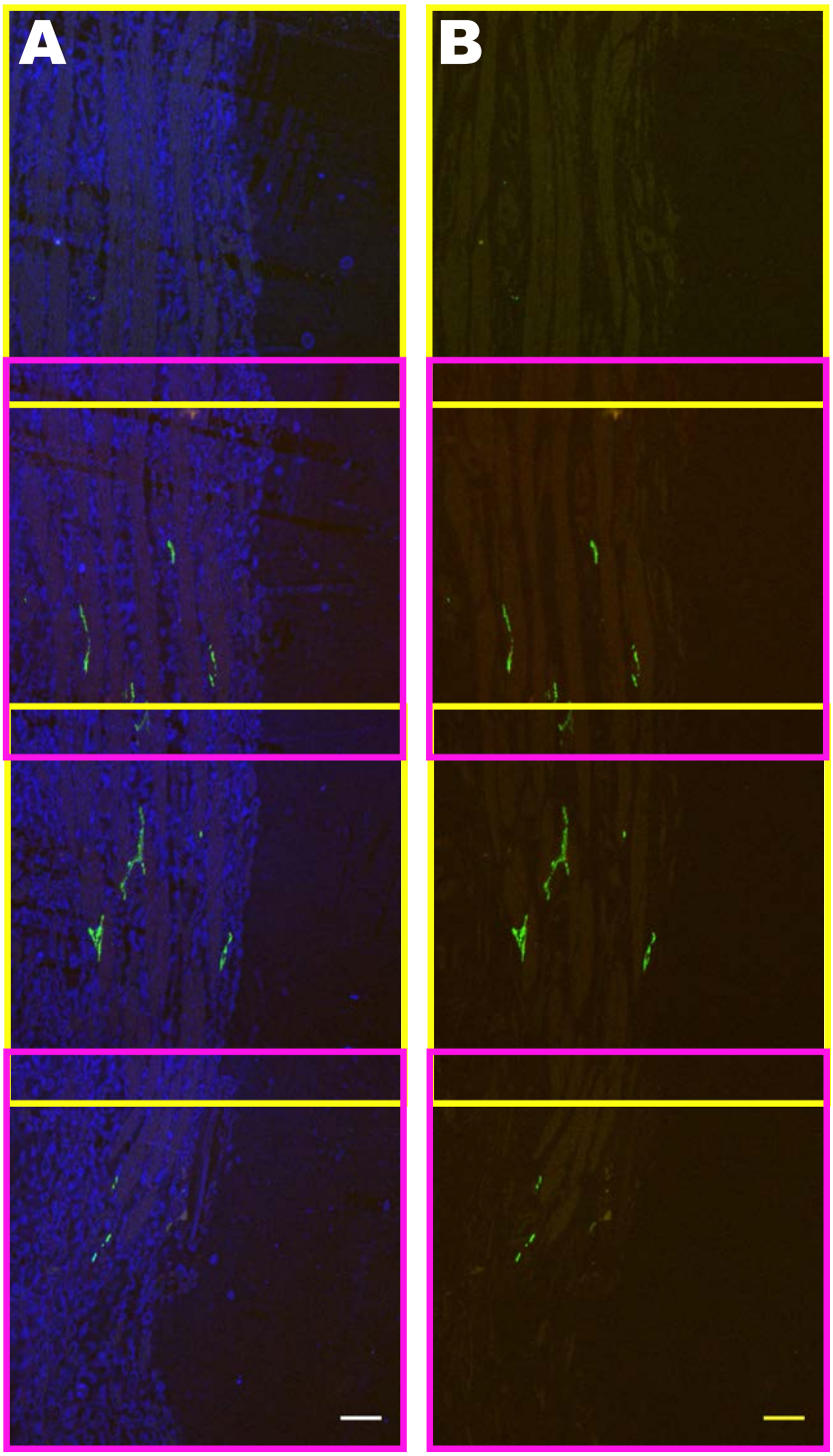

Figure 5.9: *A:Image showing a montage of four tiles covering a whole slice. The reflected light shown in blue. The yellow and pink boxes delineate each tile. B: The same image is shown as it is used for z-alignment, without the blue channel. Scale bars: 10 µm*

fluorescent signal to appear slightly wider than it should.

I wrote a plugin for imageJ to automatically select the in focus plane by selecting the slice with the highest summed pixel intensity (the sum of each pixel intensity). This worked in most cases apart from when the slice was significantly tilted. The results were verified by hand in many instances.

Two alignments of single tiles were made. The first one consisted of 89 tiles (all of which were maximum projections) with both the green and red channels. From this alignment, two things became clear: the red channel did not contain very much signal in many slices and the fluorescent structures in image stacks slightly shifted as the objective focused through the stack causing a very slight misalignment between some of the optical sections. This could be due to the objective pressing down on the coverslip and may result in worse resolution in the maximum projection than in the in-focus image plane. This alignment can be found on the DVD submitted with this thesis at `Chapter_5.../100nm_p5_4DL_alignment_89slices_singletile.avi`.

The second alignment consisted of 78 tiles of the in-focus optical slice only and the green channel only. These two alignments had an overlap of about 40 slices and allowed me to identify the location of an endplate with some axon branches innervating it and reconstruct the volume in which it was defined. This alignment can be found on the DVD submitted with this thesis at `Chapter_5.../100nm_p5_4DL_alignment_78slices_singletile.tif`, and can be opened with ImageJ or Fiji.

The third alignment consisted of 50 sections, some of which were single tiles and some of which were two tiles stitched together so that each z-plane contained the features of interest. Figure 5.10 shows the maximum projection of the 50 aligned sections. This alignment can be found on the DVD submitted with this thesis at `Chapter_5.../100nm_p5_4DL_alignment_final_50slices_whole.tif`, while the alignment of the region of interest can be found at `Chapter_5.../Figure_5.10_100nm_p5_4DL_alignment_final_50slices.avi`.

All alignments were made in Reconstruct using the Linear Align method, which takes into account translation, rotation, scaling and skew (tilt). Particular care was taken to align the endplate shown in the yellow box along with the axons below it. Features at

the edges of the image are perhaps not aligned as well. In order to create a very good global alignment it is important that slices are flat and are not stretched or wrinkled. On the right in figure 5.10 is the x/z view of the endplate. The endplate spans 40 slices therefore has a z-width of 4 μm.

Firstly, I show that this technique does indeed increase the z-resolution. Figure 5.11 on the left shows the maximum projection of the endplate and axons of interest. The yellow rectangle denotes an area where there are two axons running in parallel at different z-depths. On the right there are five consecutive x/z views of the region enclosed in the yellow rectangle. Here we can clearly see that there are at least two objects (the two axons) separated by a gap. This gap ranges from about 800 nm (8 slices) to 300 nm (3 slices). If this was an optical section, nothing separated by less than about 1 μm would be resolvable (as determined previously).

However, the increase in z-resolution is not enough for axons to be traced through the image. I will try to illustrate this point with the next figures, by showing three locations along the axon bundle. At the first and the third point I will show there are at least two axons. However, in the central point it is not possible to resolve two separate structures. The assumption is that if at least two axons are going into this spot and at least two are coming out then there should be two axons at this point as well.

Figure 5.12 shows the first location where there are at least two axons. All the images are grayscale but x/z and y/z viewing angles have been shown with the spectrum colour scheme for better contrast. The monochrome image on the upper left is the maximum projection of the alignment. Below it, is an x/z cross-section at the point shown by the horizontal dashed line. In this image there are two resolvable structures indicated by the white and blue arrows. The distance between the two peaks in the intensity profile is about 600 nm (along the x-axis). To the right of the image are three non-consecutive y/z cross-sections taken at the locations indicated by the vertical dashed lines. The white arrows show that the axons are separated along the x axis. In the first of the three y/z cross-sections there is an axon at the location indicated by the white arrow. In the second there is a gap and in the third there is an axon again. Therefore there are at least two axons at this point. However, almost immediately above the white arrows they become difficult to resolve. The black arrow indicates the point at which I have

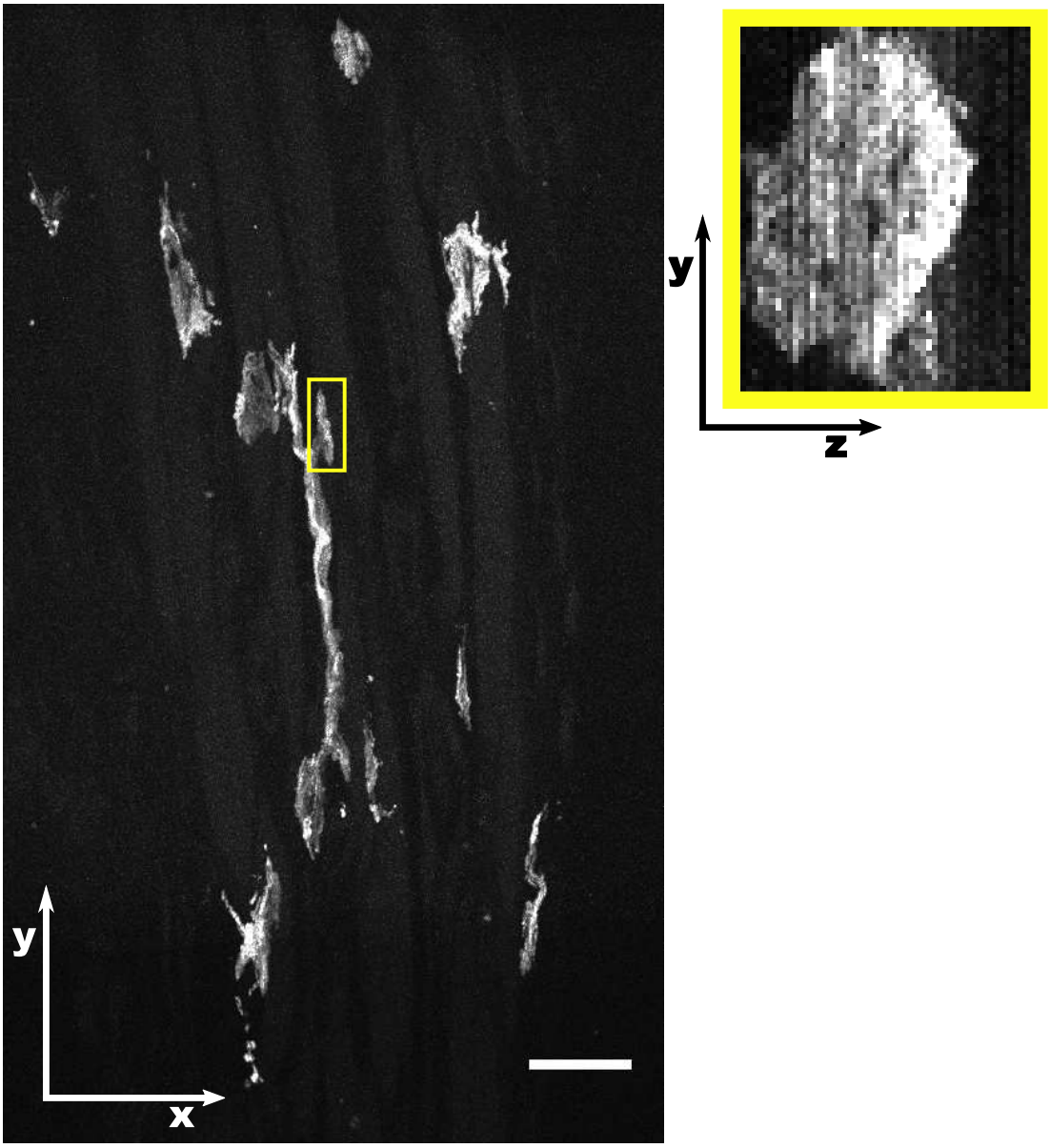

Figure 5.10: *Maximum projection from linear alignment of 50 slices. Subsequent analysis of the resolution will concentrate on the endplate shown in the yellow box plus the bundle of axons which innervate it. It is assumed this is an endplate because of its shape. The BTX staining has not showed up at this endplate. On the right is the maximum projection of that same endplate viewed from the side (z/y) compared to the image on the left. Scale bar: 10 µm*

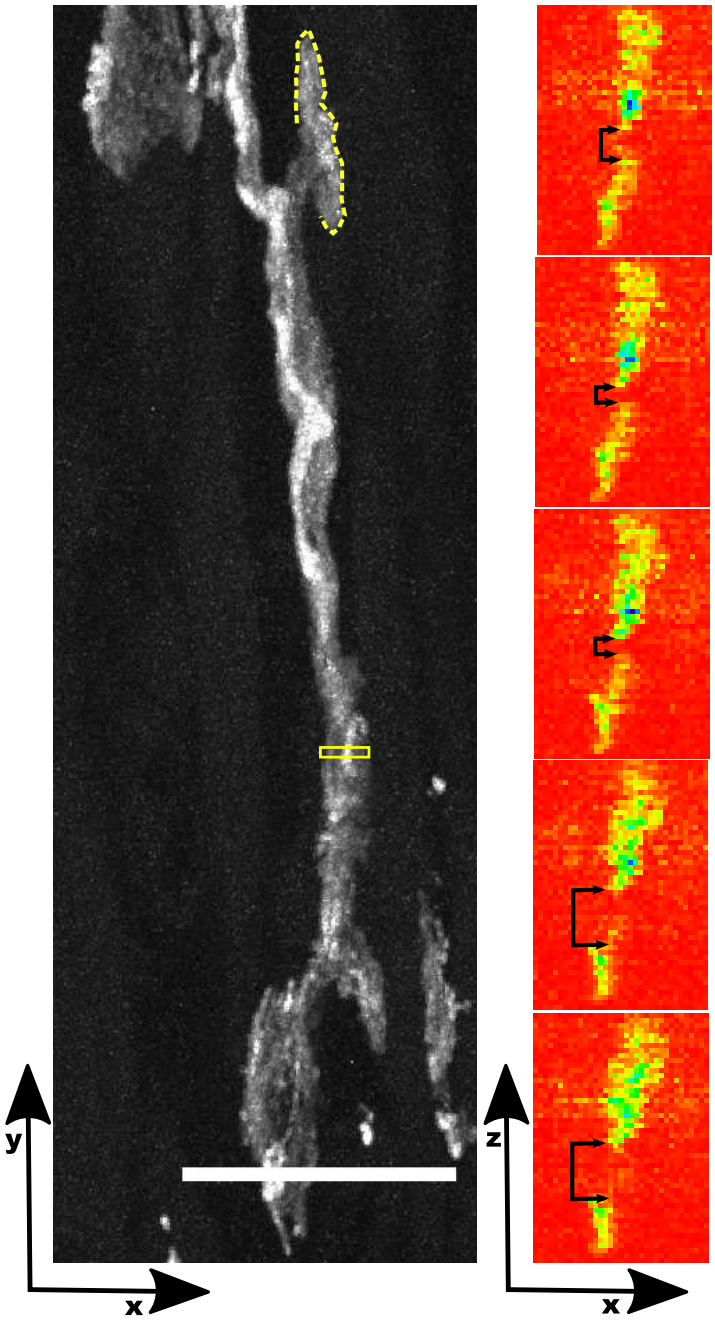

Figure 5.11: *Increased z-resolution from reconstructing serial sections. Left: Image showing maximum projection of 50 aligned sections. Right: Five x/z sections taken consecutively from where the yellow rectangle is. These are shown with a spectrum look up table (see figure 5.5). These images show that there are at least two axons travelling in parallel at different depths. They are separated by a distance under the resolution limit of the optical section of the confocal microscope. From the top the two axons are separated by 500, 300, 300, 800, 800 nm (see black arrows). Scale bar on left: 10 µm*

shown they are unresolvable (see figure 5.13).

Figure 5.13 shows the location where it is not possible to resolve two axons at the cross-section of the dashed lines. As with figure 5.12, the monochrome image is the maximum intensity projection of the 50 aligned slices. Below is the x/z cross-section taken at the location of the horizontal dashed line. It is not obvious how to segment this into two or more axons. Below the x/z cross-section are four possible segmentations which are all consistent with the image. On the right is the y/z cross-section taken from the location of the vertical dashed line. The black arrow shows the location in y/z where it is not possible to resolve two axons. Closer still to the endplate in the image there appear to be three axons as indicated by the pink, white and green arrows. It is not possible to be certain that there are three axons based only on this image because if an axon is cup shaped it might appear as two in earlier slices but as only one in later slices. However, based on looking through the x/y stack I think it is likely that there are at least two resolvable axons at this location.

Figures 5.14 to 5.17 show the individual aligned sections. The yellow dotted outline indicates where the endplate is. The large white arrow shows the unresolvable location (the same location that the large black arrow in figures 5.12 and 5.13. Note that while in some frames two axons appear to be resolvable (especially in figure 5.16) this is because of the cup shape of the x/z cross-section. Above the unresolvable region the pink and green arrows indicate the same axons as in figure 5.13 and below it the blue and white arrows show the axons referred to in figure 5.12.

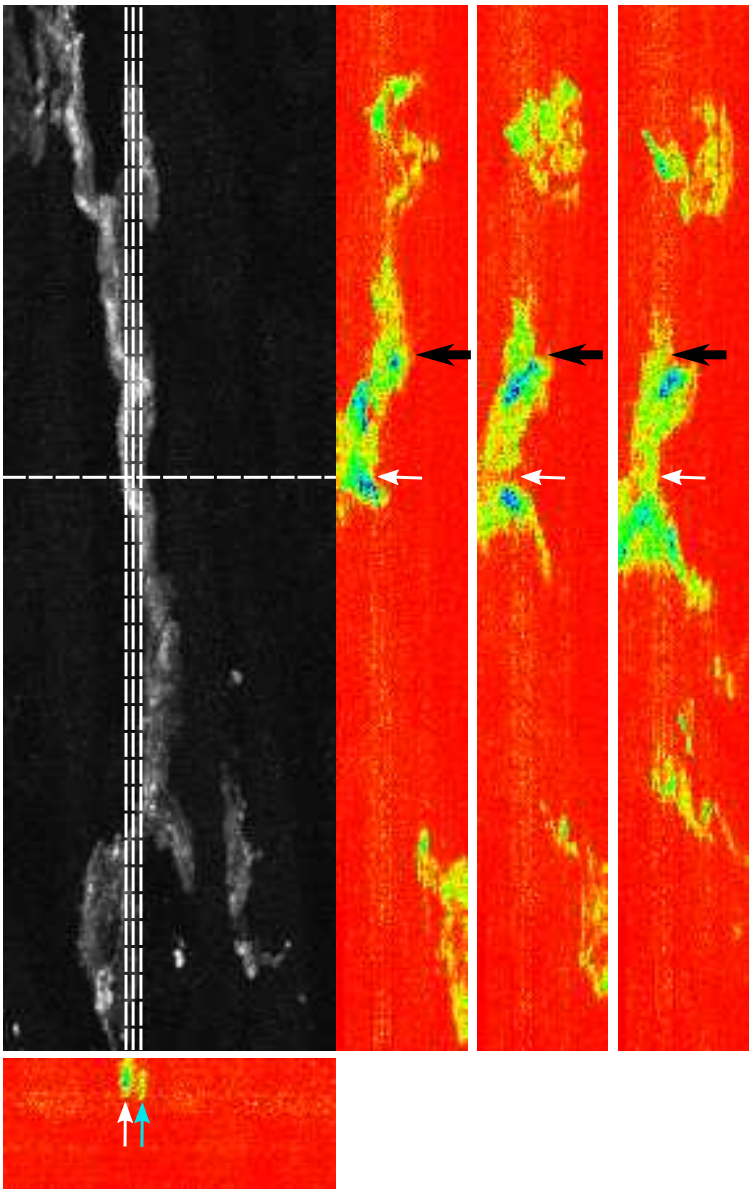

Figure 5.12: *There are two resolvable axons shown at the cross-section of the dashed lines. The monochrome image at the top left shows the maximum projection of the alignment in the x/y plane. The other images are also grayscale, but are plotted in the spectrum look up table. The lower left image is the x/z profile at the y-coordinate indicated by the horizontal dashed line. Two structures are resolvable (white and blue arrows). The three images on the right are non-consecutive y/z profiles taken from the locations indicated by the vertical dashed lines. The white arrows show the two structures separated by a gap (middle image). The black arrow shows the location where two structures are not longer resolvable (see figure 5.13).*

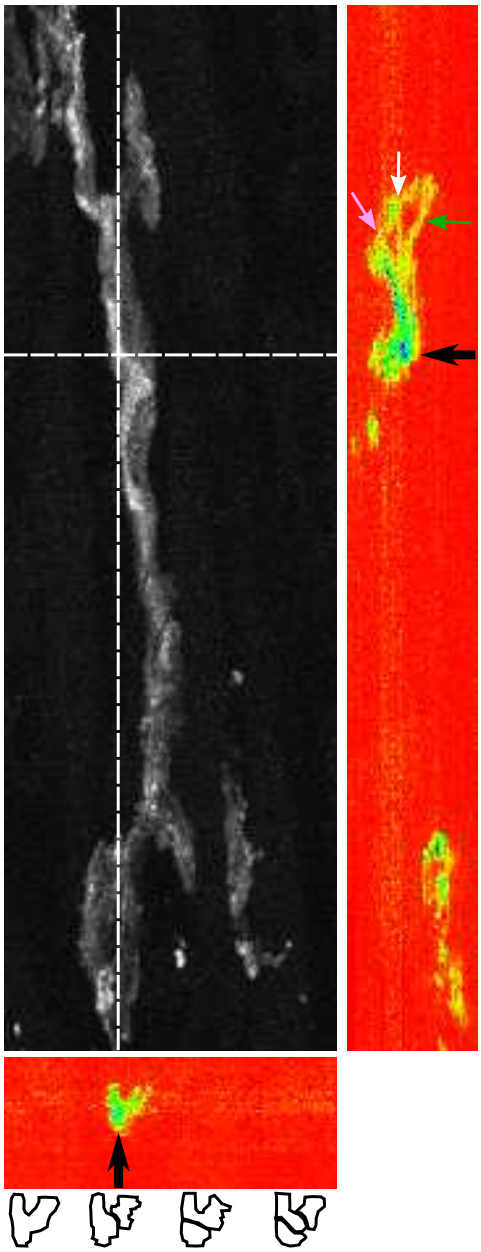

Figure 5.13: *Image showing a portion of the axon path where the axons become unresolvable. It is not clear how many axons there are (1,2 or 3). The image on the left is the maximum projection of the 50 aligned slices. Below is the x/z cross-section at the point shown by the horizontal dashed line. It is not possible to resolve two distinct axons at this location. At the very bottom of the image are four possible segmentations which are all consistent with the image. On the left is the y/z cross-section at the point shown by the vertical dashed line. The black arrow indicates the location at which more than one axon is not resolvable. However, further up the nerve more than one axon becomes resolvable again as indicated by the pink, white and green arrows. It is not clear if these represent two or three axons.*

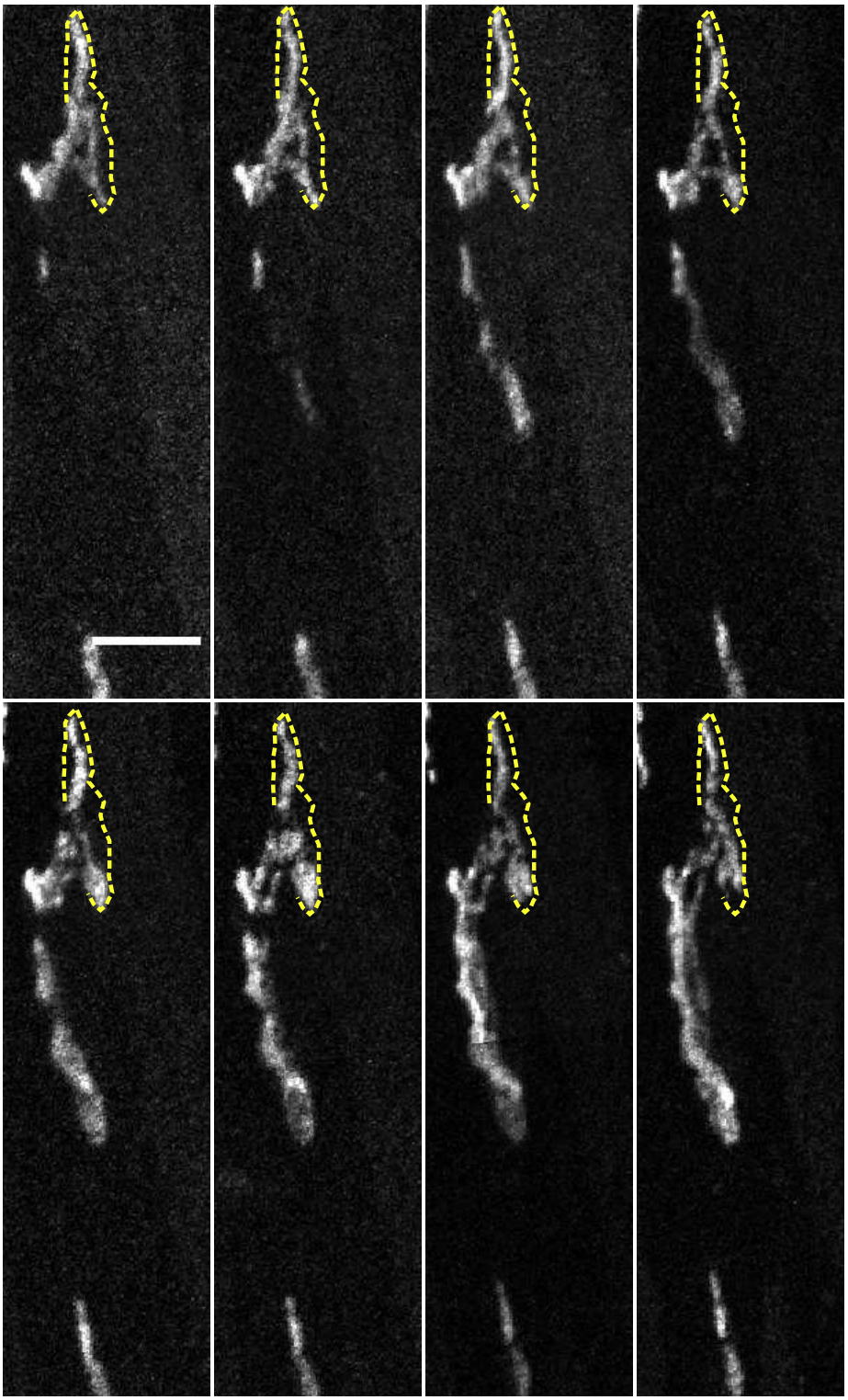

Figure 5.14: *Series of aligned sections 1-8*

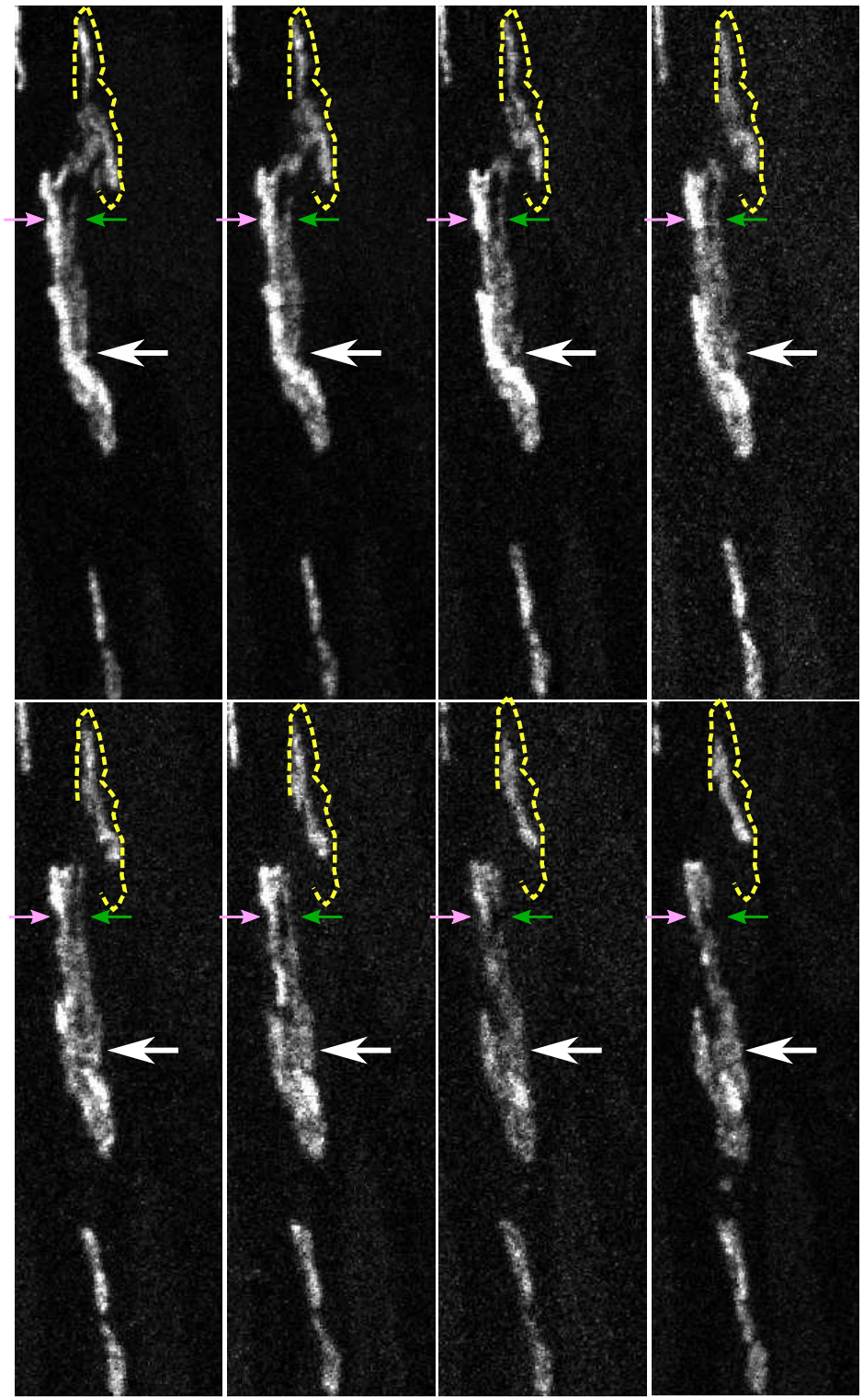

Figure 5.15: *Series of aligned sections 9-16*

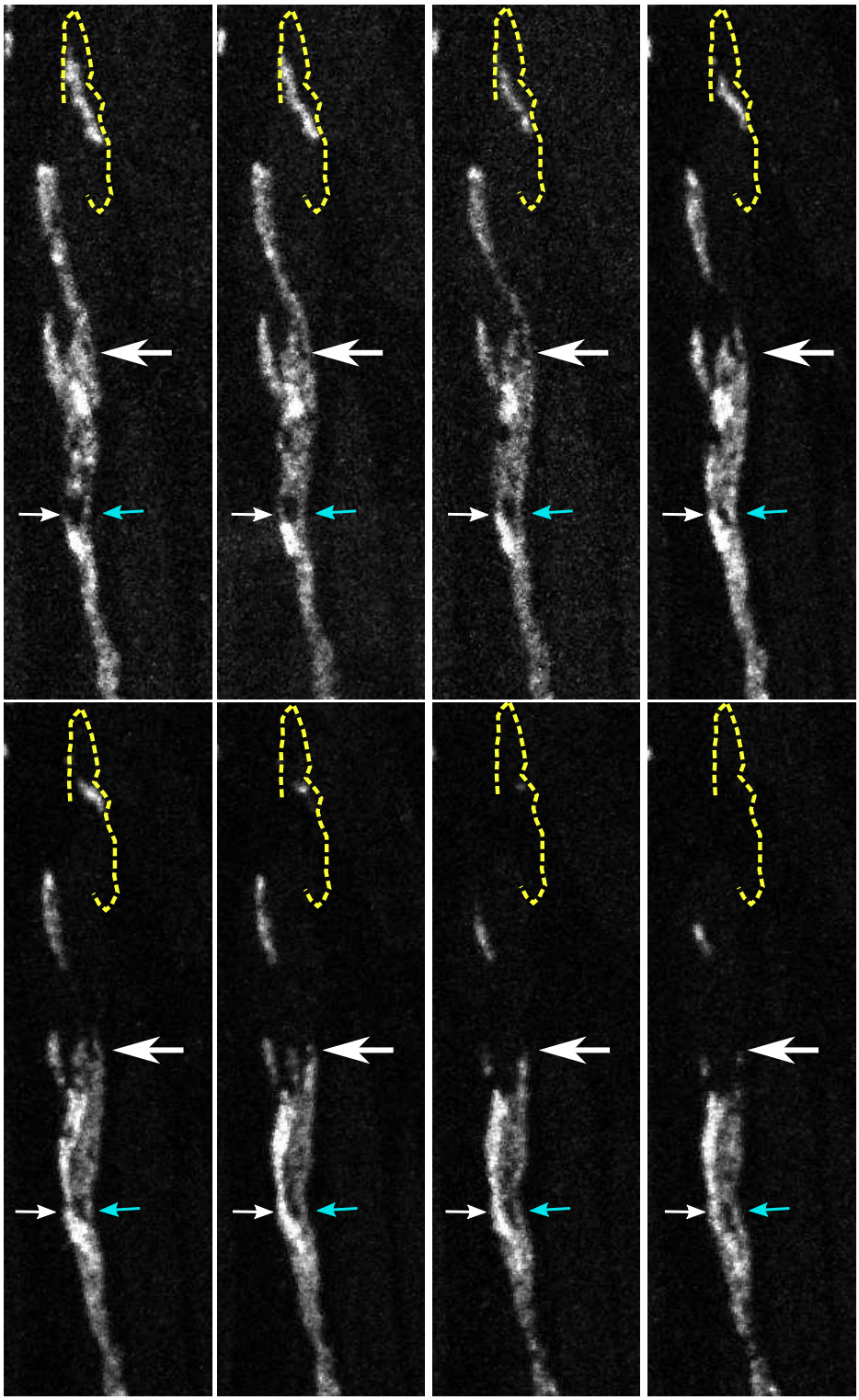

Figure 5.16: *Series of aligned sections 17-24*

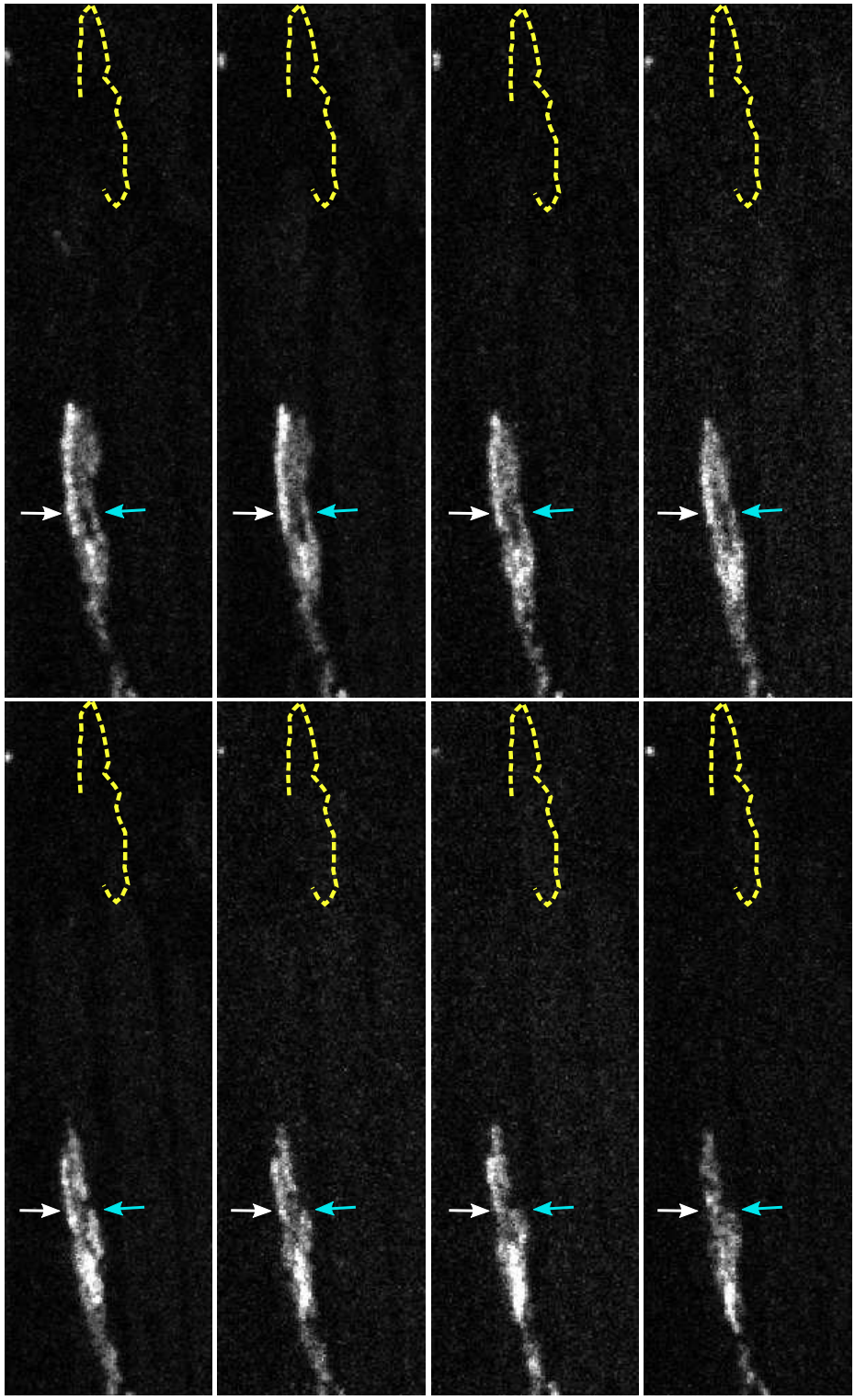

Figure 5.17: *Series of aligned sections 25-32*

5.4 Discussion/Conclusions

In this chapter I have described my attempts to resolve neonatal motor units using confocal microscopy and ultra-thin serial sectioning followed by reconstruction. I have shown that confocal microscopy does not provide sufficient resolution to distinguish between neonatal axons. Although increasing the axial resolution, physical sectioning does not do this either with the specific parameters I used. I believe there is potential for this technique, by using a super-resolution technique to image the sections, thus increasing the x/y resolution, and, possibly, by cutting thinner sections. In order for this to be feasible, as much as possible of the process should be automated.

5.4.1 Confocal microscopy on YFP16 and NF labelled muscles

I have produced confocal images of motor axons in a neonatal (p5) 4DL muscle as close as possible to the theoretical maximum resolution using a 63x magnification 1.4 NA objective lens. Images were sampled laterally at 93nm or less and axially at 300 nm or less. Despite this, individual axons are not always resolvable from each other. Furthermore, in most but not all instances, the number of axon branches innervating a specific endplate was not resolvable. This is true both for axons which endogenously express YFP and for axons marked by NF immunostaining with FITC, even though in the latter the synapses are not fluorescent which should make seeing branches near the endplate easier.

Since the image produced by the microscope is the convolution of the true image with the point spread function, one method of enhancing the microscope image is deconvolution. Deconvolution attempts to infer the true image from the acquired image and the PSF. Since the PSF spreads the photons originating from a sub-resolution point over a larger area, deconvolution assigns the captured photons to the inferred point of origin, resulting in a higher contrast image. This can work very well for images of sub-resolution beads as shown by Schrader et al. (1996). They imaged 543 nm light scattered by tiny gold beads and found that they could deconvolve the resulting digital images in order to get 80 nm resolution in the lateral direction and 40 nm in the axial

direction (as judged by using the FWHM criterion). However, as they mention in the paper, the quality of the restoration is object dependant. Objects of unknown shape and less sparse images will be less well deconvolved. Axons can vary in shape and in brightness, leading to genuinely ambiguous images in which there is no certain interpretation. Moreover, they needed a very high SNR for the resolution to be enhanced, which would not be achievable with fluorescence. Losing information about the outer regions of the PSF will also diminish the ability of a deconvolution algorithm to infer the true image.

Performing Huygens deconvolution on Nyquist sampled confocal images of fluorescently tagged NF in neonatal motor axons still did not permit individual axons to be resolvable. Therefore for neonatal (p5) 4DL the confocal microscope does not provide enough resolving power to distinguish between axons.

Many studies have counted the number of inputs to developing endplates. Traditionally these have use electrophysiology to measure endplate potentials evoked by increasing amounts of stimulation. A jump in the amplitude of the endplate potential indicates the presence of an additional input, and so the total number of jumps corresponds to the number of axons innervating that endplate (Thompson and Jansen, 1977; Betz et al., 1979, e.g.). There are also a number of studies which have quantified the number of inputs to each endplate through visual observation (Murray et al., 2008; Lanuza et al., 2002; Nguyen et al., 1998, e.g.). These are generally done on flatter and larger muscles than the mouse lumbrical (e.g. the LAL (Lanuza et al., 2002; Murray et al., 2008) or at later ages (e.g. p8 and onwards (Nguyen et al., 1998)). The lumbrical muscle is very small but also there are a large number of axon branches (since neonatal motor unit sizes appear to be relatively large). Moreover it is not flat and therefore may be particularly susceptible to the limitation in axial resolution when imaging. To the best of my knowledge no published data exists on the time-course of synapse elimination in mouse lumbrical muscle. Although it is possible to quantify the number of branches innervating an endplate in some instances, the majority of times it is ambiguous.

The shape and size of the PSF, and thus the resolution of an imaging system depend on the NA of the objective and the wavelenght of light used. Therefore, using an objective with a higher NA or using a shorter wavelength of light will increase the

imaging resolution. However, this is only feasible up to a point. The highest NA objectives routinely available at present are 1.45, which would give only a 5 nm (3%) increase to the theoretical maximum lateral resolution and a 40 nm (7%) increase to the axial resolution compared to the 1.4 NA objective used in these experiments. In terms of light, a shorter wavelength will increase resolution but that is not the only consideration when imaging. Fluorescence is a very useful tool for enhancing the contrast of the images and various fluorophores available need specific wavelength of light to be excited. Also if using more than one colour of fluorophore they need to be spectrally separable. Additionally, short wavelengths can be damaging to tissue and objectives are normally optimised for a certain range of wavelengths and thus perform sub-optimally with wavelengths outside this range.

Therefore, in order to image with enough resolution to resolve neonatal motor axons one of the techniques being developed which surpasses the diffraction limit must be used.

5.4.2 Serial sectioning and reconstruction

There are several different techniques being developed to surpass the diffraction limit. One of these techniques which is being developed in the Lichtman lab among others (Micheva and Smith, 2007) relies on physically sectioning the tissue before imaging. Tissue sections have been readily used in light and electron microscopy. Moreover, tens of serial sections have been aligned before in order to reconstruct specific structures of interest (e.g. Bishop et al., 2004). However, reconstructing a whole muscle, brain region or brain involves orders of magnitude more sections. This is difficult since sections are usually collected and placed on a slide or an imaging grid (for EM) by hand. Collecting thousands of sections by hand is not practical and, as a technique, would be prone to errors. Therefore the Lichtman lab have developed a custom made tape collecting mechanism which can collect thousands of cut sections with little human intervention (Blow, 2007; Hayworth et al., 2006). The tape collecting device used in this thesis is an early version of those described in the previous references named ATUM (Automatic Tape-collecting UltraMicrotome) as opposed to ATLUM (Auto-

matic Tape-collecting Lathe UltraMicrotome).

As discussed previously, the axial resolution of confocal microscopes is three to four times worse than the lateral resolution. Ultra-thin serial sectioning is a technique which can improve the axial resolution by an arbitrary amount, limited only by the thickness of the slice.

A z-stack taken of a 100 nm slice revealed that the z-resolution of the particular imaging system (Zeiss Pascal) was about 1 μm. Therefore, reconstructing a volume of 100 nm sections increases the z-resolution roughly ten-fold. The lateral resolution is still the same, although there may be some benefit of physical sections because objects which are close in x/y may be separated into different sections. It is not clear what the minimum separation between axons is in the neonatal lumbrical muscle. However, an EM image of lumbrical intramuscular motor axons published in Murray et al. (2008) shows the axons profiles separated by approximately 800 nm. Therefore it is reasonable to assume this technique would provide sufficient resolving power where confocal does not.

When intending to align physical sections it is important that distortion of each section is minimised. For a good alignment, each feature in one slice should be at the same position as corresponding features in other slices. If the sections are distorted when imaged, the image of them will need to be distorted in order to line up the features across sections. However, there is no guarantee that this will result in the correct shape of objects and will generally lead to a lower quality reconstruction. Therefore, it is best if the alignment can be done with as few deformations to the images as possible. Distortions, which include folds, wrinkles, stretching and tilting can be introduced both when collecting the sections on the tape and when mounting the tape on the slides. I tried a few combinations of slice thickness and tape and found that 100 nm sections on mylar or on kapton were the flattest.

Another issue is related to imaging the sections on the tape. Both mylar and kapton were autofluorescent, particularly in the red channel. Using a confocal instead of a widefield microscope may have helped to reduce some of the autofluorescence by restricting the imaging plane to less than the thickness of the tape, i.e. not collecting all the autofluorescent light emitted by the tape. Otherwise there is not much benefit of

using confocal over widefield microscopy since each section is thinner than an optical slice and widefield images would be faster to acquire. Although mylar seemed to be the less autofluorescent of the two, in the reconstructed stacks of sections on mylar the red channel is very noisy. This could also be related to the fact that the alexa-555-BTX used for staining the endplates was less bright in the slices than the alexa-488 used for the axons. The dimmer red signal could be because it was degraded more by the dehydration and embedding process, or because there is less of it per volume. A simple solution would be to use a different fluorophore for labelling the endplates that is brighter or that emits light at a wavelength at which the tape is not very autofluorescent.

Mounting the sections on a slide was not straightforward and the technique I used could be improved. It was difficult to get the sections flat on the slide. Flatness could be easily assessed by acquiring an image stack of a section and viewing the x/z cross-section (as in figure 5.7D). All the fluorescence should be centred on the same z-plane though this was not the case. One idea would be to try and use the information in the x/z profile for how the image is tilted or wrinkled in order to try and infer what the image would have looked like if it were flat. However, it is time consuming to image z-stacks and should not be necessary with 100 nm slice. Therefore a better solution would be to be able to consistently mount slices flat on the slide.

Each section did not fit into a single field of view, and so multiple tiles needed to be stitched together for each. Because the signal of interest could be sparse, which made it very difficult to align the sections in x/y, I collected the reflected light from the red channel. This provided a very rich signal for aligning in x/y although I'm not sure if the same signal could be used for the z-alignment or not. It is not clear what it represented but it seemed to be different in muscle fibres and in the space between muscle fibres. One problem with this method was that sometimes the top edge was dimmer and blurrier than the bottom edge, which made it more difficult to align the top edge of one image with the bottom edge of the other. This was probably related to the alignment of the microscope. Apart from this, it was a good technique for getting a rich signal and enabled me to align sections in x/y that otherwise I would not have had enough information to do.

Another problem was that some of the sections on the tape got caught under the glue

of the cover tape because they were too far off to the side. This ruins the particular sections and leaves gaps, which result in an incomplete reconstruction. A better preparation of the block could lead to the slices coming onto the tape straighter although, to be on the safe side, cover tape without glue could be used.

I made several large alignments. The first included 89 tiles, and each tile was the maximum projection through the z-stack I had imaged. The second large alignment included 75 tiles and overlapped by 40 tiles with the end of the first. From these two alignments I identified an endplate which was contained within these slices and a bundle of axons either leading up to it or travelling past it (it is not clear which directions the axons are travelling in from these limited images, nor if they are all travelling in the same direction). The third alignment focused on reconstructing the identified endplate along with the axons and contained 50 slices. This was used to subsequently analyse the resolution of the technique.

One interesting thing about these images is that there appears to be one bright axon and one or two dimmer ones (see figures 5.10 and 5.14-5.17). Furthermore, even the endplate appears to have a bright region and a dimmer region (figure 5.10 right, image of the y/z cross-section). However, these images were not taken with the specific idea of segregating axons based on intensity, which would require careful imaging conditions in order to preserve the intensity relationship between slices. For example, the YFP in this muscle was enhanced by immunostaining with an anti-GFP antibody before the embedding process. Immunostaining was not done in a carefully controlled way but rather the goal was to saturate the signal as much as possible. Therefore it is not clear whether any differences in brightness in the original sample, if they existed, would have remained after the immunostaining, nor whether any subsequent differences in brightness could be used to designate axon identity (rather than part of one axon being brighter than another part of it due to penetration of the antibody etc.). Furthermore, during imaging the gain and laser intensity were changed independently for different slices, depending on their overall brightness. In addition some slices were bleached more than others, specifically the first sections on a slide were more bleached than the later ones, which was probably the result of the way sections were identified (by shining a light along the tape). Finally, because Reconstruct only accepts 8-bit

images, for the alignment, images were changed to 8-bit in Fiji which seems to down-sample the gray levels of the image differently depending on the value of the brightest pixel in the image. So it is a possibility that one axon is brighter than the other, but it is not clear if the difference in intensities is a reliable way to distinguish between axons. Even if it was possible to distinguish between the axons based on intensity, the resolution would still not be enough to segment the axons in the location of interest since it is not clear if there are one or two dim axons.

Serial sectioning is only one of a few different technique being developed which could enable the reconstruction of connectomes. Other techniques include block-face imaging and multicolour imaging.

Block-face imaging takes advantage of the fact that the resolution and contrast at the surface of a tissue is better than deep into the tissue because there is less opportunity for scattering. Tissue is embedded in a block of plastic and the surface of the block is imaged. A section is then sliced off the surface and the block face (which now has new structures on the surface) is imaged again. The benefit of this technique is that it allows imaging of each structure at its maximum brightness and without blur from structures above. Although there may still be a small amount of alignment necessary, the alignment should be much easier and better than with physical sections. Furthermore, there is no need to keep track of thousands of slices. The drawbacks are that there will still be blur from the structures underneath the plane of focus. Additionally, once a section is cut it is destroyed, so there is not the potential to go back and re-image or re-stain a certain section. This technique would not provide enough resolution to distinguish every structure in mammalian brains but combined with a good deconvolution algorithm may be a good and fast technique for getting information about certain circuits.

Multicolour imaging is another way of trying to resolve structures beyond the resolution limit by tagging different structures with spectrally resolvable labels. The state of the art of this technique, at the moment, is the genetically modified brainbow mouse (Livet et al., 2007). This mouse expresses different ratios of three different fluorophores in each neuron. Consequently, different neurons exhibit different hues of colour which can help to resolve structures that would otherwise be too close together. The hope for this technique is to be able to image large networks at relatively low res-

olution, but still be able to resolve structures because of all the different colours. A difficulty with brainbow mice is that fluorophore expression is not strong at birth and so it is not possible at present to use brainbow for imaging developing networks.

Apart from techniques for trying to image large networks with sufficient resolution, there are a number of new techniques which can surpass the resolution limit like 4pi, STED, STORM and structured illumination.

A technique based on confocal microscopy, 4pi improves the resolution by using two lenses to illuminate and collect light from a sample. In order to use the 4pi technique a modified confocal microscope is needed with two lenses and a modified light path. It is especially good because it results in a uniform point spread function, i.e. the axial resolution is just as good as the lateral resolution (Heintzmann and Ficz, 2006). The z-resolution in a 4pi image can be below 100 nm (Hell et al., 1997), therefore it gives a similar resolution to the serial sectioning technique used in this chapter, but with the added benefit that sections do not have to be aligned, since the specimen is imaged as a whole mount. At the same time, imaging will be limited to relatively thin tissues, as the light must be able to travel all the way through it. In contrast, any size of tissue can be sectioned, as long as the sections can be collected and imaged without error. Another difficulty when using 4pi is that the objective lenses must be very precisely aligned.

STED, Stimulated Emission Depletion, relies on a property of fluorescent molecules, that they can be 'turned off' by stimulating them with a wavelength similar to their emission wavelength. STED can be used with a normal confocal microscope. The specimen is excited with the normal excitation wavelength but is also illuminated with a second doughnut-shaped beam which causes the fluorescence around the excitation spot (apart from in the very middle) to be forced to its ground state, preventing further emission. This has the effect of narrowing the PSF and thus increasing the resolution to on the order of tens of nanometres. However, the resulting PSF is still asymmetric (Heintzmann and Ficz, 2006).

STORM, which stands for STochastic Optical Reconstruction Microscopy, relies on precise localisation of individual fluorescent molecules by taking many sparse images of the structure of interest (Huang et al., 2008; Bates et al., 2007). The location

of a fluorophore can be found with much more precision than the space between two molecules can be imaged. Therefore by using special fluorophores that can be switched on and off, many sparse samples can be obtained, and computationally enhanced, to create images with resolution on the order of nanometres. A drawback of this technique is that the imaging can be very time consuming, as many samples are needed to build up a complete image. PALM also works by a similar principle (for a review see Heintzmann and Ficz, 2006).

Structured illumination is an imaging technique which can resolve structures below the diffraction limit by imaging a sample multiple times with patterned illumination (usually grids). This allows the imaging apparatus to capture resolvable moire fringes created by the interaction of the structure in the illumination and the sub-resolution structure of the image. This could increase the x/y resolution to 50 nm (Gustafsson, 2005). The images must be subsequently processed computationally to reconstruct the higher resolution images. This is again requires multiple images but can be relatively fast compared to STORM for example. However, this technique is only suitable for relatively thin samples as it suffers from light scattering in thick samples.

5.5 Conclusion

I have shown that the resolution from reconstructing ultra-thin serial sections is increased compared to confocal microscopy, but it is still not enough to be able to disambiguate individual axons from the bundle. It is difficult to make a strong argument about whether an image has enough resolution because the objects in the image are unknown. I have tried to make a convincing argument by finding a location in the image where I can infer that there should be two axons but more than one axon is not resolvable. This location corresponds to a point along a bundle of axons, on both sides of which there are at least two axons. At this point it is not possible to resolve two. I suspect that there are more than two axons in this bundle but there is no point at which I can conclusively show the presence of more than two axons. This is a general difficulty when working with sub-resolution images; it is hard to know that something is present but unresolvable, except by using prior assumptions of what we are looking

for.

Therefore, although I have shown that this technique does increase the z-resolution, the resolution under these imaging conditions is still not enough to distinguish between developing axons.

One possibility for improving the resolution of this technique, without using EM, is to image slices using structured illumination. Moreover if more resolution is also needed in the axial direction thinner slices can be cut. This could provide at least a four-fold increase in the lateral resolution and twice the axial resolution compared to the results obtained here. Although theoretically possible, this would be a very big job for someone and there would be a clear benefit in trying to automate as many steps as possible. There are also issues which arise with cutting, handling and imaging such thin slices. A normal microtome does not have the accuracy to cut much thinner than about 100 nm, although the Lichtman lab have been developing a cutting device which contains a sensor in order to be able to consistently cut slices as thin as about 30nm. Another issue relates to the intensity of the fluorescence in such thin slices, which will contain a very low concentration of fluorophore. If the native fluorescence is not enough these slices can be stained once they have been cut, but again this would be very time consuming if it was not automated. The collection of slices has already been automated by the ATLUM but imaging the slices, aligning the images and tracing the axons would take months, at best, and are tasks that could be automated.

In conclusion, serial sectioning in conjunction with structured illumination may provide a way of visualising neonatal motor units. This technique could only be used routinely for the reconstruction of large volumes if the required steps are fully or at least partially automated.

Chapter 6

Conclusion

The nervous system has been described as the most complicated structure in the universe and yet it is evidently the result of a self-organising process. An important step toward creating a functioning nervous system is creating the correct connections. This is achieved through a series of synaptic modifications which occurs over development. Understanding what affects the fate of a synapse is very interesting and could have an impact on how we understand what the nervous system does.

Synapses in the nervous system can be very small and each neuron can form thousands of synapses with other cells. This makes them difficult to study, especially during development when axon branches can be very thin and abundant. The neuromuscular junction is one type of synapse, however, which is accessible, large and relatively simple, therefore good for studying synaptic properties.

There are many factors which appear to affect synapse formation and synapse elimination at the neuromuscular junction. The presence of multiple terminals, the differential activity between them, access to trophic molecules, matching between neuron and muscle fibre type. All of these are factors in the environment of the axon that affect which synapses will be formed and which will be maintained. In this thesis I have investigated factors intrinsic to the neuron which may affect synapse formation or synapse elimination.

In chapter 3 I showed that some synapse elimination continues in the absence of com-

petition, which suggests that neurons could have a limited capacity for maintaining synapses. By using the Rasmussen and Willshaw model, I showed that these results are consistent with the idea that there is a limited presynaptic resource. This, in effect, means that different axon branches of the same motor neuron are competing with each other for the presynaptic resource and could affect which synapses are maintained. A prediction of this model is that, as synapses grow larger during the normal ageing of the animal, there will be an age-dependant weakening of some synapses as the presynaptic resource becomes redistributed. Therefore, this presynaptic resource, which is driving competition between axon branches of the same neuron, will continue to have an effect well beyond the period which is traditionally considered 'developmental'. This prediction is exciting in the context of studies on degenerative diseases, like motor neuron disease, where age is a known risk factor for the manifestation of the disease. There are two experiments that could be carried out to test the prediction of this model. First, 4DL muscles could be partially denervated at p5 but allowed to recover for 6 months (instead of just 4 weeks). Motor unit sizes at 6 months would be expected to be even smaller than those at 4 weeks after partial denervation. Second, a group of mice could be partially denervated at p5 and then split into three groups: a control group, one where synapses are induced to grow larger than they normally would and a third where synapses were kept smaller than they would be. The prediction would be that MU sizes would be largest in the group with the smallest synapses and decrease as the size of the synapses increases. Synaptic size could be altered by changes in the diet of the mice.

In chapter 4 I investigated whether sibling branches (i.e. those belonging to the same neuron) form synapses randomly and independently of each other. There is some evidence that synapses are formed non-randomly; for example because the position in the spinal cord could affect where a neuron makes a synapse within the muscle and also the type of motor neuron could affect which muscle fibres it synapses onto. However, there is not evidence that individual branches of the same neuron have different probabilities of innervating any given muscle fibre. Moreover it is not clear how individual branches could be differentiated. I found there is very limited evidence for within unit convergence in development and no evidence in normal adults. Therefore another constraint on synapse formation could be some kind of direct or indirect interaction

between different branches of the same neuron. However, there were some examples of convergence in development and there were a significant number of examples in regenerating muscles, which did not appear at later time points. This strongly argues that, when within unit convergence does occur, although rare, two branches from the same neuron can compete with each other. The most convincing demonstration that sibling branches do compete with each other would be to demonstrate elimination of one of the branches by time-lapse imaging. Time-lapse imaging is not possible in the lumbrical muscles because they are deep muscles, but it is a possibility in the LAL muscle. The mechanism by which intra-neuronal competition could proceed is also not clear, as most hypotheses rely on differences between neurons (e.g. in identity or activity level). I hypothesised in chapter 3 that sibling branches which innervate distinct targets compete with each other for presynaptic resource. Perhaps this could also drive competition between sibling branches which converge on the same target. It would be interesting to use the model to test competition between converging sibling branches.

It is difficult to have a complete picture of development, and one of the things that makes it difficult is that structures are very small and often beyond the resolution limits of conventional microscopy. It would be useful to have techniques which could image both large areas (whole networks) and at high resolution, to capture the detail necessary to draw conclusions about developmental processes. In chapter 5 I have investigated one such technique - array tomography, which is being developed in Professor Jeff Lichtman's lab (Harvard University, USA). This technique can give an increase in axial resolution compared to confocal microscopy. However, under the conditions used here it is still not powerful enough to resolve developing motor units. As more and more powerful imaging techniques are being developed in many different labs I am sure that the time will come when this is not only possible but routinely applied.

Appendix A

Predicting the number of innervated endplates in ANPD

This appendix explains the method I used to calculate the number of endplates that should be innervated in adults with neonatal partial denervation and two or three remaining axons, assuming intrinsic withdrawal does not occur.

I assumed that the 11 neonatal MU size values from single neonatal motor unit muscles are representative of the distribution of MU sizes in neonates. I used the `density` function in R, to create a density distribution based on these data points A.1. I set the range of possible motor unit sizes to be between 35 (which is the smallest observed motor unit size in the control group) and 223 (which is the average number of muscle fibres in a muscle). The density distribution is created by placing a Gaussian distribution centred around each data point with a standard deviation that is automatically calculated in R, and summing these Gaussians together. Because of the distribution of data points, the density plot appears bimodal, even though according to the Kolmogorov-Smirnov test the distribution of the data is not significantly different to a normal distribution. I have also tried doing the subsequent analysis using a normal distribution with a mean and standard deviation that match the data and the results are nearly identical. See table A.1 for a comparison.

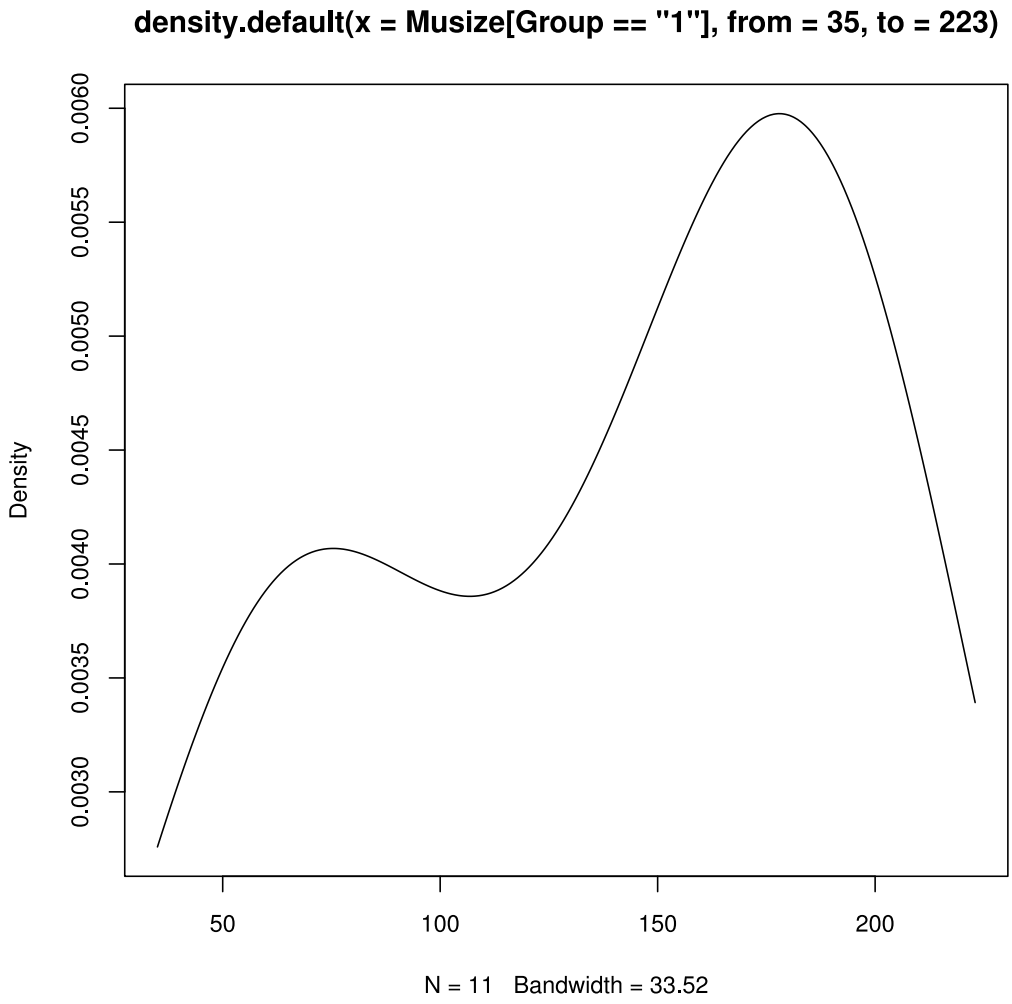

Figure A.1: *Density plot showing the distribution of neonatal motor unit sizes. Motor unit size is shown on the x-axis, and the probability of a motor unit being that size is shown on the y-axis.*

A.1 Estimating the number of innervated fibres for one remaining axon

I randomly sampled from this distribution (with replacement) in order to generate neonatal motor unit sizes. The estimated number of innervated fibres when there is one axon remaining should be equal to the MU size. Since I used the values of neonatal MU sizes to create this distribution, the predicted neonatal motor unit size should match the actual value exactly, which it does.

A.2 Estimating the number of innervated fibres for two remaining axons

When there are more than one axons remaining there may be some π-junctions left, and therefore some elimination may take place. However, if no synapse elimination occurs in the absence of competition, the same number of endplates should be innervated in the neonate and in the adult (because the only elimination will be removal of axons from π-junctions). I estimated the number of innervated junctions in muscles with two remaining axons by taking 2000 random samples of two motor unit sizes (with replacement) from the density distribution. I calculated the overlap that would occur in each of these pairs of MU sizes, given that they innervate endplates randomly. Given two MU sizes, MU1 and MU2, and assuming that there are 223 muscle fibres, the expected amount of overlap between the MUs is $MU1 \times \frac{MU2}{MF}$. Therefore, the number of uniquely innervated endplates will be $MU1 + MU2 - overlap$. I averaged this over the 2000 samples and divided by the number of motor neurons (two) in order to represent it as an average MU size. Based on this estimate, when there are two remaining motor neurons there should be about 190 innervated endplates, in other words, each axon should innervated on average 95 endplates. This value is marginally significantly different to the mean MU size in ANPD muscles with two remaining units determined experimentally (see figure 3.6.

	Density plot	Normal distribution
1 axon	135± 53	135 ± 47
2 axons	95±15	94±14
3 axons	70±5	70±5

Table A.1: *Table comparing the estimated mean and standard deviations of the number of innervated fibres with one, two or three axons, using either the bimodal density distribution (shown in figure A.1) or a normal distribution with the same mean and standard deviation as the data points. In the statistical tests I assumed that the data points were normally distributed so I wanted to show that using a normal distribution instead of the density distribution does not make a difference to the result.*

A.3 Estimating the number of innervated fibres for three remaining axons

Similarly, for three MUs, I randomly selected three MU sizes, MU1, MU2 and MU3 and calculated the number of fibres innervated by MU1 and MU2, MU1 and MU3, and MU2 and MU3 as before. I also calculated the number of fibres innervated by all three as $\frac{MU1}{MF} \times \frac{MU2}{MF} \times \frac{MU3}{MF} \times MF$. Then, in order to work out the number of innervated muscle fibres, I calculated: $MU1 + MU2 + MU3 - overlap12 - overlap13 - overlap23 + overlap123$. The reason for adding on the endplates which are innervated by all three motor neurons is because it will have been added three times originally (as it will contribute to each motor unit's size), but then it will be subtracted three times when I subtract the overlapping pairs, therefore it needs to be added again.

Taking the average of 2000, in all three cases, gives the values shown in table (A.1).

Appendix B

YFP leakage from a damaged nerve

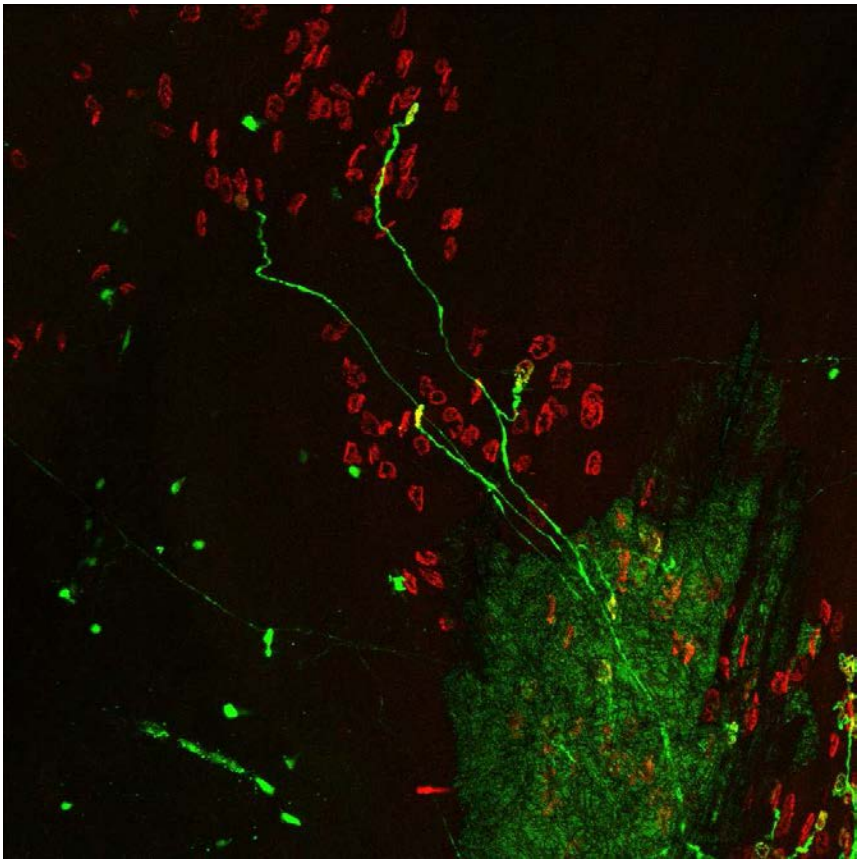

Figure B.1: *Leakage of YFP when the nerve is damaged. It is clear from this image that when the nerve is damaged and the YFP leaks from the cytoplasm it is still visible in the muscle. The axon at the damaged area is still partly visible. This strongly argues against the case that the denervated endplates seen in ANPD adults were due to YFP leakage from a damaged nerve as there was no leaked YFP visible near the endplates and the axon was completely gone.*

Appendix C

Running the model with the exponential fit

This appendix shows the result of running the model from chapter 3 (section 3.3.3) with an exponential fit.

I have tried running the model with several different equations for the postsynaptic resource, B_0, but it does not make a qualitative difference to the conclusion. Here I show an example from running the model with the equation $B_0 = \frac{a}{b+e^{c+dt}}$. The parameters are set as a = 7.94, b = 0.02, c = -2.84 and d = -0.55. I wanted to show this equation because it is the only one which reaches a limit around six months, after which there is not more growth. Using this equation does not change the main result, it only affects the time-course slightly. The main difference is that after 18 months there is not further reduction in motor unit size, since the postsynaptic resource is, by this point, stable (figure C.1).

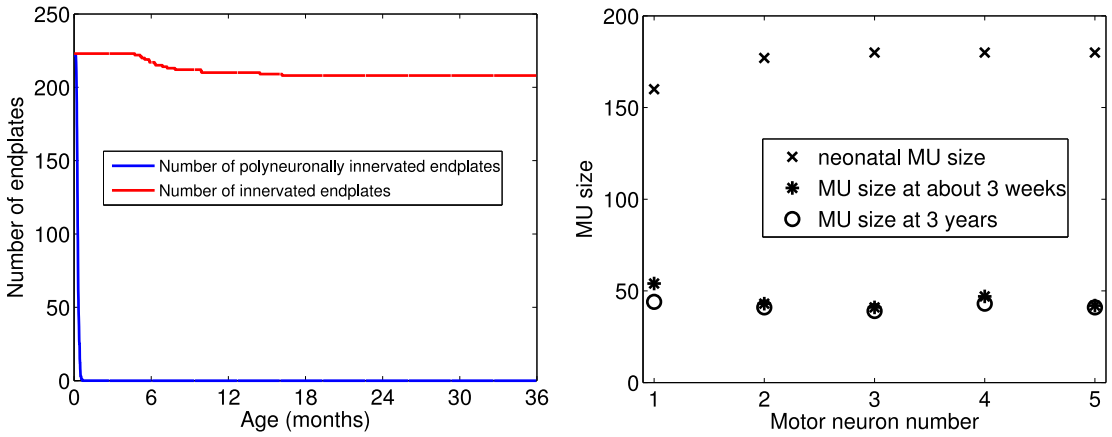

Figure C.1: *Results from running the model with the exponential fit from equation 2(b) in table 3.2. The main result, that some motor units lose synapses past the three week developmental period, remains the same. The main difference is that, because the postsynaptic resource stops growing around 6 months, MU sizes stabilise around this time. This is in contrast to the continual loss seen with the logarithmic fit.*

Appendix D

Rasmussen and Willshaw model of 4DL muscle with partial denervation

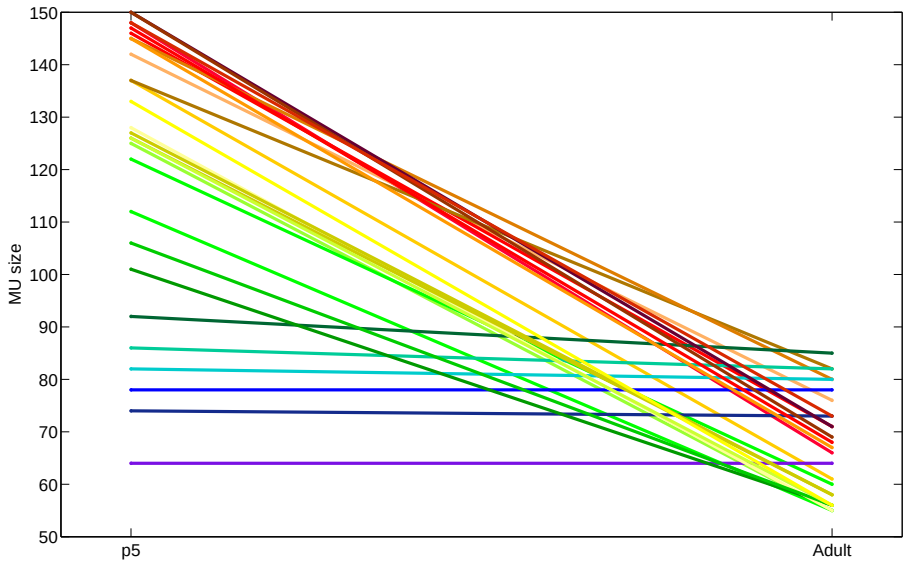

Figure D.1: *The graph shows the result of replicating the partial denervation experiment described in chapter 3 with my implementation of the original Rasmussen and Willshaw model and parameters which match the lumbrical muscle. Motor unit sizes are shown at two different timepoints: at the time of partial denervation (p5) and once the model has reached a steady state (adult) which always occured within the first three weeks (assuming, as before, that ten thousand iterations are equal to one week). Qualitatively the same kind of change occurs, where large motor units lose some synapses and smaller ones do not. However, the motor unit sizes in the adults after partial denervation at p5 are smaller than what was found in the experiments. This could be fixed by adjusting the* A_0 *parameter to fit the data. By 3 weeks the model has reached a steady state after which no further intrinsic withdrawal will occur.*

Bibliography

Andonian, M. H. and Fahim, M. A. (1987). Effects of endurance exercise on the morphology of mouse neuromuscular junctions during ageing. *J Neurocytol*, 16(5):589–599.

Andonian, M. H. and Fahim, M. A. (1989). Nerve terminal morphology in c57bl/6nnia mice at different ages. *J Gerontol*, 44(2).

Araque, A. (2008). Astrocytes process synaptic information. *Neuron Glia Biol*, 4(1):3–10.

Baker, M. W. and Macagno, E. R. (2007). In vivo imaging of growth cone and filopodial dynamics: evidence for contact-mediated retraction of filopodia leading to the tiling of sibling processes. *J Comp Neurol*, 500(5):850–862.

Balice-Gordon, R. J. (1996). Dynamic roles at the neuromuscular junction. schwann cells. *Curr Biol*, 6(9):1054–1056.

Balice-Gordon, R. J., Chua, C. K., Nelson, C. C., and Lichtman, J. W. (1993). Gradual loss of synaptic cartels precedes axon withdrawal at developing neuromuscular junctions. *Neuron*, 11(5):801–815.

Balice-Gordon, R. J. and Lichtman, J. W. (1990). In vivo visualization of the growth of pre- and postsynaptic elements of neuromuscular junctions in the mouse. *J Neurosci*, 10(3):894–908.

Balice-Gordon, R. J. and Lichtman, J. W. (1993). In vivo observations of pre- and postsynaptic changes during the transition from multiple to single innervation at developing neuromuscular junctions. *J Neurosci*, 13(2):834–855.

Balice-Gordon, R. J. and Lichtman, J. W. (1994). Long-term synapse loss induced by focal blockade of postsynaptic receptors. *Nature*, 372(6506):519–524.

Barber, M. J. and Lichtman, J. W. (1999). Activity-driven synapse elimination leads paradoxically to domination by inactive neurons. *J Neurosci*, 19(22):9975–9985.

Barker, D. and Ip, M. C. (1966). Sprouting and degeneration of mammalian motor

axons in normal and de-afferentated skeletal muscle. *Proc R Soc Lond B Biol Sci*, 163(993):538–554.

Barry, J. A. and Ribchester, R. R. (1995). Persistent polyneuronal innervation in partially denervated rat muscle after reinnervation and recovery from prolonged nerve conduction block. *J Neurosci*, 15(10):6327–6339.

Bates, M., Huang, B., Dempsey, G. T., and Zhuang, X. (2007). Multicolor super-resolution imaging with photo-switchable fluorescent probes. *Science*, 317(5845):1749–1753.

Beirowski, B., Berek, L., Adalbert, R., Wagner, D., Grumme, D. S., Addicks, K., Ribchester, R. R., and Coleman, M. P. (2004). Quantitative and qualitative analysis of wallerian degeneration using restricted axonal labelling in yfp-h mice. *J Neurosci Methods*, 134(1):23–35.

Bennett, M. R. and Pettigrew, A. G. (1974). The formation of synapses in striated muscle during development. *J Physiol*, 241(2):515–545.

Bennett, M. R. and Pettigrew, A. G. (1976). The formation of neuromuscular synapses. *Cold Spring Harb Symp Quant Biol*, 40:409–424.

Bennett, M. R. and Robinson, J. (1989). Growth and elimination of nerve terminals at synaptic sites during polyneuronal innervation of muscle cells: a trophic hypothesis. *Proc R Soc Lond B Biol Sci*, 235(1281):299–320.

Benoit, P. and Changeux, J. P. (1975). Consequences of tenotomy on the evolution of multiinnervation in developing rat soleus muscle. *Brain Res*, 99(2):354–358.

Benoit, P. and Changeux, J. P. (1978). Consequences of blocking the nerve with a local anaesthetic on the evolution of multiinnervation at the regenerating neuromuscular junction of the rat. *Brain Res*, 149(1):89–96.

Bernstein, M. and Lichtman, J. (1999). Axonal atrophy: The retraction reaction. *Curr Opin Neurobiol*, 9(3):364–370.

Betz, W. J., Caldwell, J. H., and Ribchester, R. R. (1979). The size of motor units during post-natal development of rat lumbrical muscle. *J Physiol*, 297(0):463–478.

Betz, W. J., Caldwell, J. H., and Ribchester, R. R. (1980). The effects of partial denervation at birth on the development of muscle fibres and motor units in rat lumbrical muscle. *J Physiol*, 303:265–279.

Betz, W. J., Ribchester, R. R., and Ridge, R. M. (1990). Competitive mechanisms underlying synapse elimination in the lumbrical muscle of the rat. *J Neurobiol*, 21(1):1–17.

Bishop, D. L., Misgeld, T., Walsh, M. K., Gan, W.-B., and Lichtman, J. W. (2004).

Axon branch removal at developing synapses by axosome shedding. *Neuron*, 44(4):651–661.

Blow, N. (2007). Following the wires. *Nat Methods*, 4(11):975–981.

Briggman, K. and Denk, W. (2006). Towards neural circuit reconstruction with volume electron microscopy techniques. *Curr Opin Neurobiol*, 16(5):562–570.

Brown, M. C., Holland, R. L., and Hopkins, W. G. (1981). Restoration of focal multiple innervation in rat muscles by transmission block during a critical stage of development. *J Physiol*, 318:355–364.

Brown, M. C., Holland, R. L., and Ironton, R. (1980). Nodal and terminal sprouting from motor nerves in fast and slow muscles of the mouse. *J Physiol*, 306:493–510.

Brown, M. C. and Ironton, R. (1978). Sprouting and regression of neuromuscular synapses in partially denervated mammalian muscles. *J Physiol*, 278:325–348.

Brown, M. C., Jansen, J. K., and Van Essen, D. (1976). Polyneuronal innervation of skeletal muscle in new-born rats and its elimination during maturation. *J Physiol*, 261(2):387–422.

Buffelli, M., Burgess, R. W., Feng, G., Lobe, C. G., Lichtman, J. W., and Sanes, J. R. (2003). Genetic evidence that relative synaptic efficacy biases the outcome of synaptic competition. *Nature*, 424(6947):430–434.

Buffelli, M., Busetto, G., Cangiano, L., and Cangiano, A. (2002). Perinatal switch from synchronous to asynchronous activity of motoneurons: link with synapse elimination. *Proc Natl Acad Sci U S A*, 99(20):13200–13205.

Busetto, G., Buffelli, M., Tognana, E., Bellico, F., and Cangiano, A. (2000). Hebbian mechanisms revealed by electrical stimulation at developing rat neuromuscular junctions. *J Neurosci*, 20(2):685–695.

Callaway, E. M., Soha, J. M., and Van Essen, D. C. (1987). Competition favouring inactive over active motor neurons during synapse elimination. *Nature*, 328(6129):422–426.

Cardasis, C. A. and Padykula, H. A. (1981). Ultrastructural evidence indicating reorganization at the neuromuscular junction in the normal rat soleus muscle. *Anat Rec*, 200(1):41–59.

Caroni, P. (1997). Overexpression of growth-associated proteins in the neurons of adult transgenic mice. *J Neurosci Methods*, 71(1):3–9.

Chadaram, S. R. R., Laskowski, M. B. B., and Madison, R. D. D. (2007). Topographic specificity within membranes of a single muscle detected in vitro. *J Neurosci*, 27(51):13938–13948.

Chang, Q. and Balice-Gordon, R. J. (2000). Gap junctional communication among developing and injured motor neurons. *Brain Res Brain Res Rev*, 32(1):242–249.

Chao, M. V. (2010). A conversation with Rita Levi-Montalcini. *Annu Rev Physiol*, 72:1–13.

Colman, H., Nabekura, J., and Lichtman, J. W. (1997). Alterations in synaptic strength preceding axon withdrawal. *Science*, 275(5298):356–361.

Connold, A. L., Fisher, T. J., Maudarbocus, S., and Vrbová, G. (1992). Response of developing rat fast muscles to partial denervation. *Neuroscience*, 46(4):981–988.

Costanzo, E. M., Barry, J. A., and Ribchester, R. R. (2000). Competition at silent synapses in reinnervated skeletal muscle. *Nat Neurosci*, 3(7):694–700.

Court, F. A., Gillingwater, T. H., Melrose, S., Sherman, D. L., Greenshields, K. N., Morton, A. J., Harris, J. B., Willison, H. J., and Ribchester, R. R. (2008). Identity, developmental restriction and reactivity of extralaminar cells capping mammalian neuromuscular junctions. *J Cell Sci*, 121(23):3901–3911.

Courtney, J. and Steinbach, J. H. (1981). Age changes in neuromuscular junction morphology and acetylcholine receptor distribution on rat skeletal muscle fibres. *J Physiol*, 320:435–447.

Deppmann, C. D., Mihalas, S., Sharma, N., Lonze, B. E., Niebur, E., and Ginty, D. D. (2008). A model for neuronal competition during development. *Science*, 320(5874):369–373.

Duchen, L. W. and Strich, S. J. (1968). The effects of botulinum toxin on the pattern of innervation of skeletal muscle in the mouse. *Q J Exp Physiol Cogn Med Sci*, 53(1):84–89.

Duxson, M. J. (1982). The effect of postsynaptic block on development of the neuromuscular junction in postnatal rats. *J Neurocytol*, 11(3):395–408.

English, A. (1995). Both basic fibroblast growth factor and ciliary neurotrophic factor promote the retention of polyneuronal innervation of developing skeletal muscle fibers. *Dev Biol*, 169(1):57–64.

Fahim, M. A., Holley, J. A., and Robbins, N. (1983). Scanning and light microscopic study of age changes at a neuromuscular junction in the mouse. *J Neurocytol*, 12(1):13–25.

Favero, M., Lorenzetto, E., Bidoia, C., Buffelli, M., Busetto, G., and Cangiano, A. (2006). Synapse formation and elimination: Role of activity studied in different models of adult muscle reinnervation. *J Neurosci Res*.

Feng, G., Laskowski, M. B., Feldheim, D. A., Wang, H., Lewis, R., Frisen, J., Flana-

gan, J. G., and Sanes, J. R. (2000a). Roles for ephrins in positionally selective synaptogenesis between motor neurons and muscle fibers. *Neuron*, 25(2):295–306.

Feng, G., Mellor, R. H., Bernstein, M., Keller-Peck, C., Nguyen, Q. T., Wallace, M., Nerbonne, J. M., Lichtman, J. W., and Sanes, J. R. (2000b). Imaging neuronal subsets in transgenic mice expressing multiple spectral variants of gfp. *Neuron*, 28(1):41–51.

Fiala, J. C. (2005). Reconstruct: a free editor for serial section microscopy. *J Microsc*, 218(Pt 1):52–61.

Fisher, T. J., Vrbová, G., and Wijetunge, A. (1989). Partial denervation of the rat soleus muscle at two different developmental stages. *Neuroscience*, 28(3):755–763.

Fladby, T. (1987). Postnatal loss of synaptic terminals in the normal mouse soleus muscle. *Acta Physiol Scand*, 129(2):229–238.

Fladby, T. and Jansen, J. K. (1987). Postnatal loss of synaptic terminals in the partially denervated mouse soleus muscle. *Acta Physiol Scand*, 129(2):239–246.

Futerman, A. H. and Banker, G. A. (1996). The economics of neurite outgrowth–the addition of new membrane to growing axons. *Trends Neurosci*, 19(4):144–149.

Gan, W.-B. and Lichtman, J. W. (1998). Synaptic segregation at the developing neuromuscular junction. *Science*, 282(5393):1508–1511.

Gan, W.-B. and Macagno, E. R. (1997). Competition among the axonal projections of an identified neuron contributes to the retraction of some of those projections. *J. Neurosci.*, 17(11):4293–4301.

Gates, H. J. and Betz, W. J. (1993). Spatial distribution of muscle fibers in a lumbrical muscle of the rat. *Anat Rec*, 236(2):381–389.

Gates, H. J. and Ridge, R. M. (1992). The importance of competition between motoneurones in developing rat muscle; effects of partial denervation at birth. *J Physiol*, 445:457–472.

Gillingwater, T. H., Thomson, D., and Ribchester, R. R. (2004). Myo-GDNF increases non-functional polyinnervation of reinnervated mouse muscle. *Neuroreport*, 15(1):21–25.

Gould, T. W. and Enomoto, H. (2009). Neurotrophic modulation of motor neuron development. *Neuroscientist*, 15(1):105–116.

Gouzé, J.-L., Lasry, J.-M., and Changeux, J.-P. (1983). Selective stabilization of muscle innervation during development: A mathematical model. *Biol Cybern*, 46(3):207–215.

Greensmith, L. and Vrbová, G. (1991). Neuromuscular contacts in the developing rat soleus depend on muscle activity. *Brain Res Dev Brain Res*, 62(1):121–129.

Groen, M. R. (2008). Synaptic competition at the neuromuscular junction and the limited neurotrophin theory. Master's thesis, Vrije Universiteit, Amsterdam, the Netherlands.

Gustafsson, M. G. L. (2005). Nonlinear structured-illumination microscopy: Wide-field fluorescence imaging with theoretically unlimited resolution. *Proc Natl Acad Sci U S A*, 102(37):13081–13086.

Hall, Z. and Sanes, J. (1993). Synaptic structure and development: The neuromuscular junction. *Cell*, 72:99–121.

Hamburger, V. (1952). Development of the nervous system. *Ann N Y Acad Sci*, 55(2):117–132.

Harris, A. J. and McCaig, C. D. (1984). Motoneuron death and motor unit size during embryonic development of the rat. *J Neurosci*, 4(1):13–24.

Hayworth, K. J., Kasthuri, N., Schalek, R., and Lichtman, J. W. (2006). Automating the collection of ultrathin serial sections for large volume tem reconstructions. *Microsc Microanal*, 12:86–87.

Heintzmann, R. and Ficz, G. (2006). Breaking the resolution limit in light microscopy. *Brief Funct Genomic Proteomic*, 5(4):289–301.

Hell, S. W., Schrader, M., and van der Voort, H. T. (1997). Far-field fluorescence microscopy with three-dimensional resolution in the 100-nm range. *J Microsc*, 187(Pt 1):1–7.

Henneman, E. (1985). The size-principle: a deterministic output emerges from a set of probabilistic connections. *J Exp Biol*, 115:105–112.

Huang, B., Wang, W., Bates, M., and Zhuang, X. (2008). Three-dimensional super-resolution imaging by stochastic optical reconstruction microscopy. *Science*, 319(5864):810–813.

Hughes, B. W., Kusner, L. L., and Kaminski, H. J. (2006). Molecular architecture of the neuromuscular junction. *Muscle Nerve*, 33(4):445–461.

Hutchins, I. B. and Kalil, K. (2008). Differential outgrowth of axons and their branches is regulated by localized calcium transients. *J. Neurosci.*, 28(1):143–153.

Ip, M. C. (1974). Some morphological features of the myoneural junctions in certain normal muscles of the rat. *Anat Rec*, 180(4):605–615.

Ironton, R., Brown, M. C., and Holland, R. L. (1978). Stimuli to intramuscular nerve growth. *Brain Res*, 156(2):351–354.

Jacob, J., Hacker, A., and Guthrie, S. (2001). Mechanisms and molecules in motor neuron specification and axon pathfinding. *Bioessays*, 23(7):582–595.

Jacob, J. M. and Robbins, N. (1990). Age differences in morphology of reinnervation of partially denervated mouse muscle. *J Neurosci*, 10(5):1530–1540.

Jacobson, M. (1978). *Developmental Neurobiology*. Plenum Press, New York and London, second edition.

Jansen, J. K. and Fladby, T. (1990). The perinatal reorganization of the innervation of skeletal muscle in mammals. *Prog Neurobiol*, 34(1):39–90.

Jeanprêtre, N., Clarke, P. G., and Gabriel, J. P. (1996). Competitive exclusion between axons dependent on a single trophic substance: a mathematical analysis. *Math Biosci*, 135(1):23–54.

Jessen, K. R. and Mirsky, R. (2005). The origin and development of glial cells in peripheral nerves. *Nat Rev Neurosci*, 6(9):671–682.

Jones, S. P., Ridge, R. M., and Rowlerson, A. (1987). The non-selective innervation of muscle fibres and mixed composition of motor units in a muscle of neonatal rat. *J Physiol*, 386:377–394.

Jordan, C. L. (1996). Morphological effects of ciliary neurotrophic factor treatment during neuromuscular synapse elimination. *J Neurobiol*, 31(1):29–40.

Kasthuri, N. and Lichtman, J. W. (2003). The role of neuronal identity in synaptic competition. *Nature*, 424(6947):426–430.

Keller-Peck, C. R., Feng, G., Sanes, J. R., Yan, Q., Lichtman, J. W., and Snider, W. D. (2001a). Glial cell line-derived neurotrophic factor administration in postnatal life results in motor unit enlargement and continuous synaptic remodeling at the neuromuscular junction. *J Neurosci*, 21(16):6136–6146.

Keller-Peck, C. R., Walsh, M. K., Gan, W. B., Feng, G., Sanes, J. R., and Lichtman, J. W. (2001b). Asynchronous synapse elimination in neonatal motor units: studies using gfp transgenic mice. *Neuron*, 31(3):381–394.

Kerezoudi, E. and Thomas, P. K. (1999). Influence of age on regeneration in the peripheral nervous system. *Gerontology*, 45(6):301–306.

Kiddie, G., McLean, D., van Ooyen, A., and Graham, B. (2005). Biologically plausible models of neurite outgrowth. *Prog Brain Res*, 147:67–80.

Kobayashi, N. and Mundel, P. (1998). A role of microtubules during the formation of cell processes in neuronal and non-neuronal cells. *Cell Tissue Res*, 291(2):163–174.

Korneliussen, H. and Jansen, J. K. S. (1976). Morphological aspects of the elimination of polyneuronal innervation of skeletal muscle fibres in newborn rats. *J Neurocytol*, 5(5):591–604.

Kummer, T. T., Misgeld, T., and Sanes, J. R. (2006). Assembly of the postsynaptic

membrane at the neuromuscular junction: paradigm lost. *Curr Opin Neurobiol*, 16(1):74–82.

Kwon, Y. W., Abbondanzo, S. J., Stewart, C. L., and Gurney, M. E. (1995). Leukemia inhibitory factor influences the timing of programmed synapse withdrawal from neonatal muscles. *J Neurobiol*, 28(1):35–50.

Kwon, Y. W. and Gurney, M. E. (1996). Brain-derived neurotrophic factor transiently stabilizes silent synapses on developing neuromuscular junctions. *J Neurobiol*, 29(4):503–516.

Lanuza, M. A., Garcia, N., Santafé, M., González, C. M., Alonso, I., Nelson, P. G., and Tomàs, J. (2002). Pre- and postsynaptic maturation of the neuromuscular junction during neonatal synapse elimination depends on protein kinase c. *J Neurosci Res*, 67(5):607–617.

Lanuza, M. A., Garcia, N., Santafe, M., Nelson, P. G., Fenoll-Brunet, M. R., and Tomas, J. (2001). Pertussis toxin-sensitive g-protein and protein kinase c activity are involved in normal synapse elimination in the neonatal rat muscle. *J Neurosci Res*, 63(4):330–340.

Laskowski, M. B. and High, J. A. (1989). Expression of nerve-muscle topography during development. *J Neurosci*, 9(1):175–182.

Laskowski, M. B. and Sanes, J. R. (1988). Topographically selective reinnervation of adult mammalian skeletal muscles. *J Neurosci*, 8(8):3094–3099.

Lichtman, J. and Sanes, J. (2008). Ome sweet ome: what can the genome tell us about the connectome? *Curr Opin Neurobiol*, 18(3):346–353.

Lichtman, J. W. and Balice-Gordon, R. J. (1990). Understanding synaptic competition in theory and in practice. *J Neurobiol*, 21(1):99–106.

Lichtman, J. W. and Colman, H. (2000). Synapse elimination and indelible memory. *Neuron*, 25(2):269–278.

Lichtman, J. W., Magrassi, L., and Purves, D. (1987). Visualization of neuromuscular junctions over periods of several months in living mice. *J Neurosci*, 7(4):1215–1222.

Livet, J., Weissman, T. A., Kang, H., Draft, R. W., Lu, J., Bennis, R. A., Sanes, J. R., and Lichtman, J. W. (2007). Transgenic strategies for combinatorial expression of fluorescent proteins in the nervous system. *Nature*, 450(7166):56–62.

Lu, J. and Lichtman, J. W. (2007). Imaging the neuromuscular junction over the past centuries. *Sheng Li Xue Bao*, 59(6):683–696.

Lu, J., Min, W., Conchello, J.-A., Xie, X. S., and Lichtman, J. W. (2009a). Super-resolution laser scanning microscopy through spatiotemporal modulation. *Nano Lett*, 9(11):3883–3889.

Lu, J., Tapia, J. C., White, O. L., and Lichtman, J. W. (2009b). The interscutularis muscle connectome. *PLoS Biol*, 7(2):e1000032+.

Lubischer, J. L. and Thompson, W. J. (1999). Neonatal partial denervation results in nodal but not terminal sprouting and a decrease in efficacy of remaining neuromuscular junctions in rat soleus muscle. *J Neurosci*, 19(20):8931–8944.

Luo, L. and Flanagan, J. G. (2007). Development of continuous and discrete neural maps. *Neuron*, 56(2):284–300.

Marques, M. J., Conchello, J. A., and Lichtman, J. W. (2000). From plaque to pretzel: fold formation and acetylcholine receptor loss at the developing neuromuscular junction. *J Neurosci*, 20(10):3663–3675.

McArdle, J. J. (1975). Complex end-plate potentials at the regenerating neuromuscular junction of the rat. *Exp Neurol*, 49(3):629–638.

McCann, C. M., Nguyen, Q. T., Santo Neto, H., and Lichtman, J. W. (2007). Rapid synapse elimination after postsynaptic protein synthesis inhibition in vivo. *J Neurosci*, 27(22):6064–6067.

Meunier, F. (2002). Botulinum neurotoxins: from paralysis to recovery of functional neuromuscular transmission. *J Physiol Paris*, 96(1-2):105–113.

Micheva, K. and Smith, S. (2007). Array tomography: A new tool for imaging the molecular architecture and ultrastructure of neural circuits. *Neuron*, 55(1):25–36.

Mirsky, R. and Jessen, K. R. (1996). Schwann cell development, differentiation and myelination. *Curr Opin Neurobiol*, 6(1):89–96.

Murphey, R. K. and Lemere, C. A. (1984). Competition controls the growth of an identified axonal arborization. *Science*, 224(4655):1352–1355.

Murray, L. M., Comley, L. H., Thomson, D., Parkinson, N., Talbot, K., and Gillingwater, T. H. (2008). Selective vulnerability of motor neurons and dissociation of pre- and post-synaptic pathology at the neuromuscular junction in mouse models of spinal muscular atrophy. *Hum Mol Genet*, 17(7):949–962.

Murray, L. M., Lee, S., Bäumer, D., Parson, S. H., Talbot, K., and Gillingwater, T. H. (2010). Pre-symptomatic development of lower motor neuron connectivity in a mouse model of severe spinal muscular atrophy. *Hum Mol Genet*, 19(3):420–433.

Nguyen, Q. and Lichtman, J. W. (1996). Mechanism of synapse disassembly at the developing neuromuscular junction. *Curr Opin Neurobiol*, 6(1):104–112.

Nguyen, Q. T., Parsadanian, A. S., Snider, W. D., and Lichtman, J. W. (1998). Hyperinnervation of neuromuscular junctions caused by gdnf overexpression in muscle. *Science*, 279(5357):1725–1729.

Nguyen, Q. T., Sanes, J. R., and Lichtman, J. W. (2002). Pre-existing pathways promote precise projection patterns. *Nat Neurosci*, 5(9):861–867.

Nowik, I. (2009). The game motoneurons play. *Games Econ Behav*, 66(1):426–461.

O'Brien, R. A., Ostberg, A. J., and Vrbová, G. (1978). Observations on the elimination of polyneuronal innervation in developing mammalian skeletal muscle. *J Physiol*, 282:571–582.

O'Brien, R. A., Ostberg, A. J., and Vrbova, G. (1984). Protease inhibitors reduce the loss of nerve terminals induced by activity and calcium in developing rat soleus muscles in vitro. *Neuroscience*, 12(2):637–646.

O'Brien, R. A., Purves, R. D., and Vrbová, G. (1977). Effect of activity on the elimination of multiple innervation in soleus muscles of rats [proceedings]. *J Physiol*, 271(2).

Ochs, S. (2004). *A History of Nerve Functions.* Cambridge University Press.

Oppenheim, R. W. (1991). Cell death during development of the nervous system. *Annu Rev Neurosci*, 14(1):453–501.

Personius, K. E., Chang, Q., Mentis, G. Z., O'donovan, M. J., and Balice-Gordon, R. J. (2007). Reduced gap junctional coupling leads to uncorrelated motor neuron firing and precocious neuromuscular synapse elimination. *Proc Natl Acad Sci U S A*, 104(28):11808–11813.

Pun, S., Sigrist, M., Santos, A. F., Ruegg, M. A., Sanes, J. R., Jessell, T. M., Arber, S., and Caroni, P. (2002). An intrinsic distinction in neuromuscular junction assembly and maintenance in different skeletal muscles. *Neuron*, 34(3):357–370.

Purves, D. and Lichtman, J. W. (1985). *Principles of Neural Development.* Sinauer Associates Inc, Sunderland, MA.

R (2005). *R: A Language and Environment for Statistical Computing*. Vienna, Austria.

Rasband, W. S. (1997-2009). *ImageJ*. U. S. National Institutes of Health.

Rasmussen, C. E. and Willshaw, D. J. (1993). Presynaptic and postsynaptic competition in models for the development of neuromuscular connections. *Biol Cybern*, 68(5):409–419.

Redfern, P. A. (1970). Neuromuscular transmission in new-born rats. *J Physiol*, 209(3):701–709.

Ribchester, R. R. (1988). Competitive elimination of neuromuscular synapses. *Nature*, 331(6151):21–22.

Ribchester, R. R. (1993). Co-existence and elimination of convergent motor nerve ter-

minals in reinnervated and paralysed adult rat skeletal muscle. *J Physiol*, 466:421–441.

Ribchester, R. R. and Barry, J. A. (1994). Spatial versus consumptive competition at polyneuronally innervated neuromuscular junctions. *Exp Physiol*, 79(4):465–494.

Ribchester, R. R. and Taxt, T. (1983). Motor unit size and synaptic competition in rat lumbrical muscles reinnervated by active and inactive motor axons. *J Physiol*, 344:89–111.

Ribchester, R. R. and Taxt, T. (1984). Repression of inactive motor nerve terminals in partially denervated rat muscle after regeneration of active motor axons. *J Physiol*, 347:497–511.

Ribchester, R. R., Thomson, D., Haddow, L. J., and Ushkaryov, Y. A. (1998). Enhancement of spontaneous transmitter release at neonatal mouse neuromuscular junctions by the glial cell line-derived neurotrophic factor (GDNF). *J Physiol*, 512 (Pt 3)(3):635–641.

Ridge, R. M. and Betz, W. J. (1984). The effect of selective, chronic stimulation on motor unit size in developing rat muscle. *J Neurosci*, 4(10):2614–2620.

Riley, D. A. (1977). Spontaneous elimination of nerve terminals from the endplates of developing skeletal myofibers. *Brain Res*, 134(2):279–285.

Robbins, N. and Fahim, M. A. (1985). Progression of age changes in mature mouse motor nerve terminals and its relation to locomotor activity. *J Neurocytol*, 14(6):1019–1036.

Rosenthal, J. L. and Taraskevich, P. S. (1977). Reduction of multiaxonal innervation at the neuromuscular junction of the rat during development. *J Physiol*, 270(2):299–310.

Samsonovich, A. V. and Ascoli, G. A. (2006). Morphological homeostasis in cortical dendrites. *Proc Natl Acad Sci U S A*, 103(5):1569–1574.

Sanes, J. R. and Lichtman, J. W. (1999). Development of the vertebrate neuromuscular junction. *Annu Rev Neurosci*, 22(1):389–442.

Schrader, M., Hell, S. W., and van der Voort, H. T. M. (1996). Potential of confocal microscopes to resolve in the 50–100 nm range. *Appl Phys Lett*, 69(24):3644–3646.

Slater, C. (1982). Postnatal maturation of nerve-muscle junctions in hindlimb muscles of the mouse. *Dev Biol*, 94(1):11–22.

Smalheiser, N. R. and Crain, S. M. (1984). The possible role of sibling neurite bias in the coordination of neurite extension, branching, and survival. *J Neurobiol*, 15(6):517–529.

Smith, S. J. (2007). Circuit reconstruction tools today. *Curr Opin Neurobiol*, 17(5):601–608.

Son, Y. J. and Thompson, W. J. (1995a). Nerve sprouting in muscle is induced and guided by processes extended by schwann cells. *Neuron*, 14(1):133–141.

Son, Y. J. and Thompson, W. J. (1995b). Schwann cell processes guide regeneration of peripheral axons. *Neuron*, 14(1):125–132.

Song, J. W., Misgeld, T., Kang, H., Knecht, S., Lu, J., Cao, Y., Cotman, S. L., Bishop, D. L., and Lichtman, J. W. (2008). Lysosomal activity associated with developmental axon pruning. *J Neurosci*, 28(36):8993–9001.

Sporns, O., Tononi, G., and Kötter, R. (2005). The human connectome: A structural description of the human brain. *PLoS Comput Biol*, 1(4):e42+.

Spring, K. R., Fellers, T. J., and Davidson, M. W. (n.d.). Resolution and contrast in confocal microscopy. Retreived May 25, 2010, from `http://www.olympusfluoview.com/theory/resolutionintro.html`.

Stent, G. S. (1973). A physiological mechanism for hebb's postulate of learning. *Proc Natl Acad Sci U S A*, 70(4):997–1001.

Thompson, W. (1983). Synapse elimination in neonatal rat muscle is sensitive to pattern of muscle use. *Nature*, 302(5909):614–616.

Thompson, W. and Jansen, J. K. (1977). The extent of sprouting of remaining motor units in partly denervated immature and adult rat soleus muscle. *Neuroscience*, 2(4):523–535.

Thompson, W., Kuffler, D. P., and Jansen, J. K. (1979). The effect of prolonged, reversible block of nerve impulses on the elimination of polyneuronal innervation of new-born rat skeletal muscle fibers. *Neuroscience*, 4(2):271–281.

Thompson, W. J., Condon, K., and Astrow, S. H. (1990). The origin and selective innervation of early muscle fiber types in the rat. *J Neurobiol*, 21(1):212–222.

Thompson, W. J., Soileau, L. C., Balice-Gordon, R. J., and Sutton, L. A. (1987). Selective innervation of types of fibres in developing rat muscle. *J Exp Biol*, 132:249–263.

Trachtenberg, J. T. and Thompson, W. J. (1996). Schwann cell apoptosis at developing neuromuscular junctions is regulated by glial growth factor. *Nature*, 379(6561):174–177.

Tuffery, A. R. (1971). Growth and degeneration of motor end-plates in normal cat hind limb muscles. *J Anat*, 110(Pt 2):221–247.

Tweedle, C. and Stephens, K. (1981). Development of complexity in motor nerve endings at the rat neuromuscular junction. *Neuroscience*, 6(8):1657–1662.

Van Essen, D. C. (1982). *Neuromuscular Synapse Elimination: Structural, Functional, and Mechanistic aspects.*, pages 333–376. Plenum Press, New York.

Van Essen, D. C., Gordon, H., Soha, J. M., and Fraser, S. E. (1990). Synaptic dynamics at the neuromuscular junction: mechanisms and models. *J Neurobiol*, 21(1):223–249.

van Ooyen, A. (2001). Competition for tubulin between growing neurites during development. *Neurocomputing*, 38-40(1-4):73–78.

van Ooyen, A. (2005). Competition in neurite outgrowth and the development of nerve connections. *Prog Brain Res*, 147:81–99.

van Ooyen, A. and Willshaw, D. J. (1999). Poly- and mononeuronal innervation in a model for the development of neuromuscular connections. *J Theor Biol*, 196(4):495–511.

Vital-Durand, F. and Jeannerod, M., editors (1975). *Neuroanatomical plasticity: the principle of conservation of total axonal arborization.* INSERM.

Wærhaug, O. (1992). Postnatal development of rat motor nerve terminals. *Anat Embryol (Berl)*, 185(2):115–123.

Walsh, M. K. and Lichtman, J. W. (2003). In vivo time-lapse imaging of synaptic takeover associated with naturally occurring synapse elimination. *Neuron*, 37(1):67–73.

Wernig, A., Carmody, J. J., Anzil, A. P., Hansert, E., Marciniak, M., and Zucker, H. (1984). Persistence of nerve sprouting with features of synapse remodelling in soleus muscles of adult mice. *Neuroscience*, 11(1):241–253.

White, J. G., Southgate, E., Thomson, J. N., and Brenner, S. (1986). The structure of the nervous system of the nematode caenorhabditis elegans. *Philos Trans R Soc Lond B Biol Sci*, 314(1165):1–340.

Wigston, D. J. (1989). Remodeling of neuromuscular junctions in adult mouse soleus. *J Neurosci*, 9(2):639–647.

Willshaw, D. J. (1981). The establishment and the subsequent elimination of polyneuronal innervation of developing muscle: theoretical considerations. *Proc R Soc Lond B Biol Sci*, 212(1187):233–252.

Wright, M. and Son, Y. (2007). Ciliary neurotrophic factor is not required for terminal sprouting and compensatory reinnervation of neuromuscular synapses: Re-evaluation of cntf null mice. *Exp Neurol*, 205(2):437–448.

Yang, F., Je, H.-S. S., Ji, Y., Nagappan, G., Hempstead, B., and Lu, B. (2009). Pro-BDNF-induced synaptic depression and retraction at developing neuromuscular synapses. *J Cell Biol*, 185(4):727–741.

Zoubine, M. N., Ma, J. Y., Smirnova, I. V., Citron, B. A., and Festoff, B. W. (1996). A molecular mechanism for synapse elimination: novel inhibition of locally generated thrombin delays synapse loss in neonatal mouse muscle. *Dev Biol*, 179(2):447–457.

Zuo, Y. and Bishop, D. (2008). Glial imaging during synapse remodeling at the neuromuscular junction. *Neuron Glia Biol*, First View:1–8.